UNIVERSITY OF SOUTHAMPTON

FACULTY OF ENGINEERING AND THE ENVIRONMENT

Hydrodynamic controls on nearshore sediment sizes in Poole Bay

Academic Supervisor: Dr Hachem Kassem
Industrial Supervisors: Dr Charlie Thompson (CCO),
Mr Matt Hosey (BCP)

Name: Xue Ting, Ong (Gladys)
Student ID: 30579864

A dissertation submitted in partial fulfilment of the degree of MSc in Engineering in the Coastal Environment by instructional course

September 2019

Declaration

This thesis was submitted for examination in September 2019. It does not necessarily represent the final form of the thesis as deposited in the University after examination.

I, Xue Ting Ong (Gladys) declare that this thesis and the work presented in it are my own and has been generated by me as the result of my own original research.
I confirm that:
1. This work was done wholly or mainly while in candidature for a degree at this University;
2. Where any part of this thesis has previously been submitted for any other qualification at this University or any other institution, this has been clearly stated;
3. Where I have consulted the published work of others, this is always clearly attributed;
4. Where I have quoted from the work of others, the source is always given. With the exception of such quotations, this thesis is entirely my own work;
5. I have acknowledged all main sources of help;
6. Where the thesis is based on work done by myself jointly with others, I have made clear exactly what was done by others and what I have contributed myself;
7. None of this work has been published before submission.

Acknowledgements

This work is undertaken as part of the MSc Engineering in the Coastal Environment programme of University of Southampton under the sponsorship of Housing and Development Board of Singapore. I would like to express my sincere appreciation to my academic supervisor, Dr Hachem Kassem for his valuable mentorship, unwavering encouragement and motivation for the completion of this study, industrial supervisor Dr Charlie Thompson from Channel Coastal Observatory (CCO) in giving suggestions from time to time and providing the sediment sampling and oceanographic data. Additional data and information used in this study have been supported and generously shared by Bournemouth, Christchurch and Poole Council (BCP): Particle Size Distribution records for Poole Bay and internal reports, and I would like to thank Mr Matt Hosey, Dr Dave Harlow and Dr Matt Wadey from BCP for their kind assistance. Also thanking Ms Emma Evans from CCO for the provision of topographic data. Special thanks to Dr Ian Townend for his constructive advice in the analysis of the hydrodynamic forcing. I am also grateful to Dr Sam Cope and the Standing Conference on Problems Associated with the Coastline (SCOPAC) for presenting me with the Bradbury Bursary Award based on the research's scoping report. Finally, a big thank you to my family who constantly support and believe in me in this journey to pursue the postgraduate course.

Abstract

The management of coastal zone requires not only an in-depth understanding of the shoreline, but also a good assessment of hydrodynamics, sediment characteristics and coastal interventions. Poole Bay has been suffering from coastal erosion and the beaches have been intensively managed by hard and soft engineering methods. As sandy beaches coarsen in grain size from west to the east, understanding the sediment dynamics in the nearshore coastal zone and its controlling factors will enable us to better predict, protect and defend our coastlines in the future.

The study aims to identify the influence of hydrodynamic forcing on sediment size and sorting along the frontage of Poole Bay, based on an extensive records of sediment sampling and wave data from 2005 to 2016. From the examination of sediment characteristics, there is a general increase in sediment size and deterioration in sorting with increasing distance across the bay (from west to east). Maximum surface sediment sizes are always samples from the lower intertidal beach and the coarsest sediments are usually the worst sorted. Moving away from the swash zone, sediments on the offshore bar become increasingly finer and these are the best sorted among all sampled locations.

Waves are recognized to be more important than tides in this region. The variability of sediments is largely dependent on the wave energy that the shore/beach receives. Multivariate analyses identify the key variables are mean grain size, sorting, wave-induced bed shear stress, significant wave height and wave direction. Grain size and wave-induced bed shear stress can be described in an exponential relationship. Large number of fines which have low critical shear stresses can be easily mobilised and lost to the turbulent flow even at low-energy wave conditions. Further, grain size is linearly correlated to significant wave height (Hs), and under the condition of south-westerly waves and Hs in exceedance of 0.65 m, this usually coincides with an environment that is composed of gravelly and more poorly sorted sediments. Sediment size grading is likely due to the turbulence in the highly energetic zone lifting sediment into suspension and moving the sediments up the beach. The coarser ones are deposited due to the force of gravity and bed friction, whereas finer sediments are carried furthest and deposited landward or seaward. Since Poole Bay appears as an almost closed system due to shortage of natural sediment inputs, the existing materials are being reworked and sorted across and along shore. The analysis suggests that wave action, particularly significant wave height has a considerable impact on the type and grain size occurring on the nearshore of Poole Bay.

Beach nourishment has direct impacts on the sediment size and sorting at the swash zone. As the beaches in Poole Bay have become finer than before, it is becoming more susceptible to erosion. Ultimately, to maintain a sufficient width of beach zone for future recreational activities, or as a form of coastal defence, using a coarser grade material as beach fill material is recommended so that materials can retain longer on the beach.

Contents

List of Figures

List of Tables

Abbreviations

BIS	Beach Improvement Schemes
BODC	British Oceanographic Data Centre
CCO	Channel Coastal Observatory
degTN	Degree to True North
HW	High Water
LW	Low Water
MHW	Mean High Water
MLW	Mean Low Water
OD	Ordnance Datum
OS	Offshore
PC	Principal component
SCOPAC	Standing Conference on Problems Associated with the Coastline
SMP	Shoreline Management Plan
SPM	Shore Protection Manual

Symbols

A_w	Semi-orbital wave excursion (m)
b	Distance between two wave rays (m)
C_g	Shallow water wave group celerity (m/s)
D_x	Particle diameter at x% in the cumulative distribution (mm)
D_{50}	Median grain size (mm)
E	Shallow water wave energy (W)
f_w	Wave friction factor
g	Gravitational acceleration (m^2/s)
h	Water depth (m)
H	Wave height (m)
H_b	Breaker height (m)
Hs	Significant wave height (m)
k	Wave number
K_f	Friction coefficient
K_r	Refraction coefficient
K_s	Shoaling coefficient
k_s	Nikuradze roughness (m)
Kt	Kurtosis coefficient
Mn	Mean grain size (mm or φ)
o	Deep water condition, e.g. P_o refers to deep water wave energy flux
P	Wave energy flux (W/m^2)
So	Sorting coefficient
Sk	Skewness coefficient
T	Peak wave period (s)
U_b	Maximum near bed orbital velocity (m/s)
U_{cr}	Critical bottom velocity (m/s)
V_A	Level of semi-amplitude of the sine curve
V_B	Distance of sin x = 0 to the point at which Mn = 0
V_C	Semi-wavelength of the sine curve
V_D	Level of semi-amplitude above $S_o = 0$

w_s	Fall velocity (m/s)
Z_o	Bed roughness (m)
ρ	Density of sea water (kg/m^3)
α	Wave refraction angle (degree)
φ	Dimensionless grain diameter
θ	Wave angle (degree)
$\tau_{c,b}$	Current -induced bed shear stress (Pa)
$\tau_{w+c,b}$	Combined bed shear stress (Pa)
$\tau_{w,b}$	Wave-induced bed shear stress (Pa)
Ω	Dimensionless fall velocity, Dean's parameter

1.0 Introduction

1.1 Motivation

Beaches are landforms alongside the sea and are predominantly made up of non-cohesive sediments of sand, gravel (or shingle) and in some settings, a combination of the two. The dynamics of the beach are highly dependent on the temporal and spatial variation in sediment size and hydrodynamic forcing, which in turn influence the nearshore sediment transport and morphological evolution (Cooper, et al., 2001; Van Rijn, et al., 2007).

A beach often contains a wide range of grain sizes and this is attributed by sediment transport as a result of various coastal processes or/and anthropogenic activities such as beach nourishment. In the realm of sediment transport, the incipient movement of sediment takes place when the force flowing fluid over the sediment bed exceeds the threshold of bed boundary shear stress. With the increase in flow turbulence and presence of eddies, the mode of transport advances from bed load (traction, rolling, saltation) to suspended load.

Wave, current and wind actions further mobilise sediments and sort the grains in cross-shore and along-shore directions. The extent of sediment mobilisation depends on several factors, such as the source and direction of energy, local discontinuities in the bed topography and beach slope (Kakinoki, et al., 2010; Celikoglu, et al., 2004). There are noticeable differences observed in the grain size distribution as one moves from the frontal dune or cliff base, across the beach and further offshore (Bascom, 1959). At the upper beach, finer and more well-sorted materials can be found at the dunes due to aeolian processes. From the studies conducted by Briggs (1997) and Komar (1998) on sandy beaches, coarser materials are typically found in energetic areas such as the breaker zone whilst finer grain sizes are progressively winnowed out both onshore and offshore across the surf and swash zones. McCave (1978) and Thornton et al. (2007) associated a relationship of increasing sediment grain size with increasing wave height in a net alongshore, wave-driven environment. On shingle beaches, permeability becomes more important and it is observed for larger sediments to mobilise onshore to form berms whilst fine material congregated further downslope over a period of time through repetitive tidal cycles (Duncan, 1964; Horn, et al., 2003). On the other hand, a mixed beach tends to undergo radically different behaviours (e.g. wave energy dissipation by reflection (Mason, et al., 1997) and beach permeability (Mason, 1997)) in cross-shore and longshore transport from either sand or gravel beaches due to the large variation in sediment sizes (Kirk, 1980).

Arising from this complexity of changes in sediment size and sorting along the frontage, it is commonly assumed the entire area is spatially homogenous by a single sediment size (usually the mean value) when carrying out modelling and analysis. However, such simplification of the sediment characteristics parameterises sediment transport processes with certain limitations,

leading to uncertainties in the modelling results and the efficacy of beach management works. Although coastal models such as the Telemac's SISYPHE (Hervouet & Bates, 2000) and MIKE 21's Sand Transport modules (MIKE, 2019) can model different sediment size classes, these often come at pricey cost for additional software and hence are seldom used for modelling of smaller and shorter time scale projects. Therefore, a quantifiable understanding of the variability exhibited by beach sediments in response to changes in hydrodynamic conditions is crucial to appreciate the coastal morphological changes over time and allow us to better predict, protect and defend our coastlines in the future.

1.2 Significance of the research

The beaches of Poole Bay situated in the southern coast of England have always been plagued with coastal problems owing to the eroding forces of wind and waves. To protect properties and infrastructure from coastal erosion, the coastline has been intensively managed over the past century, through the maintenance of beach volume and hard defences. During the 20th Century, hard defences were sequentially constructed to protect the cliff erosion but this in turn depletes the natural supply of sand and gravel to the shore (NFDC, 2017). Consequently, the entire frontage of Poole Bay is eroding and millions of cubic metres of beach material that have lost to natural coastal processes through the years can only be replenished by artificial means (Harlow, 2017).

Beach nourishment is a process in which sediments are added to the beach where erosion is occurring to compensate shore erosion and restore the recreational value of the beach. Beaches along the Poole Bay frontage has undergone four successive beach nourishment works, also known as 'Beach Improvement Scheme' (BIS) from 1970s and since then more than 2 million m^3 of sand has been used to replenish the beaches at Bournemouth and Poole (EU Our Coast, 2015).

The price of beach nourishment is volatile and market-driven, and can vary considerably year on year. It is dependent on a viable source based on the scale of works, suitability (grain size, volume available etc.), cost, licencing and equipment (e.g. dredger). With a growing demand for appropriate beach fill materials, the cost of beach nourishment has risen steeply, from £4.72/m^3 of sand in 2006 to £13.01/m^3 in 2010 (Harlow, 2013). The ballpark estimate for future works ranges between £10 to £15/m^3 (BCP Council, 2019). Against this background of rising costs and reduced availability of material, an efficient approach of identifying and using the appropriate material that is available for each beach is required.

Beach monitoring efforts commenced as early as 1970 in Bournemouth frontage after its first BIS. Together with the Southeast Regional Coastal Monitoring Programme that started in 2002, these have assembled a robust database of hydrographic surveys, beach profiles surveys and particle size distribution (PSD) measurements etc (CCO, 2018). This has enabled both qualitative and quantitative assessment of coastal processes in Poole Bay as well as the efficacy of the beach

nourishment schemes. However, there are still gaps of knowledge in several fields of study (e.g. uncertainties in sediment transport pathways near Hook Sands), due to lack of long-term data and insufficient coverage of survey (NFDC, 2017).

It is important to understand sediment dynamics in the nearshore coastal zone and the controlling factors so that a more informed decision can be made for the next BIS. Although the coarsening of sediment from west (Sandbanks) to east (Hengistbury Head) has been well observed, at present, little is known about the grain size variation in response to hydrodynamic processes. This knowledge gap can pose constraints to sediment transport modelling, which directly impact the model accuracy in estimating cross-shore and longshore sediment transport rates, as well as beach management practices. Therefore, the main impetus of the research is to look into and identify the underlying relationship between sediment characteristics and hydrodynamic processes along the frontage in Poole Bay.

1.3 Research Aim and Objectives

The project aims to examine the influence of hydrodynamic forcing on the textural characteristics of the sediment e.g. size and sorting along the frontage of Poole Bay. To achieve the aim, three objectives have been set out:

i) Analyse the spatial and temporal variability in sediment characteristics along beaches in Poole Bay

ii) Assess the nearshore hydrodynamic conditions and identify the relationship between hydrodynamic forcing and sediment variability

iii) Investigate the significance between beach nourishment works and sediment size and discuss its implication with regards to fill material selection for future beach management

2.0 Study Area

2.1 Geographical location

Poole Bay is a relatively shallow embayment in the English Channel, situated along the southern coast of Dorset, England (Figure 1). The 16 km log-spiral shaped shoreline spans across Sandbanks Ferry Slipway at the mouth of Poole Harbour in the west, to Hengistbury Head in the east. The beaches from Sandbanks to Alum Chine were formerly managed by Borough of Poole and beaches from Alum Chine to Hengistbury Head were managed by Bournemouth Borough Council. They have been recently amalgamated to one local authority known as Bournemouth, Christchurch and Poole (BCP) Council.

Figure 1 Site plan of Poole Bay: A quasi-log spiral shaped embayment bounded by Poole Harbour to the west and Hengistbury Head to the east. Landmark features of the bay include the Sandbanks Beach, Branksome Chine, Alum Chine, Bournemouth Beach, Boscombe Beach, Southbourne Beach, Solent Beach, Double Dykes and Hengistbury Head. (Source: ArcGIS ESRI)

The shoreline in Poole Bay is characterised by sandstone cliffs of varying heights between 4m to 36m and varying sediment grain sizes (NFDC, 2017). The urbanized sand spit of Sandbanks which extends from the east of Poole Harbour is composed of fine sandy beaches that continues to Branksome Chine across the Poole frontage. The Bournemouth frontage comprises sandy beaches that stretch from Alum Chine to Southbourne, mixed sand-shingle beaches from Southbourne to Solent Beach, and mostly shingles from Solent Beach to Hengistbury Head (Halcrow, 2004) (Figure 1).

As Bournemouth and Poole are popular coastal resort towns, many residential, commercial and recreational developments can be found on top of the cliff and across the seafront (Figure 2).

Sustainability of the tourist beaches is vital to the local economy and the beaches are heavily protected by long spans of seawalls, promenades to prevent cliff erosion and timber and rock groynes to retain materials on the beach.

Figure 2 Bournemouth's coastline populated with residential and commercial developments, and protected by engineered structures such as groynes and seawalls. (Source: Bournemouth Official Tourism)

2.2 Geology and coastal evolution

During the last Holocene epoch (about 9,000 years ago), the rising sea and fluvial levels eroded and eventually breached the chalk outcrop which ran from The Needles (Isle of Wight) to Handfast Point (Royal Haskoning, 2010) (Figure 3). This eroded more than 220 km^2 of land (Harlow, 2005), liberated very large amount of soft Tertiary sands and clays and redistributed over the coastal zone, thereby created the present-day planform of Poole Bay.

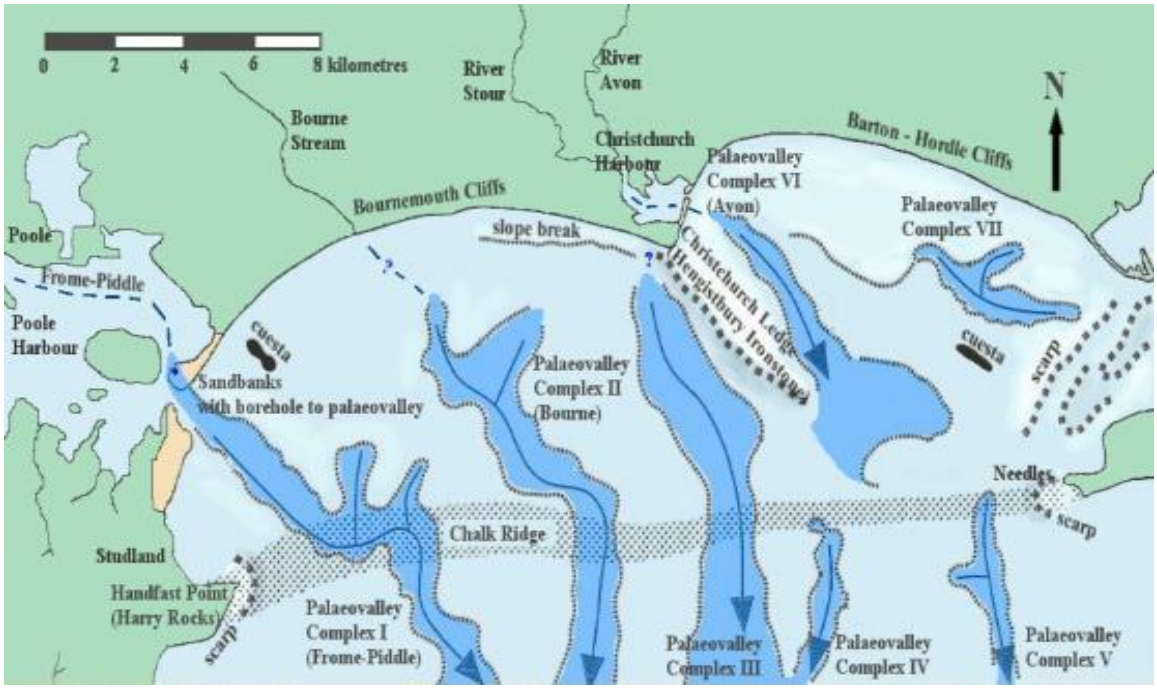

Figure 3 Map of the Paleovalley of Poole and Christchurch Bays: the flooding of tributaries and rising sea levels from Holocene transgression eroded the ridge. The river valley was exposed which was further invaded by the sea and eventually formed the present-day configuration of the two bays. Source: Sketched by Velegrakis et al (1999), modified by Ian West (2007)

The cliffs of Hengistbury Head are built on a base of Boscombe Sands (yellow sand intermixed with layers of shingle), Hengistbury Beds (ironstone doggers), Warren Hill sand and capped with Plateau Gravel (Rees, 1994) (Figure 4). This formation continues west into Poole Bay and towards Bournemouth and Poole, the cliffs are composed of Eocene sands and clays (West, 2006). The cliffs were subjected to continuous and rapid erosion throughout the Holocene, forming steep cliffs and yielding a steady supply of sediments to the beach.

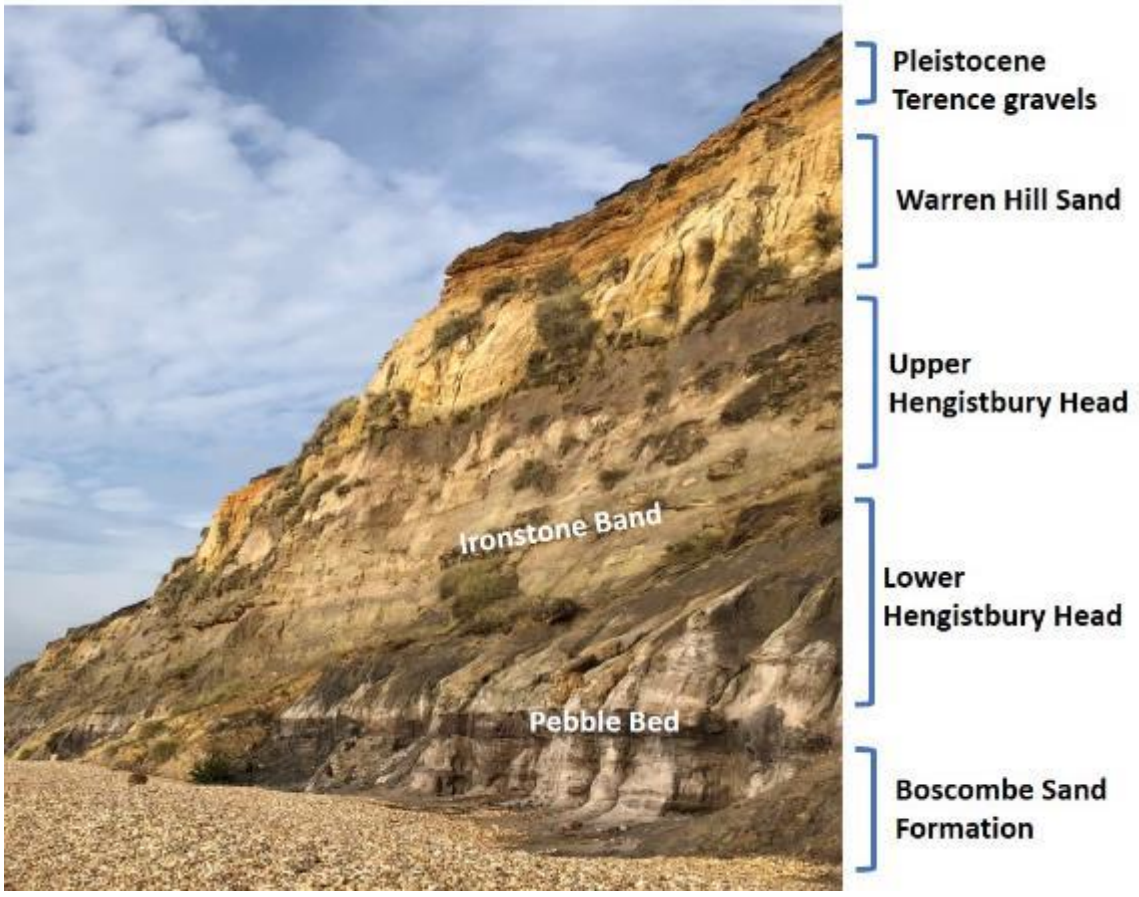

Figure 4 Cliff at Hengistbury Head. The classification of geological formation is adapted from West (2006) (Photo credit: Author's photo (2018)).

The erosion rate was estimated at approximately 1 m/year, releasing 125,000 m^3 of sediment per year in the past (Harlow, 2012a). However, human intervention in the late 18th century has modified the bay's configuration and cliff retreat rates. Apart from the unprotected cliffs along the far eastern end of Solent Beach and Hengistbury Head, the rest of the seafront are protected by hard engineering coastal protection structures (seawalls, rock and timber groynes), coupled with overgrown vegetation which have decelerated the erosion rate (Figure 5). The Long Groyne at Hengistbury Head intercepted the littoral drift, and overtime, the steadily accreting beach provided toe protection to the cliff. The frontage is now considered to be in a 'stable' form and there is virtually no more supply of natural sediment from the cliffs (Royal Haskoning, 2010).

Figure 5 Coastal protection with groyne system and vegetated cliff at Poole Bay (Photo Credit: Christophe Finot (2006))

2.3 Sediment dynamics

Beach sediment in Poole Bay originates from the sea bed during the Holocene sea-level rise however, fresh input is almost negligible. Sediments from cliffs and fluvial sources are also small in quantities, thus the bay appears as an almost closed system due to a shortage of natural fresh sediment inputs. The sediment sub-cell boundary stretches from Poole Harbour entrance to the Hengistbury Head Long Groyne (Bray, et al., 1991). Marine input mostly arrives from two sources: (i) fresh sediment from the external Poole Bay system and (ii) sediment feed to beaches from existing nearshore and/or offshore stores within the budgetary cell.

As the open frontage of Poole Bay is quite shallow, it features a drift-aligned shoreline with most incident waves arrive the shoreline at an oblique angle. According to the Sediment Transport Study 2012 conducted by Standing Conference on Problems Associated with the Coastline (SCOPAC), the littoral drift which correlated with the dominant wave climate, carries sediments alongshore in a west-to-east direction (Figure 6). The long groyne at Hengistbury Head retains most of the material while the remaining moved offshore and to Christchurch Bay.

There is a high degree of sorting along- and across shore in Poole Bay. Past studies indicated that beach materials coarsen in the same net direction as the longshore drift (Lacey, 1985; Edgell, 2008). Starting from the west, Sandbanks comprises silt to fine graded sandy materials, largely transported from Hook Sands, an ebb tidal delta store of Poole Harbour entrance. Hindcast wave models predicted a net southward or offshore sediment movement although there is limited evidence from the field as otherwise peninsula would have breached without a continual onshore feed from Hook

Sands (HR Wallingford, 2003). The central region in Bournemouth and Boscombe constituted fine to medium sand, and from Southbourne to Double Dykes, the mean particle size increased starkly and nearing the headland of Hengistbury Head where shingles dominated the sediment fraction.

Seasonal effects can cause variation in beach area, elevation and profile shape. A typical summer beach/berm profile tends to be steeper in summer compared to winter. The coarsest particles are usually found in areas of high turbulence, seawards of the backwash/surf zone and at the wave plunge point (Bascom, 1959). Seaward of mean low water, sediments generally become finer and better sorted in both landward and seaward directions with reducing wave energy (Komar, 1998). Beach profiles are more volatile in winter as the high energetic swell waves sweep the sand offshore to form transient nearshore bar and trough. However, a previous study in Poole Bay found coarsening of particles occurs in mean high water (MHW) and materials smaller than the critical value of 1.8φ (0.29 mm) are likely to disperse offshore of Poole bay (Harlow, 2012b). In addition, the beach profile in the bay appeared gentler in gradient and wider in the late summer to autumn months, a phenomenon due to the seawall which augments wave reflection and promotes offshore sediment movement. Nearshore sand bar existed smaller in size and nearer to the west in Sandbanks, and larger, further away from the shoreline to the east.

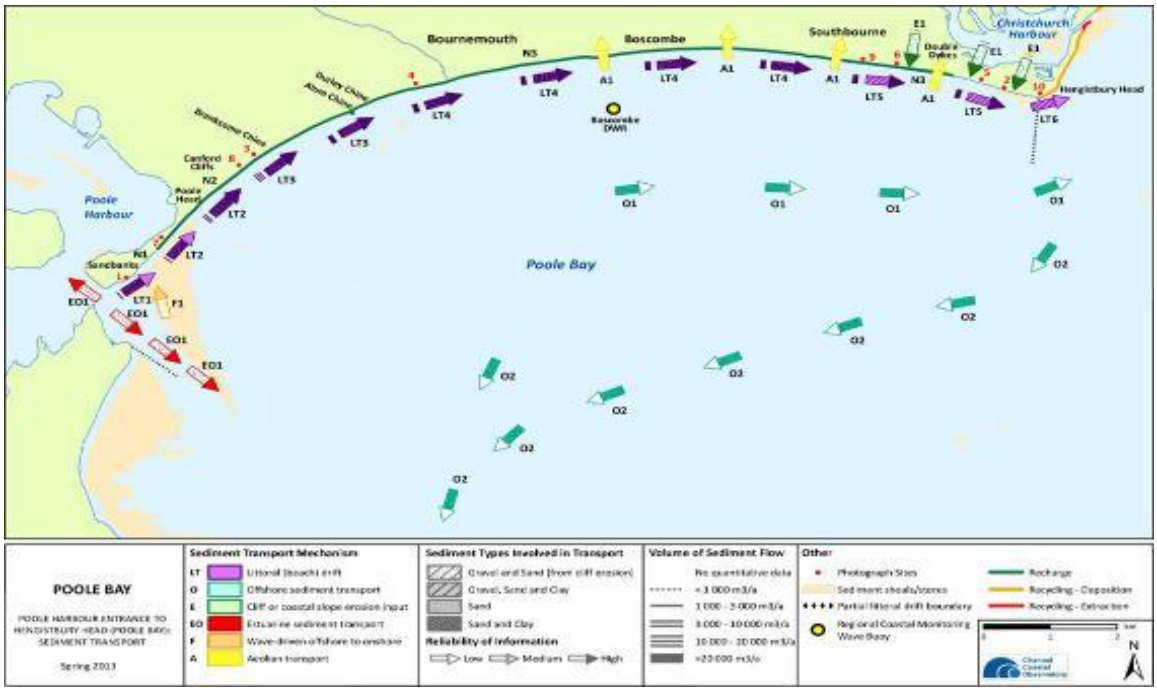

Figure 6 Sediment transport pathways from Poole Harbour Entrance to Hengistbury Head, Source: NFDC (2017)

2.4 Coastal protection strategies

The beaches in Bournemouth and Poole are amenity assets to the tourism industry and have attracted more than 6.88 million tourists (NCTA, 2013). It is crucial to improve and preserve the

existing beaches, not only as natural coastal defences for erosion and flood but also since beaches attract visitors and contribute a significant revenue to the local economy.

2.4.1 Hard defences

Historically, the implementation of hard structures was prevalent and adopted as a measure for coastal protection and management. The first coastal structure was built at Sandbanks way back in 1890s, and carried on with beaches from Bournemouth to Boscombe Pier in 1911. The defences then extended progressively eastwards to Solent Beach in 1979 with the last section of sea wall completed at Canford Cliffs in 1985. Seawalls may have afforded the cliffs with toe protection but led to intensified wave reflection and littoral drift that caused downdrift erosion (Peterson, et al., 2000). Groyne system were then erected between 1915 and 1974 to curtail these effects (Hodder, 1986) with groynes rebuilding and new rock revetment as controlling measures that continues to date (NFDC, 2017). The reduction in beach volume was approximately 10 million m^3 in 1907 to 6.5 million m^3 in 1975 (Harlow, 2005), as such there was a pressing need for beach replenishment.

2.4.2 Beach replenishment works

A shift from a 'hard' engineering approach to a 'soft' engineering approach occurred in the 1970s for the reason that beach replenishment became more widely recognised as a practical form of shoreline defence. In the last 50 years, there were four major beach improvement schemes (BIS) and intermittent recycle activities across the whole site. In 1970, the Bournemouth Borough Council piloted the pioneer replenishment project, BIS 1 that involved 84,000 m^3 of dredged sand from south east of Isle of Wight and deposited offshore at west of Bournemouth Pier to Alum Chine before repositioning to mean low water (MLW) location (Lelliott, 1989).

The success of the pilot trial is followed by a full-scale scheme, BIS 2 in 1974/1975. Approximately 1.5 million m^3 of marine sand was dredged from Dolphin Sands, an offshore sandbank south of Hengistbury Head. Half of the volume was pumped directly onto the intertidal beach. The remaining materials were initially placed at nearshore dumpsites and later migrated to the foreshore over a 5 year-period from 1975 to 1980 (Hodder, 1986). The scheme remained effective for more than a decade until the beaches reached critically low levels in 1987. It was reported that ensuing a storm in autumn that year the mean high water line moved landwards to intercept with the seawall in several parts of the beaches causing the seawall to sustain damages and breaches (Harlow & Cooper, 1995).

Due to the unexceptional low beach levels, the third replenishment scheme BIS 3 was implemented from 1988 to 1990. The timing of BIS 3 coincided with the maintenance dredging of the Poole Harbour entrance at that time and the dredged materials were used as beach fill (Turner, 1994). Purchasing and transporting sand from commercial sources can be very expensive therefore when

an opportunity arises to use sand from local dredging operations, this helps in cost savings of the scheme. A downside on this approach was the poorly sorted nature of the dredged sediments resulting in a lack of selection in grain size specifications for the beach fill materials. An estimated 990,000 m^3 of dredged materials were pumped onto the upper beach above MHW and left to form its own profile (Harlow, 2005).

During the same period, another replenishment project was undertaken at Solent Beach and Hengistbury Head. The beaches on this span were known to compose of coarser particles, hence shingle and gravels were inherently chosen for beach top-up. Some 143,000 m^3 of coarse materials were dredged off the Isle of Wight and deposited to the beach directly (May, 1990).

The then Harbour Authority in charge of the Poole frontage has adopted and maintained the groyne system to address the erosion faced in Sandbanks to create a stable environment which allowed the accretion of the beaches until late 1990s. Beaches further eastward continues to erode sufficiently and the sea front properties were at risk of damage. A beach replenishment exercise was conducted in 2003 at Sandbanks involving 88,000 m^3 of fill from the maintenance dredging within Poole Harbour (Robson, 2003) (Figure 7). More materials were placed on the western end to allow wind and waves to carry it over the central and eastern areas over time. Sand bunds were formed seawards to create a lagoon to retain the sand on the beach and avoid loses of sand to the foreshore.

Figure 7 Low beach level at Sandbanks, exposing the footing of staircase (Left). Beach replenishment works were carried out to recharge the beach (Right) (Source: Borough of Poole, 2003)

The beaches in Poole Bay were due for replenishment after the last major scheme completed 15 years ago in 1990. BIS 4 was undertaken from 2005 to 2010 over four phases. BIS 4.1 commenced during the winter of 2005/2006, over 1.1 million m^3 of beach materials from the Poole Harbour dredging operation to replenish beaches in Swanage (90,000 m^3), Poole (450,000 m^3) and

Bournemouth (600,000 m^3) (Terry, 2008). The fill included a significant proportion of gravel and shingle placed at the Solent Beach and towards the Southbourne beach. As the original Southbourne beach was composed of sandy materials, the replenishment works using the coarse sediments received negative feedback from beach-goers and posed dangers to young children and surfers due to the steep and unevenness profile (Edgell, 2008). BIS 4.2 saw the continuation of beach nourishment at Bournemouth seafront in winter of 2006/2007, between Boscombe and Alum Chine with a further 897,000 m^3 of marine dredged sand from a licensed dredging area off the Isle of Wight (Poole & Christchurch Bays Coastal Group, 2011). Three annual top-ups, BIS 4.3 to 4.5 were carried out from 2008 to 2010 to replenish beach sections between Boscombe and Southbourne using an estimated volume of 200,000 m^3 dredged materials.

A 17-year plan was formulated to protect Bournemouth's coastline from 2015 to 2032 as most of the hard defences are reaching the end of their useful life (BCP Council, 2019). The following works have been planned:

i) Replacement of existing 53 groynes
ii) Construction of additional 3 new groynes
iii) Replacement of Long Groyne at Hengistbury Head
iv) Beach replenishment every 5 years

2.4.3 Influence of coastal management works through beach monitoring efforts

Apart from the natural coastal processes, the nearshore sediment size and sorting are further altered by anthropogenic interference through the hard structures and infill materials. Beach monitoring efforts was intensively carried out in Poole Bay thereafter its first BIS in 1970 by beach profiling that extended up to 450 m offshore. In 2002, the Regional Strategic Coastal Monitoring Programme (RSCMP) was tasked to take on a more holistic approach to coastal monitoring with the planning and implementation of the monitoring programme to standardise practices and methodology for the local or lead authority to follow.

2.5 Hydrodynamic regime

Wave and tidal currents are the dominant sediment transport mechanisms. Both are mainly generated by, and dependent on wind conditions. The wave climate in Poole Bay varies spatially due to the direction of approach of the swell waves. The prevailing wave direction comes from south to south-west which corresponds with the direction of longest fetch and longer period swell waves originated in the Atlantic Ocean (Royal Haskoning, 2010). Wind waves from the east and south-east direction tend to have shorter period and are less frequent.

The coastline is sheltered from Handfast Point and the Isle of Purbeck, leading to refraction and diffraction of waves from the south south-west to south and south-east approach before entering the

bay. Halcrow (1999) predicted with a wave refraction model that 85% of the inshore environment is influenced by the refracted waves approaching from the west and south-west; whilst the dominant refracted waves from the east and south-east affect the entire coastline. Due to the presence of shallow bathymetry and underwater offshore bar, waves approaching from any angle are significantly reduced due to breaking waves.

Poole Bay experiences a semi-diurnal, low tidal range, with a range of 2.0 m during spring cycles and 1.0 m during neaps (NFDC, 2017). The tidal curve is heavily distorted by shallow water effects, producing a 'double high water' along the frontage, and its range increases slightly with distance to the east (Royal Haskoning, 2005). Figure 8 shows an example of the observed tide curve at Bournemouth for a spring-neap tidal cycle. The shape of the spring tides can be seen with a double high water with the relative height of the two high waters vary considerably. During the neap cycle, the tide displays a more erratic shape as during the neap tide periods, the tide is dominated by the higher order tidal constituents (quarter-diurnal and sixth diurnal harmonics).

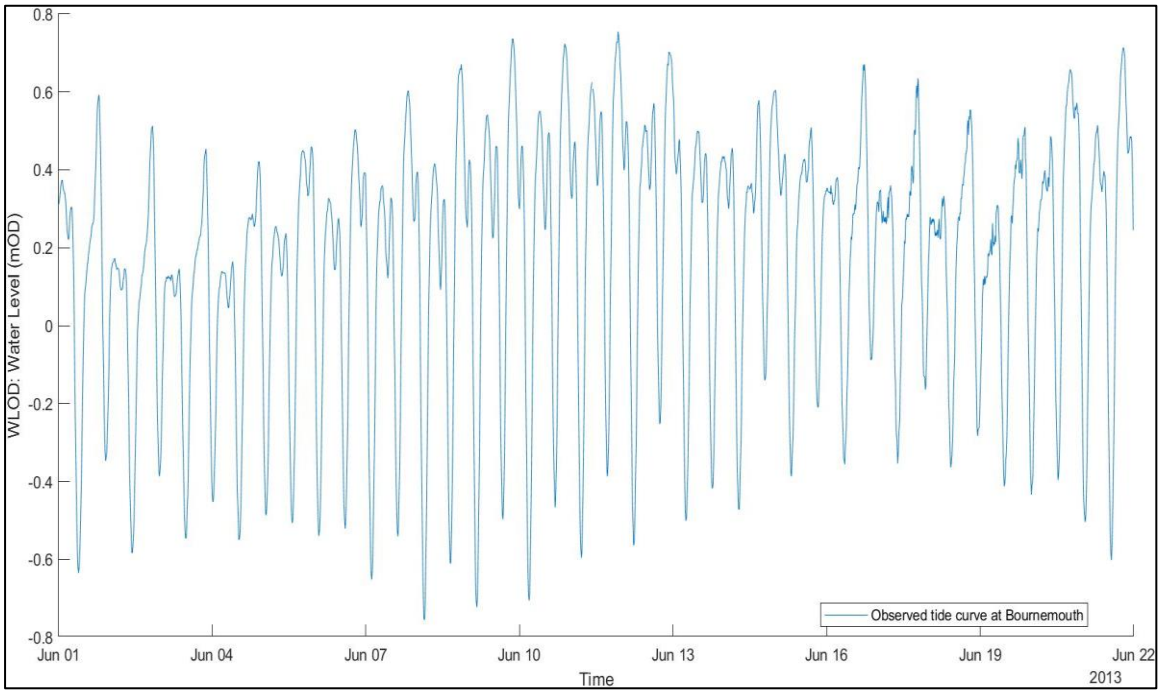

Figure 8 Observed tidal curve for a spring-neap tidal cycle at Bournemouth. (Source of data: British Oceanographic Data Centre, BODC)

Tidal currents are generally weak across the bay except at the extreme ends of the bay, offshore the Long Groyne at Hengistbury Head and at Poole Harbour mouth and the East Looe Channel. Strong currents varies in direction near to the entrance of the harbour, with ebb current velocity goes up to 2.5 m/s due to the ebb-dominant tidal regime at the Poole Harbour entrance channel (NFDC, 2017).

The low tidal currents are not capable in transporting large amount of sediments but can potentially mobilise finer sediments seawards, leaving the coarser sediments onshore. When combined with the wave induced currents, this causes a littoral transport from the west to east, although it has been

observed occasional reversal of sediment movement under the influence of changing tide and wind-generated waves (NFDC, 2017).

3.0 Background to research: Theories on sediment classification, hydrodynamics and mechanism to sediment transport & sorting

The key emphasis of this research study evolves the coupled system between hydrodynamic, sediment dynamics and mobility. This chapter provides an overview of the key concepts and assumptions used in this research.

3.1 Sediment classification

Particle size is the most important physical property of sediments, as it might represent the distance from the original source and it is correlated to the force required of the fluid stresses to entrain, transport and deposit these particles. It is also an important influence in achieving beach stability and shoreline equilibrium. For a spherical homogeneous particle, the size is distinctively defined by its diameter, *d*. The Wentworth scale has been used extensively in the coastal engineering field (Wentworth , 1922). The grades and sizes used in this scale were later supplemented by Krumbein (1934), which transformed the millimetre unit into a dimensionless parameter called phi (φ) or logarithmic scale to yield simple whole numbers:

$$\varphi = -log_2 d \qquad (3.1)$$

Figure 9 showed a simplified version of the much more detailed U.S. Geological Survey (USBS) classification.

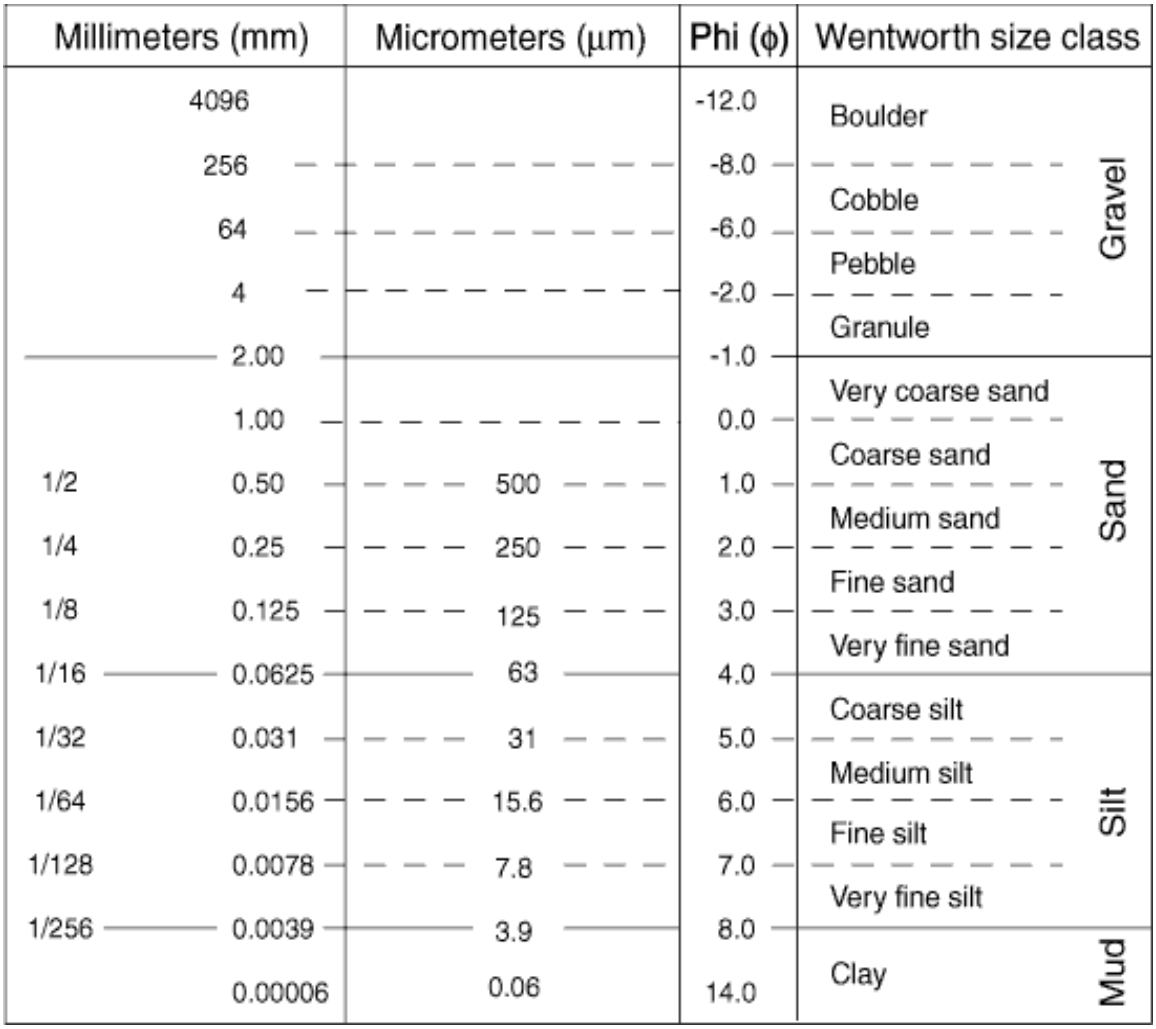

Figure 9 The common grain size thresholds using Wentworth (1922) classification

3.2 Statistical analysis of particle size distribution

Grain size analysis is fundamental to provide information on the sediment provenance, transport history and depositional conditions (Bui, et al., 1990). Various techniques are employed in grain size determination, including direct measurement, dry and wet sieving, sedimentation, and measurement by laser granulometer and Coulter counter. The most common method of sediment processing is using a sieve stack with progressively fining apertures. The overall particle size distribution is then constructed from the weights of sediment or volume percentage of sample retained on each sieve of a given range. The results are then plotted as frequency or cumulative frequency curves which gives indication on average particle size present in the sample, spreading of the particle size about this average etc.

The distribution can further be described through the application of statistical procedures. Many formulae have been proposed (Krumbein, 1934; Otto, 1939; Inman, 1952) although the most widely used are those proposed by Folk & Ward (1957) which fall into the four principal parameters:

(a) Mean grain size

The average size of sediments is usually expressed using parameters: the mode, median and the mean grain size. The mode is the most occurring particle diameter and passes through the peak of the relative frequency curve. It is useful particularly in a skewed distribution. The median represents the 50th percentile (D_{50}) of the distribution in the cumulative curve. The mean is recommended as the overall average size as it is more accurate in estimating the overall distribution by the method of moments than the mode or median (Lacey, 1985).

$$Mean, Mn = \frac{D_{16}+D_{50}+D_{84}}{3} \quad (3.2)$$

(b) Sorting

The spread of the distribution data is expressed in terms of its range, *i.e.* the difference between the minimum and the maximum sizes. Sorting (S_O) is the measure of the scatter as depicted in Figure 10 and is defined as the standard deviation equation. It can also provide information about the energy level and the rate of sediment deposition. Where samples are poorly sorted with a combination of fine and coarse grains, this usually occurs in area of high turbulence. Samples that are very well sorted would distinctly separate the finer and coarser particles into different areas according energy dissipation levels.

$$Sorting, So = \frac{D_{84}-D_{16}}{4} + \frac{D_{95}-D_5}{6.6} \quad (3.3)$$

The scale description of the sorting coefficient of a particle size distribution frequency curve is adopted from Folk & Ward (1957), presented in Table 1 and Figure 10.

Table 1 Description of the sorting coefficient, following Folk & Ward (1957)

Very Well Sorted	< 0.35
Well Sorted	0.35 to 0.50
Moderately Well Sorted	0.50 to 0.70
Moderately Sorted	0.70 to 1.00
Poorly Sorted	1.00 to 2.00
Very Poorly Sorted	2.00 to 4.00
Extremely Poorly Sorted	> 4.00

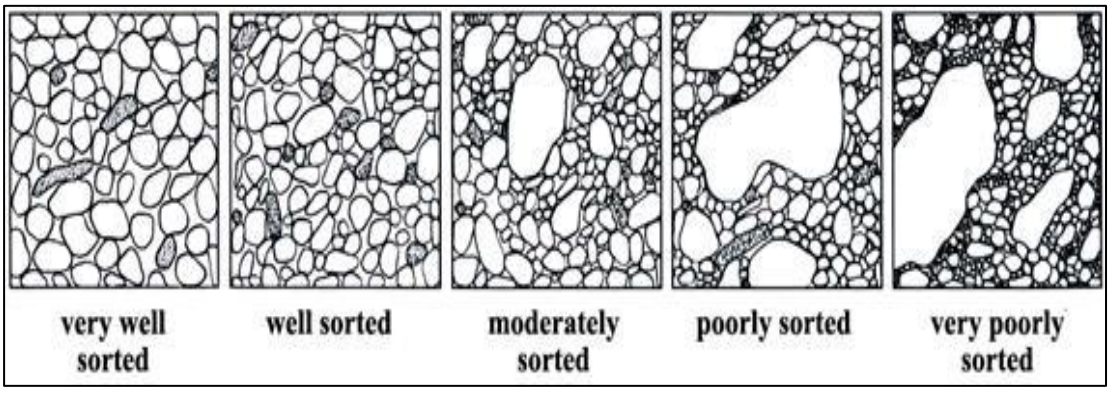

Figure 10 Sorting Chart (Bevis, 2013))

(c) Skewness

Skewness is the degree of symmetry or preferential spread to one side of the average as illustrated in Figure 11. It measures from -1.0 to +1.0. Skewness of zero refers to sample with symmetrical grain-size distribution and tends to be unimodal and more well sorted than samples with positive or negative skewness. Negative skewness implies that there are more coarse materials in the sample size and for positively skewed distribution with a higher percentage of fine materials present in the sample (Martins, 1965). The skewness of beach sands tends to be negative as a result of removal in the fine-grained tail of distribution by wave winnowing action (Friedman, 1961). The limits of skewness in the particle size distribution are described in Table 2.

$$Skewness, Sk = \frac{D_{16}+D_{84}-2D_{50}}{2(D_{84}-D_{16})} + \frac{D_5+D_{95}-2D_{50}}{2(D_{95}-D_5)} \quad (3.4)$$

Table 2 Description of the skewness coefficient, following Folk & Ward (1957)

Very Fine Skewed	+ 0.3 to + 1.0
Fine Skewed	+ 0.1 to + 0.3
Symmetrical	+ 0.1 to –0.1
Coarse Skewed	–0.1 to –0.3
Very Coarse Skewed	–0.3 to –1.0

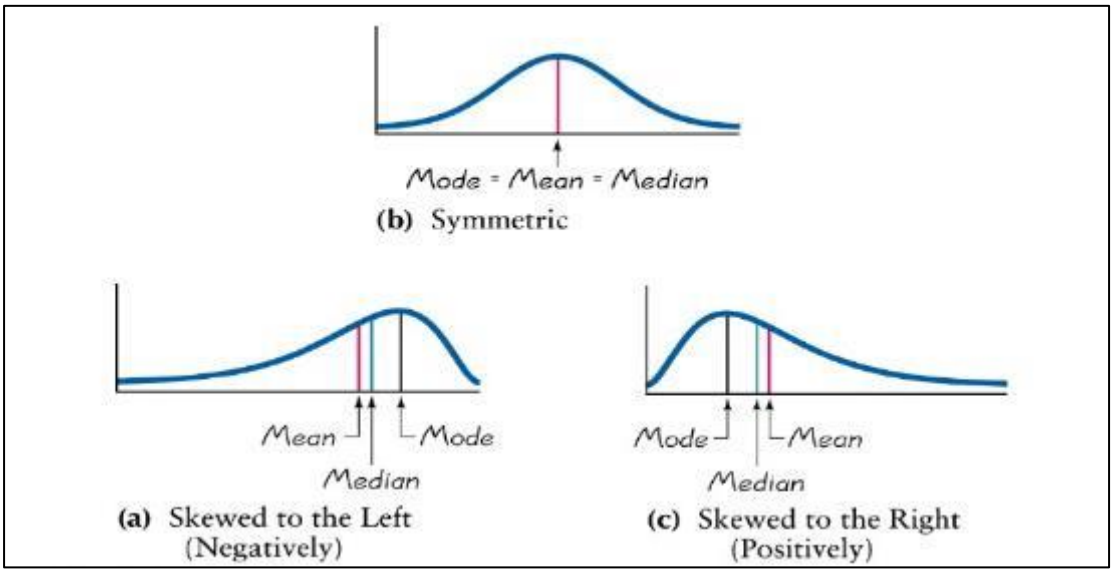

Figure 11 Distributions of (a) symmetrical distribution, (b) fine (positive) skewness and (c) coarse (negative) skewness (Leeder, 2004).

(d) Kurtosis

Kurtosis (peakedness) of a grain-size distribution is defined as the degree of concentration of the grains relative to the average. It compares sorting in the central portion of the population with that in the tails. The limits of the peakness parameter is listed in Table 3.

For a platykurtic distribution, it possesses a flatter peak compared to the pointy leptokurtic distribution that clusters near the centre of the distribution, suggesting the significance in the

tails of the distribution for a platykurtic case. Mesokurtic distribution defines a normal distribution curve and has a kurtosis value of 1.0. Figure 12 exemplified these three modes of kurtosis.

$$Kurtosis, Ku = \frac{D_{95}-D_5}{2.44(D_{75}-D_{25})} \quad (3.5)$$

Table 3 Description of Kurtosis coefficient, following Folk & Ward (1957)

Very Platykurtic	< 0.67
Platykurtic	0.67 to 0.90
Mesokurtic	0.90 to 1.11
Leptokurtic	1.11 to 1.50
Very Leptokurtic	1.50 to 3.00
Extremely Leptokurtic	> 3.00

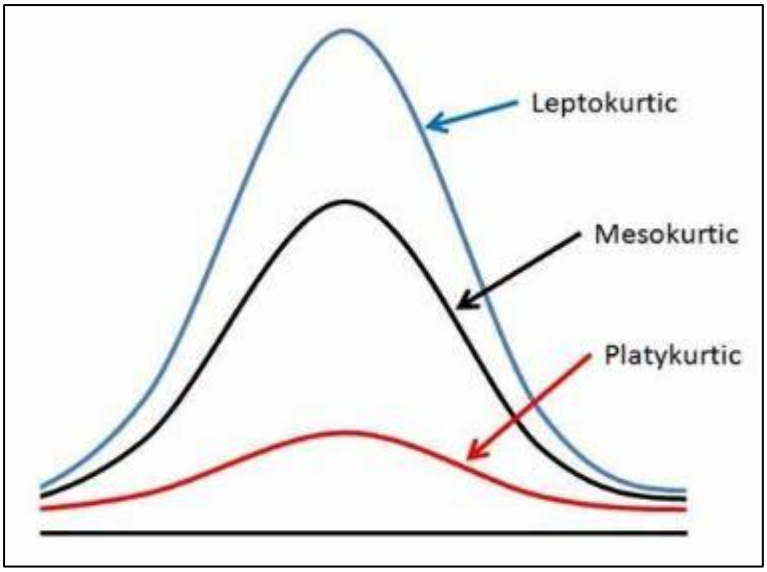

Figure 12 Illustration of Kurtosis distribution: Leptokurtic maintains a very pointy at its peak; mesokurtic owns a medium pointy and platykurtic is generally a flat curve.

3.3 Interdependency of grain textural parameters

Inter-relationships bind the textural parameters of a population of samples in several ways, yet these parameters are often theoretically, considered geometrically independent of each other (Lacey, 1985). The relationships can be expressed in mathematical equations through scatterplots of the sampled data. This approach has proven beneficial as it allows a more in-depth understanding on how the four parameters evolve around each another as well as in spatial and temporal settings rather than examining each parameter in isolation.

3.3.1 Bi-variate relationship between sorting and mean grain size

Folk & Ward (1957) first discovered the significance of the textural characteristics in his work on the sediments of Brazos River bar. There is a bi-variate relationship between the mean grain size and sorting embodied by a sinusoidal curve. This was further explored in coastal settings and found

applicable by Harlow (1982) and Lacey (1985) in the bays of Christchurch and Poole. The relations are expressed as shown in the equations below. The parameters V_A and V_D exhibited the level of sorting within the sediment population, V_B and V_C indicated the range of mean sizes present. Figure 13 reflects the bi-variate relationship of the sorting and mean coefficients and Figure 14 are plots from the previous studies.

$$S_o = V_D - V_A \sin\left[\frac{180}{V_C}(M_N - V_B)\right] \quad (3.6)$$

Where V_A = Level of semi-amplitude of the sine curve

V_B = Distance of $\sin x = 0$ to the point at which $M_N = 0$

V_C = Semi-wavelength of the sine curve

V_D = Level of semi-amplitude above $S_o = 0$

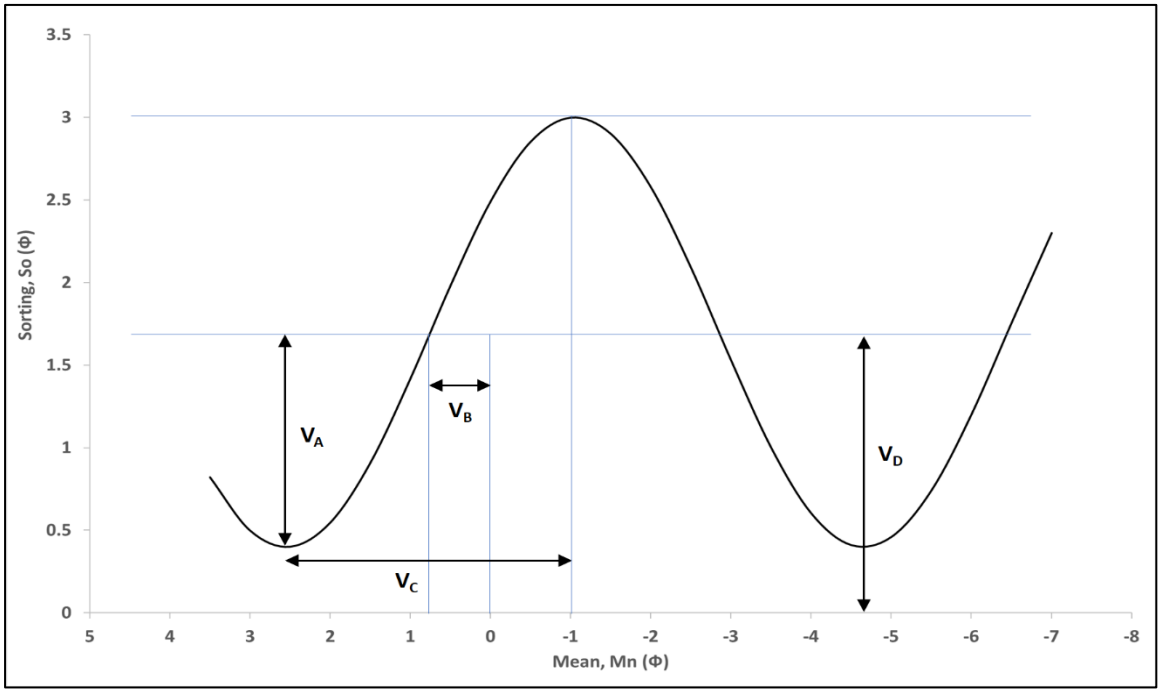

Figure 13 Relationship between the mean and sorting coefficients expressed in a sinusoidal curve, adapted from Harlow (1982) in equation 3.8.

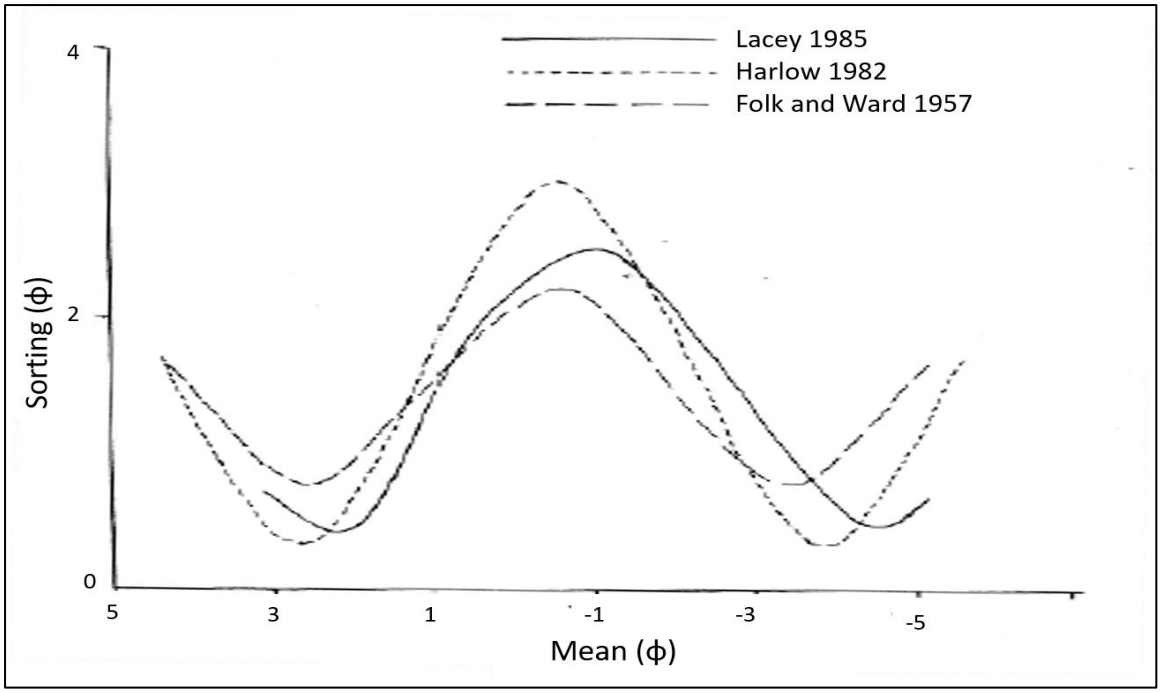

Figure 14 Sinusoidal relationship between mean and sorting for riverine (Folk & Ward, 1957) and beach (Harlow, 1982; Lacey, 1985) sediment populations.

Referring to the troughs of the curve, the degree of sorting of the modes is observed to be higher for river gravels, *i.e.* less well sorted than the beach sediments. This is anticipated since river sediments usually get buried quickly when deposited onto the river bed, whereas beach sediments are continually subject to wave action. However, when the population is no longer a unimodal distribution, the sorting varies according to the proportion of the materials as shown in the crest of the curves.

The following relationships are obtained from Folk & Ward (1957) for Brazos River bar sediments (Equation 3.7), Harlow (1982) for beach sediments from Selsey Bill to Portsmouth (Equation 3.8), Lacey (1985) for sediments in Christchurch and Poole Bay (Equation 3.9). Edgell (2008)'s analysis focussing on sediments along the Bournemouth beach front developed a similar sinusoidal relationship (Equation 3.10 and Figure 15).

$$So = 1.50 - 0.75\ sin\ [60(Mn - 0.75)] \quad (3.7)$$

$$So = 1.67 - 1.33\ sin\ [55(Mn - 1)] \quad (3.8)$$

$$So = 1.50 - 1.10\ sin\ [51.5(Mn - 0.75)] \quad (3.9)$$

$$So = 1.61 - 1.08\ sin\ [47(Mn - 0.44)] \quad (3.10)$$

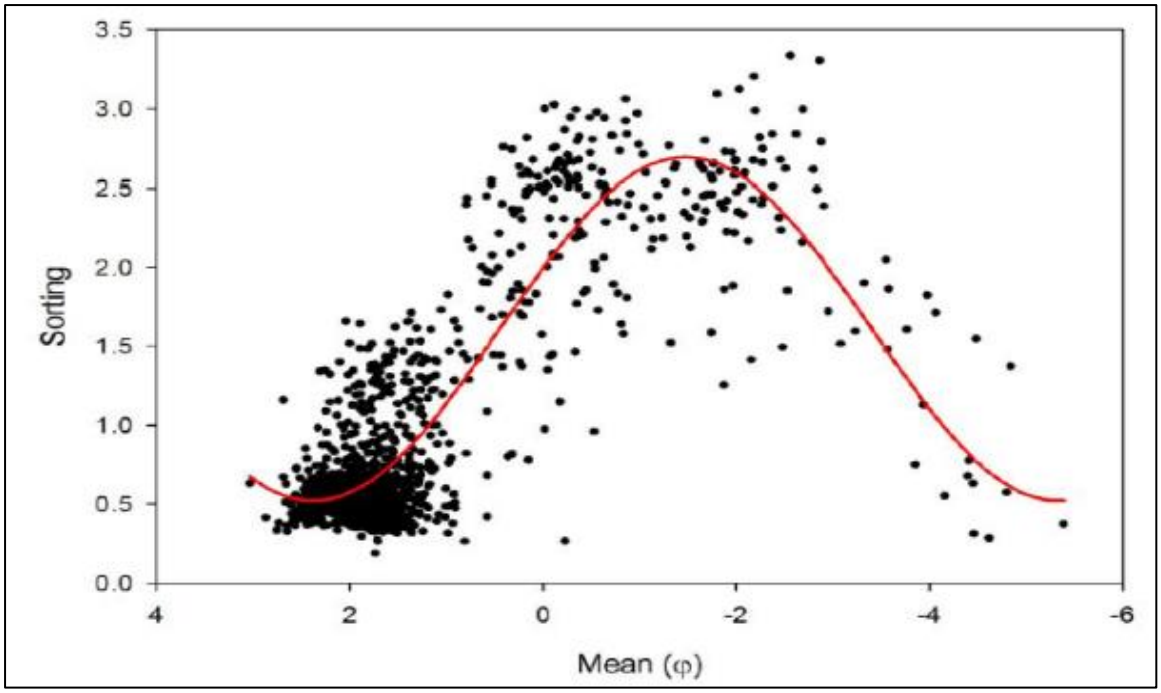

Figure 15 Mean grain size plotted against sorting for sediments at Bournemouth beach (Source: Edgell (2008))

3.3.2 Multi-variate relationship for statistical parameters

A multi-variate relationship was realised in a helical form for the grain textural parameters as shown in Figure 16 (Folk & Ward, 1957). The shape of the helical curve is dependent on the nature and combination of polymodal sediments made available and the conditions in which they were deposited.

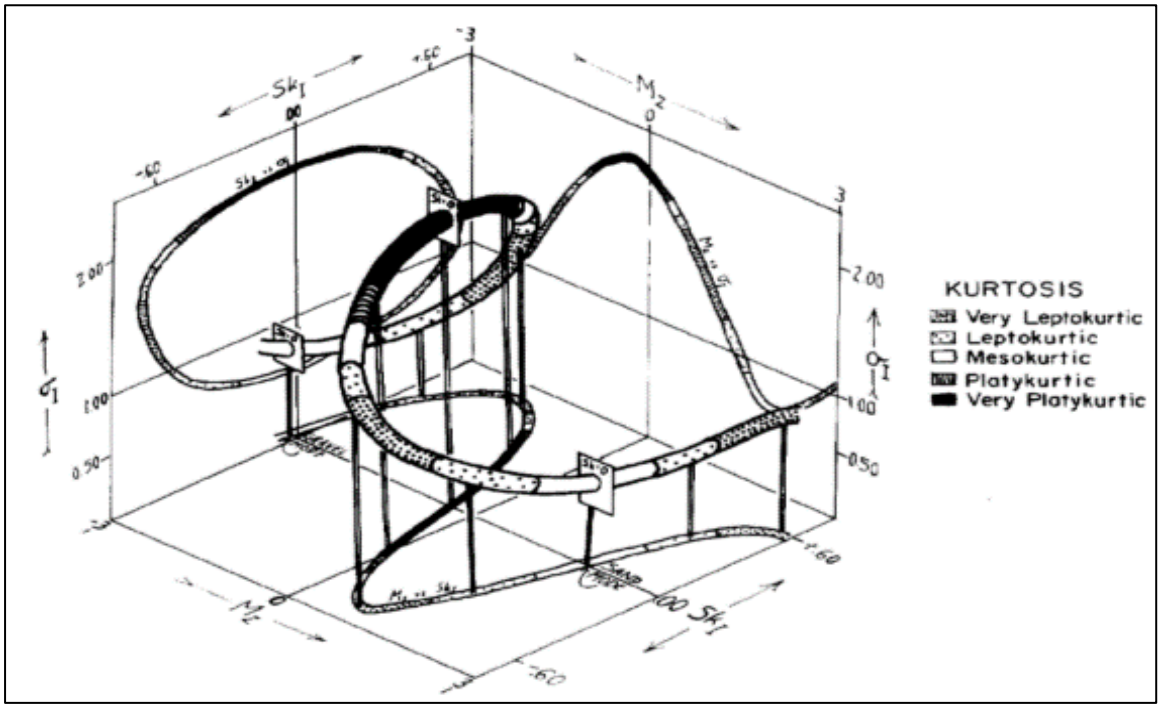

Figure 16 Multi-variate relationship established based on the helix form using the parameters: sorting, mean, skewness and kurtosis.

3.4 Hydrodynamic influence

3.4.1 Wave refraction and diffraction

Because the coastal zone is usually made up of bays, beaches and headlands, the depth of water around a coast varies and as an offshore wave approaches the coast, its propagation is modified due to friction from the seabed, disrupting the motion of waves (Reeve, et al., 2018). The approaching waves get refracted with energy focussed around headlands but reduced as the wave paths around bays diverge or spread out. Waves then tend to approach coastline parallel to it, and shoals with reducing water depth until the threshold of wave steepness is reached. Wave energy is dissipated by seabed friction and as wave breaking finally takes place, the sediments are deposited on the nearshore bars or/and foreshore beach. Shoaling and breaking waves generate larger sediment transport rates than tidal currents (Kana & Ward, 1980) and is therefore one of the key aspects to be looked into in this study.

It is common for refraction and diffraction to occur together. Waves traveling over irregular bathymetry may create a region where wave rays cross, spreading wave energy away from regions of large wave height (Reeve, et al., 2018). Diffraction can also occur around coastal structures such as offshore breakwaters or islands. These elements result in wave spreading as its energy is radiated normal to the direction of wave propagation into the lee of an island or breakwater. At times, superposition of the waves can occur as the diffracted waves cross path through each other. Therefore, a change in configuration of bottom contours will affect the wave period, direction of approach and wave height. Using offshore waves for analysis of the inshore wave parameters would therefore need to account for these effects.

Swells coming from the south-west which coincides with the longest fetch would arrive at Durlston Head, get diffracted and refracted before entering the bay (NFDC, 2017). Because the solution of the Laplace equation (Equation 3.11) for diffraction is highly complex and beyond the scope of this study, furthermore there are no breakwater or man-made islands in the vicinity, this study would focus on refraction and shoaling processes.

Mild slope equation (Berkhoff, 1972): $\frac{\partial}{\partial x}\left(cC_g\frac{\partial \phi}{\partial x}\right)+\frac{\partial}{\partial y}\left(cC_g\frac{\partial \phi}{\partial y}\right)+\omega^2\frac{C_g}{c}\phi=0$ (3.11)

3.4.2 Hydrodynamic interactions with the seabed

In the previous section of refraction and shoaling, it was assumed that there is no loss of energy as waves are transmitted inshore. In reality, at shallow and transitional water depths, the water particle movements induced by surface waves have a strong effect in the entire water column from the surface to the bottom of the sea through seabed friction. Wave energy dissipation can be estimated using the linear wave theory in an analogous way to open channel flow frictional relationships. The flow in this region is induced by surface waves and currents, where the bottom wave boundary layer

is very small (a few millimetres or centimetres) at the seabed controlled by friction due to the bottom roughness. Since the wave velocity shear is much larger than that of current boundary layers, the wave friction factor is expected to be many times larger. As such, the wave boundary layer flow is the controlling factor on the bottom shear stress can in turn brings about sediment transport (Reeve, et al., 2018). Hence, it is of interest to review also, in our case, the influence of the bottom shear stresses on sediment grain parameters.

The wave-induced bed shear stress τ_b, is found using

$$\tau_b = \frac{1}{2} f_w \rho u_b^2 \quad (3.12)$$

Where wave friction factor $f_w = 1.39 \frac{A_w}{z_o}^{-0.52}$ (Soulsby, 1997) (3.13)

Semi-orbital wave excursion $A_w = \frac{u_w T}{2\pi}$ (3.14)

Bed roughness $z_o = \frac{k_s}{30}$ (3.15)

Nikuradze roughness $k_s = 2.5 D_{50}$ (3.16)

and maximum near bed orbital velocity $u_b = \frac{\pi H}{T \sinh \frac{2\pi d}{L}}$ (Komar, 1976) (3.17)

The critical bottom velocity (u_{cr}) for the initiation of sediment motion under waves was given by Soulsby (1997):

$$u_{cr} = (1.09 g\ (s-1))^{4/7} {D_{50}}^{3/7} T^{1/7} \text{ (Soulsby, 1997)} \quad (3.18)$$

3.5 Mechanism of sediment transport and sorting

Current-induced transport is associated with mean currents such as tide- and wind-driven currents carrying sediments in the direction of the main flow, while wave-related transport processes are due to oscillating and mean currents generated in the wave boundary layer by high-frequency waves (Van Rijn, 1997). Sorting of beach materials occurs either parallel with or perpendicular to the coastline, and varies with depth. It may be observed over various spatial and temporal scales: from a short span of beach in terms of cusps to alongshore grading over kilometres length of foreshore beach; from each tidal cycle to seasonal changes.

Sediments are sorted and redistributed by hydrodynamic regime when there is a non-uniformity of sediment sizes along the cross-shore section (Celikoglu, et al., 2006). Part of the cross-shore sorting of sediment is due to the orbital motions under waves they propagate into shallow water region. Waves become more asymmetrical in shape as they shoal, and velocity under the wave crest that is directed onshore is higher but shorter period than the trough that is directed offshore (Komar, 1976).

This results in finer sediments to be transported offshore and coarser sediment onshore (Cornish, 1898). In the surf zone, waves breaking initiated the near surface onshore directed flow and a strong undertow which promotes the migration of suspended sediment landwards and bedload seawards (Reeve, et al., 2018). Crossshore sorting and transport also depend on the wave intensity. If the energy of the oncoming waves is high, the onrush of water can transport both fine and coarse sediments landwards. The backrush is slow and transport smaller size sediments seawards which eventually deposit on the offshore bar. On the other hand, waves of lower energy levels can only move the finer sediment landwards but its backrush could transport the finest sediment in the offshore direction (Celikoglu, et al., 2006).

On sandy beaches, sediment reduces in size from backshore to foreshore due to decreasing swash intensity and the largest variation of sediment sizes occur when the energy dissipation is the highest (Komar, 1998). However, if beaches are composed of coarse sediments like gravel, high beach permeability due to high porosity between particles leads to the asymmetry of swash. The strong uprush pushes the gravel onshore to form berms while displacing the finer materials downslope with each successive wave (Horn, et al., 2003). Transverse sorting on a mixed beach is more complex due to the broad mixture of sediments which influence beach permeability and energy dissipation by reflection. Mixed beaches can reflect more energy than a sandy beach due to a steeper gradient. Although, the slope of mixed beach is gentler than gravel beach, this reduction in reflection may be offset by the sediment grading and composition which influence permeability. A mixed beach will reflect more energy than a gravel beach due to less energy dissipation through infiltration (Mason, et al., 1997).

For longshore sorting, the angle of wave approach and longshore current become relevant. When an oblique wave approaches the shore and breaking occurs in the surf zone, longshore currents are generated and mobilised the finer sand grains from updrift to downdrift section. This develops an armouring effect as the coarser materials are retained in the updrift section (Celikoglu, et al., 2004). In cases where alternating waves approach the coast, the stronger waves will mobilise more materials in that direction and the coarser sediments displaced may not return when the weaker waves move back the finer materials (Bird, 1984). This causes the alongshore sorting until the motion is disrupted by headland or breakwater. The most favourable condition for longshore drifting is when the wave approaches the shoreline at an angle of 45^{o} (Gourlay & Apelt, 1978). Longshore sorting of gravel beach is different from sand beaches due to the beach slope. Plunging breakers occur in steeper gradient and surf zone tends to be narrower in this environment. Grading is usually limited to the surface and within the swash zone.

3.6 Morphodynamic states of beaches and nearshore zone

Hydrodynamic processes and the relative contributions of different mechanisms to sediment transport and morphological change differ differently depending on the beach state. Beach states are broadly classified according to the ability of the slope of the shore zone in dissipating or reflecting the wave energy (Figure 17). This led to the definition of reflective, dissipative or intermediate states (Wright & Short, 1984).

Steeply sloping beaches are exposed to relatively small waves and are typically reflective with an almost-absent surf zone, other than beach cusps. Whereas, sandy beaches which are exposed to larger waves are typically dissipative and have a wide surf zone. Intermediate beaches are the transitions between these two states and thus contain both dissipative and reflective elements. The morphological beach state can be determined by a non-dimensional sediment fall velocity (Gourlay, 1968; Dean, 1973), and is also known as the Dean's parameter.

$$\Omega = \frac{H_b}{(w_s T)} \tag{3.19}$$

Where H_b is breaker height (m), w_s is sediment fall velocity (m/s) and T is wave period (s).

Dissipative beaches are associated with $\Omega > 6$, while reflective beaches occur when $\Omega < 1$ and intermediate state ranges from 1 to 6.

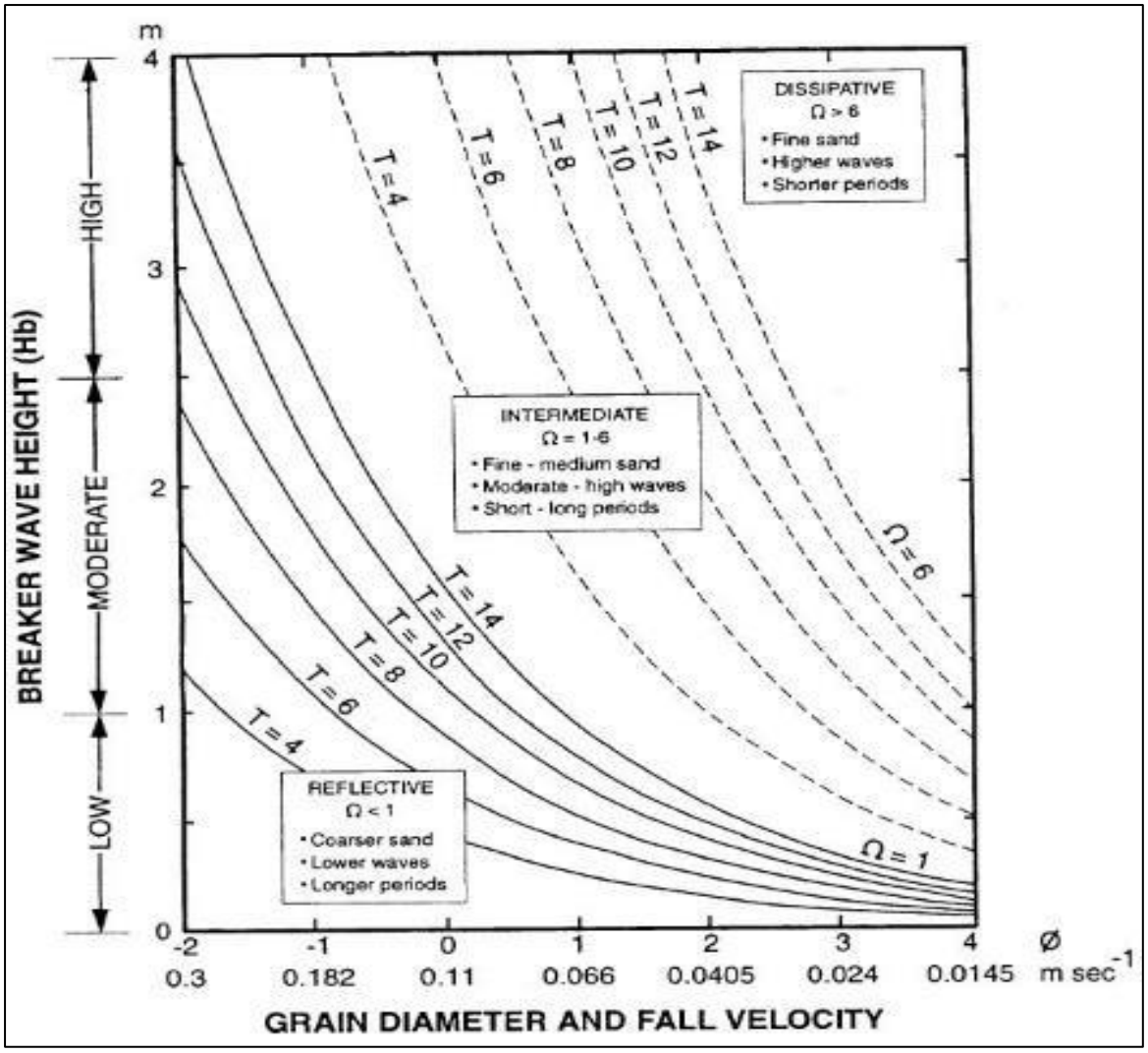

Figure 17 Diagram to determine whether a beach is reflective, dissipative, or intermediate on the basis of breaker height (m), wave period (s), and fall velocity (m/s) or grain diameter (Φ) of the beach particles (Gourlay, 1968). Reflective beaches (for which the dimensionless fall velocity (Ω<1) lie below the solid line for a given wave period, dissipative beaches (Ω>6) lie above the dashed lines for a given wave period, and intermediate beaches (Ω = 1 to 6) lie between the two lines.

4.0 Methodology

The aim and objectives revolve around three questions: i) How have the Poole Bay frontage changed in terms of sediment grain size and sorting in the recent years? And, ii) What is the role of hydrodynamic agents contributing to this transformation? iii) How have beach nourishment works alter the beach sedimentology? It is recognised that there has been vast research conducted previously in the area coupled with annual beach monitoring surveys. The beach is modified (to a certain extent) during and after every beach nourishment program, therefore the trend in the sedimentological transformation is of interest. The last beach nourishment took place in 2015/2016, it is thus timely and advantageous to revisit and update the analysis of sediment characteristics. The first question requires the spatial examination of the sediment sampling data and how the variables have changed over time. The second question requires, to first analyse the coastal flow conditions around the Poole Bay, followed by inspect whether a trend co-exists between the forcing and the sediment parameters. To address the final question, a trace-back on which part of the beach has been nourished, the fill characteristics and associate with the beach condition before and after nourishment.

4.1 Particle size distribution (PSD)

4.1.1 Sediment sampling surveys

The study examined the PSD data from 2005 to 2016 that were supplied by Channel Coastal Observatory (CCO) and Bournemouth, Christchurch and Poole (BCP) Council. Since 2004, CCO has been the organisation engaged to implement the sediment sampling surveys for the Strategic Regional Beach Monitoring Programme (SRBMP) and this is beneficial as sampling approach and processing techniques have been maintained and kept consistent.

The survey occurs typically on an annual interval, but were missed in 2007 and 2012. The dates of survey are recorded in Table 4. Each sampling was undertaken at three locations, approximately 300 m offshore on the bar (OS), Mean Low Water (MLW) and Mean High Water (MHW) along 8 profiles in Bournemouth (between Alum Chine and Hengistbury Head). An ad-hoc sampling exercise was conducted by British Petroleum in 2013 and 2014 along Poole beaches with sediment samples taken along 4 profiles at offshore, MLW and MHW positions.

Table 4 Sediment sampling survey locations and dates

Survey No.	Beach Frontage	Date of Survey
1	Bournemouth	20 Dec 2005
2	Bournemouth	20 Aug 2006
3	Bournemouth	28 Aug 2008
4	Bournemouth	24 Jul 2009
5	Bournemouth	7 Jul 2010
6	Bournemouth	31 Aug 2011
7	Bournemouth & Poole	3 Oct 2013 & 10 Oct 2013
8	Bournemouth & Poole	2 Oct 2014
9	Bournemouth	27 Nov 2015
10	Bournemouth	20 Dec 2016 & 9 Jan 2017

Surveys took place at mean low water springs and when the weather and sea state were calm. Before the completion of BIS 4 (which occurred between 2005 to 2010), the sediment samplings took the onshore samples (MHW and MLW) at fixed locations. But after a review on the sampling approach, it was decided to sample at High Water and Low Water positions on the day of sampling, in preference to fixed locations. Based on a cursory examination, the positions do not differ much, as such the sampling locations used in this study shall take on from the 2005 survey.

For notation purpose, the sampling locations are renamed from the original dataset as below. The prefix e.g. 3HW indicates the sampling location at Profile 3 near Bournemouth Beach at High Water (the coordinates of which are listed in the table below). The number increases from west to east. The prefix 'BP' corresponded to the sediment sampling at Poole beaches and distinguished from the Bournemouth surveys. The locations of the 36 sample sites are given in Table 5 and shown in Figures 18 and 19.

Table 5 Coordinates of sampling locations (in British National Grid reference) along Poole Bay. 3 sampling locations are set out namely, A – nearshore, LW – Low Water and HW – High Water.

Bournemouth			Poole		
Sample Number	Easting	Northing	Sample Number	Easting	Northing
1OS	407432	89775	BP04OS	406699	89387
1LW	407318	90070	BP04LW	406533	89552
1HW	407305	90093	BP04HW	406523	89588
2OS	408665	90319	BP09OS	405702	88610
2LW	408487	90552	BP09LW	405555	88768
2HW	408480	90580	BP09HW	405533	88808
3OS	410350	90719	BP14OS	405204	88063
3LW	410320	90999	BP14LW	405029	88197
3HS	410315	91028	BP14HW	404995	88228
4OS	411757	90877	BP22OS	404600	87286
4LW	411831	91188	BP22LW	404407	87426
4HW	411827	91215	BP22HW	404392	87440
5OS	413210	90909			
5LW	413191	91212			
5HW	413191	91253			
6OS	414657	90697			
6LW	414738	91055			
6HW	414744	91079			
7OS	416200	90580			
7LW	416235	90796			
7HW	416239	90817			
8OS	417591	90150			
8LW	417635	90347			
8HW	417642	90373			

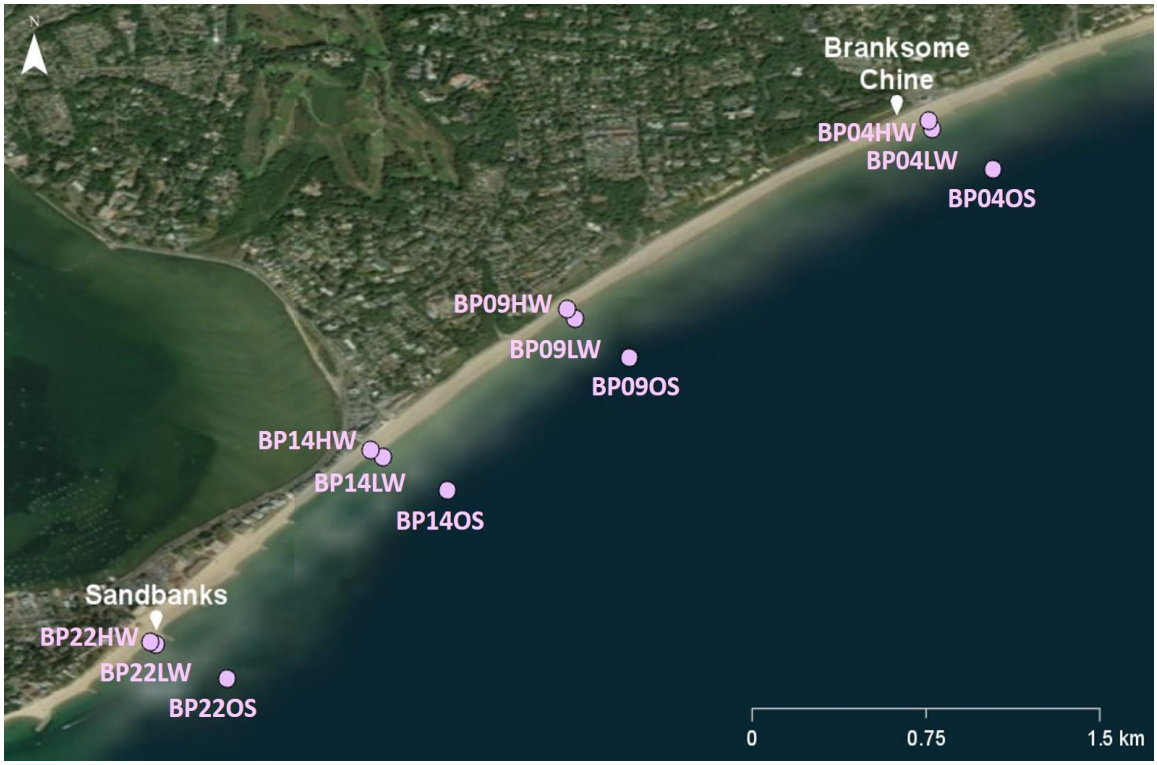

Figure 18 Ad-hoc sampling conducted across four profiles along Poole beaches in 2013 & 2014 (Source: ArcGIS ESRI)

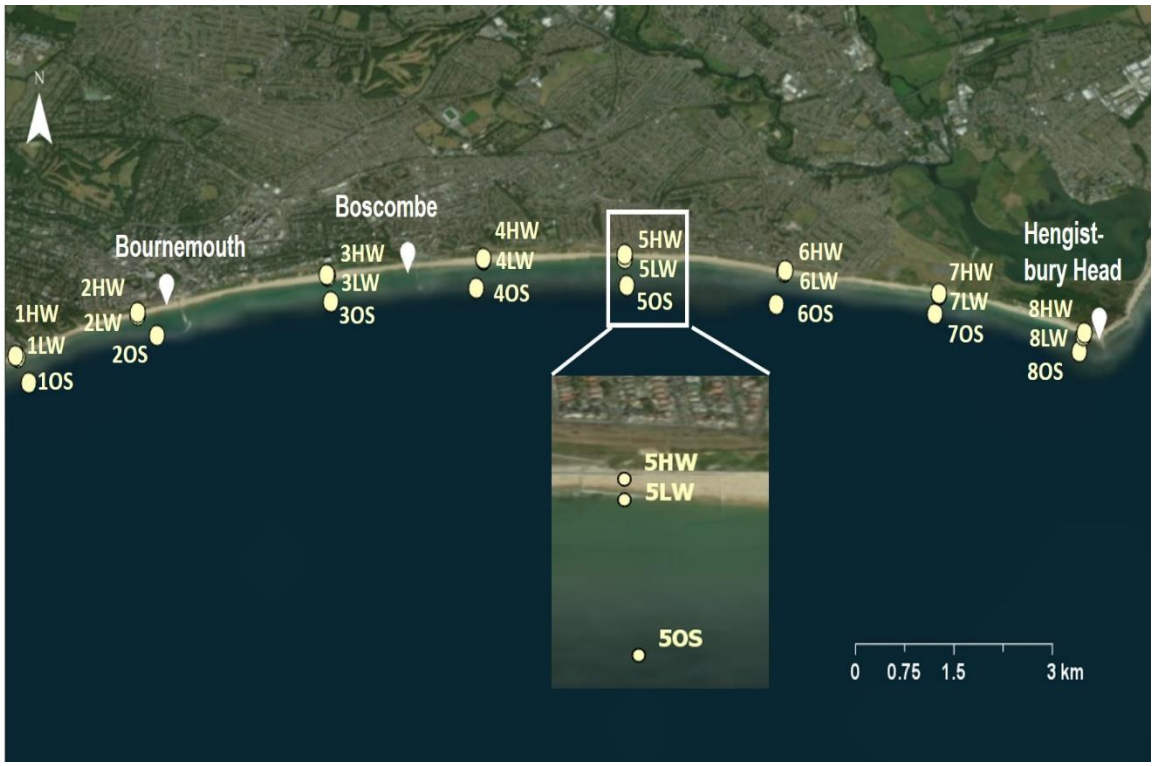

Figure 19 Annual sampling conducted at offshore (OS), High Water (HW) and Low Water (LW) positions across eight profiles along Bournemouth beaches (Source: ArcGIS ESRI)

The sampling procedure was performed using a Shipek Grab from a small vessel for offshore sampling. For onshore sampling at Low Water and High Water, samples were taken using hand-held grab pan by the surveyor. Samples of particles between 50 to 1000g dry weight were taken

and placed in labelled plastic bags for subsequent laboratory processing. The onshore sampling could be slightly subjective from the surveyor's selection of the sediments from within an area of $1m^2$ that was deemed representative of the proportions of sand and gravels present. This can lead to bias and ambiguities in the sediment distribution results.

4.1.2 Sampling recovery

The study covers the period from 2005 to 2016 of which, a total of 279 out of the possible 288 samples were retrieved. This is considered as a very high sample recovery of 97 %. Most of the missing samples came from Profile 8OS, near Hengistbury Head. Due to shallow bathymetry and exposed headland, collection of samples was challenging and samples were often returned without any sediments. The recovery rate for this site is approximately 27%, hence the reliability of data from this profile is compromised and interpretation of the data need to be taken with caution.

4.1.3 Samples processing and analysis

Each sample is washed and dried at 100ºC for at least 48 hours. Samples were passed through a sieve with 2mm apertures to separate the gravel and sand fractions. In accordance to BS 1377, where gravel is present (grain sizes greater than 2mm), a large volume was required and the whole sample is processed in the sieve nest while the sand fraction is subdivided to a reduced size of 100g of sandy material to prevent sieve clogging or multiple sieving which adds time and cost. The samples are vibrated for 10 minutes on a mechanical shaker, using a nest of sieves sizes that range from 0.063 mm to 64 mm in 0.5φ increments (CCO, 2017).

4.1.4 Calculation of graphic moments of PSD

PSD characteristics are determined based upon the sieve weights using a computer program, GRADISTAT, developed by Blott and Pye (2001). It provides rapid and automated calculation of grain size statistics by both method of moments and graphical parameters. The program, written in Microsoft Visual Basic is integrated with Microsoft Excel spreadsheet to generate tables and graphs as outputs. The sample statistics computed are mean, mode(s), sorting, skewness, kurtosis and a range of cumulative percentile values (e.g. D_{25}, D_{50}, D_{75} and D_{90}). The textural characteristics are based upon the formulae of Folk & Ward (1957) as shown in equations 3.2 to 3.5. The program outputted these values for every sample, as well as calculating the proportions of sand and gravel as a percentage, and gives a physical description of the textural class (e.g. Slightly gravelly sand) (Folk, 1954) as illustrated in Figure 20.

SAMPLE STATISTICS

SAMPLE IDENTITY: **1LW (2016)** ANALYST & DATE: GO, 4 Jun 2019

SAMPLE TYPE: Bimodal, Poorly Sorted TEXTURAL GROUP: Slightly Gravelly Sand

SEDIMENT NAME: Slightly Very Fine Gravelly Fine Sand

	μm	ϕ
MODE 1:	215.0	2.237
MODE 2:	605.0	0.747
MODE 3:		
D_{10}:	155.1	-0.179
MEDIAN or D_{50}:	352.4	1.505
D_{90}:	1132.2	2.689
(D_{90} / D_{10}):	7.301	-15.009
(D_{90} - D_{10}):	977.2	2.868
(D_{75} / D_{25}):	3.069	3.576
(D_{75} - D_{25}):	436.2	1.618

GRAIN SIZE DISTRIBUTION

GRAVEL: 4.6%	COARSE SAND: 25.2%
SAND: 95.4%	MEDIUM SAND: 28.4%
MUD: 0.0%	FINE SAND: 33.4%
	V FINE SAND: 1.3%
V COARSE GRAVEL: 0.0%	V COARSE SILT: 0.0%
COARSE GRAVEL: 0.0%	COARSE SILT: 0.0%
MEDIUM GRAVEL: 1.1%	MEDIUM SILT: 0.0%
FINE GRAVEL: 1.3%	FINE SILT: 0.0%
V FINE GRAVEL: 2.2%	V FINE SILT: 0.0%
V COARSE SAND: 7.2%	CLAY: 0.0%

	METHOD OF MOMENTS			FOLK & WARD METHOD		
	Arithmetic	Geometric	Logarithmic	Geometric	Logarithmic	Description
	μm	μm	ϕ	μm	ϕ	
MEAN ($\bar{x}$):	707.4	404.6	1.305	377.9	1.404	Medium Sand
SORTING (σ):	1424.3	2.355	1.236	2.192	1.132	Poorly Sorted
SKEWNESS (Sk):	6.391	1.211	-1.211	0.206	-0.206	Coarse Skewed
KURTOSIS (K):	50.18	5.161	5.161	0.957	0.957	Mesokurtic

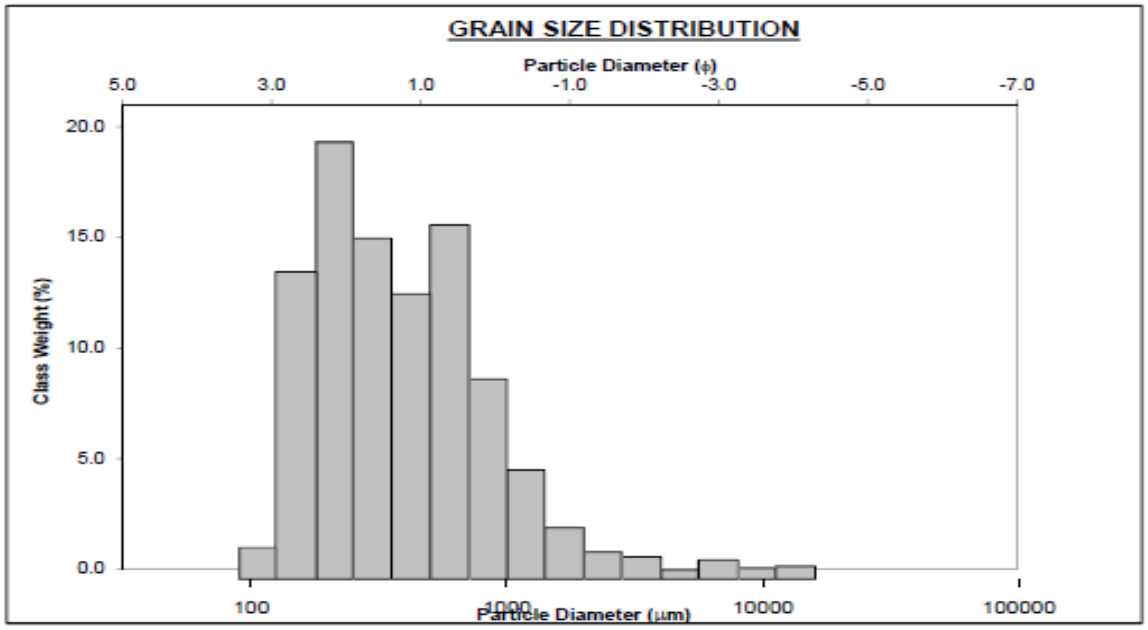

Figure 20 Example of sediment statistics processed using Gradistat program

Past studies have compared statistics derived by moments and graphical methods, as well as geometric and logarithmic statistics. Geometric or logarithmic scales are commonly used in characterizing sediments (Blott & Pye , 2001). The geometric mean and sorting values for both methods are related to each other by simple logarithmic relationships (Equation 3.1). The inverse relationship between the geometric and logarithmic skewness parameters is because the metric and phi scales function in opposite directions and geometric and logarithmic kurtosis are comparable in values. The key difference of the two methods lies on the emphasis placed on different part of the grain size distribution. Folk & Ward's graphical method focus on the middle point of the grain size curve and less on the tails, keeping the upper and lower limits at 95 and 5 percentiles respectively. While both methods produce comparable results for mean grain size and sorting values, the

graphical technique provides more robust basis for routine comparison of compositionally variable sediments, as such, the Folk & Ward method is adopted for this study.

4.2 Nearshore hydrodynamics

The prediction of the evolution of the coastal environment requires detailed information about inshore wave conditions. This becomes possible only through the transformation of offshore sea states, particularly when information from global forecasting models such as satellite or offshore buoy measurements are readily available, but usually at a distance of many kilometres away from the coast. In many instances, the inshore wave characteristics of the site of interest are determined by the use of computationally intensive, highly spatially resolved numerical wave models from offshore wave climatology. Nevertheless, developing such a model can be quite time consuming and require high performance computing capabilities.

For the study of the morphological changes of the coastline in Poole Bay, the main challenge is obtaining representative nearshore waves, particularly on its western end as this is sheltered by the headlands out to Durlston Point. A simple inshore wave approximation is devised to simulate the refracted/diffracted waves entering the bay. The approach to treat this problem is to apply shallow-water wave models to transform offshore wave directional spectra to inshore spectra, exploiting the available geographical information (bathymetry, coastline) which will be elaborated in Section 4.4.

4.3 Data compilation

4.3.1 Wave data

As Poole Bay is a wave-dominated environment (NFDC, 2017), the emphasis is on the assessment of wave climate. To quantify this forcing at a regional scale, some approximation or averaging of the causal processes is required. Specifically, waves in any particular part of the ocean at any particular time are not all the same and are made up of fluctuating amplitude and period (Dyer, 1986). The characteristics of this variable sea can be described by measuring the wave height, period and direction. The wave parameters used in this study are i) Significant wave height (Hs): the mean wave height of the highest third of the waves in an interval; ii) Maximum peak period (T): period of the peak of the wave energy spectrum and iii) Wave direction (θ): angle at which the wave approaches the shoreline from True North.

A Directional Waverider MkIII wave buoy was deployed offshore from Hengistbury Head (50°38'.02N, 001°43'.13W) in 28 m water depth to collect data since 17 December 2003. The offshore wave information included the significant wave height, peak wave period, wave direction, sea temperature which were downloaded from CEFAS Wavenet (https://www.cefas.co.uk/cefas-data-hub/wavenet/). Although data collection for this buoy commenced in 2003, the assessment

period for this research was governed by the particle size distribution data which was made available to the author from 2005 to 2016, hereby denoted as the study period.

There is another existing wave buoy, Datawell Directional Waverider Buoy located in 10.4 m water depth near Boscombe Pier (50°42'.68N, 001°50'.38W) provided by Channel Coastal Observatory (CCO). Data collection commenced since 11 July 2003. Wave data for the study period were downloaded from the database (http://www.channelcoast.org/), which include the significant wave height, peak wave period and wave direction measured at every half-hourly interval. The locations of the wave buoys can be referred to Figure 21.

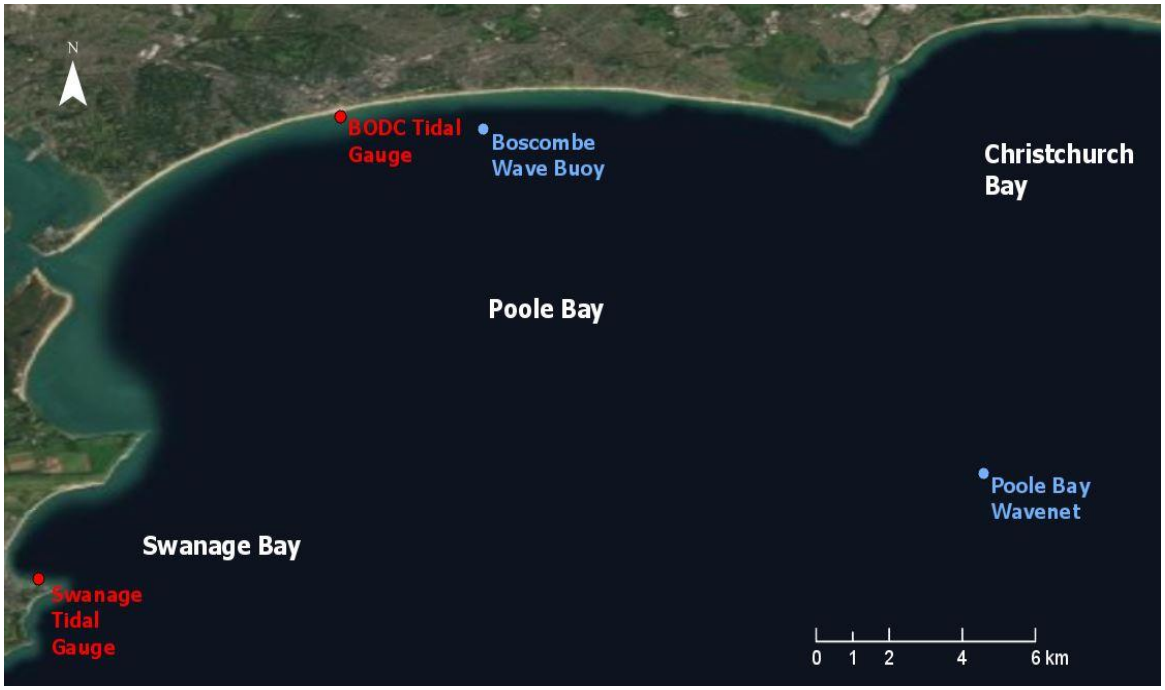

Figure 21 Locations of Boscombe wave buoy, Poole Bay Wavenet, Bournemouth and Swanage tidal gauges (Source: ArcGIS ESRI)

4.3.2 Tidal data

Tidal data were taken from CCO 's Swanage Pier Wave radar (50°36.56'N, 001°56.95'W). Records are measured at a 10-minute frequency and extended from 2008 to 2016 (Figure 21). The information provides tidal levels both in Ordnance and Chart Datums. To cover the entire study period (*i.e.* from 2005 to 2016), processed tidal data which have been quality controlled from any transmission problems that will be blanked out accordingly, are separately obtained from Bournemouth tide gauge (50°42.51'N, 001°52.29'W) of British Oceanographic Data Centre (BODC) between 2005 and 2008. The information included the measured (with reference to Chart Datum) and residual values at 15-minute interval.

4.3.3 Bathymetric data

Bathymetric surveys were retrieved from ADMIRALTY Marine Data Portal (https://data.admiralty.co.uk/portal/apps/sites/#/marine-data-portal) which has been accredited by the Marine Environmental Data and Information as the National Data Archive Centre for this information. The bathymetric surveys were conducted in blocks from 26 August 2011 to 6 April 2012. Figure 22 shows the bathymetric survey blocks of No. 7, 11, 12 and 14 that made up the region. As there are missing bathymetric data at the entrance of Poole Harbour, the data are obtained from other sources e.g. navigational chart. The bathymetric data are used for various purposes, in the nearshore forcing parameterisation as well as the analysis of bedform dynamics for sediment transport. ArcGIS Pro, a desktop GIS application from ESRI is used to explore, visualize and extract the bathymetric data (Figure 23).

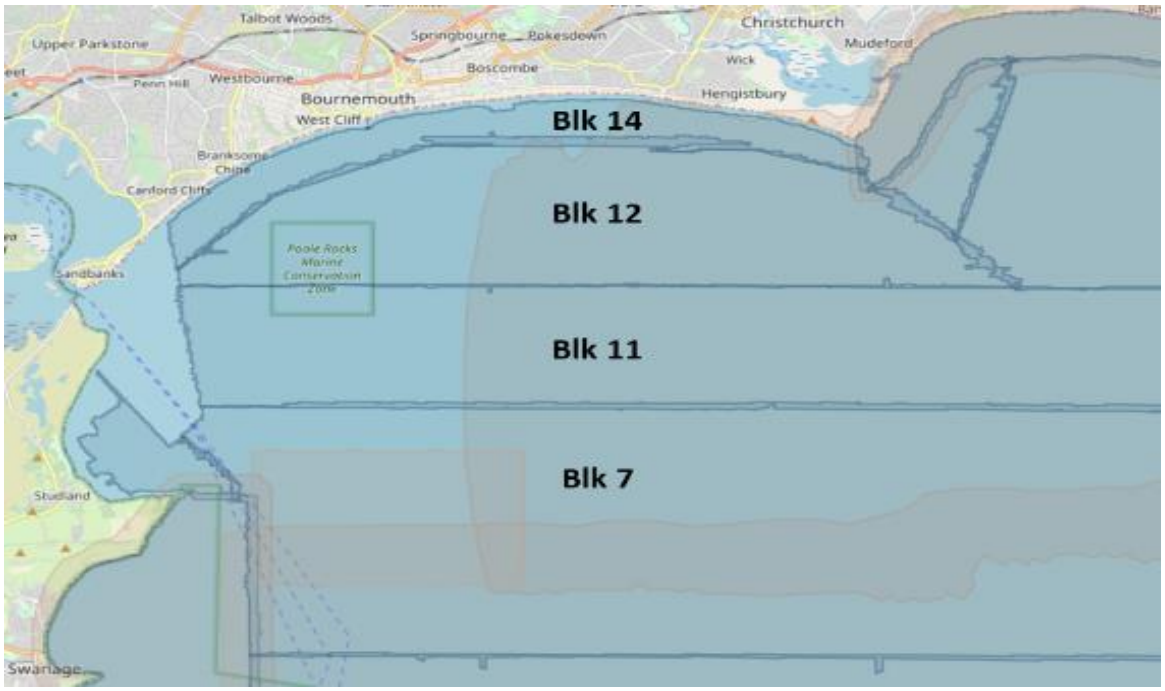

Figure 22 Bathymetry survey conducted in block segments in 2012 (Source: Admiralty Maritime Data Solutions)

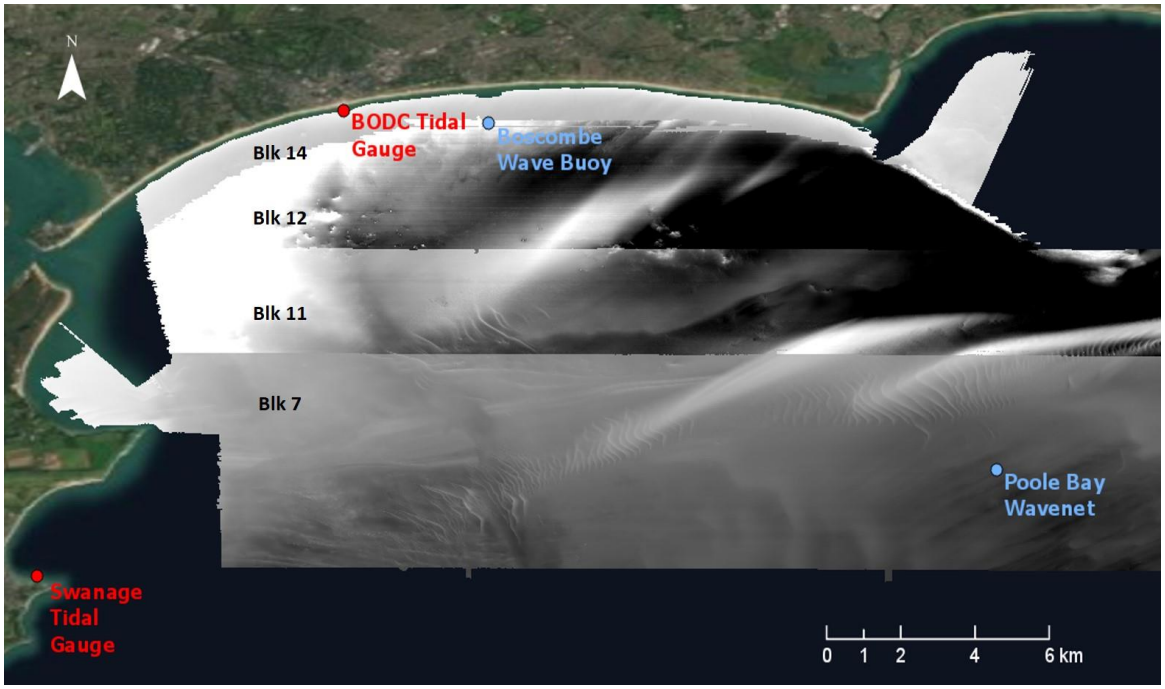

Figure 23 The use of ArcGIS Pro to extract the necessary bathymetric data for processing of bedform and wave dynamics.

4.3.4 Topographic data

Topographic beach profiles were downloaded from CCO for the geometry of onshore beach as inputs definition in the inshore wave approximation. For instance, at profile 431 which is closest to Boscombe Pier, the upper beach slope is estimated to be 1:20 (Figure 24). The profiles are also used to investigate the morphologic change of the coastline in the discussion of beach state analysis in Section 6.

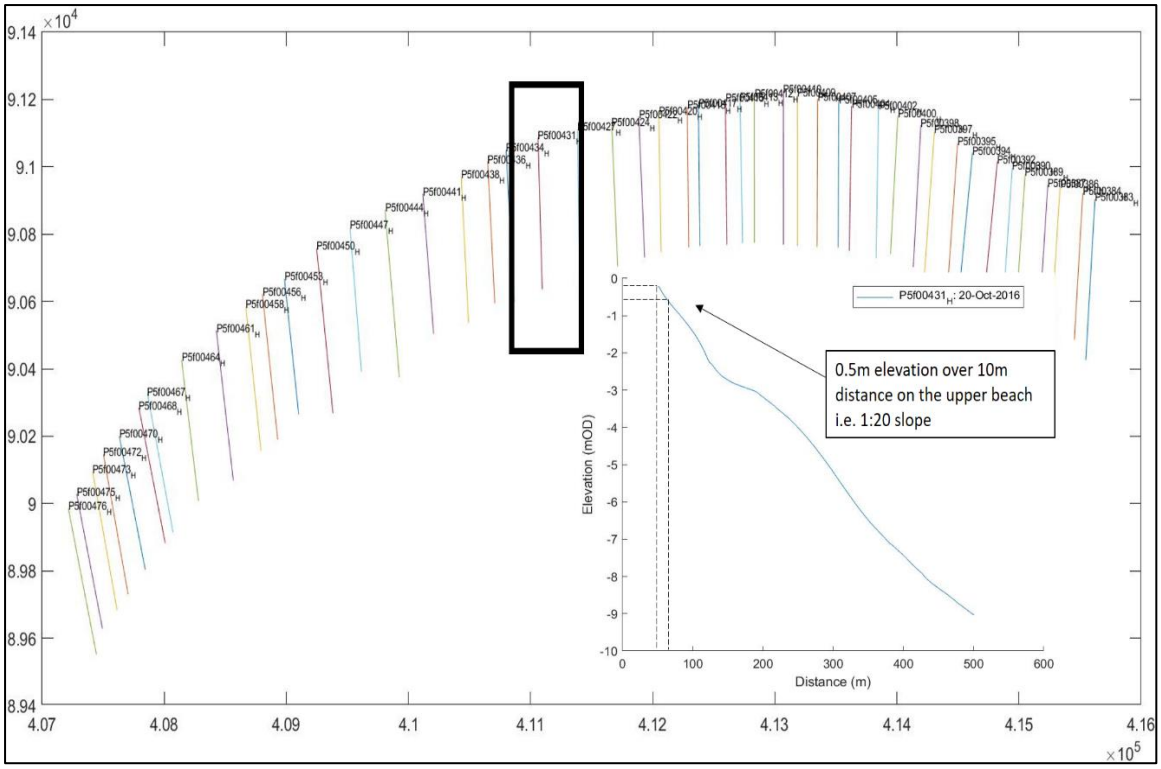

Figure 24 Derivation of beach slope using CoastalTools. Profile 431 has a 1:20 slope at the upper beach.

4.4 Inshore wave approximation

The offshore wave data from Wavenet buoy were first processed using the CoastalTools (https://www.channelcoast.org/ccoresources/coastaltools/). The Coastal Tools is a program written in MATLAB language code and provided as Open Source (Townend, 2016). The software has provision for waves, water levels, beach profiles data set with modelling capability, relating to wave parameters and changes to shoreline/beach volume. Statistical analysis functions within the CoastalTools were employed to generate the mean monthly significant wave height Hs, wave period T, wave angle θ, then collated and plotted in time series and wave rose plots for offshore wave climate.

The nearshore wave model which is based on the principles of linear wave theory, plane bed refraction and shoaling was run to simulate the inshore waves from offshore condition. For each time interval, the model uses the offshore values of wave height, period and direction. Wave refraction and shoaling is computed based on the inshore depth. The output generated a time series of inshore wave heights and wave angles. Wave period is assumed to remain constant. Given that there are available nearshore wave measurements at Boscombe, the Wavenet data were loaded into CoastalTools to create the inshore condition at Boscombe site. Table 6 showed the inputs definition for the model. The model outputs were then compared with the measured nearshore wave buoy data for calibration and adjustment.

Table 6 Site parameters defined for the nearshore wave model at Zone D

Description	Inputs defined	Remarks
Bed level offshore (mOD)	-28	Offshore Wavenet buoy's bed level
Bed level inshore (mOD)	-10.4	Nearshore Waverider buoy's bed level
Angle of shoreline (degTN[1])	75	Angle of contour line at wave buoy location (based on Navigational Chart from www.visitMyHarbour.com)
Friction coefficient, k_f	1	Default value (*i.e.* no frictional attenuation) The lower the k_f means higher frictional forces and greater amount of energy is lost as wave propagates to the coast (Bryant, 1979).
Bed elevation 1km from shore (1:m)	-14	Bathymetry data from Admiralty Maritime Data Solutions
Upper beach slope	20	Topography profiles from CoastalTools
Grain size D_{50} (mm)	3.4	Zone D's LW
Wave breaking model	1	SPM breaking on the slope based on JONSWAP method (Townend, 2016; Reeve, et al., 2018)

[1]degTN refers to degree from True North

4.4.1 Model calibration

Model calibration is essential to ensure the model is robust and reliable. The 2016 wave data were used for calibration. Results for January month are provided in Figures 25 and 26. This is selected for illustration as January is usually stormier than other months and expected to have more fluctuations in the water level. The remaining monthly time series graphs are attached in Appendix A. Figure 25 depicts the modelled and measured wave direction in blue and orange respectively. Most waves received at Boscombe site are from south south-easterly (SSE) to south-westerly (SW) waves (*i.e.* between 140º to 220º). The modelled waves coincided with the measured waves from the easterly direction. However, for SSE to SW wave approaches, the modelled waves were inferior to the measured waves, with the model over-estimating up to 30º at certain intervals.

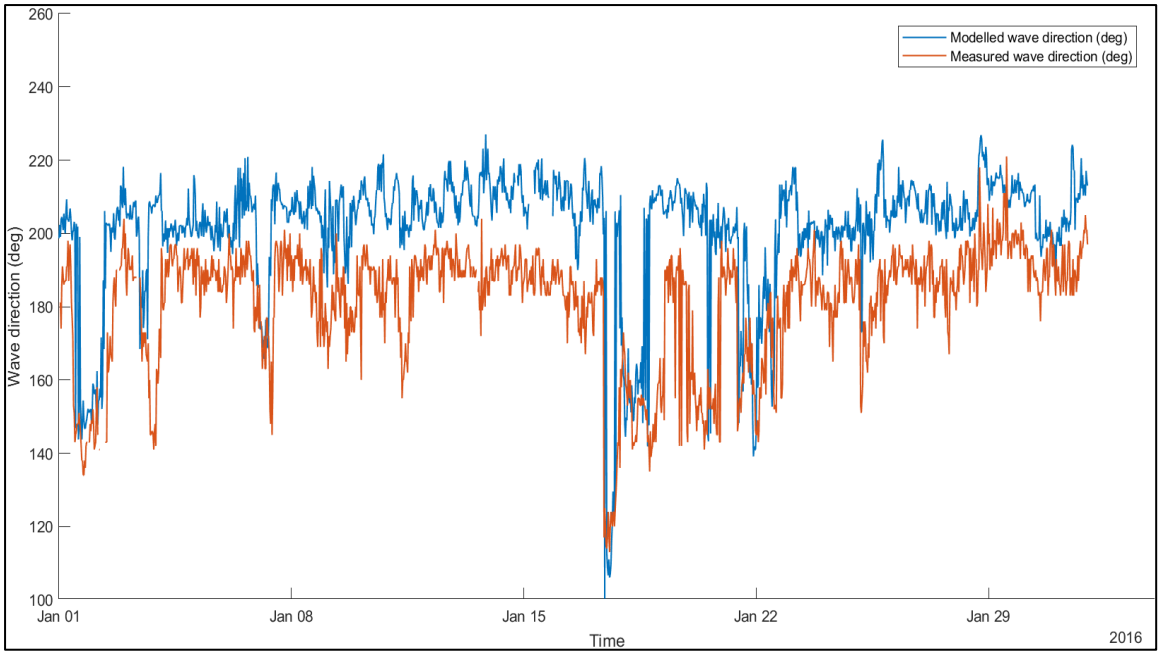

Figure 25 Time series of 2016's modelled (blue) and measured (orange) waves direction. The modelled nearshore waves arriving from SSE and SW directions do not associate well with the measured waves at Boscombe site.

The time series graph for the significant wave height is shown in Figure 26, with the blue curve representing the modelled inshore waves and orange curve as the measured waves at Boscombe. The nearshore wave model lacks performance for it could only capture 3 peaks across January month (circled in black). Table 7 presented the mean monthly measured and modelled Hs for 2016, of which the overall mean percentage deviation was 39%.

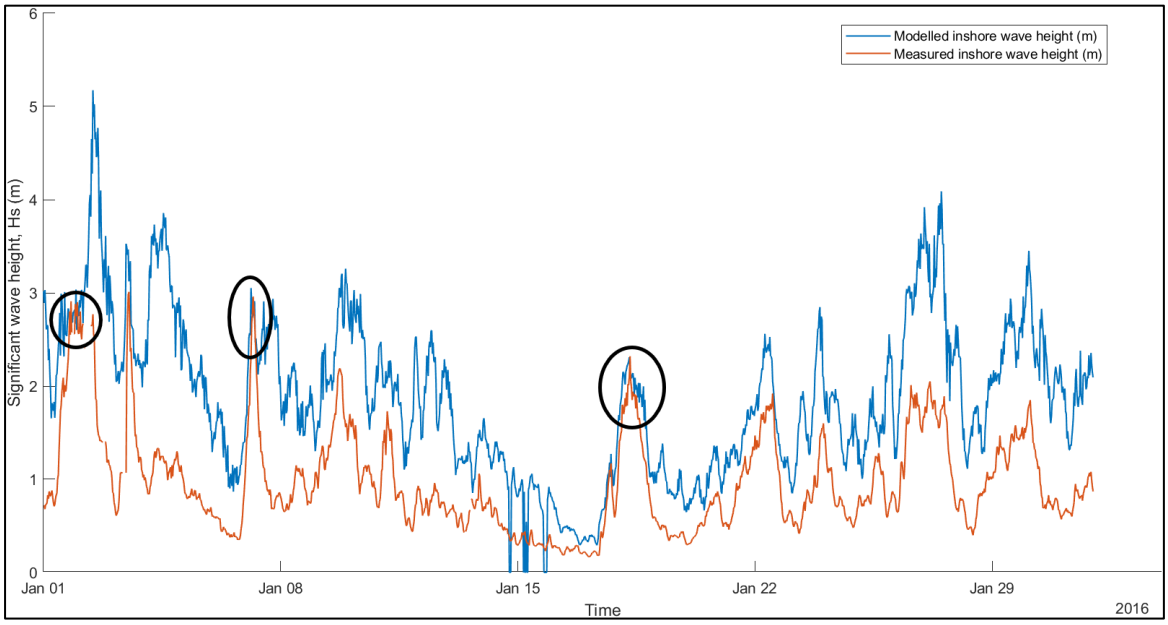

Figure 26 Time series of 2016's modelled (blue) and measured (orange) significant wave height. The modelled nearshore waves captured only 3 clusters/peaks of the measured waves at Boscombe site circled in red.

Table 7 Monthly mean significant wave heights of measured and modelled Hs in 2016 with percentage deviation

2016													
Statistic	All	Jan	Feb	Mar	Apr	May	Jun	Jul	Aug	Sep	Oct	Nov	Dec
Measured Hs (m)	0.54	0.97	0.78	0.55	0.46	0.33	0.37	0.41	0.46	0.49	0.50	0.57	0.58
Modelled Hs (m)	0.88	1.73	1.42	0.98	0.76	0.49	0.57	0.63	0.71	0.76	0.71	0.85	0.99
Difference	39%	44%	45%	44%	40%	32%	34%	35%	35%	36%	30%	34%	42%

The calibration took several iterative rounds of parameters testing with friction coefficient (K_f) and shifting of wave direction to achieve a good match. The optimum model adopted the K_f value of 0.55 (Bryant, 1979; Kurain et al., 1985). and 20º counter-clockwise shift in wave direction. The results of the calibrated model in 2016 are presented in Figure 27. Appendix A provides the monthly time series comparison between the calibrated model and the field data for wave angle and significant wave height. The plots in Figure 27 a) and b) showed that the Hs and θ time series for measured and predicted waves have peaks and clusters in the same pattern. Also, the wave rose diagrams in Figure 27 c) and d) indicated similar direction and magnitude. The dominant waves approach is SSW and wave height ranges from 0.5 to 1.5m.

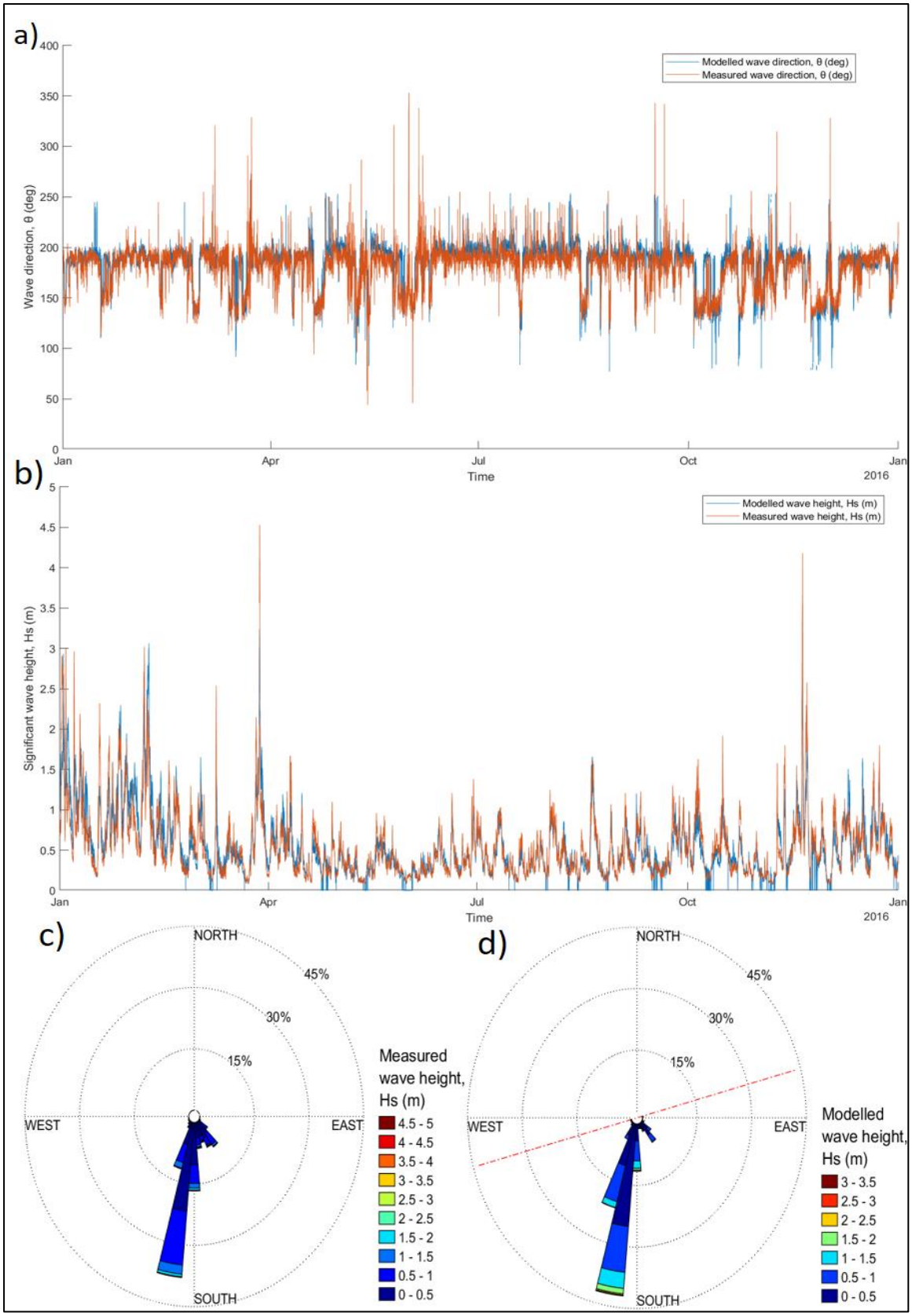

Figure 27 Calibrated results with adjustment to friction coefficient and wave direction: a) Times series plot of modelled and measured waves direction in 2016; b) Times series plot of modelled and measured waves direction in 2016; c) Wave rose plot for measured wave height d) Wave rose for modelled wave height (the dashed red line indicated the shore line angle (to True North) used for the inshore wave calculations)

The percentage deviations of the calibrated and measured wave height and direction in 2016 were found to be 1% and 3% respectively (Table 8). To check if the model also works well for the remaining wave data, Taylor diagram, a statistical tool, is used to conduct a comparative assessment of the annual scenarios (Taylor, 2001). The tool compared three statistics: Pearson correlation coefficient (R^2), normalized root-mean-square and normalised standard deviation. A normalized standard deviation (closer to the red dotted line) indicated a modelled time series that has similar wave amplitude. A correlation coefficient of 1 indicated the modelled time series has the same pattern with the measurements. The ultimate target is to derive a model series as close to the red dotted line and point 0. Refer to Figure 28 a), all annual scenarios except 2005 have a high correlation (>0.8) and normalised standard deviation (close to 1.0) for significant wave height. Whereas for angle of wave approach (Figure 28 b), all except 2005 have good normalised standard deviation although its correlation values are lower, ranging from 0.6 to 0.7. The month of November 2005 has the highest disparity of 56% between the measured and modelled wave Hs. Based on the CCO Annual Wave Report 2005, the buoy was badly damaged prior to the November/December 2005 storms (CCO, 2005). During this period, no data were retrieved and this could be the reason for the large discrepancy. Despite the model performance being the worst for 2005 scenario, on the whole, the statistical results and time series showed good agreement with the observed nearshore waves at Boscombe. The model can still be considered as a decent fit to the observation dataset, and shall be used for the subsequent establishment of inshore waves.

Table 8 Monthly mean significant wave heights and directions of measured and modelled Hs in 2016 after calibration. The annual mean percentage deviation for wave height and wave direction diminished to 1% and 3% respectively after calibration.

2016													
Statistic	All	Jan	Feb	Mar	Apr	May	Jun	Jul	Aug	Sep	Oct	Nov	Dec
Measured Hs (m)	0.54	0.97	0.78	0.55	0.46	0.33	0.37	0.41	0.46	0.49	0.50	0.57	0.58
Modelled Hs (m)	0.54	1.07	0.88	0.60	0.47	0.30	0.36	0.39	0.44	0.48	0.42	0.51	0.61
Difference	1%	9%	11%	9%	2%	-12%	-5%	-6%	-4%	-3%	-17%	-10%	6%
Measured θ (deg)	179	181	182	181	178	175	185	189	184	183	164	169	179
Modelled θ (deg)	185	186	183	183	186	186	193	196	190	192	171	174	182
Difference	3%	3%	1%	1%	4%	6%	4%	3%	3%	4%	4%	3%	2%

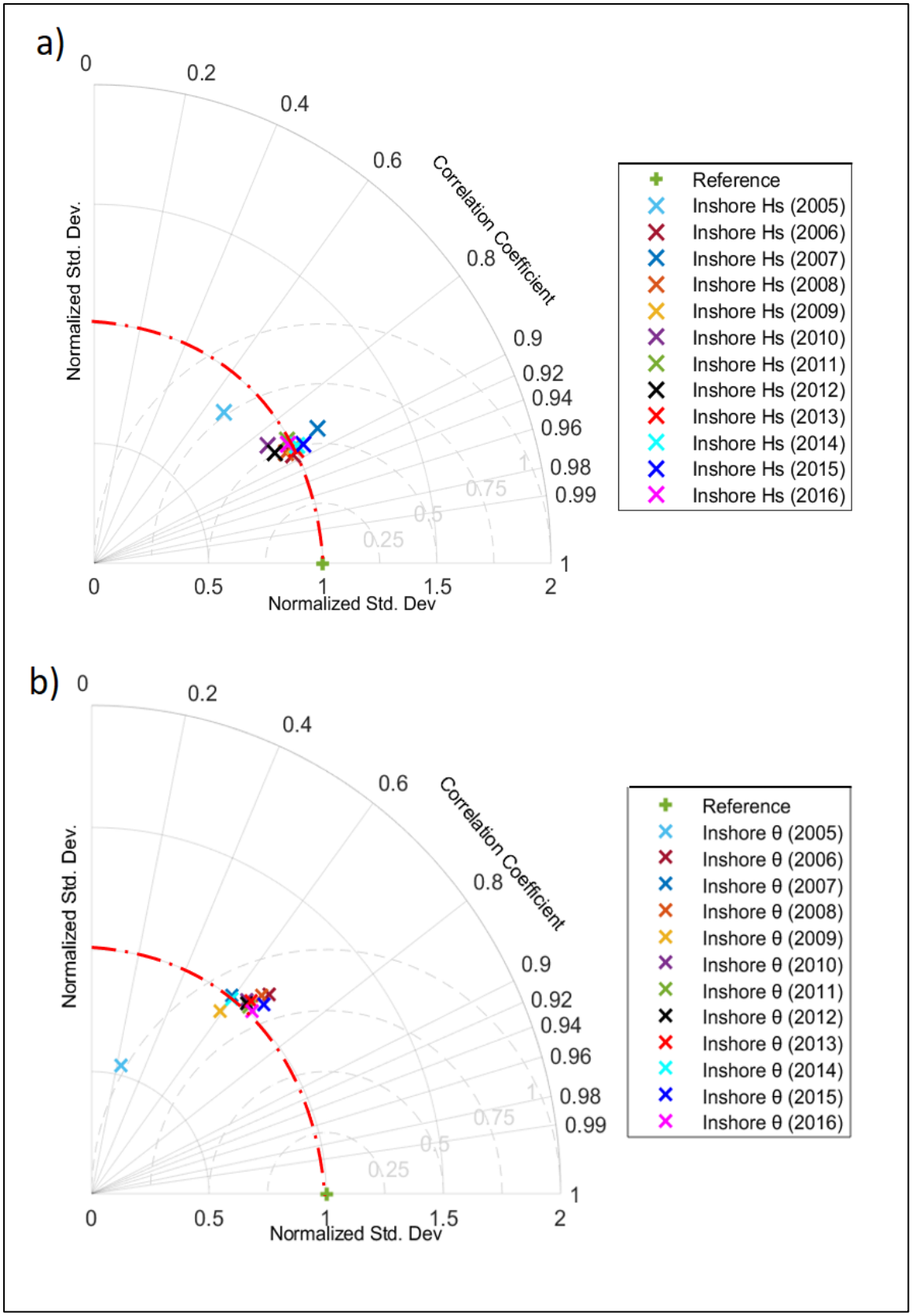

Figure 28 Taylor Diagram was used to compare modelled inshore results with actual wave data from 2005 to 2016. a) For wave height, apart from 2005, all yearly scenarios have a high correlation (>0.8) and normalised standard deviation (close to 1.0) b) In terms of the angle of wave approach, all annual modelled scenarios except 2005 have good normalised standard deviation while the correlation is of lower values ranging from 0.6 to 0.7.

4.4.2 Inshore waves along Poole Bay

The zonation of Poole Bay is on the basis of the shoreline orientation, from Zone A at Sandbanks to Zone I at Hengistbury Head as indicated in Figure 29. The annual mean wave approach and significant wave height from 2005 to 2016 are computed for each zone and the results are elaborated in Section 5.

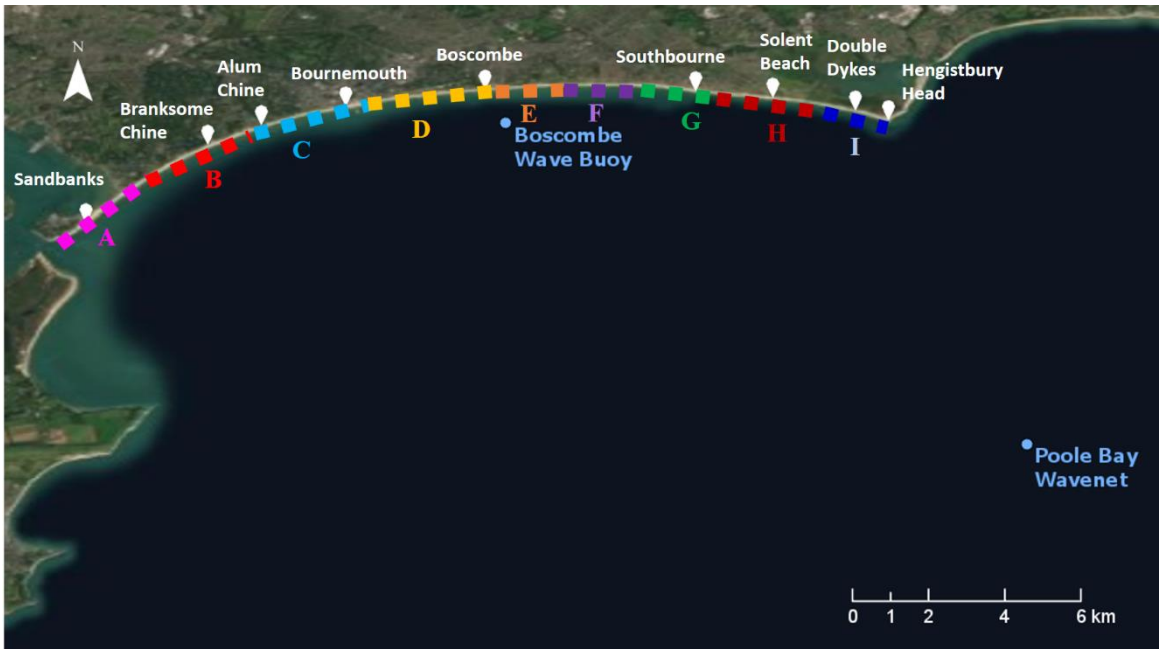

Figure 29 Poole Bay is configured into 9 zones based on the orientation of shoreline to evaluate the inshore wave parameters (Source: ArcGIS ESRI)

4.5 Computation of bed shear stress and beach characterisation

Sedtrans05, a single point sediment transport model conventionally used for continental shelf and estuaries is employed to calculate the effective bed shear stress (Neumeier, et al., 2008). Inputs relating to water depth, sediment type, waves parameters are derived as explained in the previous sections and inserted into the program. The program also computes the boundary layer thickness for combined current-waves conditions. Rightfully, it is necessary to define the combined wave and current shear stress at the bed which constitute to the total sediment transport. But since field measurements on currents are not available and effects of waves are more dominant, only wave conditions are analysed in this study.

Sediment mobility is then determined by a simple empirical approach where maximum bed orbital velocity, u_b must exceed a critical bottom velocity, u_{cr}. (Equations 3.17 and 3.18). Dean's parameter, Ω (Equation 3.19) is also computed to assess the thresholds between various beach morphodynamic states ranging from reflective, through intermediate, to dissipative.

4.6 Statistical analysis

Sediment characteristics information was compiled in a matrix including the mean grain size, median, sorting, and skewness of the distribution. The information on the wave properties comprises significant wave height, peak wave period, wave angle and wave-induced bed shear stress. Data sets extracted from the results of the sediment and wave analyses were combined on a 9-column by 279-row matrix for statistical analysis. Given that there are numerous variables to be considered and a large dataset compiled for the entire coastline and slightly over one-decade duration, it is necessary to deploy a statistical technique capable of discerning patterns, identifying and grouping the key factors.

Principal Components Analysis (PCA) is a multivariate, statistical technique that can be used to examine the data variability. It is frequently applied to environmental datasets such as sediments (Spencer, 2002) and soils (Zhang, 2006) with complex inter-relationships between variables are difficult to visualise. The use of PCA aims to identify a small number of derived variables (known as principal components (PCs)) from a larger number of original variables so that they can be more easily interpreted (Manly, 1997). This was implemented using the SPSS (statistical software system), a software package acquired by IBM and is widely used for statistical analysis in social science but has since expanded to many other fields. Multiple linear regression was performed between the variables and the Pearson's coefficient was taken as an indicator of the relationship of those variables.

5.0 Results

5.1 Textural sediment characteristics

A total of 279 samples were surveyed and analysed during the study period from 2005 to 2016. Sediments in Poole Bay were mostly sandy (less than -1 φ or 2mm) and sand constituted 90% of the samples collected. As the length of coastline is extensive, sediments sampled from one part of the beach may vary differently from another part. Broadly speaking, the characteristics of the coastline can be described as having a mean grain size (Mn) of 1.25 φ (0.42 mm, medium sand), sorting (So) of 1.03 φ (poorly sorted), skewness (Sk) of -0.17 (coarse skewed) and kurtosis (Ku) of 1.34 (leptokurtic). These values are comparable to the earlier studies conducted by Lacey (1985) and Edgell (2008). The main dissimilarity lies in the sediment sorting, their samples recorded the population as moderately sorted (0.74 in Lacey's and 0.99 in Edgell's study). Another observation is that the mean sediment size has decreased over time, from 0.89 φ by Lacey (1985) to 1.22φ by Edgell (2008), and the present study of 1.25 φ.

The mean and median (D_{50}) grain sizes are plotted in Figure 30. The two variables are represented in a linear function as shown in Equation 5.1 (R = 0.94; n = 279). Majority of the samples fall on the line mean = median. Mn has a tendency to produce smaller value or coarser sediment grain size than D_{50} (circled in red) because of the small percentage of gravels in the population that cause coarse skewness in predominantly sand samples (1.0 φ < Mn < -1.0 φ). Contrarily, Mn can generate bigger value or finer sediment grain size than D50 (circled in green) where sand produces fine skewness in predominantly gravel samples (-1.0 φ < Mn < -3.0 φ).

$$D_{50} = 1.04\,Mn + 0.03 \qquad (5.1)$$

Although it has been debatable as to which property is more suitable to use, using this Mn vs D_{50} approach shows that most samples fall on the equated line for samples, particularly for grain size between 1 φ to 3 φ. The high R value of 0.94 further suggests there is no major difference in using either property. It is noticeable that a small number of samples deviate from the straight line due to bimodality distribution, and thus to avoid under or over estimating the particle size distribution, the mean grain size is adopted in this study. The samples with unimodal distribution take up approximately 66 % of the entire population in the study period. Figure 31 illustrated the frequency distribution of sediments sampled in 2013. Given that unimodal distribution still prevails, it can be assumed that the sample population are of singular mode, thus a unimodal analysis approach is undertaken in this study.

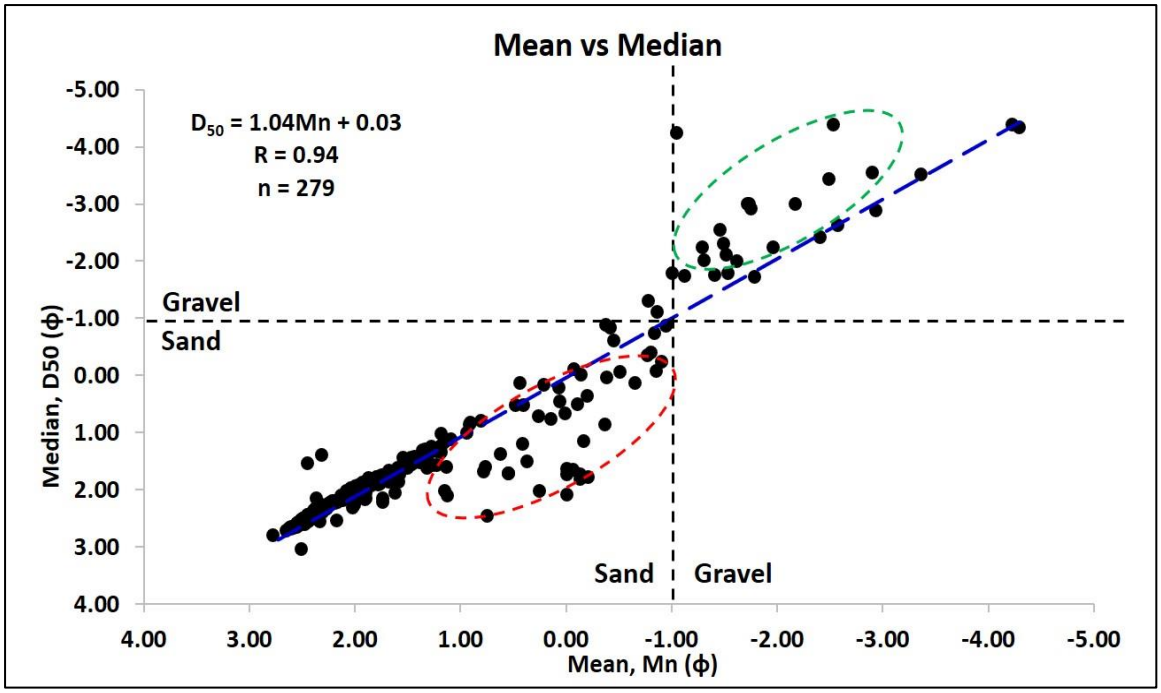

Figure 30 Linear relationship between mean and median parameters

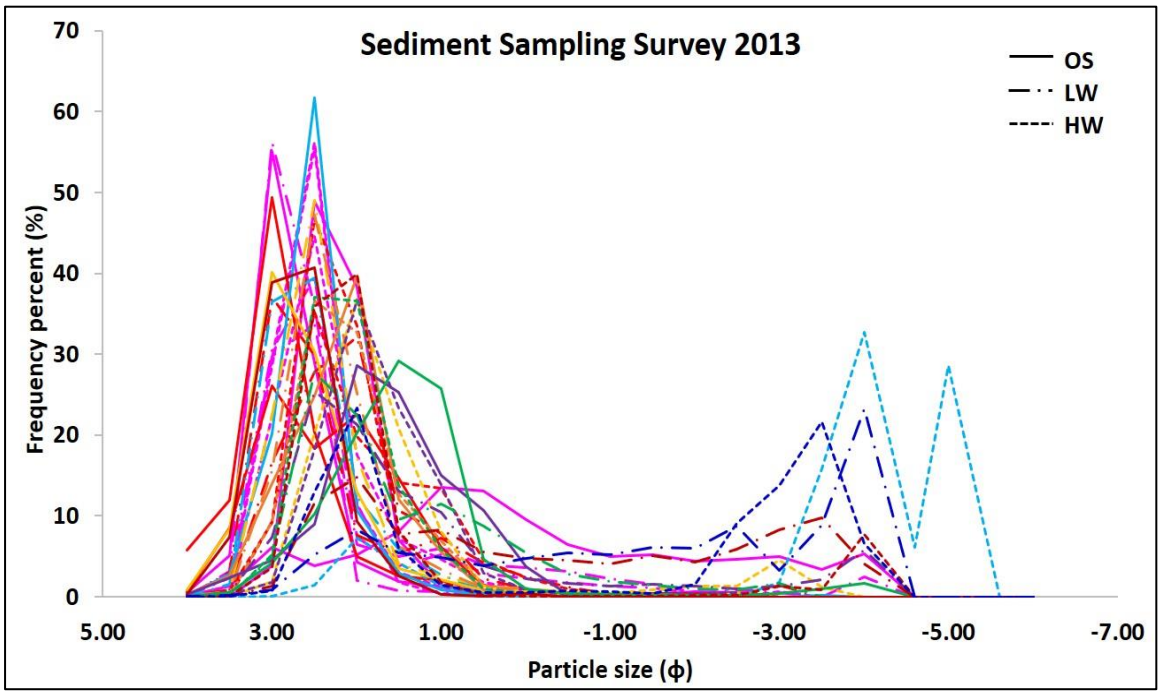

Figure 31 Frequency distribution of sediment samples collected in 2013's survey indicating most samples are unimodal (Note: Different colour lines represent the samples from zones A to I according to the zonal colour codes - see Figure 29).

Figure 32 shows a sinusoidal curve for the mean grain size and sorting of all samples collected at offshore, low water and high water positions. The two parameters are expressed through a function as shown in Equation 5.2. This is alike to the relationships observed in Lacey (1985), Harlow (2005) and Edgell (2008), with some variances in amplitude and wavelength of the sine curve (V_A to V_D) due to morphological changes throughout the years. Bulk of the samples contains Mn ranging from 1.5 φ to 2.5 φ in the fine sand category and sorting below 1.0 φ (well sorted). Referring to the peak

of the curve, as the particle size becomes coarser, the sorting becomes poorer from the mixing of gravel and sand fractions. As gravel proportion starts to dominate the sample size (Mn > 4.5 φ), the sorting is expected to improve. The offshore (blue points) and high water (red points) samples were distinctively well sorted whilst the low water samples (green points) were rather mixed and poorly sorted.

$$So = 1.5 - 1.1\, sin\,[\,48\,(Mn - 0.8)] \qquad (5.2)$$

Note: V_A (Level of semi-amplitude of the sine curve) = 1.1;

V_B (Distance of $\sin x = 0$ to the point at which $M_N\ is\ 0$) = 0.8;

V_C (Semi-wavelength of the sine curve) = 3.75 and

V_D (Level of semi-amplitude when S_o is above 0) = 1.5

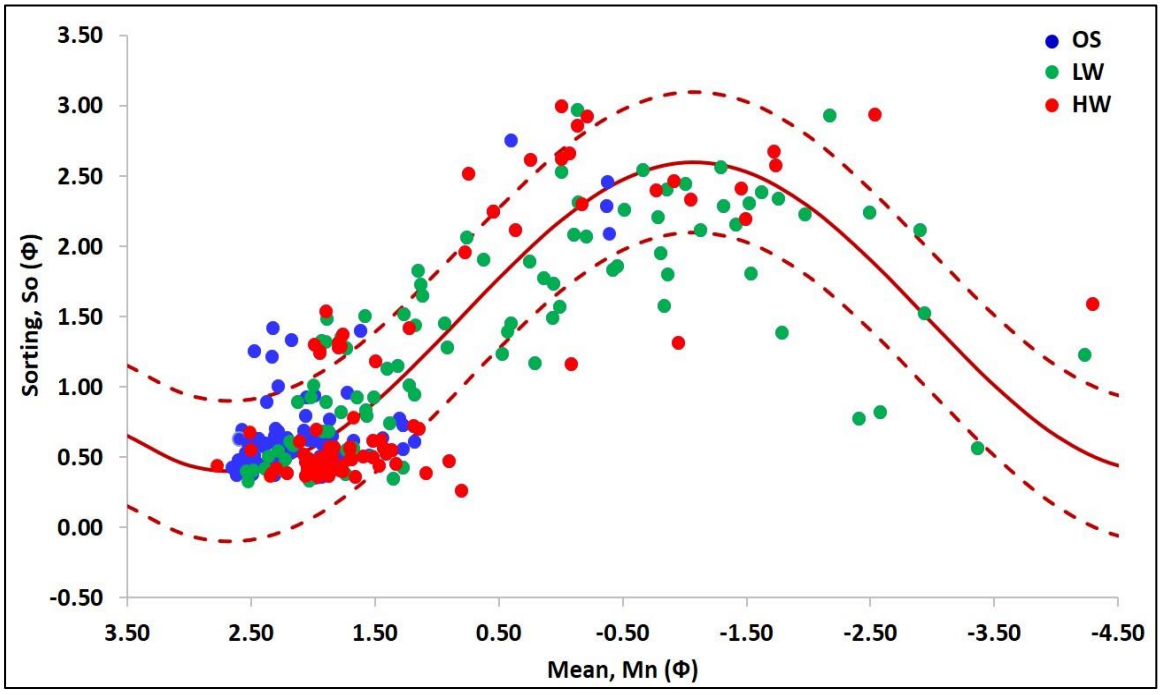

Figure 32 Mean grain size and sorting expressed a sinusoidal relationship.

A multi-variate relationship is observed as a helical trend on mean, sorting and skewness of the frequency distribution (Folk & Ward, 1957) and this is related to the relative abundance of the two (gravel and sand) modes as indicated in Figure 33. Best sorting occurs when sample is entirely of sand mode (circled in black). As the proportion of gravel in the sample increases, the grain size increases, sorting worsens and skewness goes to maximum negative value (arrow in black which runs diagonally across the plot). When gravel mode becomes more dominant, the sequence of changes is reversed until (red arrow), in pure gravel state (red circle), better sorted normal curves again appear.

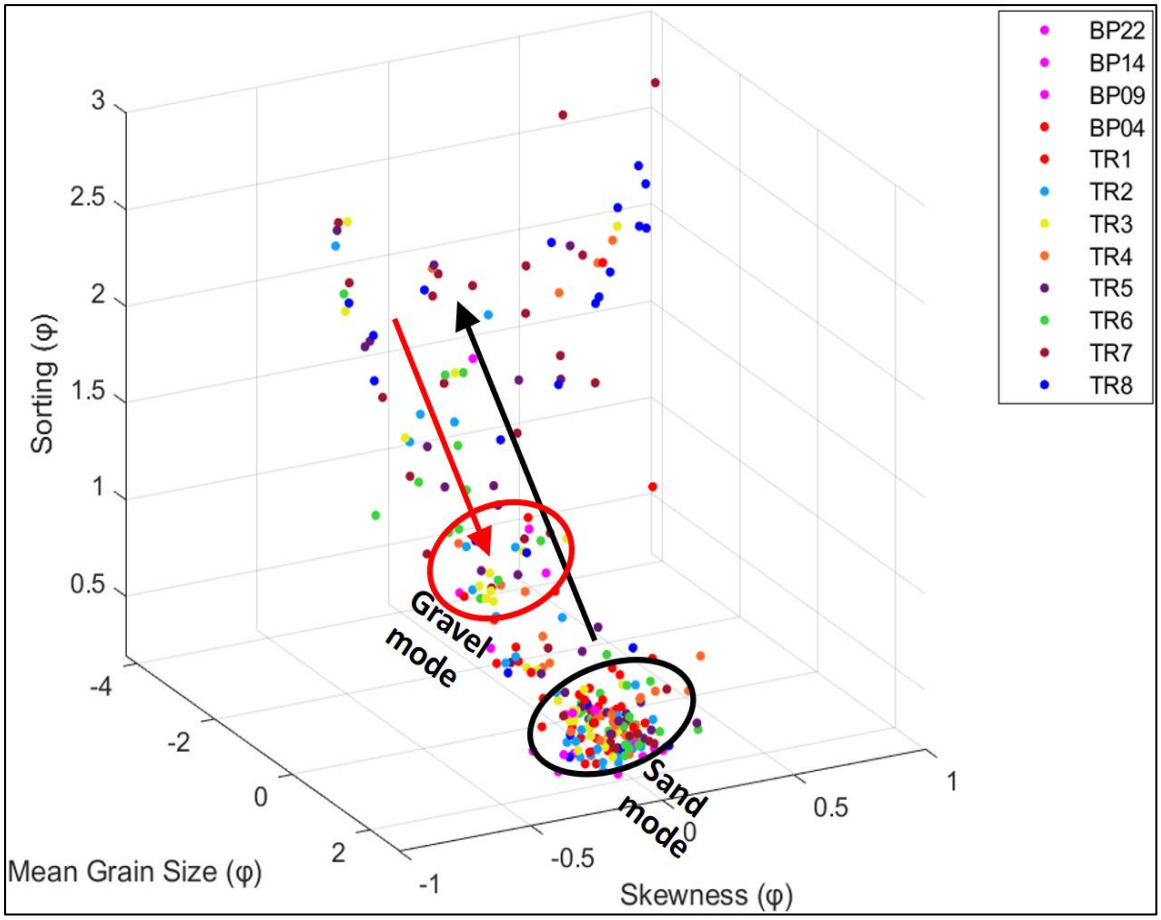

Figure 33 Relationship between mean, sorting and skewness of the sampled population. (Note: Different colours of data points are based on the zonal colour codes - see Figure 29)

5.2 Spatial-temporal variability

Beaches are highly complex and dynamic, with sediments continuously rework and redistribute to reach the equilibrium steady state under the highly variable hydrodynamic regime (Splinter, et al., 2014). As the length of coastline is extensive, sediments sampled from one part of the beach may vary differently from another part. Characterising the beach with a single sediment size only provides a glimpse of the beach condition as it assumes the sediment distribution remains fixed in both space and time. A single sediment size is unable to provide an accurate reflection of the actual evolution of a beach system. It is therefore preferred to analyse the sediment variability in the directions longitudinal and traverse to the shoreline.

5.2.1 Alongshore direction

The zonation of 16 km coast in Poole Bay begins in Zone A (Sandbanks) and terminates in Zone I (Hengistbury Head). Figure 34 shows the equivalent (average) values of the textural parameters in the longshore direction.

Sediments across the entire coast have been found to be mostly composed of fine-grained materials. There is an increase in Mn across the bay from 2.09 φ (0.23 mm or fine sand) in Zone A to 0.46 φ

(0.72 mm or very coarse sand) in Zone I. In general, samples are moderately sorted in the western and central bay, but become poorly sorted after Zone F. This can be understood from the gravel-sand percentage as from this point on, there is a rise in the gravel content. Zone H has the largest equivalent mean grain size which is explained by the highest gravel content received in this area. The whole distribution is negatively coarse skewed (*i.e.* computed mean is lower than median values) although the skewness values are relatively close to the lower bound of the symmetrical range ($-0.1 < Sk_{symmetric} < 0.1$). Kurtosis values range from 1.18 to 1.70 and are thus leptokurtic to very leptokurtic (*i.e.* clustering at the centre of the distribution and the tails are of lower significance).

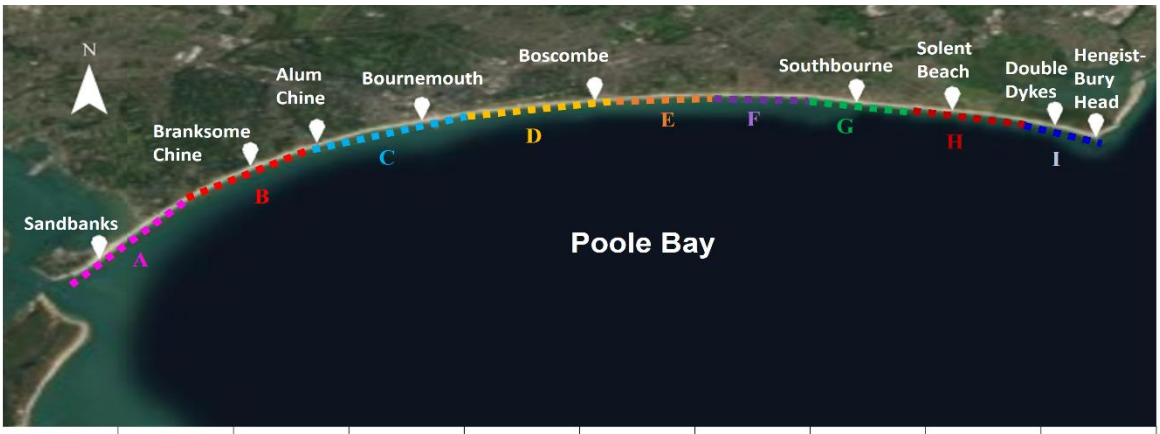

	A	B	C	D	E	F	G	H	I
Mn (φ)	2.09	1.87	1.71	1.55	1.48	1.06	1.25	0.31	0.46
So (φ)	0.74	0.73	0.86	0.98	0.86	1.09	0.89	1.50	1.47
Sk (φ)	-0.25	-0.16	-0.23	-0.26	-0.09	-0.18	-0.17	-0.12	-0.06
Ku (φ)	1.22	1.18	1.59	1.70	1.31	1.37	1.22	1.19	1.14
% Gravel	3.5	2.2	7.0	7.8	8.4	13.1	11.0	29.4	27.2
% Sand	96.5	97.8	93.0	92.2	91.6	86.9	89.0	70.6	72.8

Figure 34 Equivalent textural characteristics for Zones A to I over the longshore distance

As the sampling survey is conducted at offshore (OS), low water (LW) and high water (HW), the characteristics of sediments vary differently in each location due to exposure to different hydrodynamic loading, bed/beach elevation and other environmental aspects. It is thus more meaningful to analyse the longshore trends at each of these locations (see Sections 5.2.1.1 to 5.2.1.3). The complete set of sediment characteristics at OS, LW and HW for the longshore distance are provided in Appendix B.

5.2.1.1 Offshore region

Figure 35 indicates the mean grain size trend for offshore region. Across the bay, there is a nominal variation in the mean grain size: Mn measures at 1.88 φ (0.27 mm) at the western bay and 1.99 φ (0.25 mm) at the eastern bay. For sorting, it changes from 0.76 to 0.72, overall the sediments are

moderately sorted (Figure 36). The sediments become poorly sorted at Zone F as Mn is 0.13 φ coarser than in Zone E. Zone G has better sorting from Zone F although this trend is not continuous in the downdrift.

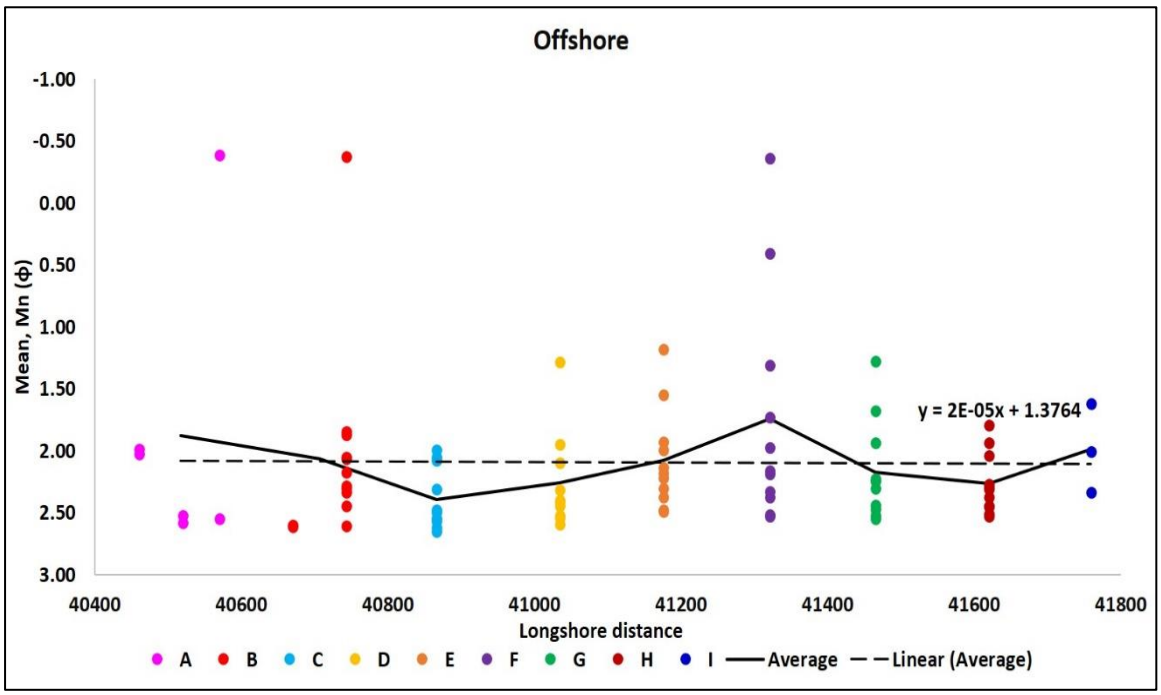

Figure 35 Sediment's mean grain size trend for offshore region from Sandbanks to Hengistbury Head.

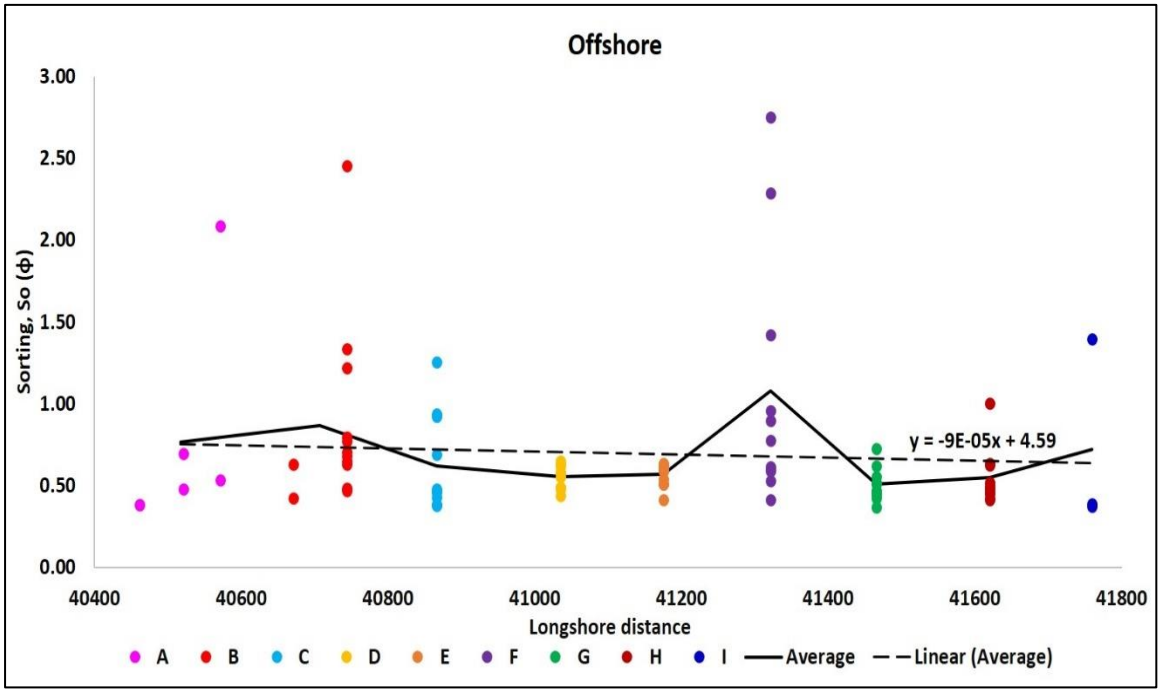

Figure 36 Sediment's sorting trend for offshore region from Sandbanks to Hengistbury Head.

The earlier plots examined how sediment characteristics vary spatially. By analysing the temporal variability of sediment characteristics of the coastline, this provides another insight on how sediments behaved and changed over time, as a result of different environmental or/and anthropogenic conditions at that specific timeframe.

Table 9 shows the offshore mean grain size for the sampling sites from 2005 to 2016 and Figure 37 plots the periodic change in mean grain size at offshore region. Metric units are adopted for ease of interpretation and visualization of the temporal change. A total of three peaks are observed: Zone A (BP 09) in 2013; Zone B (TR 1) in 2014 and Zone F (TR5) in 2006 (values in bold in Table 9). In all three periods, the sediments are classified as very coarse sand and they varied starkly from the fine sand sediments in the adjacent zones. Sediment size variability can be attributed to several factors such as wave and currents, storm effects, anthropogenic actions etc. These effects are discussed and examined in Section 6.

Table 9 Mean grain size of offshore samples from 2005 to 2016. Mn values in bold refers to very coarse sand (> 1 mm) observed in the sample population. (Note: Grey-out boxes refer to no sampling done or samples returned without sediments)

Zone	A			B		C	D	E	F	G	H	I
Sampling site /Date	BP22	BP14	BP9	BP4	TR1	TR2	TR3	TR4	TR5	TR6	TR7	TR8
2005					0.24	0.25	0.41	0.44	0.25	0.31	0.29	
2006					0.28	0.24	0.26	0.34	**1.29**	0.26	0.26	0.25
2007					0.18	0.17	0.20	0.19	0.75	0.17	0.18	0.20
2008					0.20	0.24		0.22	0.22	0.21	0.18	
2009					0.21	0.17	0.17	0.25	0.17	0.21	0.17	
2010					0.22	0.18	0.19	0.23	0.22	0.20	0.21	0.33
2011					0.27	0.16	0.18	0.22	0.30	0.21	0.24	
2013	0.25	0.17	**1.31**	0.17	0.24	0.20	0.19	0.26	0.40	0.41	0.18	
2014	0.25	0.17	0.17	0.16	**1.29**	0.16	0.17	0.18	0.19	0.18	0.20	
2015					0.20	0.17	0.17	0.20	0.18	0.17	0.19	
2016					0.16	0.18	0.23	0.18	0.20	0.18	0.20	

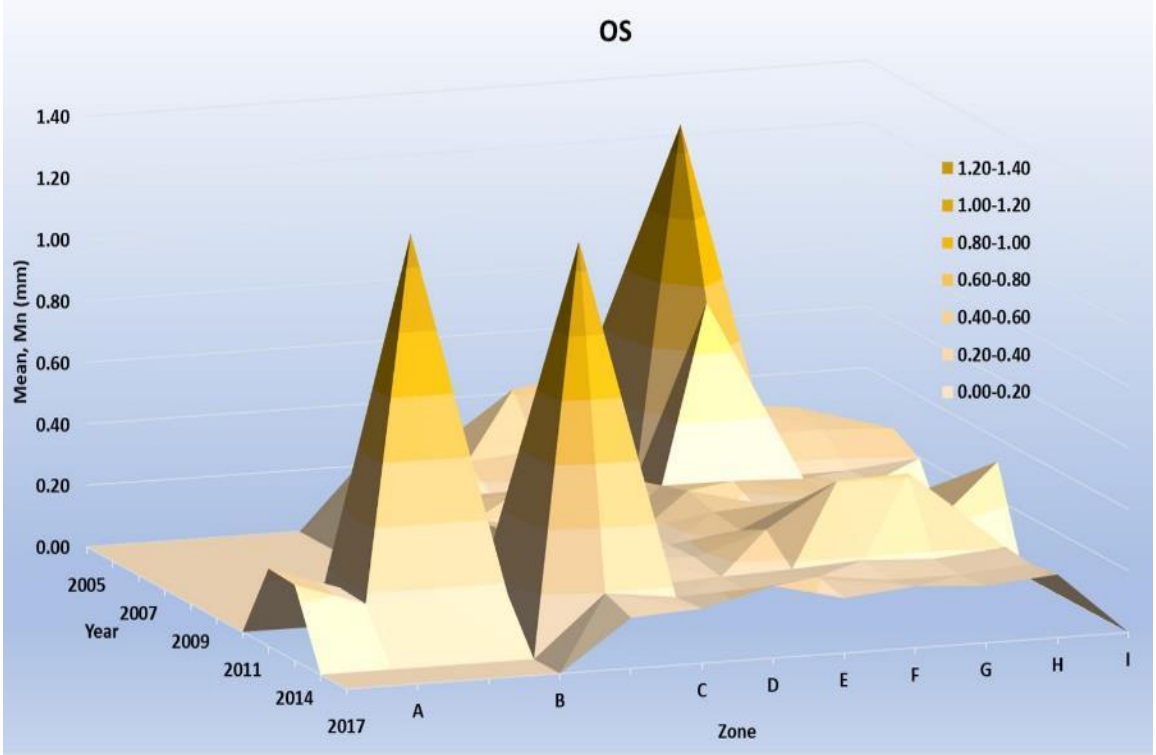

Figure 37 Temporal plot of sediment mean grain size at offshore region

5.2.1.2 Low Water

Figure 38 plots the mean grain size of the lower beach around mean low water springs. The graph exhibits a rising trend of particle size from 1.98 φ (0.25 mm fine sand) to -0.74 φ (1.67 mm very coarse sand) across the bay. There is a wider spread of particle sizes at the central bay, with Zone F having the most varied sediment sizes *i.e.* variance of 6.45 φ.

Sediment sorting also increases with distance across the bay (Figure 39), changing from 0.97 φ (moderately sorted) at the western bay to 1.80 φ (poorly sorted) in the eastern end. In terms of sediment fraction, the LW region at Zone H is found to have a 58.3% - 41.7% of gravel-sand content and is the highest among other zones (Table 10).

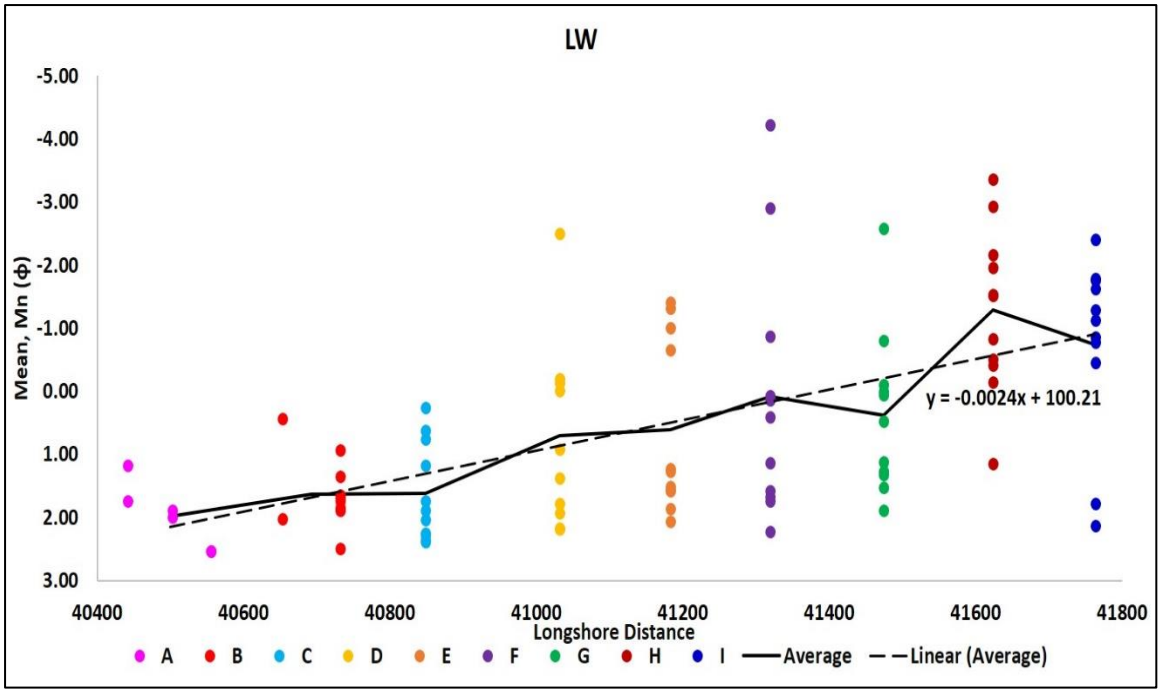

Figure 38 Sediment's mean grain size trend at Low Water.

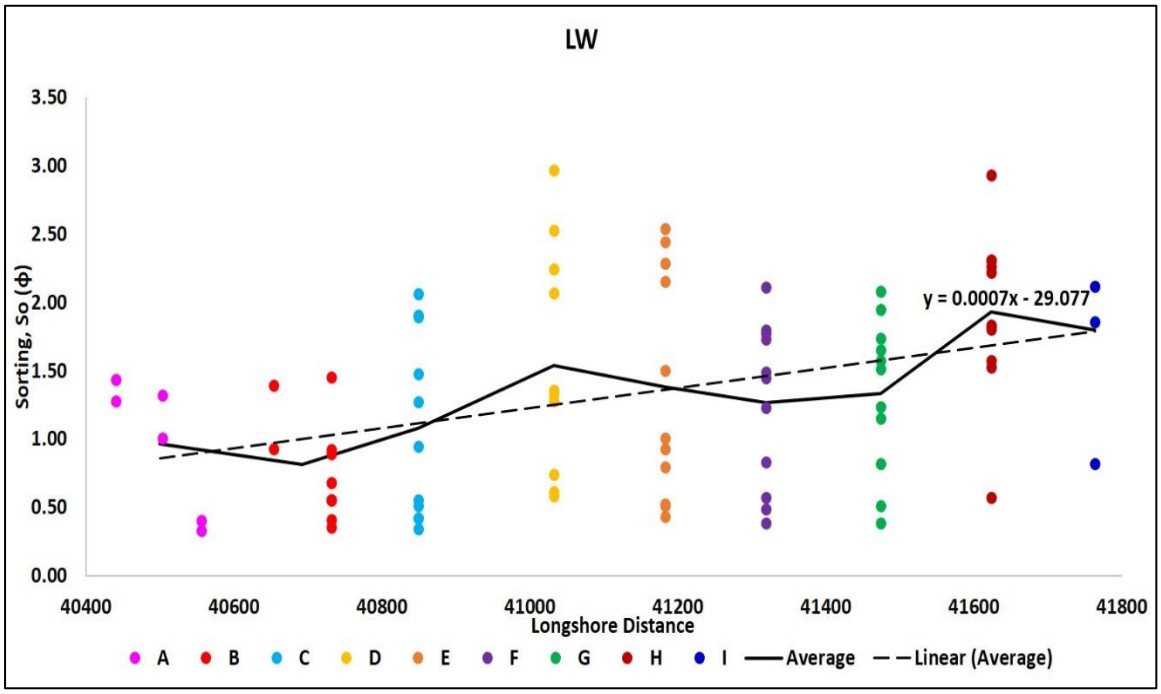

Figure 39 Sediment's sorting trend at Low Water.

Table 10 Gravel-Sand Fraction for offshore, Low Water and High Water samples

	OS		LW		HW	
Zone	% Gravel	% Sand	% Gravel	% Sand	% Gravel	% Sand
A	5.8	94.3	4.7	95.4	0.1	99.9
B	4.3	95.7	2.1	97.9	0.1	99.9
C	1.9	98.1	6.9	93.1	12.2	87.8
D	0.4	99.6	18.2	81.8	4.9	95.1
E	0.2	99.8	22.6	77.4	2.4	97.6
F	5.3	94.7	27.6	72.4	6.4	93.6
G	0.4	99.6	24.9	75.1	7.6	92.4
H	1.3	98.7	58.3	41.7	28.7	71.3
I	1.2	98.8	51.2	48.8	29.3	70.7

Table 11 and Figure 40 shows the mean grain size for the LW sampling sites from 2005 to 2016. Particle size varies considerably and multiple peaks are observed to cluster around the central and eastern bay. Significant increase in the particle size (pebbles greater than 5 mm) are observed in Zones F and H in 2009, Zone D, F and G in 2010 and Zone H in 2014.

Table 11 Mean grain size of LW samples from 2005 to 2016. Mn values in bold refers to pebble > 5 mm observed in the sample population. (Note: Grey-out boxes refer to no sampling done or samples returned without sediments)

Zone	A			B		C	D	E	F	G	H	I
Sampling site /Date	BP22	BP14	BP9	BP4	1	2	3	4	5	6	7	8
2005					0.32	0.65	0.53	0.43	0.91	1.08	1.34	0.29
2006					0.39	0.84	0.38	0.41	0.30	0.99	2.87	2.17
2007					0.30	0.27	0.29	0.33	1.82	0.41	1.78	1.36
2008					0.28	0.21	1.15	1.58	0.33	0.35	3.90	1.81
2009					0.31	0.24	1.00	2.48	**7.47**	0.27	**7.63**	3.37
2010					0.27	0.59	**5.62**	0.34	**18.70**	**5.95**	0.45	2.44
2011					0.18	0.19	0.22	2.01	0.21	0.46	1.10	1.72
2013	0.30	0.25	0.17	0.25	0.27	0.21	0.22	0.24	0.46	0.40	1.43	3.07
2014	0.44	0.27	0.17	0.74	0.52	0.44	1.10	0.35	0.75	1.75	**10.28**	3.44
2015					0.26	0.19	0.26	0.28	0.31	0.96	4.49	0.23
2016					0.38	0.30	0.86	2.66	0.95	0.72	2.89	**5.29**

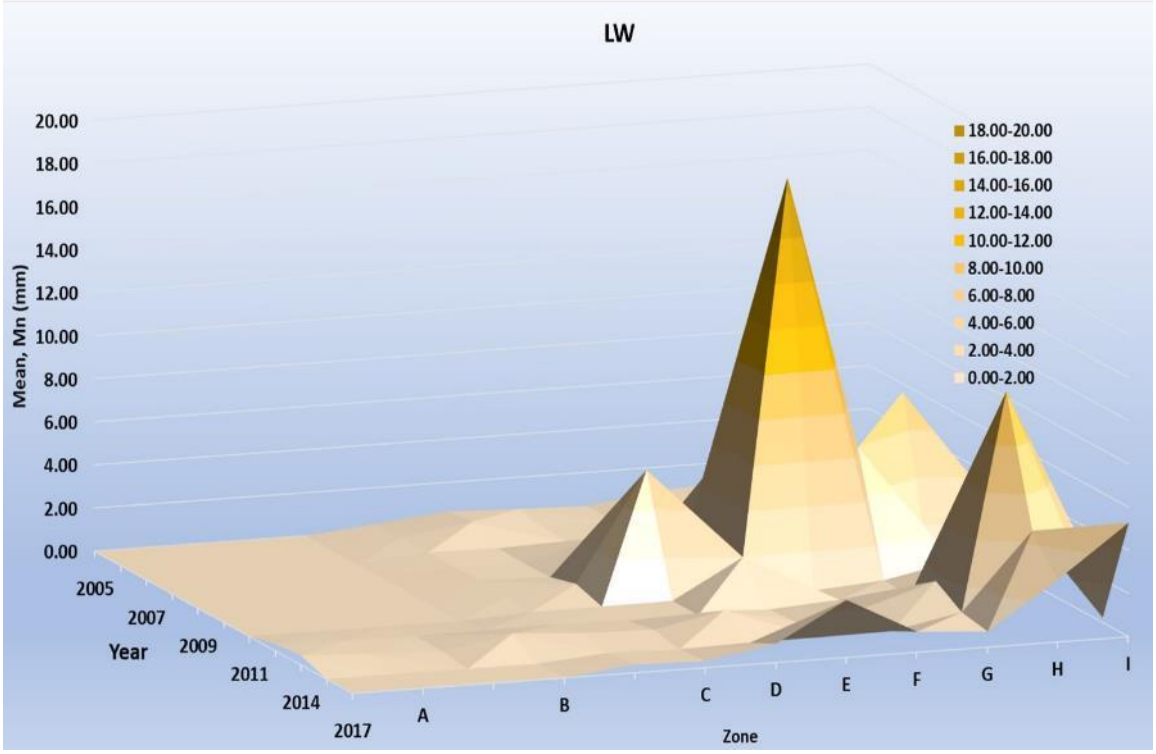

Figure 40 Temporal plot of sediment mean grain size at low water from Zone A to I

5.2.1.3 High Water

There is a degree of similarity for Mn and So between LW and HW regions. Figures 41 and 42 show the upward trends of sediment mean and sorting on the upper beach at High Water (HW). Mean and sorting of all except Zone C increase with distance. Mn increases from 2.40 φ (0.19 mm or fine sand) at Zone A to 0.14 φ (0.91 mm or coarse sand) at Zone I. There is a spike in mean grain size at Zone C because of an outlier sample with -4.29 φ (19.82 mm or pebble). Sorting peaks at 2.03 φ in Zone H is classified as very poorly sorted category due to a high gravel content of 28.7% (refer to Table 10). On the whole, sediments are finer and better sorted in the west, with the occurrence of coarser gravels increasing eastwards.

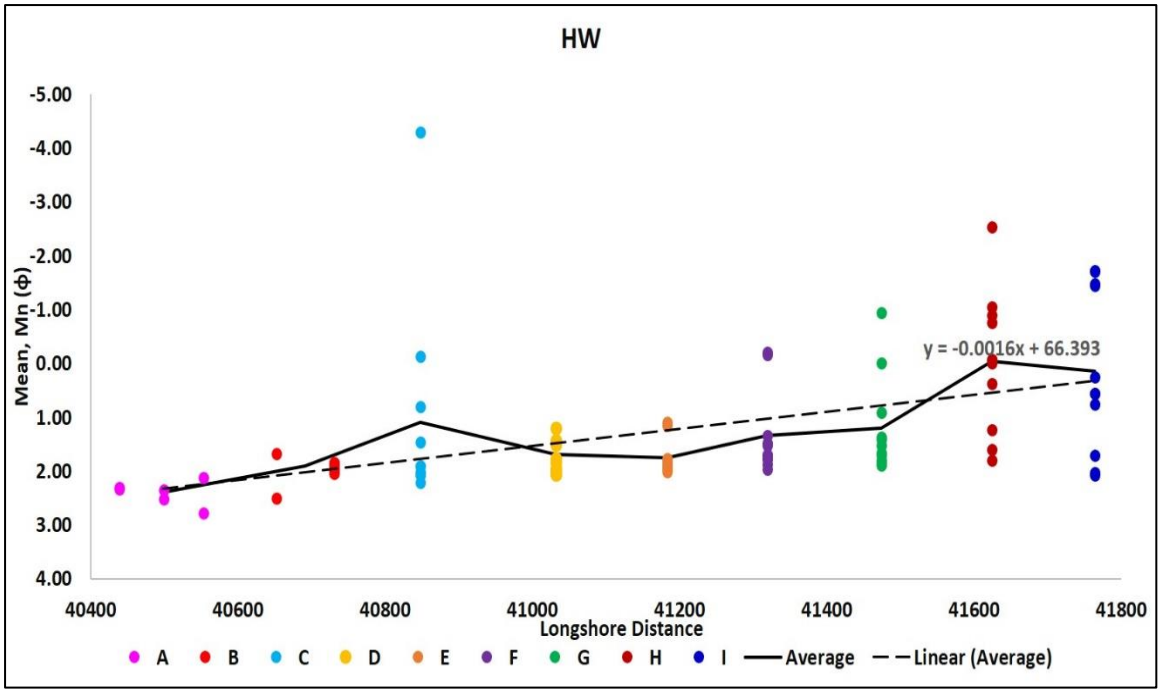

Figure 41 Sediment's mean grain size trend for High Water region.

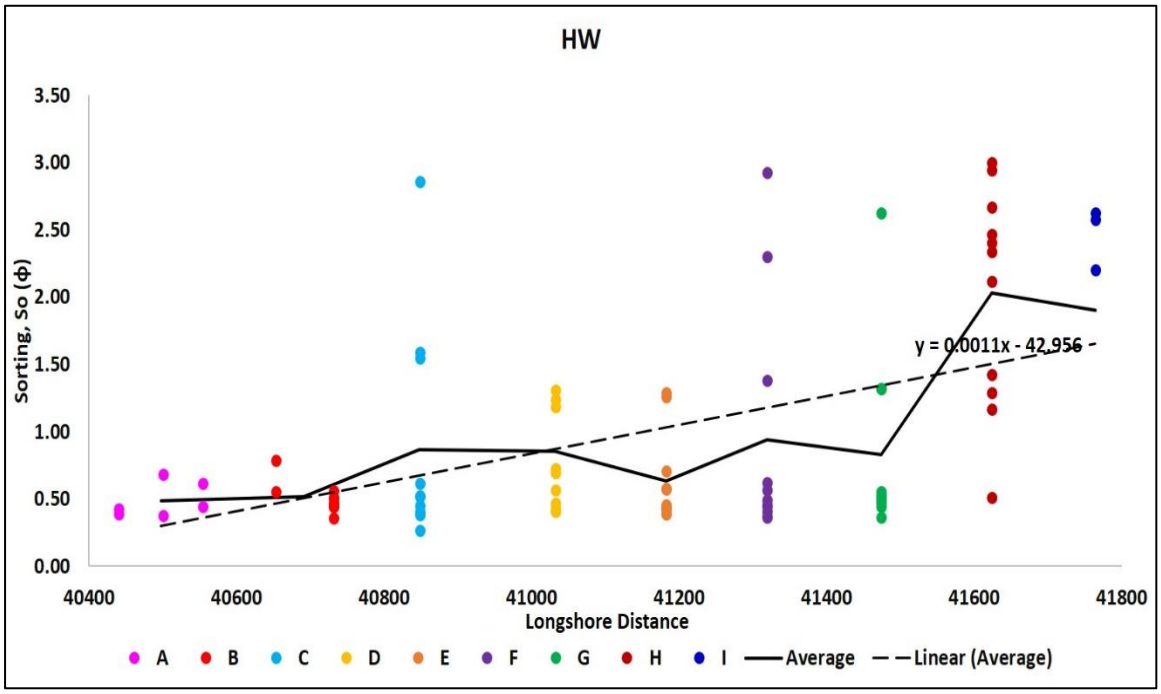

Figure 42 Sediment's sorting trend for High Water region.

Table 12 and Figure 43 shows the mean grain size for the LW sampling sites from 2005 to 2016. For the periodic trend at high water, there is a gradual increase in sediment sizes from Zone A to I with the exception of Zone C where mean was 19.62 mm in 2013. There are several smaller apexes with coarse sand and granules observed in Zone H in 2011 and 2017, Zone I in 2005, 2006 and 2013.

Table 12 Mean grain size of HW samples from 2005 to 2016. Mn values in bold refers to gravel > 2 mm observed in the sample population. (Note: Grey-out boxes refer to no sampling done or samples returned without sediments)

Zone	A			B		C	D	E	F	G	H	I
Sampling site /Date	BP22	BP14	BP9	BP4	1	2	3	4	5	6	7	8
2005					0.27	0.57	0.44	0.45	0.36	0.32	0.43	**3.32**
2006					0.25	0.36	0.37	0.47	0.40	0.53	1.87	**2.81**
2007					0.27	0.24	0.25	0.26	0.31	0.38	1.70	0.84
2008					0.28	0.24	0.29	0.26	0.27	0.35	0.77	0.31
2009					0.27	0.24	0.28	0.27	0.29	0.39	1.06	0.24
2010					0.26	0.22	0.26	0.26	0.29	1.92	1.05	0.24
2011					0.24	1.10	0.24	0.28	0.26	0.29	**2.07**	0.68
2013	0.20	0.20	0.23	0.31	0.25	**19.62**	0.35	0.27	0.35	0.28	0.29	**2.74**
2014	0.20	0.18	0.15	0.18	0.28	0.27	0.24	0.25	1.15	0.27	1.00	0.59
2015					0.37	0.25	0.25	0.29	1.12	0.31	0.33	0.68
2016					0.28	0.27	0.58	0.29	0.31	1.00	**5.79**	3.28

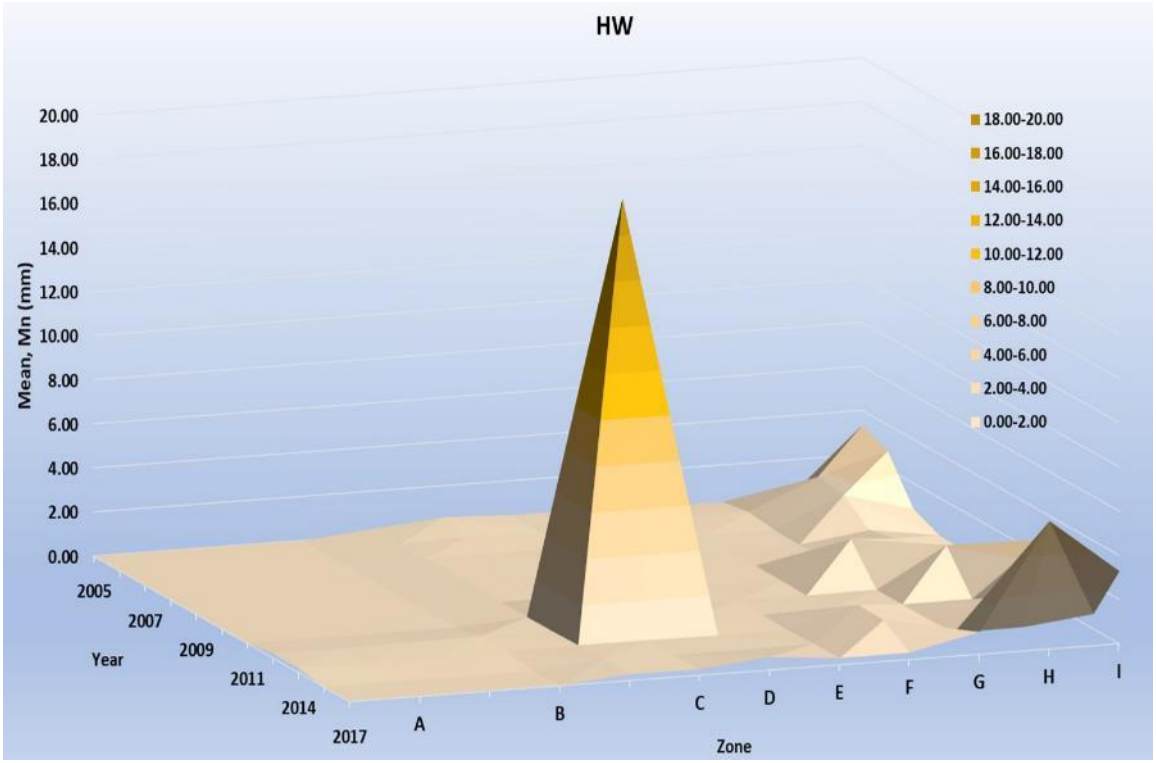

Figure 43 Temporal plot of sediment mean grain size at high water

5.2.2 Cross-shore direction

The overall sediment textural characteristics in the cross-shore direction are given in Table 13. The equivalent Mn at offshore is 2.09 φ (0.23 mm fine sand), Low Water is 0.55 φ (0.68 mm coarse sand) and High Water is 1.27 φ (0.41 mm medium sand). Lower beach sediments are 66% coarser

and 49% less sorted than offshore sediments and 40% coarser and 25% less sorted than upper beach sediments. The distribution is negatively coarse skewed and leptokurtic at all three sites. The complete set of cross-shore plots for Zone A to I are provided in Appendix C.

Table 13 Equivalent textural characteristics at offshore, LW and HW.

	Region		
	OS	LW	HW
Mn (φ)	2.09	0.55	1.27
So (φ)	0.69	1.34	1.01
Sk (φ)	-0.16	-0.17	-0.18
Ku (φ)	1.30	1.27	1.40

The differential characteristics of sediment population across the cross-shore distance (from HW to OS) for the zones are presented in Table 14. It suggested that sediments typically diminished in size in the seaward direction. A positive change in Mn (e.g. 0.52 in Zone A), means that sediment size is smaller at HW than OS. Appendix C provides the plots of mean and sorting in the cross-shore direction. In general, all with the exception of Zone A exhibited grain size reduction between HW and OS (*i.e.* offshore sediments are finer than the intertidal beach). Sediments are the coarsest at LW and there is a fairly wide range of sediment sizes observed here.

For sorting, negative value refers to sorting becomes poorer with increasing distance from shore. The west side of the bay e.g. Zone B experienced negative sorting changes, in other words, the upper beach has a better sorted distribution while offshore sediments are more mixed (Figure 44). The other zones (e.g. Zone F) display improved sorting with offshore fining. The mean values (black solid line) in Figure 45 showed the coarsest and worst sorted materials at LW.

Zones A and B see a small increment of approximately 5% in gravel content while the remaining zones experienced a decrease in gravel content in the cross-shore direction (Table 14). On the other end of Poole Bay, Zones H and I see more than a quarter of the distribution comprising gravelly materials. A potential gravel source is from the erosion of high cliffs at Double Dykes (West, 2018), thereby explaining the large deviation in textural characteristics from the remaining parts of the bay.

Table 14 Changes in sediment textural characteristic for Zones A to I in the cross-shore direction.

	A	**B**	**C**	**D**	**E**	**F**	**G**	**H**	**I**
Distance from shore (m)	280	316	328	319	352	348	395	253	250
Mn (φ)	0.52	-0.16	-1.30	-0.57	-0.33	-0.40	-0.97	-2.31	-1.85
So (φ)	-0.28	-0.35	0.25	0.30	0.06	-0.14	0.33	1.48	1.19
Sk (φ)	0.21	0.14	0.11	-0.09	-0.14	0.02	-0.17	-0.24	0.04
Ku (φ)	-0.28	-0.34	-0.45	0.78	0.53	-0.20	0.53	-0.10	0.47
Gravel Content %	-5.7	-4.1	10.4	4.5	2.2	1.0	7.1	27.4	28.1

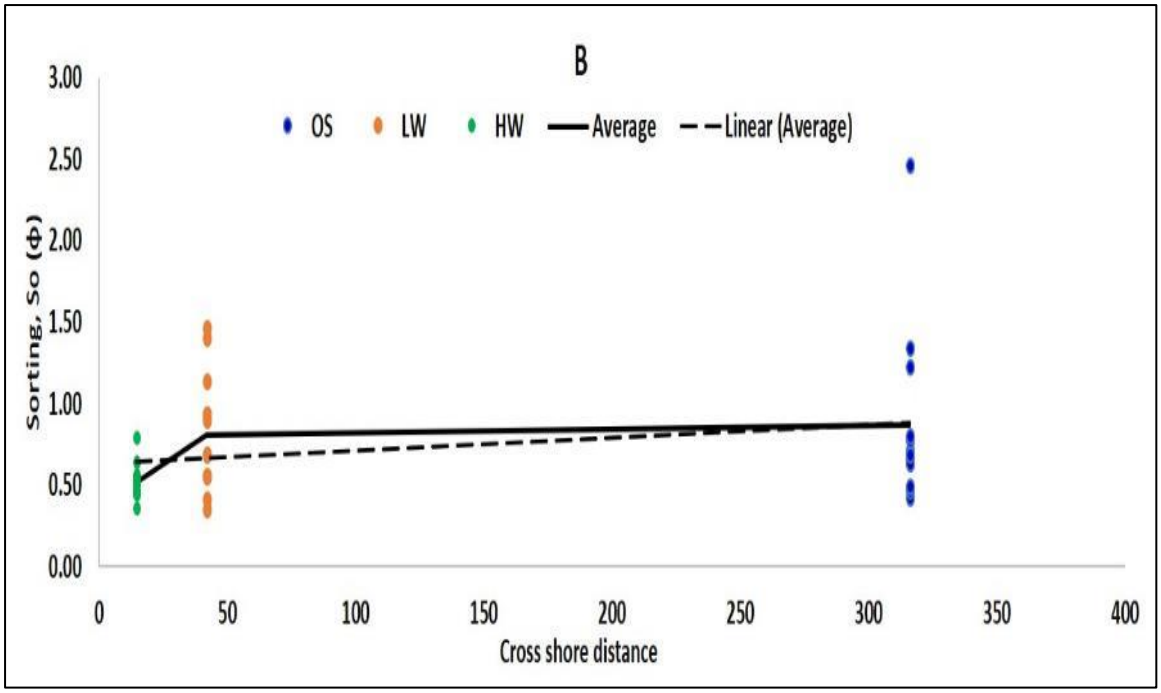

Figure 44 Sorting trend in cross shore direction at Zone B

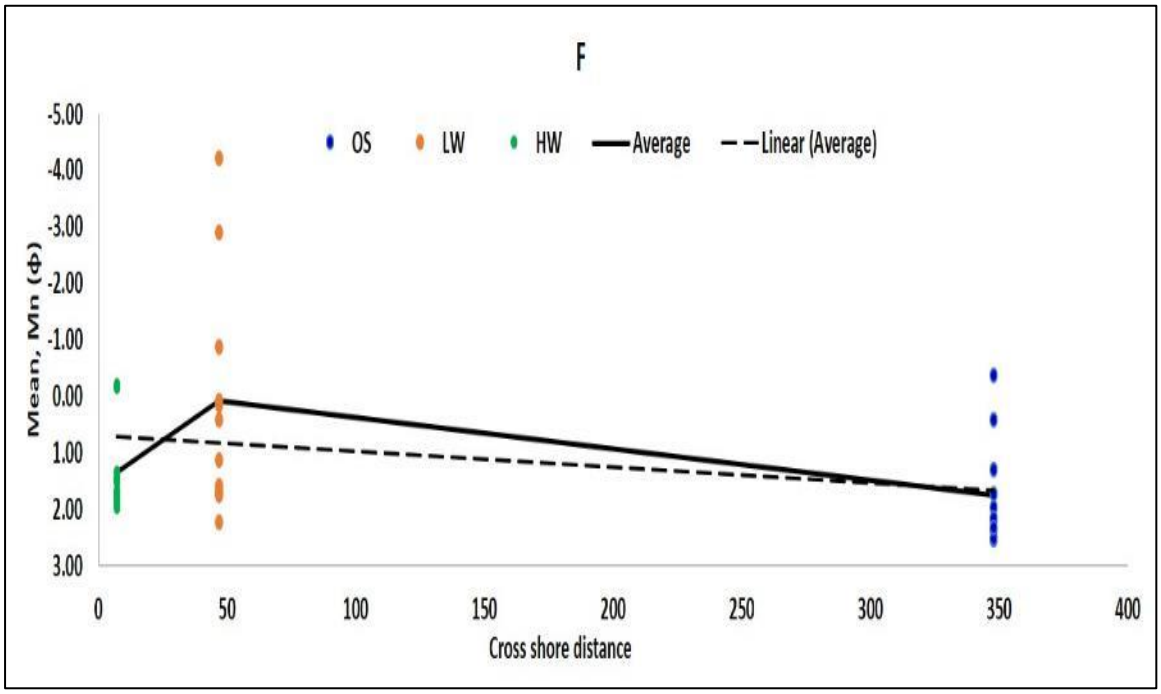

Figure 45 Mean trend in cross shore direction at Zone F

5.3 Hydrodynamic regime by waves only

Wave-induced processes play an important role for non-cohesive sediment motion and can trigger surficial sediment distribution patterns in the nearshore region. The headlands at Hengistbury and Durlston Point, as well as the sea bottom topography affect the waves approaching the shoreline. Therefore, the offshore wave parameters are redefined to inshore conditions. The results of the equivalent (average) significant wave height Hs, period T and direction θ are given in Table 15. Data relating to the annual wave parameters are provided in Appendix D. Because the nearshore model assumes the same wave period as the offshore waves, it was decided to adopt the wave period measurements from the nearshore Boscombe wave buoy for better representation of the site.

The annual mean wave direction and significant wave height from 2005 to 2012 are plotted in Figures 46 and 47. Wave angle increases steadily to the east. At Sandbanks, the main direction is coming from the south-east, whereas the central beach receives waves almost perpendicular to the shore, and near Hengistbury Head, the dominant waves that approach the shoreline is from south-west direction. Similarly, Hs increases from Sandbanks to Hengistbury Head (Figure 47). The mean wave climate has been relatively consistent throughout the years although there is a decline of 20% in Hs in 2010. Mean Hs ranges from 0.51 to 0.66 m. The mean wave period is recorded at 7.2 s.

The offshore and nearshore wave parameters are also compared. Wave roses at the western, central, eastern bay and the offshore wave buoy are shown in Figure 48, illustrating the change in wave direction due to shoaling, refraction and diffraction processes. The original south-easterly waves at the external bay bent approximately 90º anti-clockwise upon reaching Zone A whereas the waves near the central beach are almost perpendicular to the shoreline. At the headlands of Hengistbury, the waves are slightly refracted as this is closer to the offshore wave origin and continued to move in the same (south-west) direction.

Table 15 Wave height, period and direction in the longshore distance.

	θ (deg)			Hs (m)			T (s)		
Zone	Mean	Min	Max	Mean	Min	Max	Mean	Min	Max
A	166	58	227	0.51	0.03	3.02			
B	176	68	244	0.54	0.03	3.37			
C	181	76	252	0.55	0.05	3.44			
D	184	82	258	0.56	0.06	3.47			
E	188	89	266	0.56	0.05	3.44			
F	190	95	272	0.62	0.07	3.74			
G	192	101	277	0.66	0.06	4.01			
H	194	110	283	0.70	0.05	4.19			
I	196	113	288	0.68	0.07	4.28	7.2	1.9	19.3

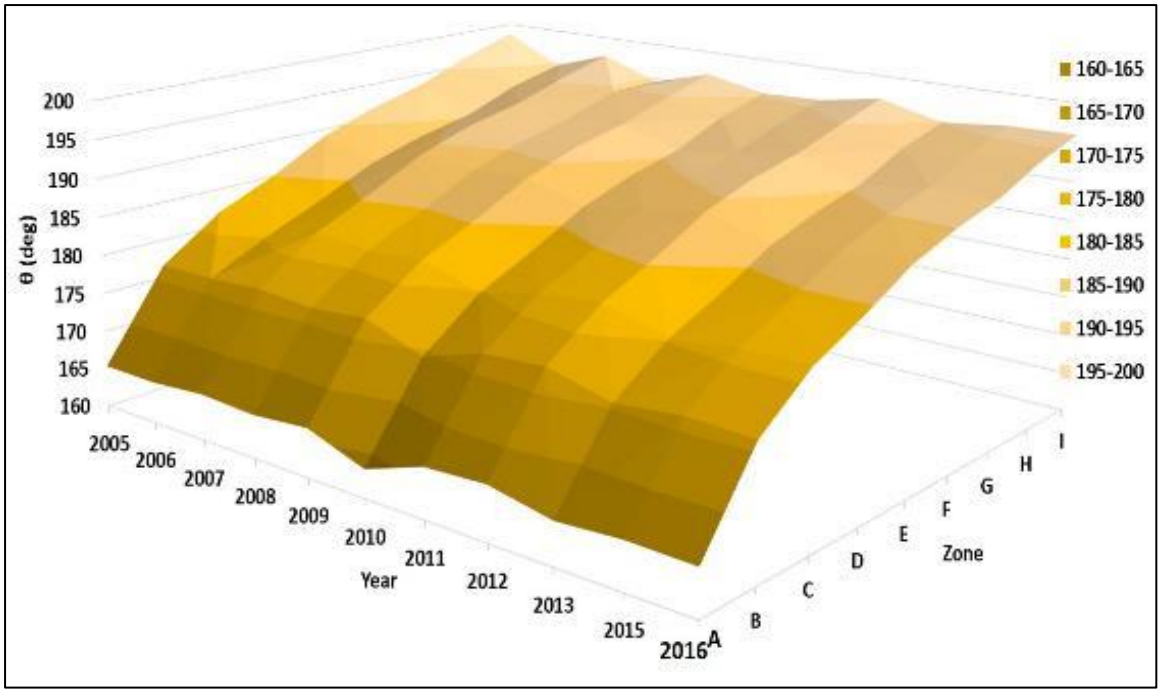

Figure 46 Variability of wave direction from 2005 to 2016.

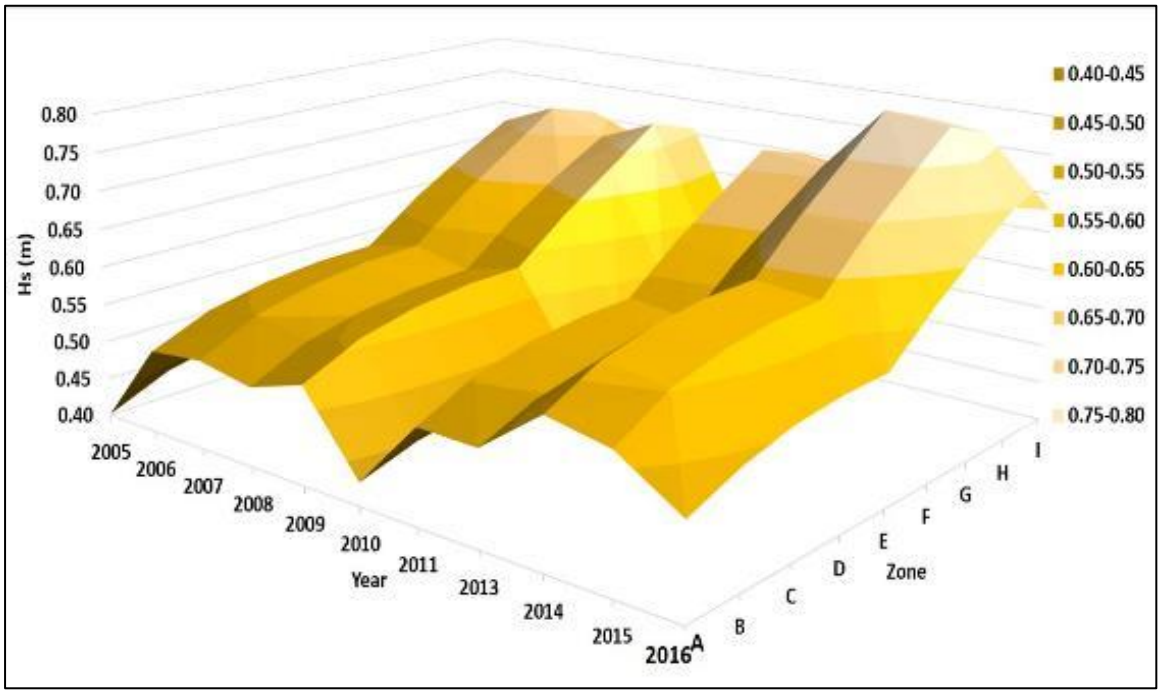

Figure 47 Significant wave height increases across the bay from Zone A to I.

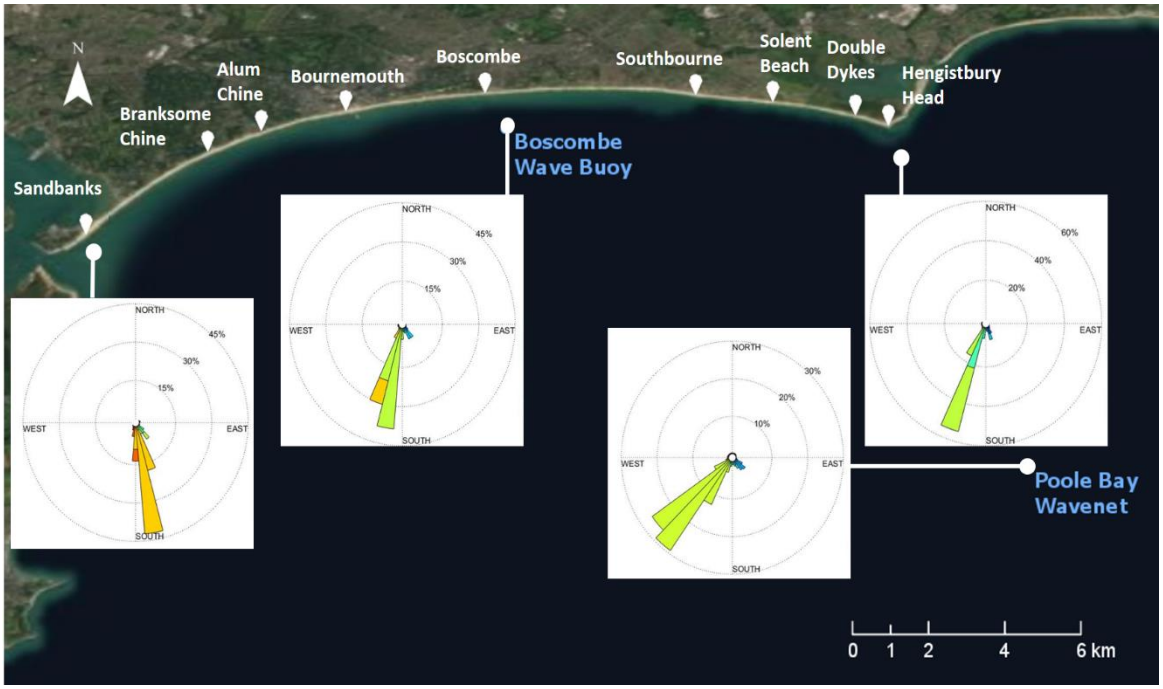

Figure 48 Wave rose plot for nearshore and offshore waves.

5.4 Sediment entrainment and bed shear stress due to waves

The average effective wave induced bed shear stress, $\tau_{w,b}$ is calculated based on the respective water depth, mean wave characteristics of each zone and using a wave friction factor derived by Soulsby (1997) (Equation 3.13). The bed shear stress, which is a function of the mean significant wave height and D_{50} is plotted for all the zones as shown in Figure 49. It ranges from 0.33 to 0.64 Pa in the west but increases with distance after Zone E. In the cross-shore direction, LW location has the highest maximum bed shear stress for all zones with the exception of Zone C, followed by HW and OS having the least.

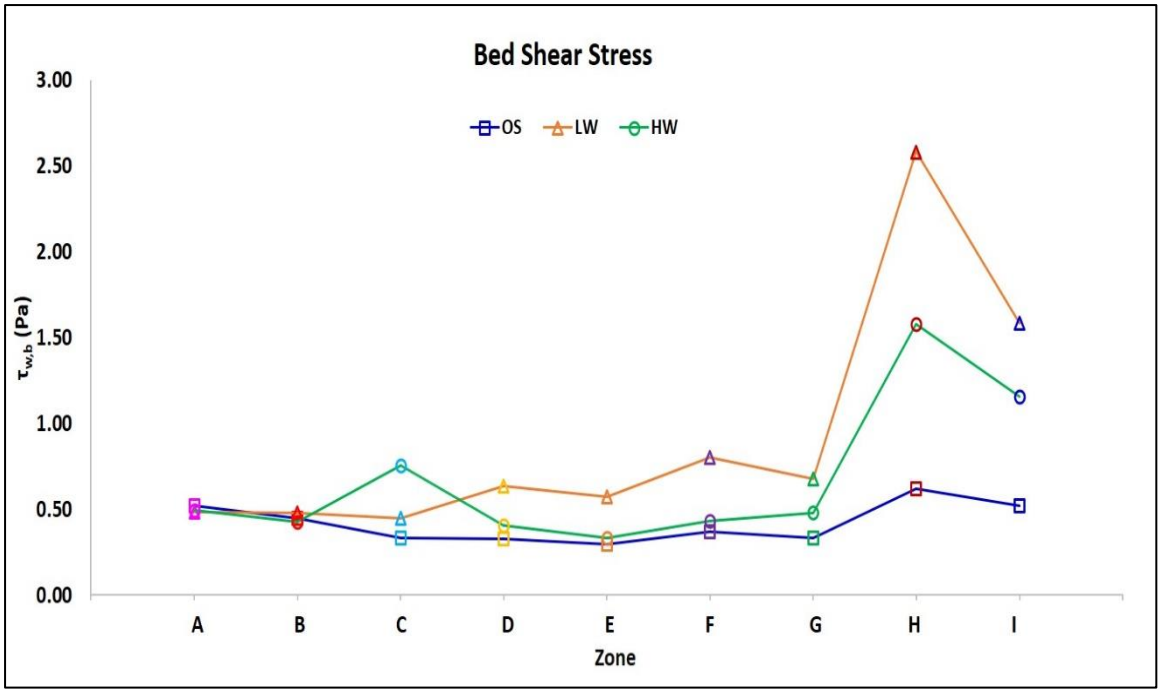

Figure 49 Average effective wave-induced bed shear stress along Poole Bay during the study period.

Because sediment sampling was complete for all zones (including Poole beaches and Hengistbury Head) in 2013, this is used as a case study to investigate the threshold of sediment mobility. The average effective wave-induced bed shear stress $\tau_{w,b}$, maximum orbital velocity u_b, critical bottom velocity u_{cr}, threshold limit of sediment motion and beach category are calculated using SEDTRAN05 and provided in Table 16. The thresholds of sediment motion for bedload and suspension are exceeded at 88% and 15% of the sample stations respectively. Where fine-graded sediments are present, both bedload and suspension are expected (e.g. In 2013, at the low water of Zone A, for D_{50} = 0.17 mm, the time fraction with only bedload transport is 44.7%; suspended load transport is 34.7% and no transport is 20.6%). Waves at certain areas (e.g. Zone C) were unable to bring about sediment movement, because these areas are characterized by coarse-grained materials and coarser materials have higher u_{cr}. Higher wave intensity would be required for the critical limit to be exceeded. For instance, the threshold of sediment movement will only be exceeded when Hs > 2.40m at water depth of 6.4m. It is to note that tidal currents and any residual currents in the coastal zone have not been considered for this analysis.

Table 16 Bed shear stress, maximum orbital and bottom critical velocities and threshold of sediment mobility of samples from 2013's survey.

Location	Zone	A	B	C	D	E	F	G	H	I
OS	$\tau_{w,b}$	0.53	0.41	0.35	0.32	0.32	0.41	0.46	0.59	0.62
	u_b	0.36	0.31	0.29	0.28	0.25	0.25	0.27	0.43	0.36
	u_{cr}	0.19	0.19	0.17	0.17	0.20	0.23	0.24	0.17	0.22
	Threshold for bedload	Exceeded	Exceeded	Exceeded	Exceeded	Exceeded	Exceeded	Exceeded	Exceeded	Exceeded
LW	$\tau_{w,b}$	0.45	0.44	0.35	0.35	0.30	0.44	0.45	1.72	1.97
	u_b	0.36	0.31	0.29	0.28	0.25	0.25	0.27	0.43	0.36
	u_{cr}	0.16	0.20	0.18	0.18	0.19	0.25	0.23	0.40	0.56
	Threshold for bedload	Exceeded	Exceeded	Exceeded	Exceeded	Exceeded	Exceeded	Exceeded	Exceeded	Not exceeded
HW	$\tau_{w,b}$	0.52	0.42	3.77	0.44	0.32	0.38	0.37	0.75	1.85
	u_b	0.36	0.31	0.29	0.28	0.25	0.25	0.27	0.43	0.36
	u_{cr}	0.18	0.19	1.24	0.22	0.20	0.22	0.20	0.20	0.53
	Threshold for bedload	Exceeded	Exceeded	Not exceeded	Exceeded	Exceeded	Exceeded	Exceeded	Exceeded	Not exceeded

In reality, a combined flow condition exists. The presence of currents with waves enhance the bed shear stresses that the grains are exposed to. As current measurements during the study period are not available, there is insufficient information to estimate the combined wave-current shear stress. Although bed shear stress under wave-current flows interact non-linearly, using a linear summation approach provides a lower bound of stress that the grains are subjected to and if this exceeds the threshold, then the non-linear interaction which result in even higher stress that are beyond the threshold would further increase sediment transport. Figure 50 depicts the current-only bed shear stress (at ebb tide) from a numerical model in a recent analysis for current flows in the region, as well as the current-only, waves-only shear stresses and the linear addition of the two.

Maximum current-induced bed shear stress is observed in Zone A and in deep water. As Zone A is next to the Poole Harbour mouth which is generally an ebb-dominated tidal inlet, the fast current flows at ebb tides would therefore increase bed friction and yield higher stresses, $\tau_{c,b}$. The bed shear stress imparted by tidal currents represented only about 20% of the total bed shear stress. Given the low tidal current velocities, these alone are unlikely to mobilise sediments, thus stresses from shoaling and breaking waves become the key mechanisms to bring about sediment transport. From this analysis, it shows that waves are the dominant forcing in the inshore zone of Poole Bay.

Table 17 indicates the Dean's parameter (Ω) and its corresponding beach state. In 2013, most parts of the beaches (Zones A to G) indicate the occurrence intermediate beach states with beaches in Zones H and I as reflective beach states. A transformation in Ω is observed for Zones A and G in 2014. Zone A switched from intermediate to dissipative and Zone G from intermediate to reflective.

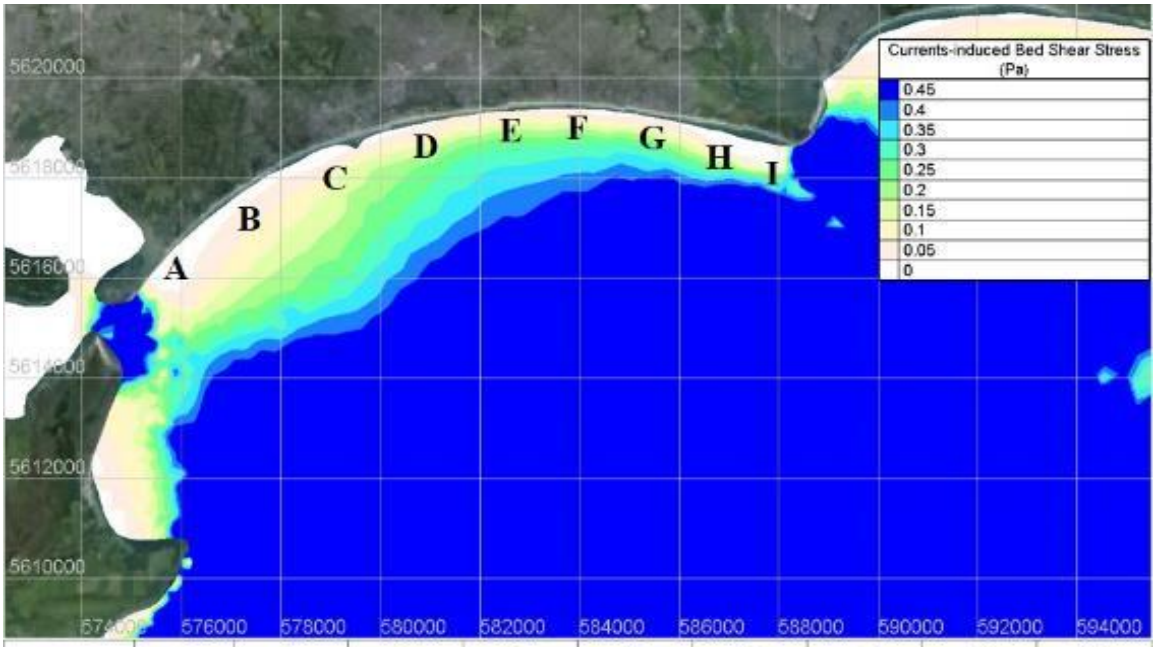

	A	B	C	D	E	F	G	H	I
$T_{w,b}$ (Pa)	0.45	0.44	0.35	0.35	0.30	0.44	0.45	1.72	1.97
$T_{c,b}$ (Pa)	0.21	0.05	0.05	0.10	0.14	0.15	0.18	0.03	0.02
$T_{w+c,b}$ (Pa)	0.66	0.49	0.40	0.45	0.45	0.59	0.64	1.75	1.99

Figure 50 Bed shear stress plot during spring tide (peak ebb) at Bournemouth. $T_{w,b}$ indicates wave-induced bed shear stress, $T_{c,b}$ indicates currents-induced bed shear stress and $T_{w+c,b}$ indicates combined bed shear stress.(Source: Telemac numerical model for Feasibility assessment of constructing a trans-shipment terminal on Bramble Banks)

Table 17 Beach state descriptors (D: Dissipative, I: Intermediate and R: Reflective) of Poole Bay from 2013 to 2014.

Description/ Zone	A	B	C	D	E	F	G	H	I
Dean's parameter, Ω in 2013	3.90	3.64	5.14	4.83	4.23	2.05	2.50	0.99	0.63
Beach State in 2013	I	I	I	I	I	I	I	R	R
Dean's parameter, Ω in 2014	6.84	1.31	2.07	1.04	2.66	1.45	0.90	0.38	0.64
Beach State in 2014	D	I	I	I	I	I	R	R	R

5.5 Statistical results

Given that a large matrix and variables are involved, Principal component analysis (PCA) which is a variable-reduction technique is employed to reduce and identify the key variables that associate between the sediment and wave characteristics. Prior to performing PCA, the suitability of data for analysis was assessed by Bartlett test of Sphericity and the Kaiser-Meyer-Olkin (KMO) measure of sampling adequacy test. The Bartlett Test of Sphericity checks for the hypothesis that the correlation matrix is an identify matrix, *i.e.* all the variables are uncorrelated. A score with significance at 95% ($p<0.05$) led us to reject the null hypothesis and conclude that there are correlations in the data set that are appropriate for PCA. KMO measures the proportion of variance among the variables that might be common variance and range from 0 to 1. A value closer to 1 is ideal for PCA to yield distinct and reliable results. The Bartlett's test of sphericity showed significance at 95%, which reasonably supports the correlation. KMO measured at 0.53 is marginally accepted for the score of 0.50 is the minimum value required for a good PCA (Kaiser, 1974).

The PCA results based on the correlation matrix analysis indicate four principal components with eigenvalues greater than 1, which correspond to an overall cumulative variance of 82.5% (Table 18). The order of significance of these variables is determined by the magnitude of their eigenvalues. The different variables considered in the PCA and their loadings within their respective PCs are presented in Table 19. The higher weighted variables for PC1 consists of the surficial sediment and flow characteristics on mean grain size (Mn), median size (D_{50}), bed shear stress (τ) and sorting (So); PC2 consists of wave properties (significant wave height (Hs) and wave angle (θ)); PC3 consists of properties that give the shape of the sediment size distribution (skewness and kurtosis) and PC4 consists of wave period (T) only. As a rule of thumb, the cut-off for principal components is at the 'elbow' of the scree plot (Figure 51) where the first two PCs are sufficient to describe the essence of the data. Figure 52 shows the component loading plot between PC1 and PC2. The further away these vectors are from a PC origin, the more influence they have on that PC. Mean grain size, D50, sorting, bed shear stress, wave height and angle have large positive loadings on both principal components. Bed shear stress is a function of Hs and grain size therefore suggest that these components primarily measures sediment mobility thus signifying the ability of materials to sort and redistribute in the coastal zone.

Multiple linear regression of these variables is presented in Table 20. It shows variables with significant relationship at $p<0.01$ are bed shear stress with mean grain size ($R = 0.759$); bed shear stress with D_{50} ($R = 0.757$), significant wave height with wave angle ($R = 0.590$), and mean grain size with wave angle ($R = 0.180$). Mean grain size with significant wave height is statistically significant at $p<0.05$ ($R = 0.120$). Given that correlation coefficient for bed shear stress with mean grain size is higher than D_{50}, and earlier section (section 5.1) has suggested the use of mean grain

size, D_{50} will not be pursued further. The relationships of mean grain size and sorting with wave height, wave angle and bed shear stress shall be explored and discussed.

Table 18 Principal components (PCs) for sediment characteristics and forcing factors.

PCs	Eigenvalues	Variance (%)	Cumulative Variance (%)
1	3.396	37.730	37.730
2	1.599	17.767	55.497
3	1.287	14.295	69.792
4	1.145	12.728	82.519
5	0.798	8.866	91.385
6	0.318	3.537	94.923
7	0.278	3.084	98.007
8	0.125	1.389	99.396
9	0.054	0.604	100.000

Table 19 Results of Principal component analysis (rotation method) for the study site. Figures in bold indicate variables which contribute most strongly to the variance.

Variables	PC1	PC2	PC3	PC4
D_{50}	**0.95**	0.03	-0.18	-0.05
Mean grain size	**0.94**	0.01	-0.09	-0.03
Sorting	**0.50**	0.47	-0.33	0.07
Skewness	-0.38	0.03	**0.81**	0.15
Kurtosis	0.01	-0.11	**0.81**	-0.10
Sig. wave height	0.09	**0.82**	-0.13	0.42
Wave angle	0.11	**0.88**	-0.06	-0.28
Wave period	0.02	0.003	0.01	**0.97**
Bed shear stress (wave)	**0.84**	0.35	-0.13	0.13

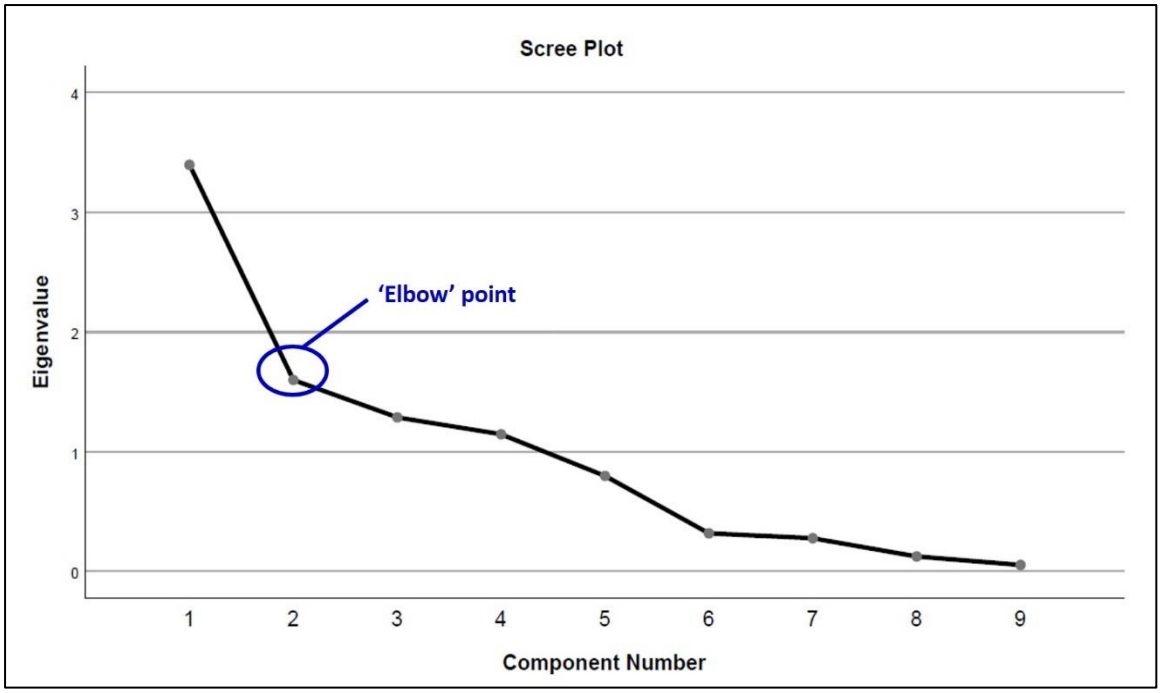

Figure 51 Scree plot displays how much variation each principal component captures from the data. The 'elbow' point that cuts off at Component No. 2 indicates the first two PCs are sufficient to account for most of variance in the original variables.

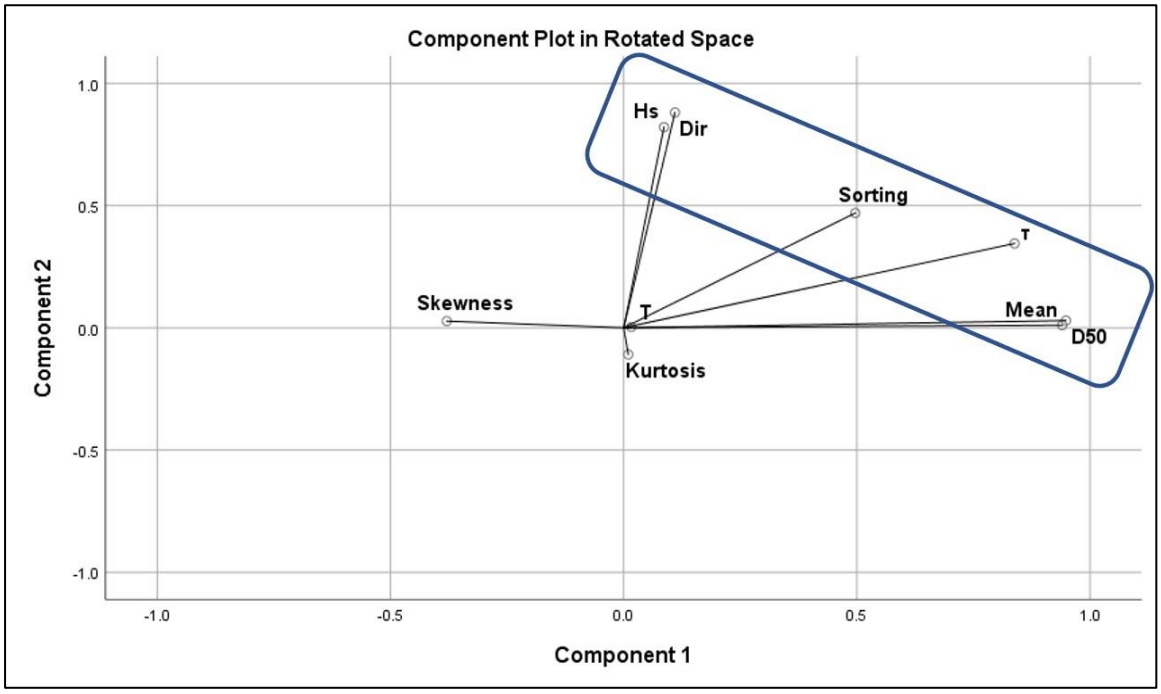

Figure 52 Component loading plot in rotated space. The further away vectors are from a PC origin: the more influence they have on the PC i.e. in this case, Hs, Dir, Sorting, τ, Mn and D_{50}.

*Table 20 Correlation matrix (Pearson's coefficients) between sediment properties and wave characteristics. From multilinear regression analysis, correlation value with ** means significance at p<0.01 and * means significance at p<0.05 (two-tailed test).*

Correlation Matrix								
	D_{50}	Mean	Sorting	Skewness	Kurtosis	Hs	Dir	T
D_{50}								
Mn	0.916**							
So	0.373**	0.316**						
Sk	-0.524**	-0.385**	0.130*					
Kt	-0.092	-0.047	-0.042	0.439**				
Hs	0.123*	0.120*	0.276**	-0.081	-0.127*			
θ	0.197**	0.180**	0.308**	-0.140*	-0.027	0.590**		
T	-0.009	0.003	0.040	0.092	-0.025	0.367**	-0.173**	
τ	0.757**	0.759**	0.538**	-0.359**	-0.173**	0.436**	0.303**	0.079

5.6 Relationship of shortlisted sediment and wave characteristics

Figure 53 defines the relationship between mean grain size and effective bed shear stress experiences at the locations where the mean size exists. The power (exponential) trendline appears to have a closer fit as compared to the linear trendline for it has a higher R^2 value of 0.77. Furthermore, τ is related to wave friction factor (Equation 3.12) which in turn is inversely proportionate to grain size expressed with a power exponent (Equation 3.13). Clustering of data ranges from 3 φ to 0 φ with bed friction below 1.0 Pa. Large number of fines have low critical shear stresses and therefore can be easily mobilised and lost to the turbulent flow even when subjected to low effective stresses. This can be further shown in Figure 54 that majority of the sediments have excess bed shear stress above 0 Pa (i.e. bedload movement threshold has been exceeded). As grain size magnitude increases, higher critical bed shear stress occurred, implying a more agitated environment is necessary to initiate sediment movement for coarser grains. The bivariate histogram in Figure 55 displays the power trend similar to Figure 53, further indicate the relationship between bed shear stress and sediment size as an exponential relationship.

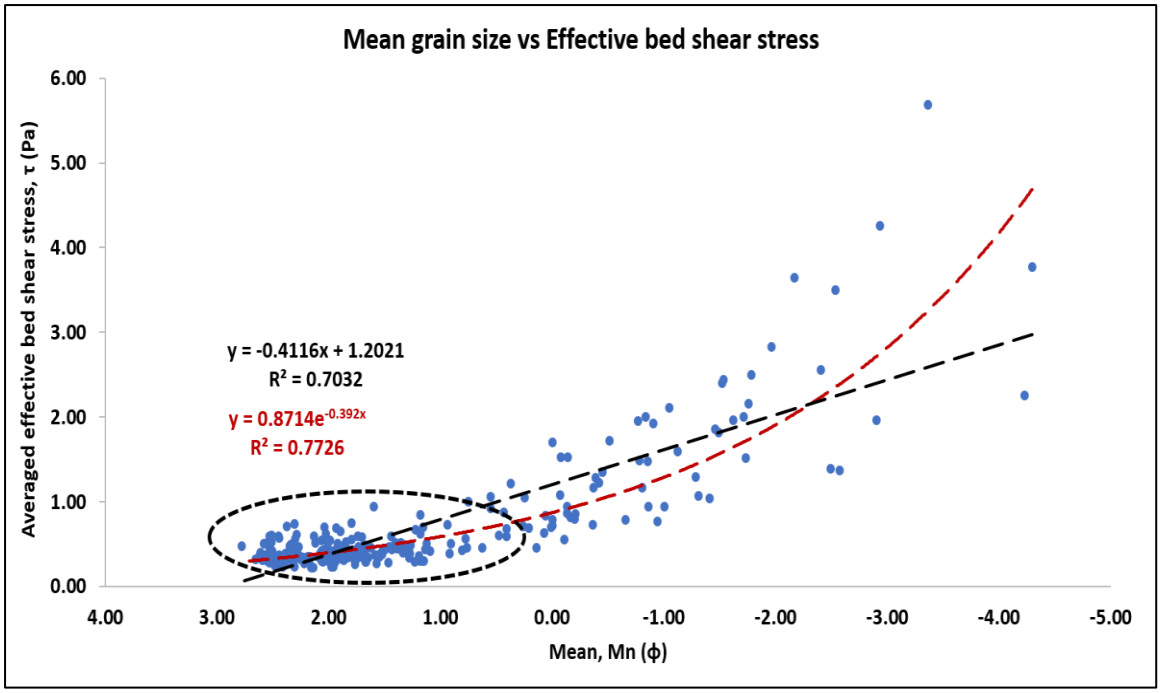

Figure 53 Comparison of Mean grain size with effective bed shear stress (wave-induced)

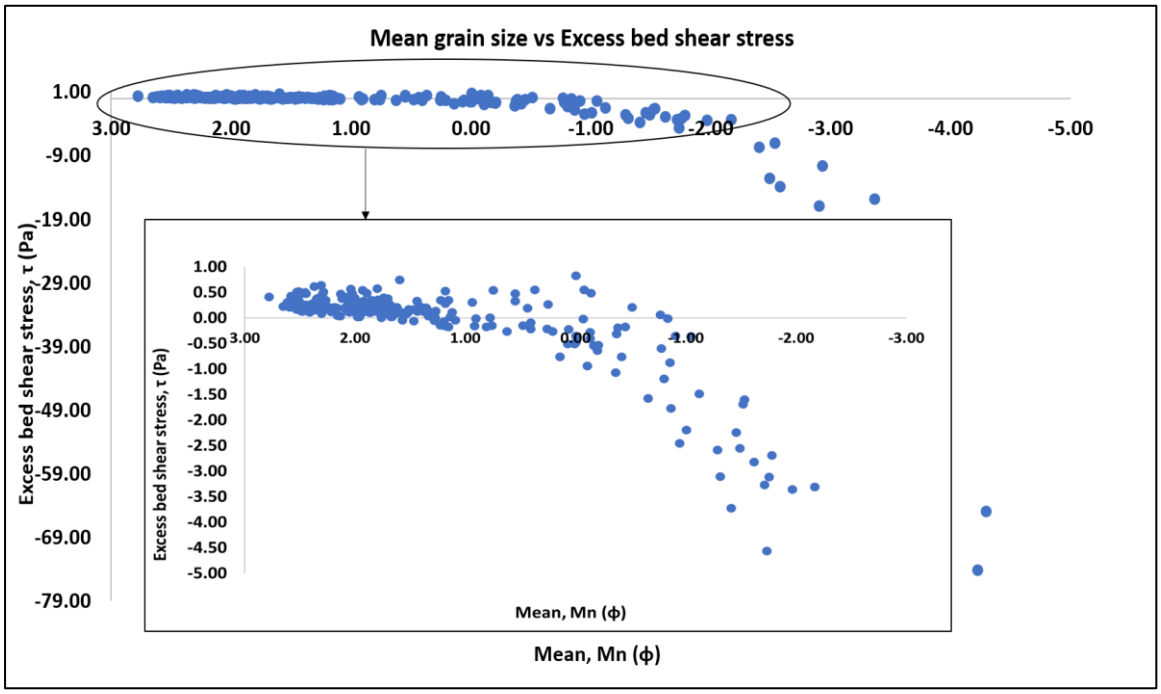

Figure 54 Comparison of Mean grain size with excess bed shear stress

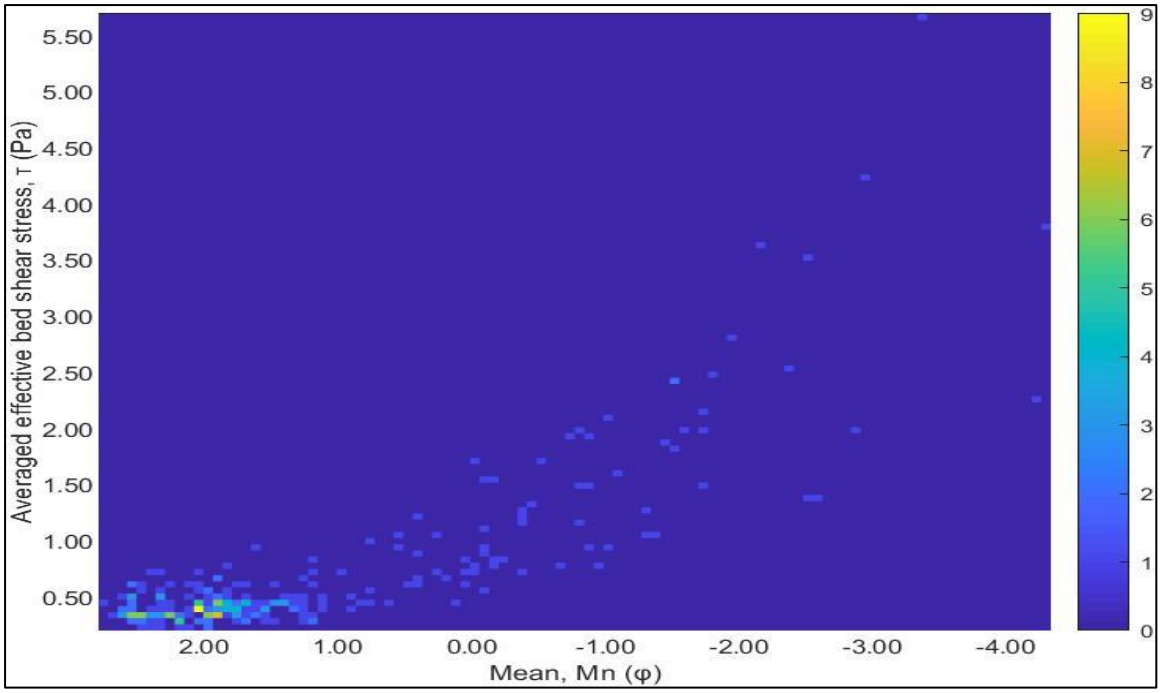

Figure 55 Bivariate histogram displays mean grain size and bed shear stress as a density plot

Figure 56 shows the comparison of wave height with Mn and So. Under the condition of progressively increasing wave height, the grain-size composition is found to be coarser, and more poorly sorted. For wave heights greater than 0.65 m, there is higher occurrence of poorly sorted sediments (red box in Figure 56), implying that under more intense wave conditions, coarse sediment grains can be mobilised more easily, deposition and erosion processes take place more frequently and the mixing between the fine and coarse sediments leads to less homogenous beaches.

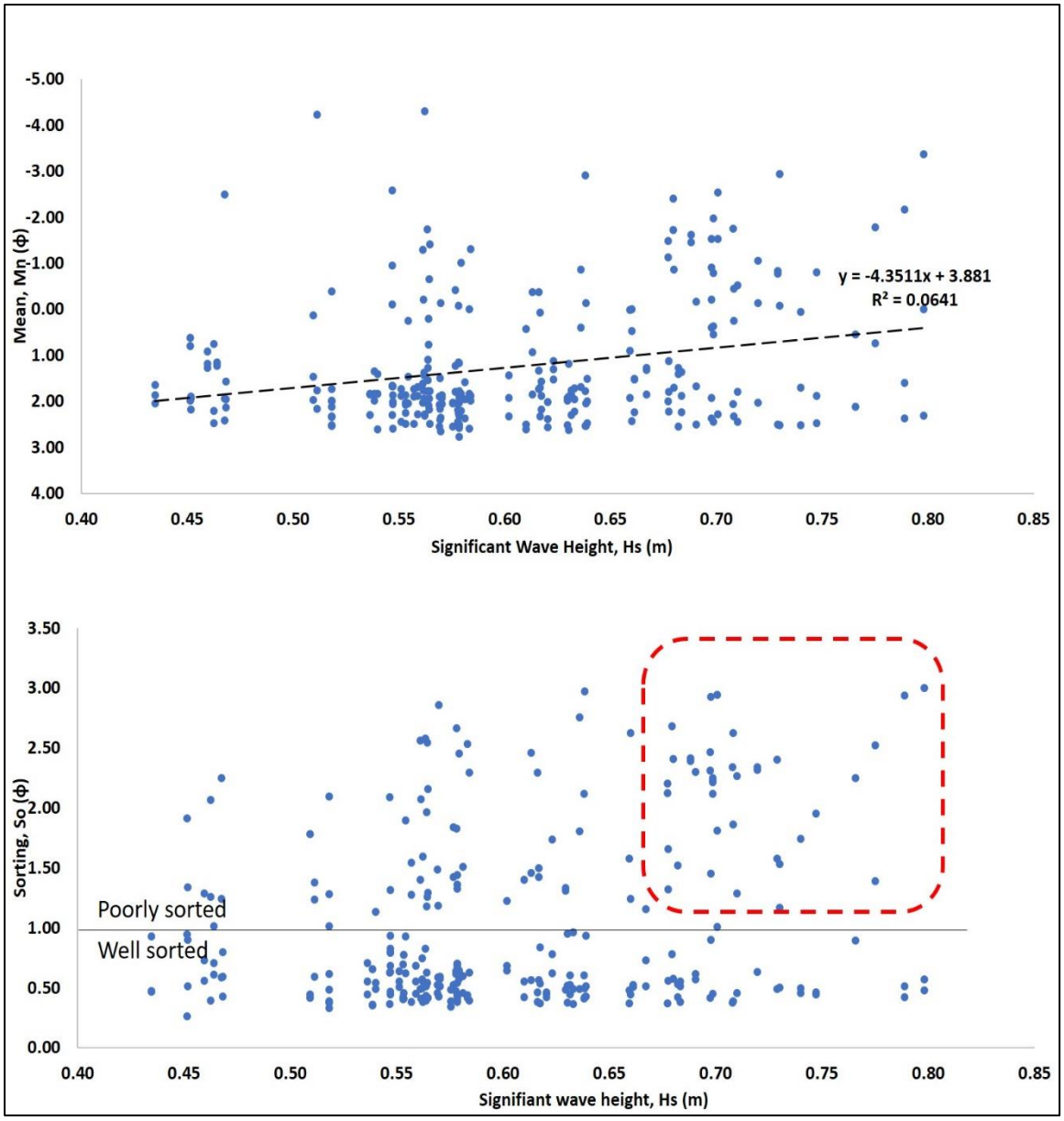

Figure 56 Comparison of mean grain size and sorting with significant wave height

The comparison of Mn and So with θ is given in Figure 57. Sediment size increases from very fine sand to pebble grade with increasing wave angle. For wave angle below 188º, this mainly contributed to sandy sediments (black box). Beyond this angle, coarser grain size tends to occur more frequently (red box). Sorting is weaker where waves approaching the shore at greater than 188º (*i.e.* from south to south west direction) (green box).

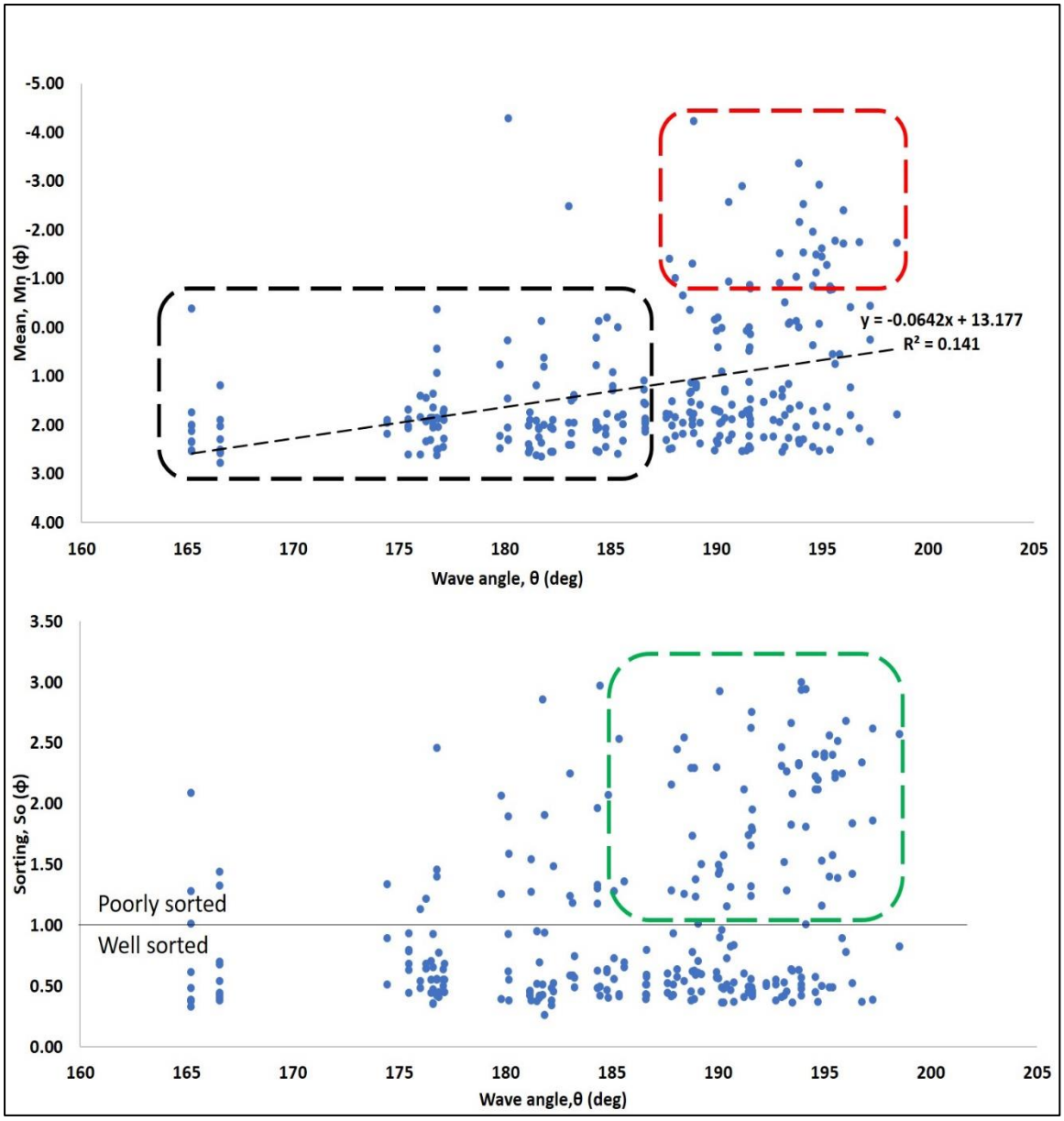

Figure 57 Comparison of mean grain size and sorting with wave angle

6.0 Discussion

This chapter seeks to address the findings described in Section 5, taking into consideration past studies and relevant literature review. In addition, it attempts to clarify the uncertainties in the analysis as well as to review the limitations of this study. The decade-long, annual sediment surveys carried out in Poole Bay compiled over hundreds of samples and the samples demonstrated several relationships amongst the key sediment textural parameters in terms of mean grain size, median, sorting, skewness and kurtosis. The linear, sinusoidal and helical relationships (Folk & Ward, 1957; Lacey, 1985) provide a different perspective in characterising and identifying patterns in the sediment distribution, particularly in more complex situations where surficial sediments vary differently.

6.1 Spatial variability

6.1.1 Alongshore trends

An examination of the alongshore sediment characteristics expresses the offshore region to be uniform with negligible change (average zonal change = ~ 0.055 φ or 0.01 mm). The distribution is moderately sorted and materials are composed of medium sand. These results are logical since the hydrodynamic forcing here is expected to be less energetic compared to shallower and more active depths, hence the sediments are mostly fine graded and have uniform sorting.

Unlike other zones, the sample recovery at Zone I near Hengistbury Head is limited to three occasions (out of the possible 11 annual sampling surveys) due to the presence of jutted bedrocks. The lack of samples can skew the distribution and affect reliability of the results. Results from another study were used for comparison. In Edgell (2008), the mean grain size was 1.77 φ (0.29 mm) at the eastern end of the bay and this equated to 16% increase in the mean grain size of the current study (1.99 φ or 0.25 mm). The sediments for this zone are similarly classified as medium sand and have not varied much since 2008's study, therefore the results and trend of this current study are deemed acceptable even though these are based on 3 annual sampling surveys.

At LW, there is a generic coarsening of grain size to the east (Figure 37). Sorting trend displays a similar upward trend (sorting deteriorated) across the bay as moderately sorted samples in the west became poorly sorted in the east (Figure 38). According to Kraus et al (1999), in a wave dominant environment, sediment transport is driven by longshore current which mostly takes place inside the breaker zone but decreases in magnitude both landwards (to the beach) and seawards to the depth of closure. Poorer sorted environment is due to mixing of sediment populations of different origins (offshore sediments washed onshore or cliff eroded materials). This alongshore grading is attributed by higher wave energy levels (wave energy is related to square of wave height) in the east, causing systematic removal of finer grains offshore by waves. Sorting became poorer after Zone E due to the higher proportion of gravel in the eastern bay (Table 9).

The lower beach at Zone H saw a peak for sediment mean grain size and sorting. This observation is consistent with literature review stating that finer sediments around Southbourne and Solent Beach are less stable and easily mobilised and this is because of the increase in wave exposure and longshore drift in the easterly direction (NFDC, 2017).

Zone I sees a reduction in sediment grain size but improved sorting from other zones. This phenomenon arises from the decrease in the wave height received in this area. The reduction in wave exposure and littoral drift may be explained by the terminal groyne effect at Hengistbury Head. Brampton & Motyka (2015) described that groynes can reduce incident wave energy through reflection and diffraction, thereby acts as a barrier to the littoral drift. Thus, the groyne is presumably to provide some form of shielding and deflects the wave trains. Consequently, more fine-graded materials get accumulated in this area.

Sediments also become coarser in the longitudinal direction at the upper intertidal beach (HW) from Sandbanks to Hengistbury Head. Apparently, HW samples are less sparsely spaced than the LW samples, suggesting that sediment grain size and distribution remained relatively constant. This can be explained by the lower intensity current flow received at HW compared to LW as more energy is dissipated with decreasing water depth. The peak at Zone C indicated the presence of mean grain size of 19.6 mm pebble at Zone C could be a one-off occasion as other surveys sampled sandy sediments. A visit to the beach in Bournemouth (Zone C) during April 2019 also noticed that the beach is mostly composed of fine sands (Figure 58).

Figure 58 Bournemouth Beach masked with fine sandy materials seen across the intertidal zone (Source: Author's photo, taken in Apr 2019).

6.1.2 Cross shore trends

Sediments consistently became coarser and poorly sorted in the seaward direction across the intertidal zone. Sediments then became finer and better sorted beyond LW towards offshore. These suggest the sediment transport in waves as they are re-worked in the cross shore direction: the coarser materials are transported onshore due to higher wave crests in non-linear waves but are unable to mobilise by weaker stresses (due to lower wave troughs) on the downrush, therefore only finer materials are returned offshore (Komar, 1976).The observations are consistent with prior studies by Lacey (1985) and Edgell (2008). The LW exists along the profile which has greater exposure to wave turbulence. As waves are efficient sediment sorter and winnow finer grains from the bed in the most energetic areas by a turbulent process and are carried away to less energetic areas, this results in a coarsening of the bed in more energetic areas (Friedman, 1967), whereas finer sediment is carried furthest and deposited landward or seaward (Lacey, 1985; Komar, 1998). Subsequently, the armour layers (coarse grain setting) has a stabilizing effect on the morphology (Celikoglu, et al., 2006). This can be seen from most of the LW sampled sites that coarser and poorly sorted materials are usually found here.

6.2 Temporal variability

The long-term beach monitoring programme in Poole Bay has benefited a quantifiable understanding of temporal changes in sediment properties. From the longitudinal plots of Figures 37, 40 and 43, there have not been systematic nor consistent changes observed during this period. Fundamentally, changes in sediment grain size can be due to a single or combined factor such as (i) normal hydrodynamic forcing (ii) extreme storm events (ii) human factors (e.g. introducing fresh inputs of coarser or finer size than native materials during beach improvement works). These have been assessed in the following sections accordingly.

6.3 Hydrodynamic influence

The analysis of wave height and angle from the offshore buoy concluded that waves from the south-west affected the inshore for more than 75% of the time. Waves in the inshore environment undergo a change in direction as the wave angle decreases with decreasing wave height to the west due to the sheltering effect along the shoreline (Table 15). This suggests the effect of increasing shelter in the west as waves at Zone A are the least severe. In contrast, Zones G to I appeared to be the most energetic environment with waves approaching from directions from south-west to east. The maximum wave height exceeded 4.0 m in these three areas. Mean Hs at Zone I (0.68 m) is lower than Zone H despite having the highest mean Hs recorded at 4.28 m here. The reduction in wave height can be explained by compounded effects from wave breaking upon the bedrocks and the Long Groyne. Waves were the highest (range from 1.18m in Zone A to 1.56m in Zone I) during the period from December 2013 to February 2014 (Appendix D) due to the severe storms that affected

the entire UK (BBC, 2014). Coastal defences were overtopped and multiple locations (streets, parks and quayside) in Poole and Bournemouth were flooded during that period (Haigh, et al., 2017) .

Davidson et al. (2013) explained that extreme storm events could cause beach profile to be out of equilibrium and extreme changes to the beach volume and sediment conditions, with erosion typically occurring alongside a coarsening of the beach surface. The energetic but destructive forces can bring about mass transport of both fine and coarse materials offshore and after the storm, part of the materials transported offshore returned to the foreshore under normal wave condition. The multiple storm events (and subsequent beach recovery) can produce a more well-sorted composition in the swash zone but poorer sorted offshore. That being said, the storms in 2013/2014 is very likely to cause the huge sediment variability in Zones B and F (also in other zones) since there were no beach nourishment taking place during this period (Note: the next nourishment took place in December 2014).

The difference in hydrodynamic loading has resulted in a regular sorting pattern: environments with higher wave heights (*i.e.* increased wave energy) produce beaches with grains coarser and less well sorted as seen from Figure 56. This outcome also reaffirms the earlier spatial examination that larger sediments coincided with the areas of greater wave heights. In addition, the south to south-westerly waves have more impacts on the sediment size and sorting. These wave directions tend to lead to poorly sorted and coarser sediments.

6.4 Human factors

The impacts of anthropogenic actions on littoral evolution have been acknowledged and documented worldwide (Komar, 1998; Stanica & Ungureanu, 2010). Several beach nourishments are undertaken during the study period, including BIS 4 (https://poolebay.net/bis.html) and nearshore replenishment trial (Mason, 2018). The estimated volume of materials, timing of the works and approximate locations are gathered from different sources (CCO, 2018; NFDC, 2017; Harlow, 2016 and www.PooleBay.net) and summarised in Figure 59. Full details are provided in Appendix E. It is to note that the last beach nourishment record prior to the study period was in 1989.

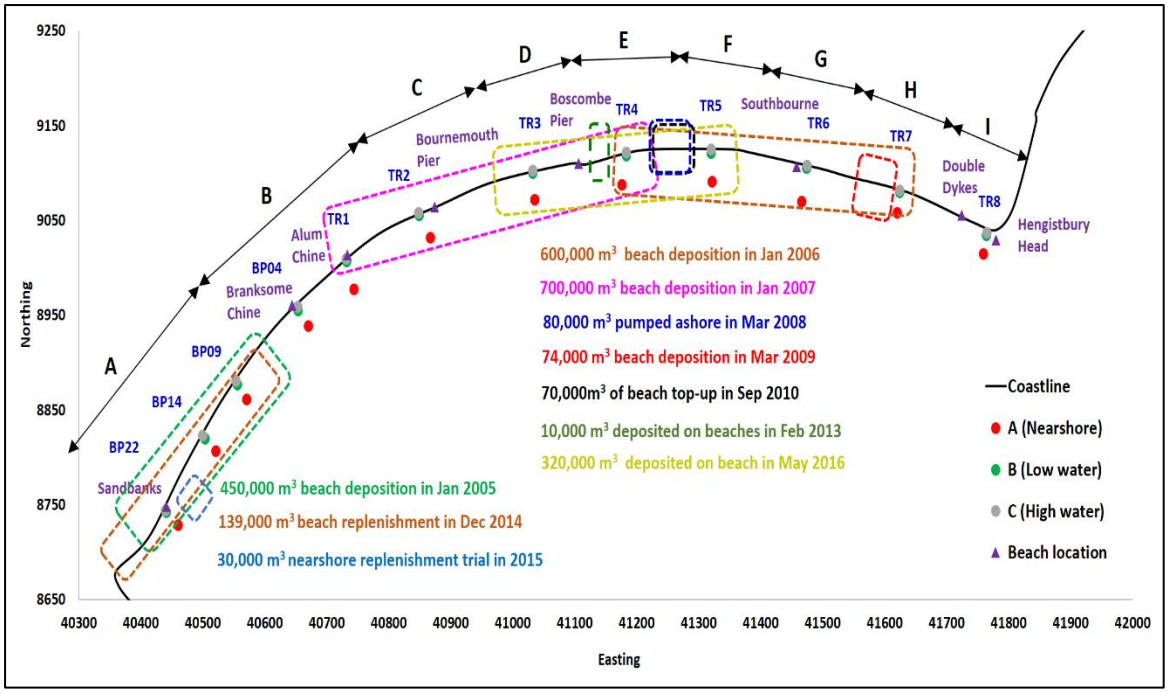

Figure 59 Diagram mapping out beach nourishment works carried out in Poole Bay from 2005 to 2016 (Full details to refer to Appendix E)

The maximum sediment variability (in terms of number of peaks, and differential sediment size between adjacent zones) occurred in LW, followed by HW and then OS. This can be related to beach nourishment since most replenishment works took place directly on the beach. Zones B and H are selected to represent the west and east of the Bay for discussion. The mean grain size relationship with time for these zones are presented in Figures 60 and 61 respectively.

For Zone B, between 2005 and 2006, there was a gain of approximately 20% in its mean grain size (Figure 60). This is likely related to the replenishment that took place in the winter of 2005/2006 that covered Swanage, Poole and Bournemouth. The replenished materials from Poole Swashway and Poole Harbour were coarser (average = 0.53 mm from PSD records compared to native beach materials ranging from 0.24 to 0.32 mm) and more poorly sorted since tidal deltas are less energetic than beaches (Harlow, 2016). The peak in 2014 see almost threefold increase in the mean grain size from previous year was, however, was unable to trace back to any beach nourishment programmes for the works only occurred after the sampling exercise. From 2014 to 2015, there was a reduction in the mean grain size of 58 %. This is possibly triggered by the replenishment works carried out in December 2014. Although no PSD information of the beach fill materials can be found, given that the beach fill materials are from Swash Channel and by assuming these have similar PSD characteristics as 2005 (*i.e.* average = 0.53 mm) the fining of the materials found in Zone B after the beach nourishment can thus be justified.

The beach materials used for 2005/2006 replenishment on Bournemouth ranged from 0.14 to 5.82 mm. Since the deposition on the beach, there has been an increase beach sediment size to the east,

and it is inferred that this transformation is caused by the sorting effects of littoral drift in the easterly direction. Zone H sees an increase of mean grain size for more than 140 % and 300 % at LW and HW (Figure 61). The next peak is observed in 2009 where mean sediment size almost doubled (from 3.90 to 7.63 mm). This can be associated with BIS 4.4 in Mar 2009 where very coarse materials were deliberately used to recharge the site (Harlow, 2016). Contrarily, Mn at OS was 0.27 mm and unaffected by the beach top-up, indicating that coarse beach sediment movement is restricted to intertidal region. A significant increase in the mean grain size from 1.43 mm to 10.28 mm took place between 2013 and 2014. Since there are no nourishment works during this period, the sediment variability is unlikely to have been affected by human intervention, but possibly related to sediment inputs (e.g. pebbles) from cliff erosion by the major storms in 2013/2014 as discussed in Section 6.3.

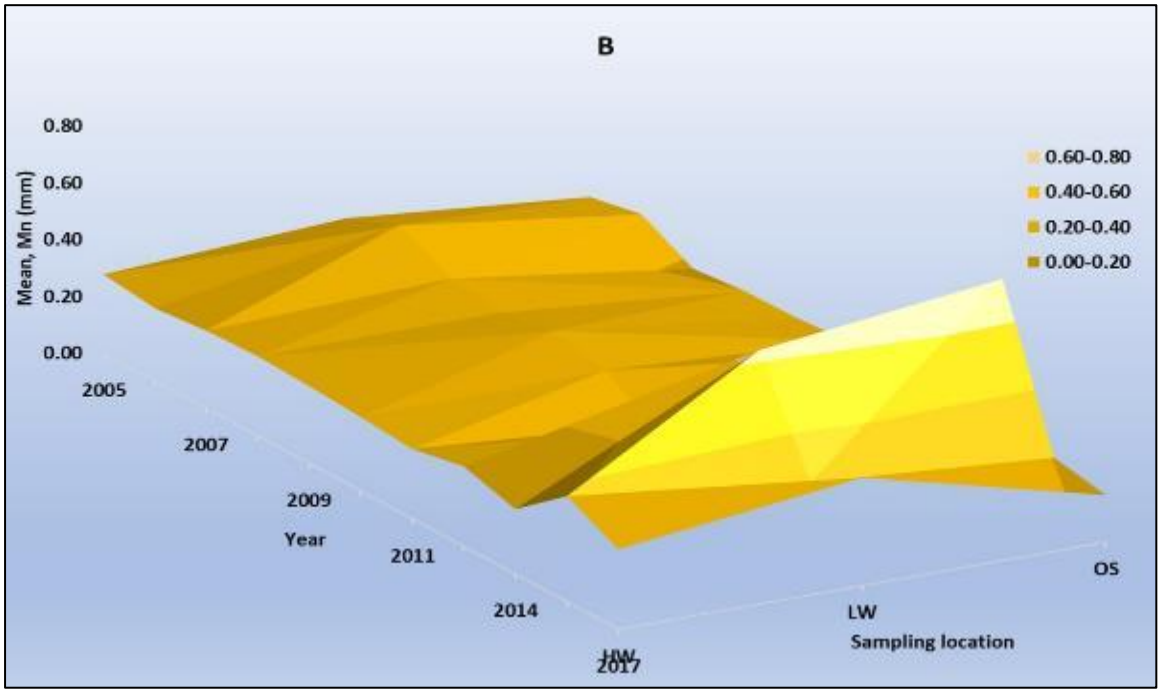

Figure 60 Periodic change in sediment grain size at Zone B in the cross-shore direction

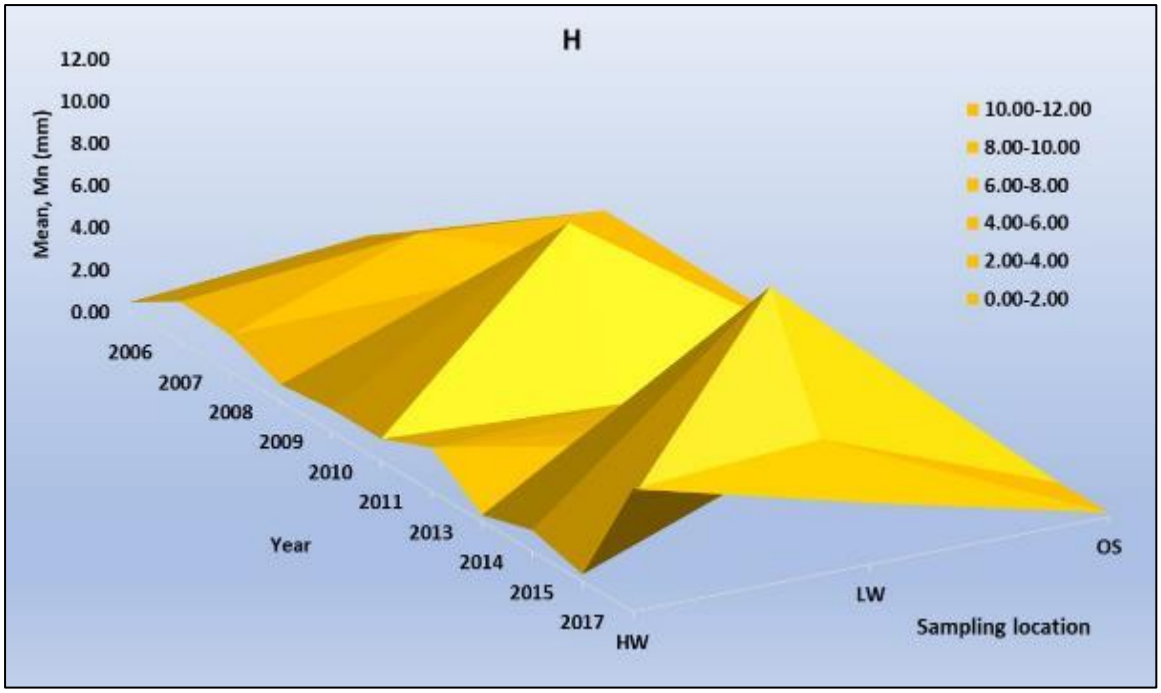

Figure 61 Periodic change in sediment grain size at Zone F in the cross-shore direction

6.5 Significance of beach nourishment fill

The fining of beaches in Poole and Bournemouth has been observed over the past four decades as highlighted in Section 5.1. Taking Zone B for example, the sediment grain size of the beach fill, native beach before and after nourishment are provided in Figure 62. The cumulative effect of the nourished materials has resulted in a downward trend of sediment grain size over time. The normal wave regime (*i.e.* without storms) during the study duration has maintained at a relatively consistent level, however, with sea levels rising (projection up to 1 m sea level rise to year 2105 (Royal Haskoning, 2011)), this will increase the littoral drift and loss of beach sediment. The deficit of sediment can only be compensated for by recharge activities. It is typical to select recharge materials similar to the existing beach textural characteristics to retain the current state. Finer materials can be deposited at the upper beach locations and coarser materials can be placed at a steeper gradient so that they can retain longer on the beach.

Fundamentally, a fine sandy beach is more well-received by public because of aesthetic, recreational, safety and perception reasons, though finer materials hardly retain on the beach as they can be easily winnowed out by currents and blown away by wind (Wong, 2014). For instance, wind-blown sands can accumulate to form dunes at the upper foreshore (e.g. at Hengistbury Head) and can act as a form of protection to the shoreline. But, in anticipation of harsher climate in the future, beaches and dunes will be undermined at a higher and faster rate and regular maintenance will be required although this is not sustainable. To lengthen the beach nourishment life span, fill material should be slightly larger than the in-situ material (Van Rijn, 2014). In this case, Zone B has an equivalent grain size of 0.28 mm at HW and 0.38 mm at LW (both medium sand) in 2016, the

selection of fill material is suggested to select from the next tier of sediment size *i.e.* coarse sand ranging from 0.50 to 1.0 mm. It is to note that the nourishment in 2006, 2007 and 2014 have adopted grain size about 0.53 mm or less. Therefore, the subsequent nourishment may adopt a coarse grade sand that is larger than 0.53 mm to coarsen the beach profile. However, too coarse a material may invite negative feedbacks, and is an area that coastal managers planning for the next BIS would need to consider striking a balance between public perception and practicality.

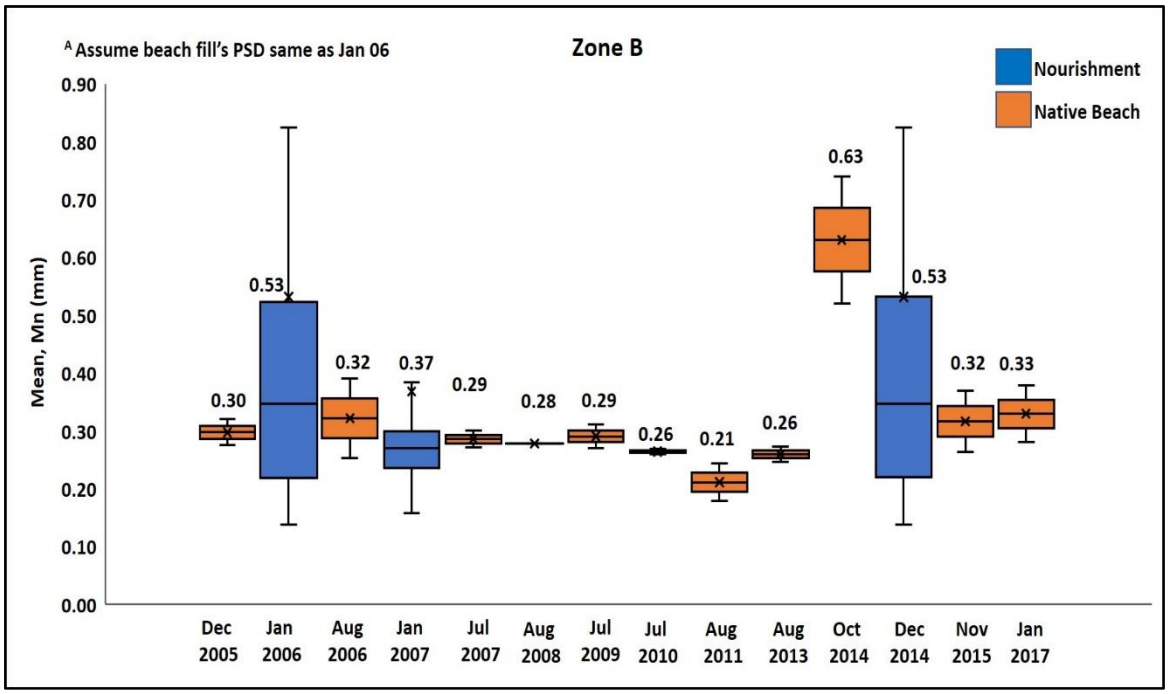

Figure 62 Changes in mean grain size at low water position of Zone B due to beach nourishment works. Orange bar refers to the range and average sediment size found on the native beach and blue bar refers to the fill materials used. The introduction of nourished materials has a direct impact on the mean grain size and resulted in an increase or decrease in beach grain size.

6.6 Morphological predictions

The morphological prediction of a beach using the relationship between grain size parameters and wave characteristics through the non-dimensional fall velocity can yield a qualitative understanding of the conditions that closely associate with each state (Dean, 1973; Wright & Short, 1984; Masselink & Short, 1993). It is well understood that sediment sizes determine the fall velocity at which the grains will return to the bed. Finer sediments will have a slower sediment fall velocity than grains that are coarser, thus beaches with finer sediments will drive beach evolution to more dissipative and coarser materials drives to an intermediate/reflective beach state. The same changes can also be caused by variations in wave height. An increase in wave height tend to lead to dissipative beach and lower wave intensity lead to a more reflective form.

In 2013, the beaches in Poole and Bournemouth were mostly in intermediate states (Ω = 1 to 6) but become reflective (Ω <1) nearer to Solent Beach and Hengistbury Head. In 2014, Zone A is reclassified as dissipative, Zone B to F remained as intermediate forms and Zone G and I are termed

as reflective states. The differences lie in Zone A when it transformed from intermediate to dissipative state meaning that the beach is characterised by finer sediments and the sub-tidal profile becomes flatter and has less features; also in Zone G where the beach became reflective and constituted of coarser materials.

Since beaches to the east of Poole Bay are typically coarse-grained beaches, it is foreseeable for beaches to be reflective. However, the area is also under exposure to larger waves and this is contrary to the morphological evolution of becoming more dissipative. According to Prodger (2017), larger waves can cause erosion of the bed and carry the finer sediments further seaward, which leave the larger grain size materials behind on the beach. The larger pores between coarse sediments result in greater percolation and less backwash. Also, coarse material has higher angle of repose and develop a beach slope with steeper gradient. This then restricts the development of dissipative states, resulting in a more reflective beach as what is observed from Zones G to I. The reverse is true for the flatter, less permeable and finer grained beaches in Poole and Bournemouth where backwash volume is greater and these beaches are more towards the dissipative end.

The temporal variations are also related to the change in beach profile. The beach profiles of Zones A, D and I which represent the west, center and east of the bay from 2013 to 2016 are provided in Figure 63. Zone A shows low sloping including two to three shore-normal bars and troughs. It displays a dissipative-intermediate characteristic which is correctly described by the dimensionless fall velocity. In 2013, the beach has a shallow slope of about 1:20 and a bar at around 45 m from the shoreline. While in 2014, there is a 0.5 m drop at the 0 m mark which signified the erosion of beach crest and draw-down of materials by storm waves from the 2013/2014 winter storms. Several bars are formed nearer to the shore showing signs of initial phases of beach recovery from onshore transport of materials. In 2015, there is an significant increase in the beach volume and these materials are reworked and redistributed in the cross-shore direction into a gentle sloping beach. Zone D concerns an intermediate beach characterised by approximately 1:50 flat profile. An offshore bar was present at around 120 to 140 m away from the shore in 2013. It became less distinctive and shifted nearer to the shore in 2014, a sign of beach recovery similar to Zone A. The beach has not undergone much changes from 2015 to 2016. In contrast, Zone I showed a steep cliff profile that is fronted by a flat and relatively featureless beach, fully exemplifying the reflective beach state. A well-defined wide berm of approximately 2 m height is observed before the profile stepped down into the almost linear gradient in the nearshore zone. The berm receded in size in 2015 before finally faded away into the offshore zone in 2016.

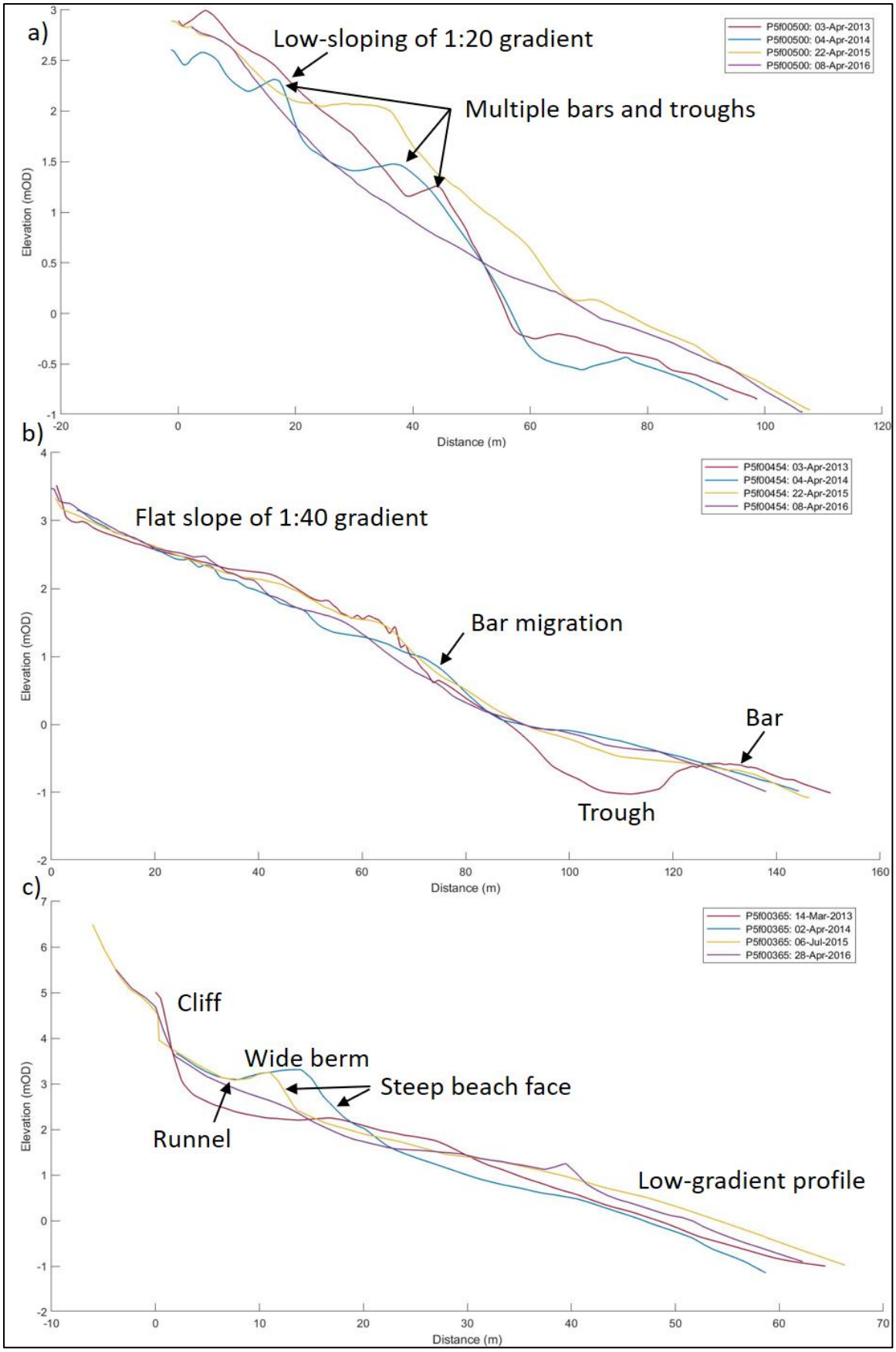

Figure 63 Beach profiles for a) Zone A; b) Zone D and c) Zone I depicting the dissipative, intermediate-dissipative and reflective beach states respectively and their temporal variability from 2013 to 2016.

6.7 Limitations and uncertainties

6.7.1 Data coverage

The coverage and reliability of the data are critical to produce representative results for this study. The study area spans from Sandbanks to Hengistbury Head, although there have been intensive monitoring works along the Bournemouth frontage, there is a shortage of survey coverage for the beaches along the Poole frontage. Only two years of annual sediment surveys were conducted as opposed to eleven years of records from the Bournemouth frontage. Quantifying for the spatial and temporal changes in sediment characteristics, particularly for the western bay has thus been challenging due to limited information.

The sampling site is an important determinant for the analysis of sediment textural characteristics. Sampling was carried out at fixed locations previously, even though the mean high water and low water positions vary from time to time. In fact, the survey in 2009 conducted sampling at both fixed locations and the actual MLW and MHW found substantial discrepancies (CCO, 2009). The deviation in mean grain size at Profile TR6 (near Southbourne) was 83%: the fixed LW location sampled a poorly sorted, very coarse sand sample while the actual low water sampled a well sorted medium sand sample. Whether or not the samples between 2005 and 2008 (whose results are based on samples taken at fixed locations) reflects the actual sediment characteristics at high and low tidal conditions contains a certain degree of uncertainty. The existing practice to sample based on the positions of high water and low water of the sampling day is more accurate and reasonable (CCO, 2017).

6.7.2 Nearshore conditions uncertainties and model assumptions

Another limitation is the uncertainties in estimating inshore wave data using the simple approximation method. To better predict nearshore conditions and parameterise hydrodynamic forcing, numerical modelling would be necessary. Phase-averaged wave models (e.g. SWAN) that are based on energy balance equation on source terms can be used to transform offshore wave directional spectra to inshore spectra, with the use of wind and geographical information (e.g. bathymetry and topography) (TUDelft, 2017). It accounts for processes of wave generation by wind, dissipation due to whitecapping, wave refraction and diffraction, bottom friction and depth-induced wave breaking (Ris, et al., 1994). Due to limited timeframe of this study and wind field information are not available, a simple approximation method using the nearshore model from CoastalTools is adapted instead. Also, calibration works are limited to measurements from a nearshore buoy at Boscombe Pier only.

Wave period is an intrinsic property of a wave and will thus not readily change through shallow or intermediate water wave transformation. Inshore wave period is assumed the same as offshore waves in the model, however, a comparison between the measured wave periods of offshore and

nearshore wave buoys indicated a deviation ranging from 10 to 15%. The inshore wave period is eventually based on the measured wave period from the nearshore buoy at Boscombe, but the same wave period is assumed throughout the entire bay. This may not be true due to the irregular shallow water deformation of nearshore waves along the long span of coastline (Mizuguchi, 1982). The mean wave period is an important variable that controls sediment sorting on the beach (Medrek, et al., 2015). Thus, the assumption of constant value can affect the statistical analysis in determining the principal controlling factors to a certain extent.

6.7.3 Tidal effects

So far, the study has only considered hydrodynamic forcing in terms of wave properties. Currents generated by tides can be important in areas (e.g. estuary, tidal inlets) where tidal influence is significant (Figure 50). The analysis of the bed shear stress has shown that tidal effects can be extensive in Zone A due to its close proximity to the Poole Harbour entrance. However, for the rest of the bay, tidal effects are proven to be rather minimal. Besides, there is a need to account for the combined current-waves stresses and non-linearity effects on hydrodynamic forcing (e.g. wind-induced and tidal residual currents, wave setup and setdown due to breaking waves) as these affect the mean elevation of water level.

7.0 Recommendations for future studies

This research project is an initial analysis on the hydrodynamic influence on the sediment variability in Poole Bay. The following are some suggestions and improvements to enhance the research.

i) Nearshore hydrodynamic forcing

The use of numerical models such as SWAN (TUDelft, 2017), WAVEWATCH III (Tolman, 1997) to simulate the nearshore zone is beneficial to accurately parameterise the inshore hydrodynamic conditions. Calibration and validation works should expand beyond Boscombe wave buoy. Site deployment to measure the inshore hydrodynamic conditions can be undertaken at the two ends of Poole Bay (Sandbanks and Hengistbury Head) and used to calibrate the model. For a more regional-based model, calibration works can further be extended to the nearby Milford and Swanage buoys.

ii) Sediment sampling surveys

For a more comprehensive analysis of the entire bay, more sampling at Poole frontage is required. Routine sampling surveys should include Sandbanks to Alum Chine (Poole frontage) as the current annual survey run by CCO only covers Alum Chine to Hengistbury Head (Bournemouth frontage). In addition, a more regular sampling such as quarterly interval is more beneficial to capturing the dynamics of sediment characteristics.

Abnormalities in the sediment analysis can easily skew the distribution and misrepresent the trend. It is suggested that surveying team to include the sample & site description and pictorial documentation so that subsequent analysis can easily identify and exclude any outliers.

iii) Seasonal effects

Seasonal effects have not been considered in this study since most samples are collected are between August to November (calmer weather). It is worth investigating the effects of seasonality a more complete study in sediment dynamics in Poole Bay.

8.0 Conclusions

An 11-year dataset of sediment sampling and waves from 2005 to 2016 along the frontage and in the offshore of Poole Bay has been collated. An investigation was set out to examine the influence of hydrodynamics on sediment variability in this region. The sediments across the nearshore zone are classified as medium sand, poorly sorted, coarse skewed and leptokurtic distribution. Two-third of the samples exhibited unimodal distribution and are largely made up of sandy materials with gravel content varying between 2% to 29 %.

This study explored both magnitude and potential drivers behind the spatial and temporal variability in sediment grain size and sorting. The longshore and cross-shore spatial sediment trends were assessed. The key observations are as follows 1) At the swash zone (for both LW and HW), sediments were found to consistently become coarser and less well sorted to the east of the bay. Offshore samples, however, do not display this trend. The degree of sediment sorting is controlled by the sand-gravel content in the sample composition. Therefore, samples that contained higher gravel content, e.g. in Solent beach, tend to display poorer sorting than the lower gravel content samples, e.g. in Sandbanks. 2) In the direction transverse to the shore, sediments became coarser and more poorly sorted in the seaward direction across the swash zone up to LW position with peak sediment sizes observed on the lower beach. 3) Although the sediments coarsened up to LW, further offshore from this point, sediments were significantly finer and better sorted than the surface samples collected from the swash zone. The temporal changes in sediment size and sorting exhibited relatively high degree of variability, attributed to differing hydrodynamic loading and anthropogenic interference which promoted further winnowing and distributing of the materials across the beach.

Analysing the nearshore waves indicated that the sheltering effect becomes more prominent to the west. Waves that reach the western inner bay have lower wave heights and since wave energy is proportional to the square of wave height, this area received lower energy levels compared to the central or eastern bay. The increase in wave angle from west to east implies that the littoral drift is also in this direction. Bed friction induced by wave currents have a high tendency to mobilise sediments from the seabed as the thresholds for bedload sediment movement were exceeded for more than 80% of the time, suggesting a considerable amount of sediment transport in the nearshore region.

Multivariate analysis identifies the principal controlling factors between the sediment characteristics and wave parameters are mean grain size, sorting, bed shear stress, significant wave height and wave angle. Grain size and wave-induced bed shear stress can be described as an exponential function. Large number of fines which are subjected to lower bed shear stresses can be easily displaced by turbulence under suitable energy environment. Mean grain size is linearly correlated to significant wave height. Coarser and poorly sorted sediment distribution occurs more when Hs is above 0.65 m. This translates to how the exposure to higher waves in the eastern coast has led to a more mixed composition of sand

and gravel which was evidently shown in the particle size distribution analysis. Wave direction also has a bearing on the sediment characteristics. The prevailing south and south easterly waves are the ones that arrive to the western end of the bay and the south-westerly waves reaching the other end. Understanding the beach states also help to interpret the effects of hydrodynamic and beach morphological change over time.

Despite various shortcomings, the study has shown the response of the nearshore zone to sediment and morphological change is stimulated by hydrodynamic (wave) regime to a large extent. There is a close correlation between textural parameters and wave properties. On the basis of the data shown and observations made, it is certain that increasing wave height and direction accelerates the longshore drift from west to east, resulting in higher rates of sorting and winnowing out the finer grains from the intertidal zone seawards. Consequently, the grain increases in size to the east. Anthropogenic factors must also be considered since introducing fresh sediments into the system can disrupt but also can restore the beach equilibrium state. Beach fining is observed over the years therefore using a larger material grade could help to regain the initial condition and also strengthen the beach's ability to defend against sea level rise and stormier events.

9.0 References

Bascom, W. N., 1959. The Relationship Between Sand Size and Beach Face Slope. American Geophysical Union Transactions, 32(6), pp. 866-874.

BBC, 2014. 10 key moments of the UK winter storms. London: BBC.

BCP Council, 2019. Beach Management Scheme: A 17-year plan to protect Bournemouth's coastline during 2015 to 2032. [Online]
Available at:
https://www.bournemouth.gov.uk/AttractionsLeisure/BeachesandWaterfront/BeachManagementScheme/BeachManagementScheme.aspx
[Accessed 14 Jun 2019].

Berkhoff, J. C., 1972. Computation of combined refraction–diffraction. Vancouver, 13th International Conference on Coastal Engineering, pp. 471-490.

Bevis, K. A., 2013. The Geology of Sedimentary Rocks. [Online]
Available at: http://intheplaygroundofgiants.com/geology-of-the-grand-canyon-region/the-geology-of-sedimentary-rocks/
[Accessed 21 Aug 2019].

Bird, E., 1984. Coasts: An Introduction to Coastal Geomorphology. 3rd ed. Canberra: National Univ. Press.

Blott, S. J. & Pye , K., 2001. Gradistat: A grain size distribution and statistics package for the analysis of unconsolidated sediments. Earth Surface Processes and Landforms, 26, pp. 1237-1248.

Brampton, A. H. & Motyka, J. K., 2015. The effectiveness of groynes. In: Shoreline Protection. s.l.:Institution of Civil Engineers, pp. 111–123.

Bray, M. J., Carter, D. J. & Hooke, J. M., 1991. Coastal sediment transport study, Portsmouth.

Briggs, D., 1977. Particle size analysis. Sources and methods in geography: Sediments. pp. 55-110.

Brompton, A. H., Evans, C. D. R. & Velegrakis, A. F., 1998. Seabed sediment mobility study - West of the Isle of Wight, Project Report PR 65, London: CIRIA.

Bryant, E., 1979. Comparison of computed and observed breaker wave heights. Coastal Engineering, Volume 3, pp. 39-50.

Bui, E. N., Mazullo, J. & Wilding, L. P., 1990. Using quartz grain size and shape analysis to distinguish between aeolian and fluvial deposits. Earth Surface Processes and Landforms, 14, pp. 157-166.

CCO, 2005. Regional Coastal Monitoring Programme: Boscombe Annual Wave Report. [Online]
Available at: http://www.channelcoast.org/reports/
[Accessed 25 Jul 2019].

CCO, 2009. Southeast Strategic Regional Coastal Monitoring Programme - Bournemouth Sediment Sampling , Bournemouth: CCO.

CCO, 2017. Bournemouth Sediment Sampling 2016, Bournemouth: Southeast Regional Coastal Monitoring Programme.

CCO, 2018. Southeast regional coastal monitoring programme. [Online]
Available at: http://www.channelcoast.org/southeast/
[Accessed 21 Aug 2019].

Celikoglu, Y., Yuksel , Y. & Kabdas¸lı, S. M., 2004. Longshore sorting on a beach under wave action. Ocean Engineering, 31, pp. 1351-1375.

Celikoglu, Y., Yuksel, Y. & Kabdasli, M. S. ., 2006. Cross-shore Sorting on Beach under Wave action. Journal of Coastal Research, 22(3), pp. 487-501.

Cooper, N., Hooke, J. M. & Bray, M. J., 2001. Predicting coastal evolution using a sediment budget approach: a case study from southern England. Ocean & Coastal Management, 44, pp. 711-728.

Cornish, V., 1898. On sea beaches and sand banks. The Geographical Journal, 11(5), pp. 528-543.

Davidson, M., Splinter, K. & Turner, I., 2003. A simple equilibrium model for predicting shoreline change. Coastal Engineering, 73, pp. 191-202.

Dean, R.G., 1973. Heuristic models of sand transport in the surf zone. Engineering dynamics in the surf zone. Coastal Engineering. pp. 208-214

Duncan, J. R., 1964. The effects of water table and tidal cycle on swash–backwash sediment distribution and beach profile development. Marine Geology, 2, pp. 186-197.

Dyer, K. R., 1986. Coastal and Estuarine Sediment Dynamics. Chichester: John Wiley & Sons, Ltd.

Edgell, 2008. An analysis of particle size distribution trends associated with an artificially nourished beach and implications for future fill selection, Bournemouth UK. Southampton: University of Southampton.

EU Our Coast, 2015. Long-term monitoring programmes for more effective coastal planning, Bournemouth - UK. [Online]
Available at:
http://discomap.eea.europa.eu/map/Data/Milieu/OURCOAST_048_UK/OURCOAST_048_UK_Case_LongTermMonitoringBournemouth.pdf
[Accessed 8 Jul 2019].

Folk, R. L., 1954. The distinction between grain size and mineral composition in sedimentary-rock nomenclature. Journal of Geology, 62, pp. 344–359.

Folk, R. L. & Ward, W. C., 1957. Brazos River bar: A study in the significance of grain size parameters. Journal of Sedimentary Petrology, 27(1), pp. 3-26.

Friedman, G., 1961. Distinction between dune, beach and river sands from their textural characteristics. Journal of Sedimentary Petrology, 31(2), pp. 514-529.

Friedman, G. M., 1967. Dynamic processes and statistical parameters compared for size frequency distribution of beach and river sands. Journal of Sedimentary Research, 37(2), pp. 327-354.

Giraldo, D. F. M., 2015. Controls on the evolution of mid-latitude continental shelf bedforms. Southampton: University of Southampton.

Gourlay, M. R., 1968. Beach and dune erosion tests, Delft: Delft Hydraulics Laboratory.

Gourlay, M. R. & Apelt, C. J., 1978. Coastal Hydraulics and Sediment Transport in a Coastal System. 1st ed. Queensland: Dept. of Civil Engineering, University of Queensland.

Haigh, I. D. et al., 2017. An improved database of coastal flooding in the United Kingdom from 1915 to 2016. Scientific Data, 4, pp. 1-10.

Halcrow, 1999. Poole and Christchurch Bays Shoreline Management Plan, Report to Poole Bay and Christchurch Bay Coastal Group Volume 2: Physical Environment.

Halcrow, 2004. Poole Bay & Harbour Strategy Study Technical Annex 9 - Sources of Beach Recharge Material, Poole: Poole Bay & Harbour Coastal Group.

Harlow, D. A., 2005. Bournemouth Beach Monitoring, Bournemouth : Bournemouth Borough Council.

Harlow, D. A., 2012a. Bournemouth Beach Monitoring, Chapter 1: Introduction, Bournemouth: Bournemouth Borough Countil.

Harlow, D. A., 2012b. Bournemouth Beach Monitoring, Chapter 5: Beach Profiles, 1974 to 2012, Bournemouth: Bournemouth Borough Council.

Harlow, D. A., 2013. Future replenishment in Poole Bay. [Online]
Available at: https://scopac.org.uk/wp-content/uploads/2018/11/Dave_Harlow-compressed.pdf
[Accessed 25 Feb 2019].

Harlow, D. A., 2016. Bournemouth Beach Monitoring, Chapter 9: Particle Size distribution of one-off sampling sites, Bournemouth: BCP.

Harlow, D. A., 2017. Bournemouth Beach Monitoring, Chapter 8: Particle Size Distribution of Native Beach, Bournemouth: BCP.

Harlow, D. A. & Cooper, N. J., 1995. Coastal management: putting policy into practiceBournemouth Beach Monitoring: The first twenty years. London: Thomas Telford.

Hervouet, J. M. & Bates, P., 2000. The telemac modelling system special issue. Hydrol. Process, 14, pp. 2207–2208.

Hodder, J. P. D., 1986. Coastal Sediment Processes in Poole Bay with Particular Reference to the Bournemouth Beach Renourishment of 1974/75. Southampton: Department of Civil Engineering, University of Southampton.

Horn, D. P., Li, L. & Holmes, P., 2003. Measurement and modelling of gravel beach groundwater response to wave run-up. New York, pp. 121-146.

HR Wallingford, 2003. Poole Bay and Harbour Strategy Study: Computational Model Studies., Bournemouth.

Inman, D.L., 1952. Measures for describing the size distribution of sediments. Journal of Sedimentary Petrology, 22, pp. 125–145.

Kaiser, H. F., 1974. An index of factor simplicity. Psychometrika, 39(1), pp. 31-36.

Kakinoki, T., Tsujimoto, G. & Uno, K., 2010. Grain size sorting in the swash zone on unequilibrium beaches at the timescale of individual waves. Shanghai, Coastal Engineering Proceedings.

Kana, T. W. & Ward, L. G., 1980. Nearshore suspended sediment load during storm and post-storm conditions. Seventeenth Coastal Engineering Conference, 2, pp. 1158-1174.

Kirk, R. M., 1980. Mixed sand and gravel beaches: morphology, processes and sediments. Physical Geography, 4, pp. 189-210.

Komar, P. D., 1976. Beach Processes and Sedimentation. Englewood Cliffs, NJ: Pearson.

Komar, P. D., 1998. Beach morphology and sediments, Beach processes and sedimentation. Second Edition ed. s.l.:Prentice Hall.

Krumbein, W. C., 1934. Size frequency distributions of sediments, Journal of Sedimentary Petrology, 4(2), pp. 65-77.

Krumbein, W.C., 1938. Size frequency distribution of sediments and the normal phi curve. Journal of Sedimentary Petrology, 8, pp. 84–90.

Kurain, N. P., Baba, M. & Shahul Hameed, T. S., 1985. Prediction of nearshore wave heights using a refraction programme. Coastal Engineering, 9, pp. 347-356.

Lacey, S., 1985. Coastal Sediment Processes in Poole and Christchurch Bays and the Effects of Coast Protection Works, Southampton: University of Southampton.

Lelliott, R. E. L., 1989. Evolution of the Bournemouth defences. Bournemouth: Thomas Telford.

Manly, B. F. J., 1997. Multivariate Statistical Methods: A Primer. 2nd ed. London: Chapman and Hall.

Martins, L. R., 1965. Significance of skewness and kurtosis in environmental interpretation. Journal of Sedimentary Petrology, 35(3), pp. 768-770.

Mason, T., 1997. Hydrodynamics and sediment transport on a macro-tidal, mixed (sand and shingle) beach, Southampton.

Mason, T., 2018. Trialling a new approach to beach replenishment in Poole Bay, Bristol: Environmental Agency.

Mason, T., Voulgaris , G., Simmonds, D. J. & Collins, M. B., 1997. Hydrodynamics and sediment transport on composite (mixed sand/shingle) and sand beaches: A comparision. Coastal Dynamics, pp. 48-51.

Masselink, G. & Short, A. D., 1993. The effect of tide range on beach morphodynamics and morphology: a conceptual beach model. Journal of Coastal Research, 9(3), pp. 785-800.

May, V. J., 1990. Replenishment of the Resort Beaches at Bournemouth and Christchurch, England. Journal of Coastal Research, 6, pp. 11-15.

Medrek, K. et al., 2015. Impact of wave action on the structure of material on the beach in Calypsobyen (Spitsbergen). [Online]
Available at: https://meetingorganizer.copernicus.org/EGU2015/EGU2015-11496-3.pdf
[Accessed 11 September 2019].

MIKE, 2019. Modelling all aspects of sediment processes in 1D, 2D and 3D. [Online]
Available at: https://www.mikepoweredbydhi.com/products/mike-21/sediments
[Accessed 23 Mar 2019].

Mizuguchi, M., 1982. Individual Wave Analysis of Irregular Wave Deformation in the Nearshore Zone. Cape Town, 18th International Conference on Coastal Engineering.

Moutzouris, C. I., 1991. Beach Profiles vs Cross shore distributions of sediment grain sizes. s.l., Coastal Sediments'91ASCE Conference Proceedings, pp. 860-874.

NCTA, 2013. Tourism. [Online]
Available at: https://www.bournemouth.gov.uk/CouncilDemocratic/Statistics/Themes/Tourism.aspx
[Accessed 6 Jul 2019].

Neumeier, U. et al., 2008. Sedtrans05: An improved sediment-transport model for continental shelves and coastal waters with a new algorithm for cohesive sediments. Computer & Geosciences, 34(10), pp. 1223-1242.

NFDC, 2017. Update of Carter, D., Bray, M., & Hooke,J., 2004 SCOPAC Sediment Transport Study, New Forest District Council.

Otto, G.H., 1939. A modified logarithmic probability graph for the interpretation of mechanical analyses of sediments. Journal of Sedimentary Petrology, 9, pp. 62–75.

Peterson, C. H., Hickerson , D. H. M. & Johnson , G. G., 2000. Short-term consequences of nourishment and bulldozing on the dominant large invertebrates of a sandy beach. Journal of Coastal Research , 16(2), pp. 368–378.

Poole & Christchurch Bays Coastal Group, 2011. Poole & Chirstchurch Bays Shoreline Management Plan. [Online]
Available at: https://twobays.net/poole_bay.htm
[Accessed 9 Jul 2019].

Poolebay.net, 2015. Coastal & Flood Risk Management: A record of projects along the coast of Poole Bay, Dorset. [Online]
Available at: https://poolebay.net/past-projects/
[Accessed 6 Jul 2019].

Prodger, S., 2017. Spatial and Temporal variability of sandy beach sediment grain size and sorting Plymouth: University of Plymouth.

Rees, B., 1994. Hengistbury Head. [Online]
Available at: https://www.hengistbury-head.co.uk/hengistbury-head-geology.php
[Accessed 23 Mar 2019].

Reeve, D., Chadwick, A. & Fleming, C., 2018. Wave Theory. In: Coastal Engineering: Processes, Theory and Design Practice (3rd edition). Lomdon: CRC Press, pp. 40-44.

Ris, R. C., Holthuijsen, L. H. & Booij, N., 1994. A Spectral Model for Waves in the Near Shore Zone. Kobe, Coastal Engineering Proceedings.

Robson, D., 2003. Sandbanks coast protection, Poole: Borough of Poole Leisure Services.

Royal Haskoning, 2005. Poole Harbour Approach Channel Deepening and Beneficial Use Schemes EIA. [Online]
Available at: https://www.phc.co.uk/downloads/channeldeepening/es3_hydrodynamic.pdf
[Accessed 28 Jul 2019].

Royal Haskoning, 2010. Poole and Christchurch Bays SMP2 Review of Coastal processes and geomorphology - Appendix C Baseline Process Understanding, Bournemouth, Poole, Christchurch: Bournemouth Borough Council.

Royal Haskoning, 2011. Poole and Christchurch Bays Shoreline Management Plan Review Sub-cell 5f Section 4. Policy Development Zone 2. [Online]
Available at:
http://www.twobays.net/SMP2%20Final/Main%20Report/Section%204%20-%204.3%20PDZ2.pdf
[Accessed 25 Aug 2019].

Soulsby, R., 1997. Dynamics of marine sands.. London: Thomas Telford..

Spencer, K. L., 2002. Spatial variability of metals in the inter-tidal sediments of the Medway Estuary, Kent, UK. Marine Pollution Bulletin, 44, pp. 933-944.

Splinter, K. D. et al., 2014. A Generalized Equilibrium Model for Predicting Daily to Interannual Shoreline Response. Journal of Geophysical Research: Earth Surface, 119, pp. 1936-1958.

Stanica, A. & Ungureanu, G., 2010. Understanding coastal morphology and sedimentology. Terre et environnement, 88, pp. 105-111.

Taylor, K. E., 2001. Summarizing multiple aspects of model performance in a single diagram. Journal of Geophysical Research, 106, pp. 7183–7192.

Terry, S., 2008. www.Poolebay.net : Beach Replenishment 2005/06. [Online]
Available at: https://www.poolebay.net/PhaseI/
[Accessed 9 Jul 2019].

Thornton, E.B. et al., 2007. Rip currents, mega-cusps, and eroding dunes. Mar. Geol., 240, pp. 151–167.

Tolman, H. L., 1997. User manual and system documentation of WAVEWATCH-III version 1.15. [Online]
Available at: https://polar.ncep.noaa.gov/mmab/papers/tn151/OMB_151.pdf
[Accessed 11 Sep 2019].

Townend, I. H., 2016. CoastalTools Manual and Software. Southampton: CoastalSEA.

TUDelft, 2017. SWAN. [Online]
Available at: http://swanmodel.sourceforge.net/
[Accessed 11 Sep 2019].

Turner, N., 1994. Recycling of capital dredging arisings - The Bournemouth experience. Lymington, SCOPAC, pp. 57-67.

Van Rijn, L. C., 1997. Sediment transport and budget of the central coastal zone of Holland. Coastal engineering, 32, pp. 61-90.

Van Rijn, L. C., 2014. WWW.LEOVANRIJN-SEDIMENT.COM. [Online]
Available at: www.leovanrijn-sediment.com
[Accessed 25 Aug 2019].

Van Rijn, Walstra, D. J. R. & van Ormondt, M., 2007. Unified view of sediment transport by currents and waves. Journal of Hydraulic Engineering, 133, pp. 776.

Velegrakis, A. F. et al., 1999. Late Quaternary Evolution of the Upper Reaches of the Solent River, Southern England, Journal of the Geological Society, 156, pp. 73-87

Wentworth , C. K., 1922. A Scale of Grade and Class Terms for Clastic Sediments. The Journal of Geology.

West, I., 2006. Geology of the Wessex Coast of Southern England. [Online]
Available at: http://www.soton.ac.uk/~imw/Field-Guides-Introduction.htm
[Accessed 23 Mar 2019].

West, I., 2018. Geology of Hengistbury Head. [Online]
Available at: http://southampton.ac.uk/~imw/Hengistbury-Head-Geology-Revised.htm
[Accessed 21 Aug 2019].

Wong, C. Y., 2014. An investigation of wind-blown sand on nourished beach case study: Bounemouth Beach, Southampton: University of Southampton.

Wright, L. D. & Short, A. D., 1984. Morphodynamic variability of surf zones and beaches. Marine Geology, 56, pp. 93-118.

Zhang, C., 2006. Using multivariate analyses and GIS to identify pollutants and their spatial patterns in urban soils in Galway, Ireland. Environmental Pollution, 142, pp. 501-511.

Appendix A

This section provides the (monthly) time series of significant wave height and wave approach of i) modelled inshore waves from offshore waves at Wavenet buoy (by CEFAS) ii) measured inshore waves from Boscombe wave buoy (by CCO).

Before calibration

i) Significant wave height, Hs (m)
The graphs indicated a substantial difference in wave height between the modelled and observed data. Modelled inshore waves appeared to be higher than the measurements, even up to 40% difference at certain intervals.

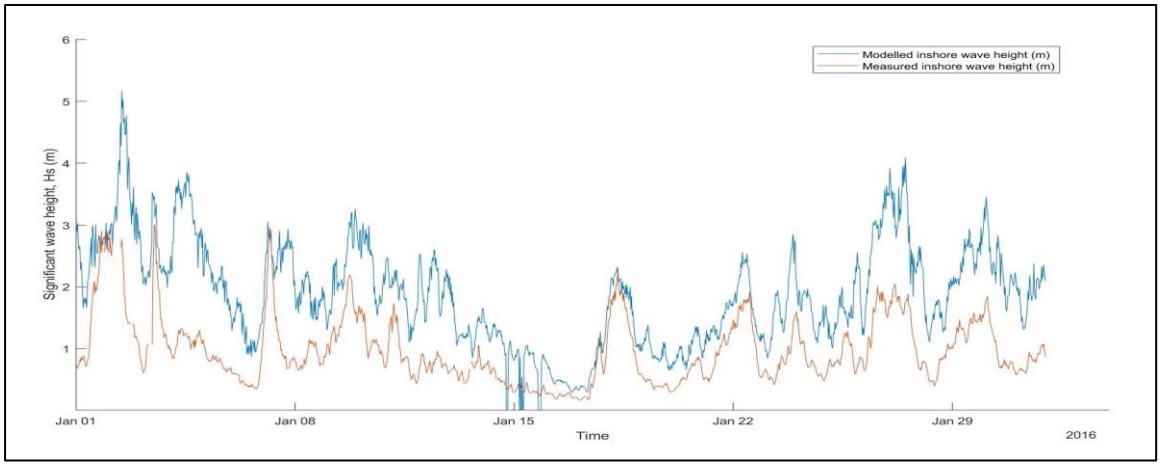

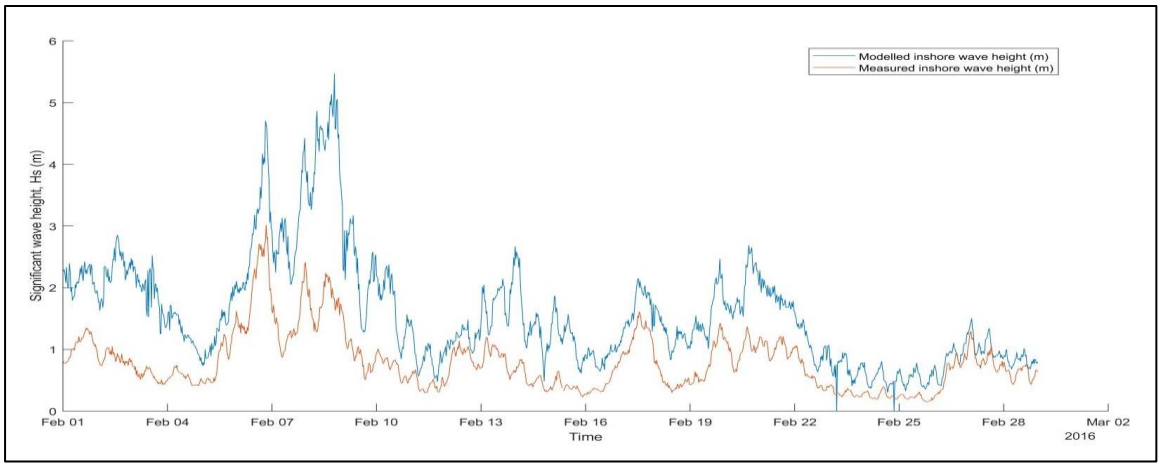

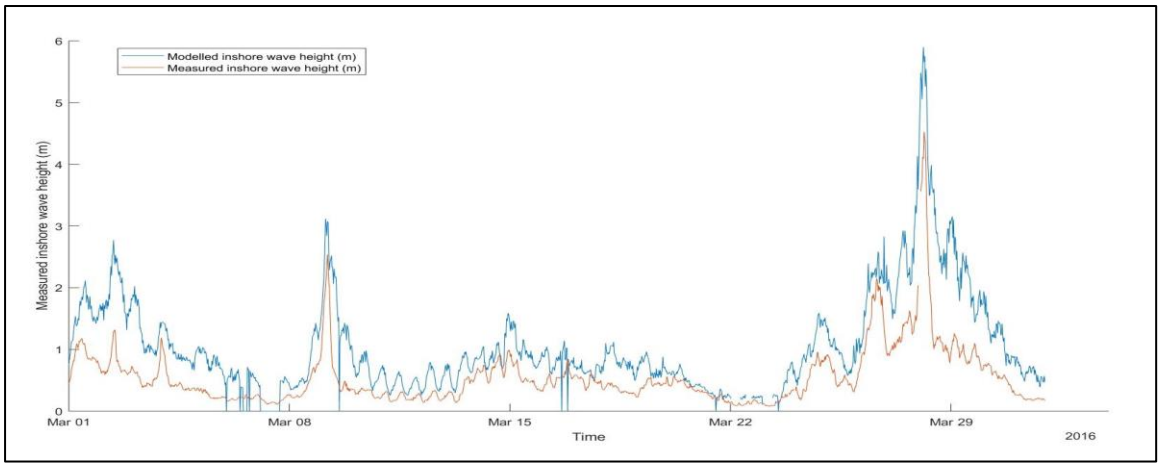

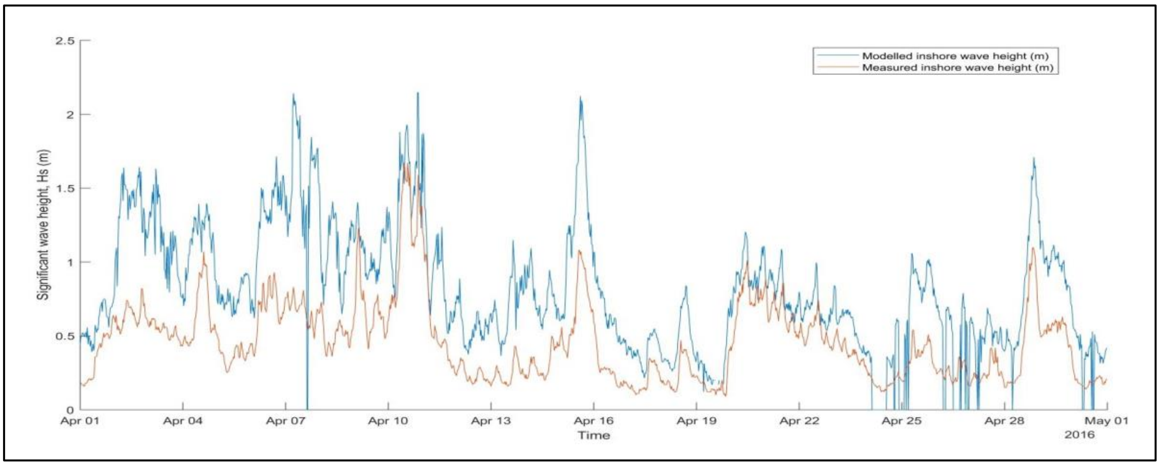
Modelled inshore wave height (m)
Measured inshore wave height (m)
Significant wave height, Hs (m)
Time
2016

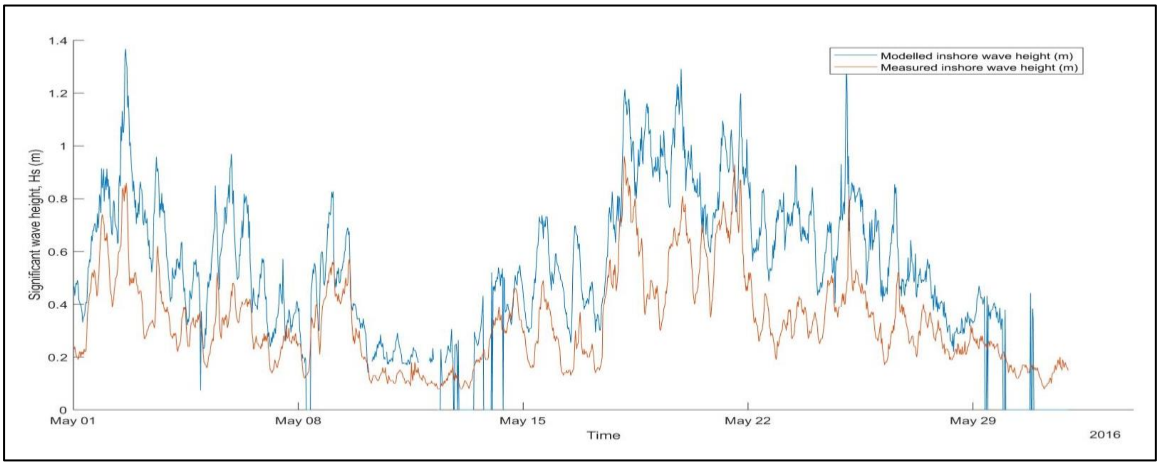
Modelled inshore wave height (m)
Measured inshore wave height (m)
Significant wave height, Hs (m)
Time
2016

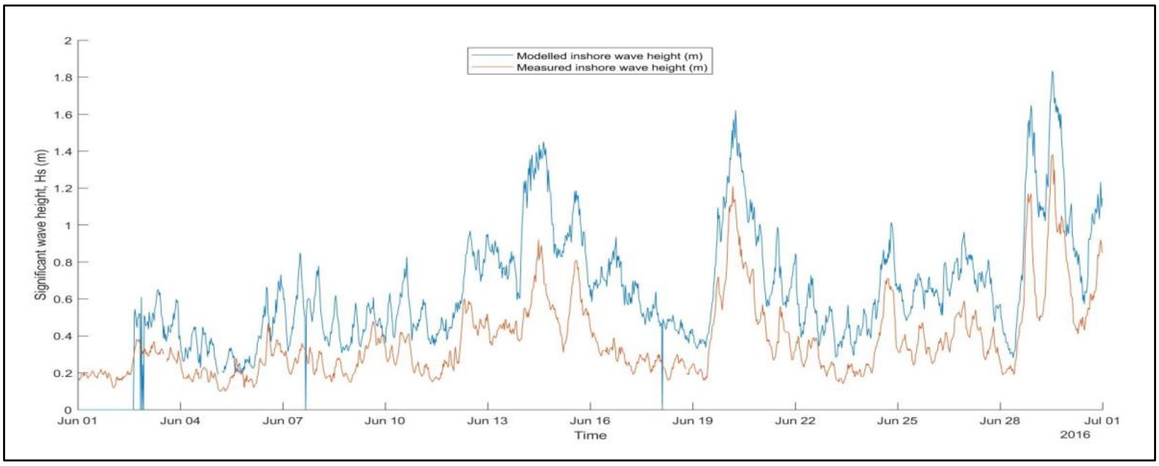
Modelled inshore wave height (m)
Measured inshore wave height (m)
Significant wave height, Hs (m)
Time
2016

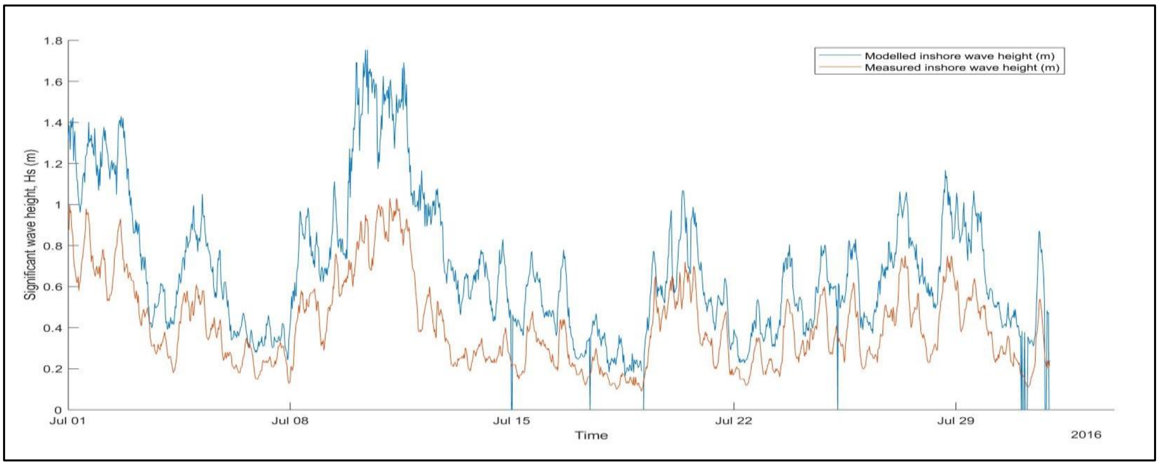
Modelled inshore wave height (m)
Measured inshore wave height (m)
Significant wave height, Hs (m)
Time
2016

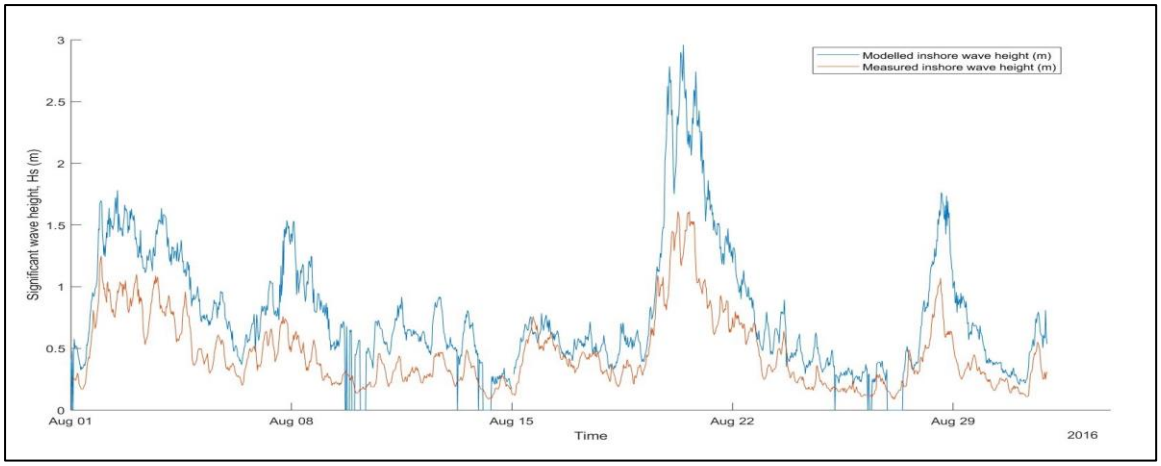
Modelled inshore wave height (m)
Measured inshore wave height (m)
Significant wave height, Hs (m)
0
0.5
1
1.5
2
2.5
3
Aug 01
Aug 08
Aug 15
Aug 22
Aug 29
Time
2016

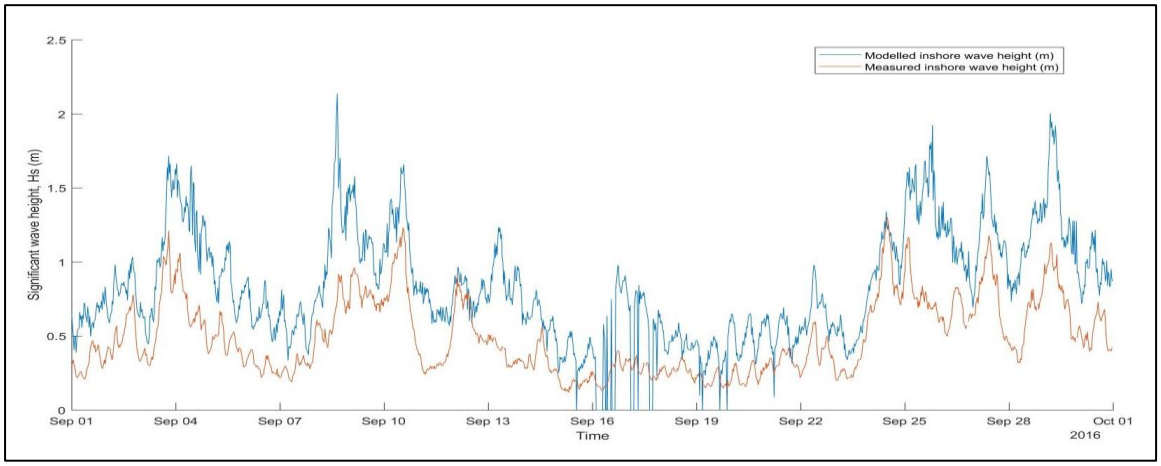
Modelled inshore wave height (m)
Measured inshore wave height (m)
Significant wave height, Hs (m)
0
0.5
1
1.5
2
2.5
Sep 01
Sep 04
Sep 07
Sep 10
Sep 13
Sep 16
Sep 19
Sep 22
Sep 25
Sep 28
Oct 01
Time
2016

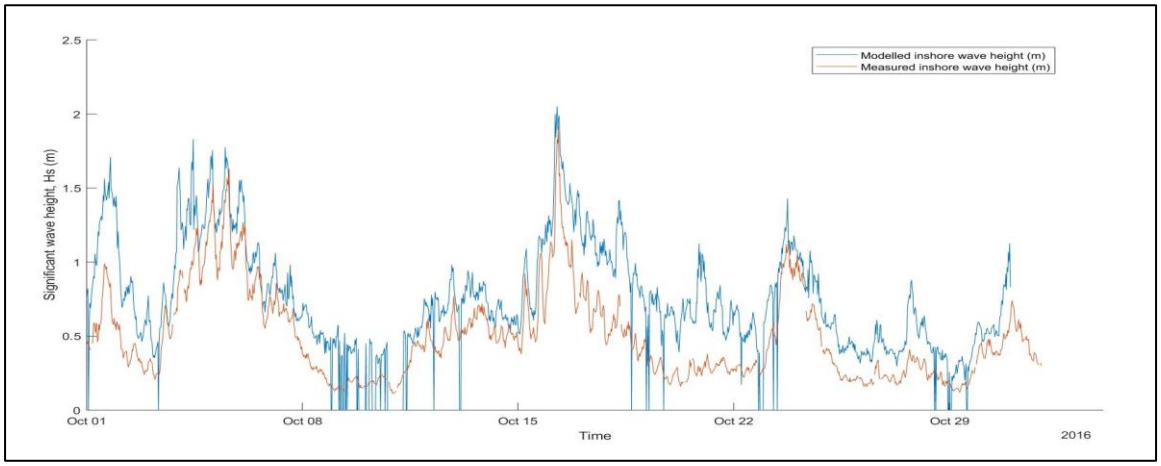
Modelled inshore wave height (m)
Measured inshore wave height (m)
Significant wave height, Hs (m)
0
0.5
1
1.5
2
2.5
Oct 01
Oct 08
Oct 15
Oct 22
Oct 29
Time
2016

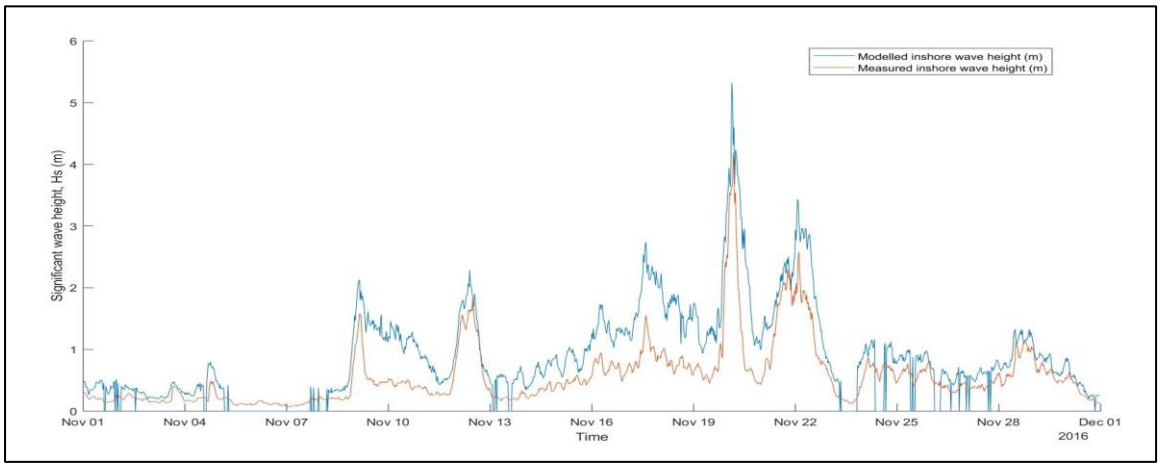
Modelled inshore wave height (m)
Measured inshore wave height (m)
Significant wave height, Hs (m)
0
1
2
3
4
5
6
Nov 01
Nov 04
Nov 07
Nov 10
Nov 13
Nov 16
Nov 19
Nov 22
Nov 25
Nov 28
Dec 01
Time
2016

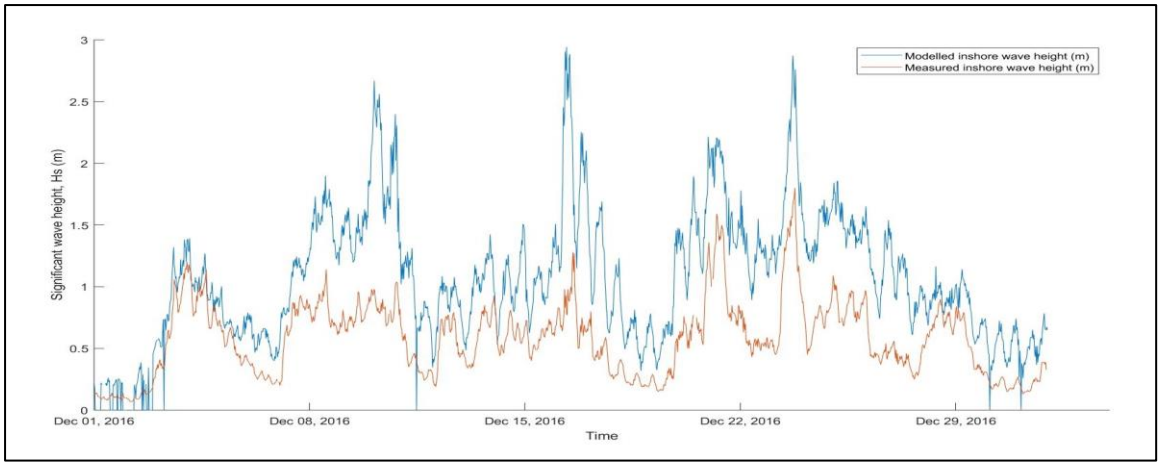

ii) Wave approach

Measured waves mainly came from south west direction but modelled waves indicated south easterly direction.

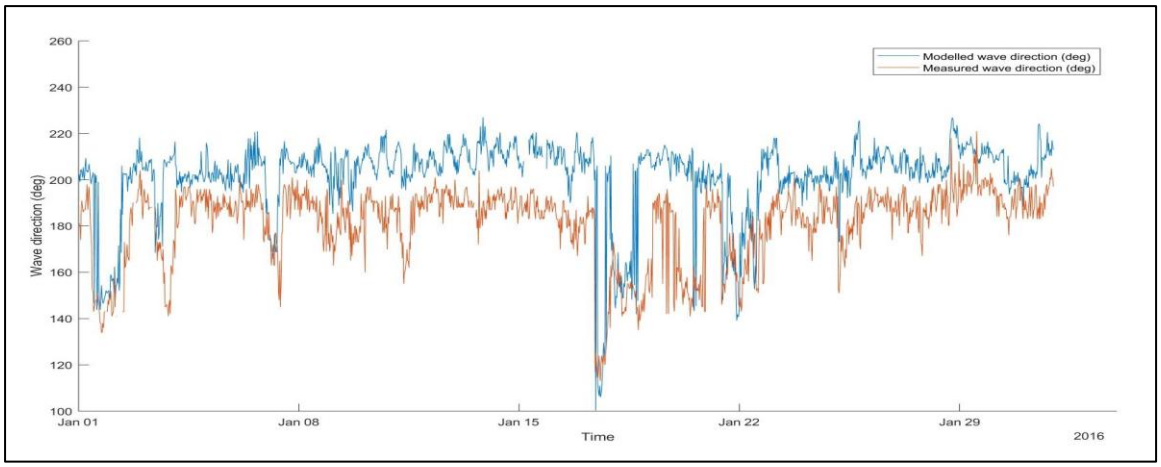

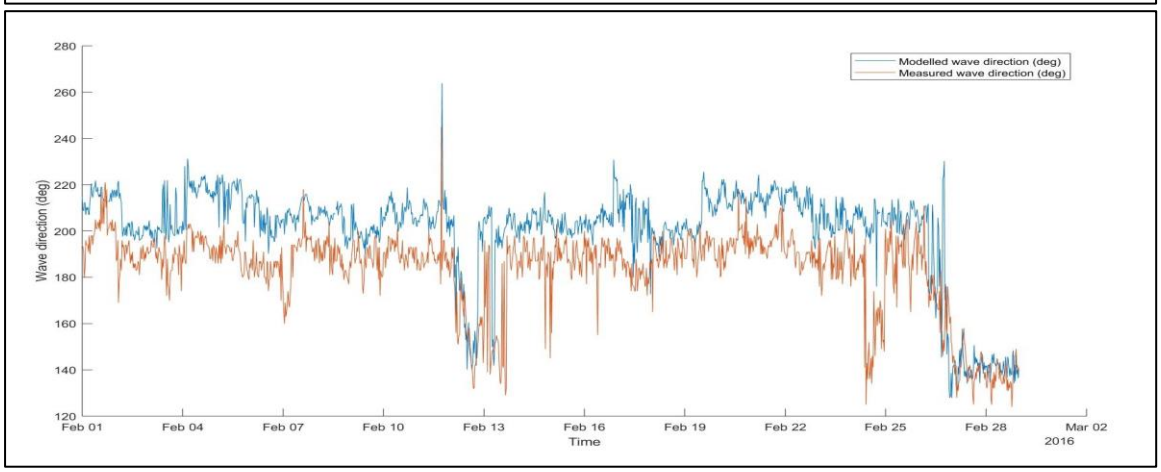

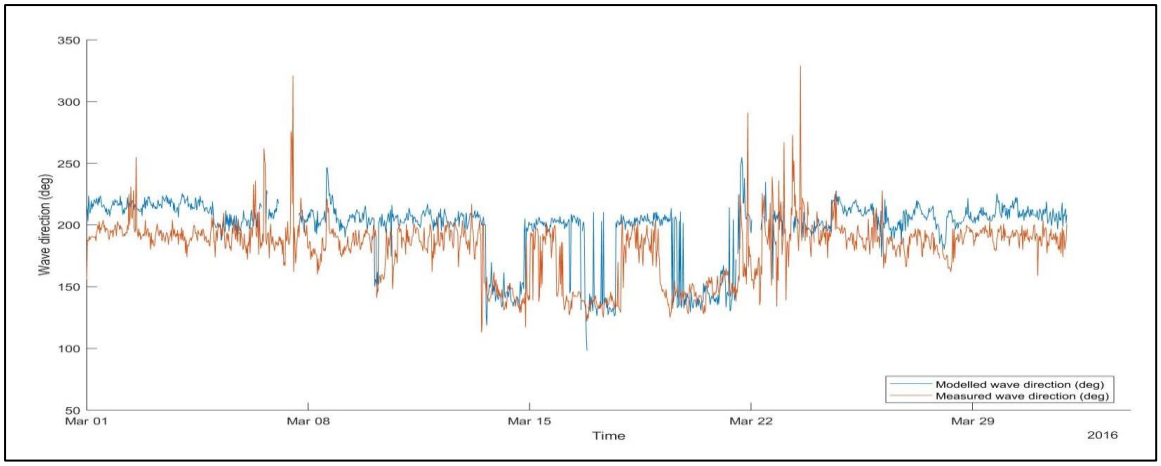
Wave direction (deg)
350
300
250
200
150
100
50
Mar 01
Mar 08
Mar 15
Mar 22
Mar 29
Time
2016
Modelled wave direction (deg)
Measured wave direction (deg)

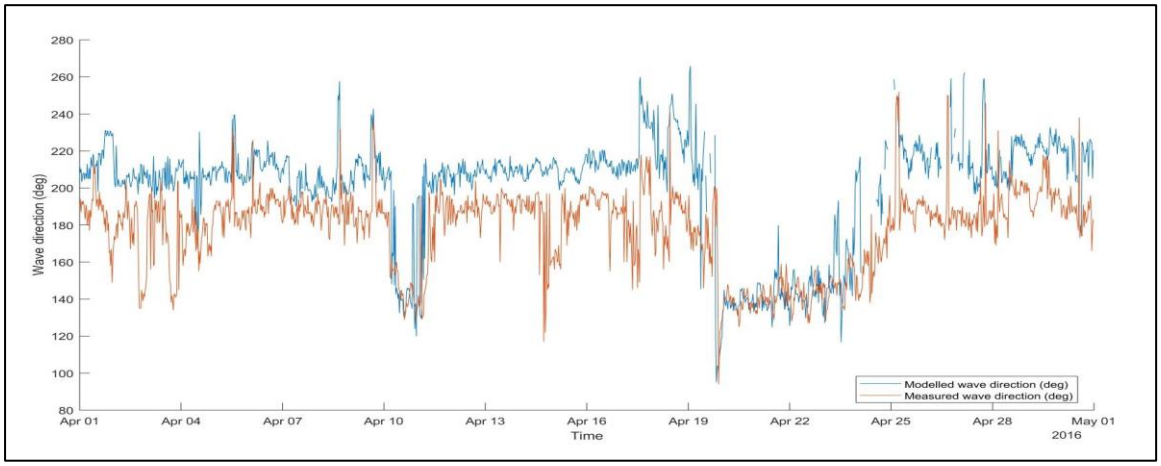
Wave direction (deg)
280
260
240
220
200
180
160
140
120
100
80
Apr 01
Apr 04
Apr 07
Apr 10
Apr 13
Apr 16
Apr 19
Apr 22
Apr 25
Apr 28
May 01
Time
2016
Modelled wave direction (deg)
Measured wave direction (deg)

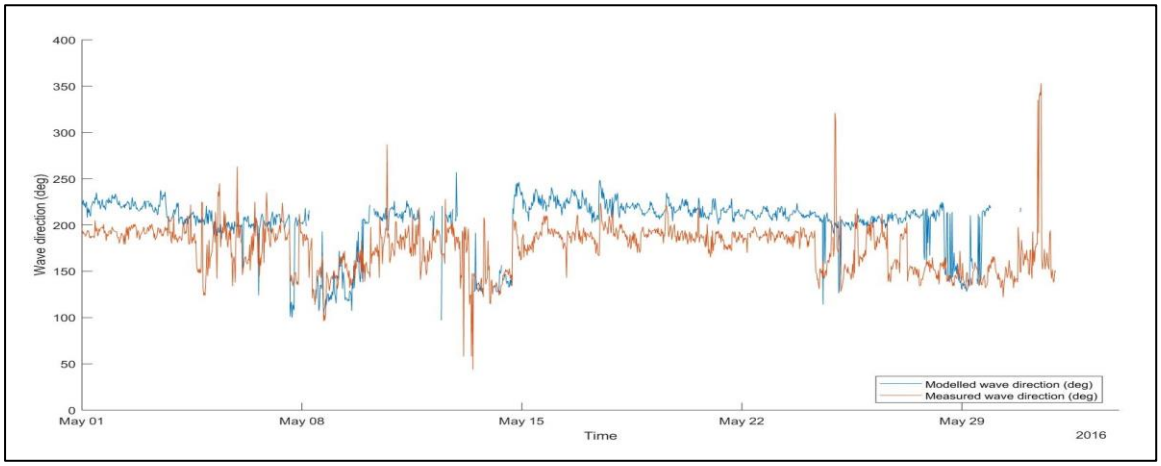
Wave direction (deg)
400
350
300
250
200
150
100
50
0
May 01
May 08
May 15
May 22
May 29
Time
2016
Modelled wave direction (deg)
Measured wave direction (deg)

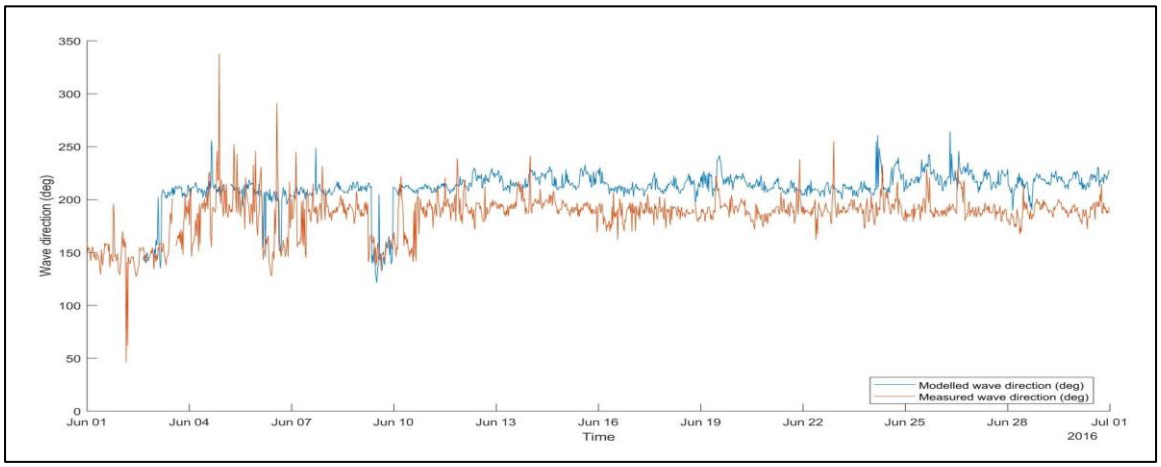
Wave direction (deg)
350
300
250
200
150
100
50
0
Jun 01
Jun 04
Jun 07
Jun 10
Jun 13
Jun 16
Jun 19
Jun 22
Jun 25
Jun 28
Jul 01
Time
2016
Modelled wave direction (deg)
Measured wave direction (deg)

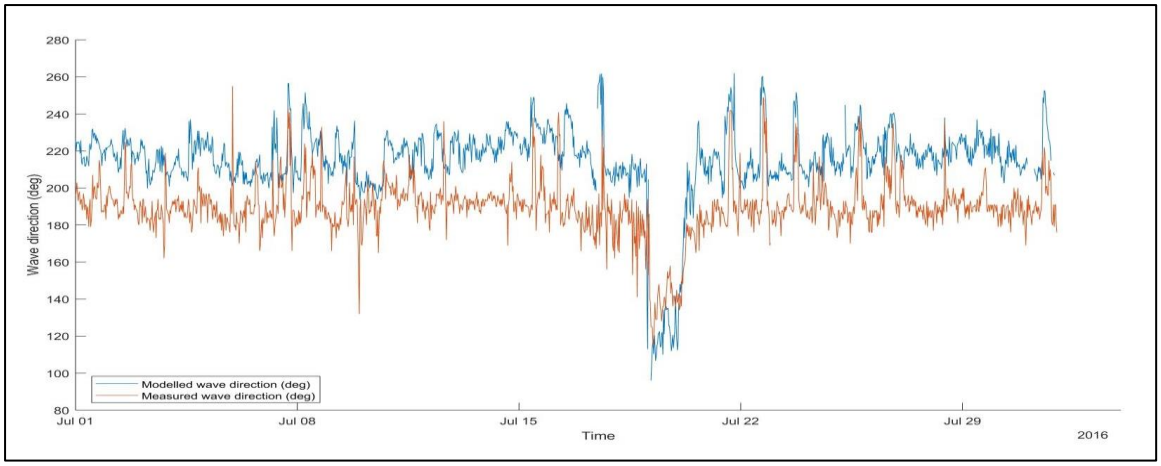
Wave direction (deg)
Modelled wave direction (deg)
Measured wave direction (deg)
Jul 01
Jul 08
Jul 15
Jul 22
Jul 29
Time
2016

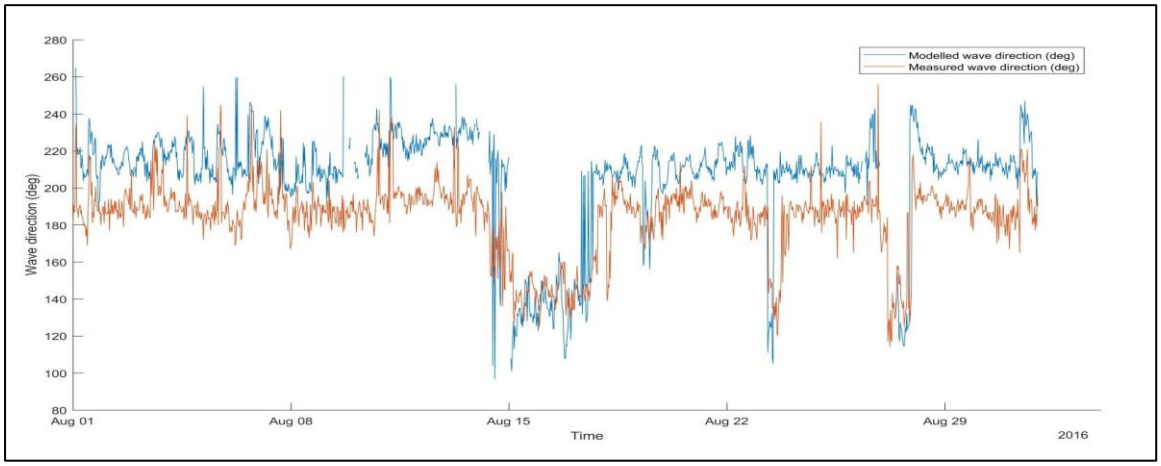
Wave direction (deg)
Modelled wave direction (deg)
Measured wave direction (deg)
Aug 01
Aug 08
Aug 15
Aug 22
Aug 29
Time
2016

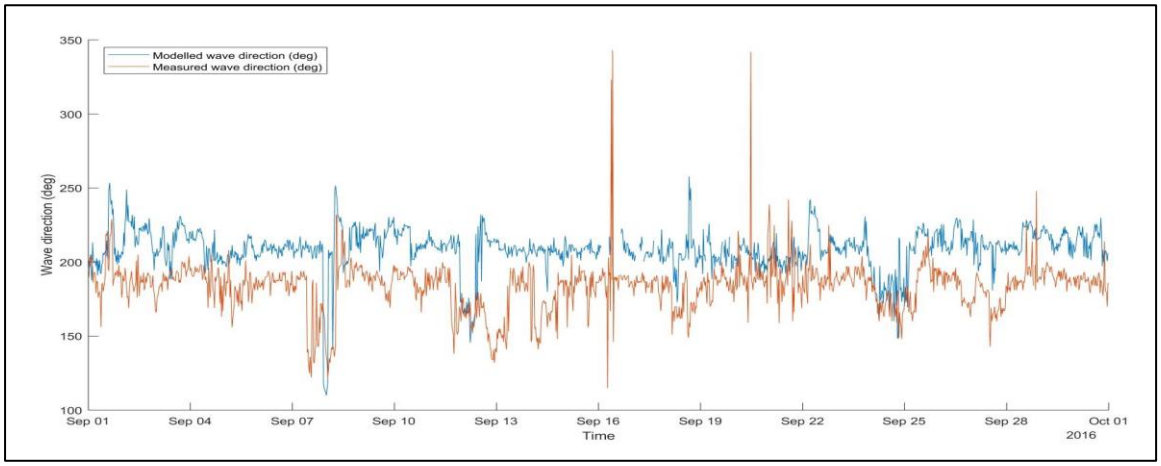
Wave direction (deg)
Modelled wave direction (deg)
Measured wave direction (deg)
Sep 01
Sep 04
Sep 07
Sep 10
Sep 13
Sep 16
Sep 19
Sep 22
Sep 25
Sep 28
Oct 01
Time
2016

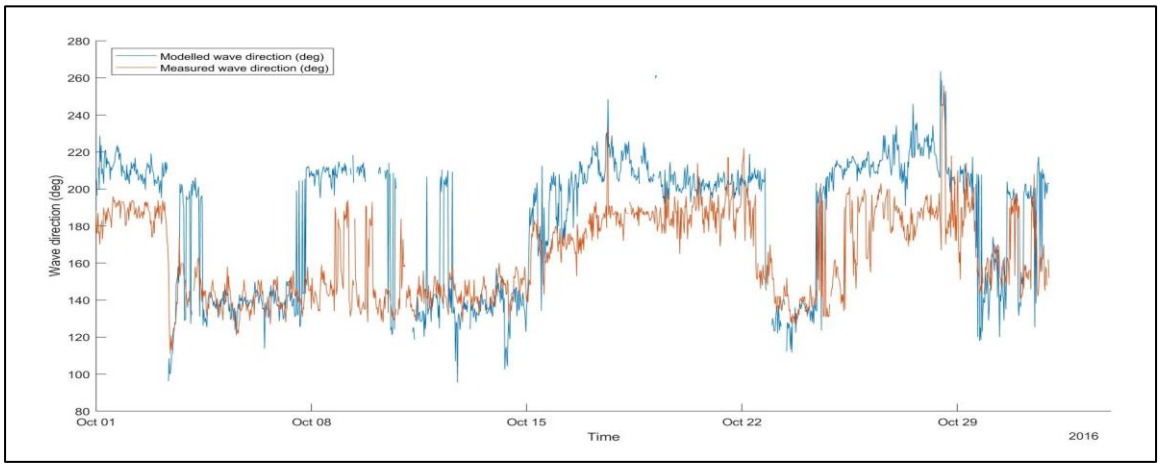
Wave direction (deg)
Modelled wave direction (deg)
Measured wave direction (deg)
Oct 01
Oct 08
Oct 15
Oct 22
Oct 29
Time
2016

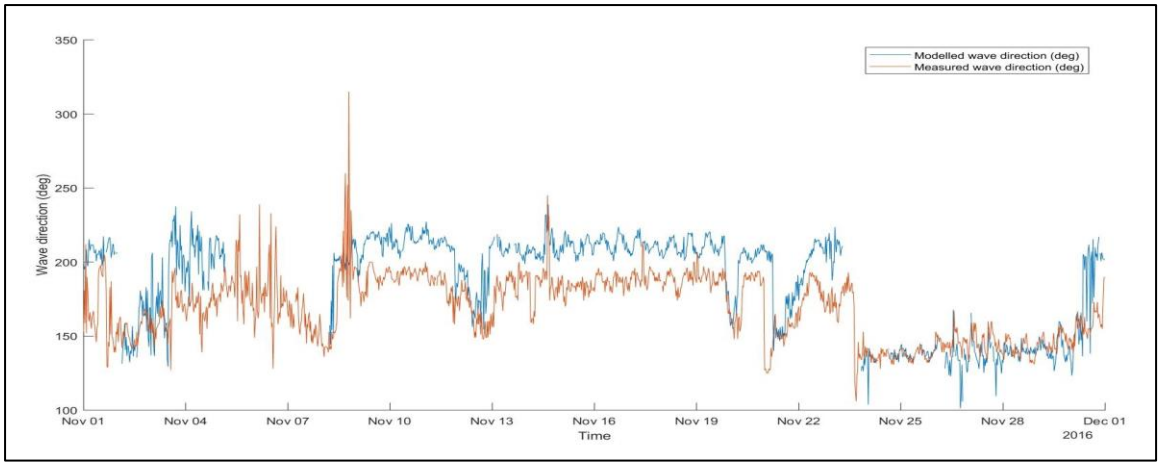
Modelled wave direction (deg)
Measured wave direction (deg)
Wave direction (deg)
350
300
250
200
150
100
Nov 01
Nov 04
Nov 07
Nov 10
Nov 13
Nov 16
Nov 19
Nov 22
Nov 25
Nov 28
Dec 01
2016
Time

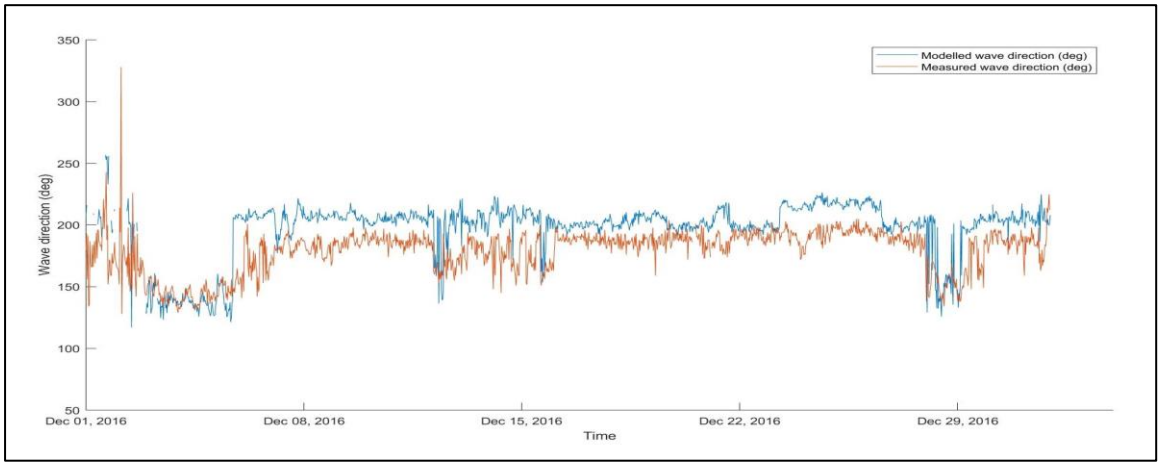
Modelled wave direction (deg)
Measured wave direction (deg)
Wave direction (deg)
350
300
250
200
150
100
50
Dec 01, 2016
Dec 08, 2016
Dec 15, 2016
Dec 22, 2016
Dec 29, 2016
Time

After calibration

i) Significant wave height, Hs (m)

After calibration, there is a higher degree of conformity between the two sets of data. More than half of the modelled Hs are in the same magnitude as the measurements.

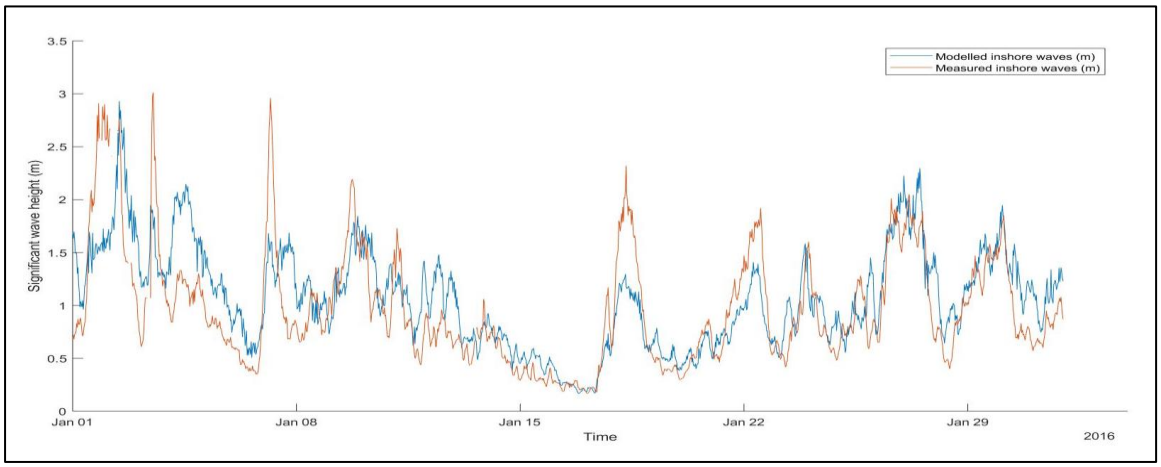

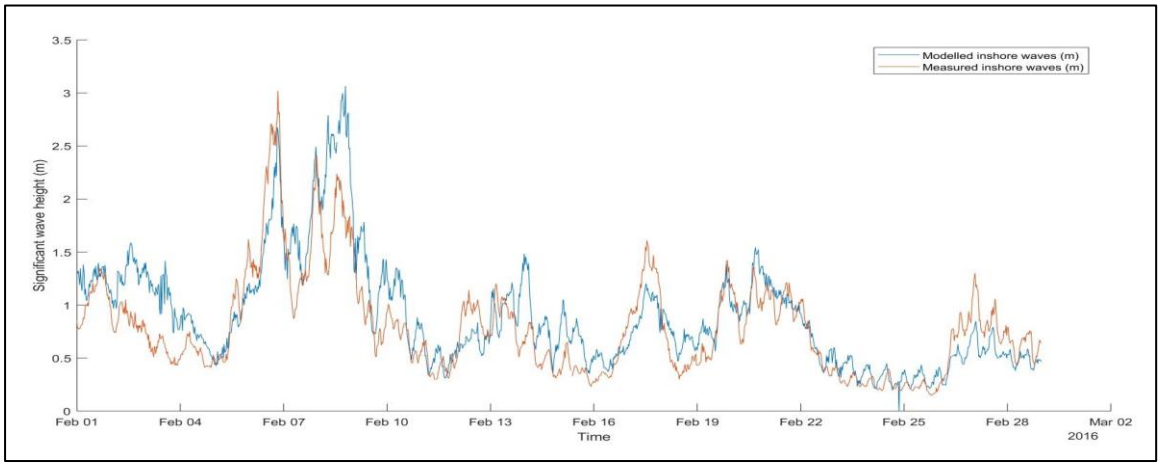

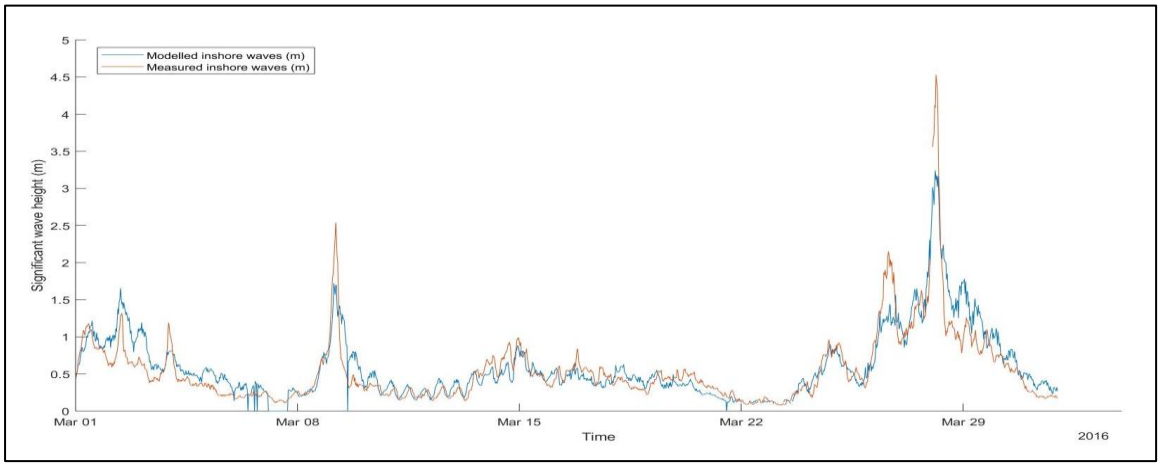

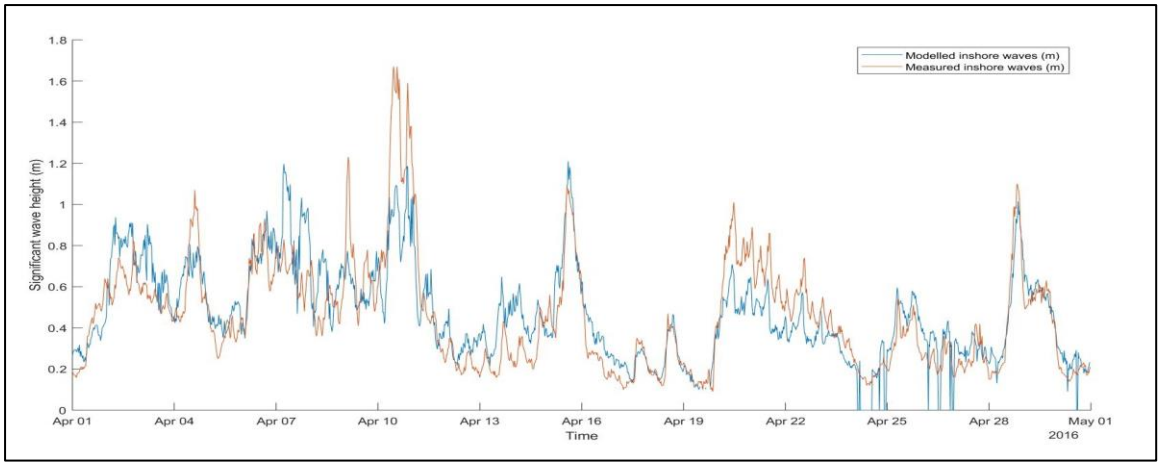
Modelled inshore waves (m)
Measured inshore waves (m)
Significant wave height (m)
Time
Apr 01
Apr 04
Apr 07
Apr 10
Apr 13
Apr 16
Apr 19
Apr 22
Apr 25
Apr 28
May 01
2016

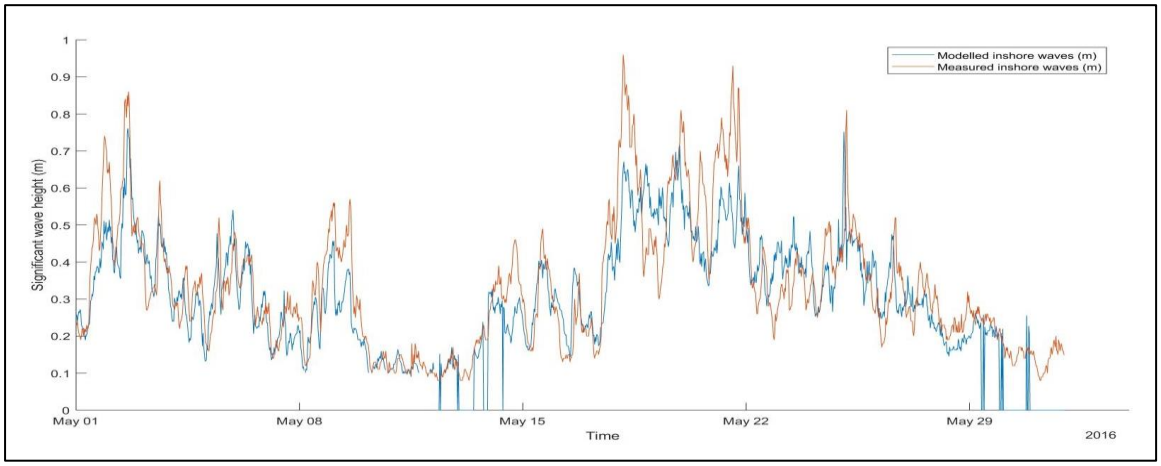
Modelled inshore waves (m)
Measured inshore waves (m)
Significant wave height (m)
Time
May 01
May 08
May 15
May 22
May 29
2016

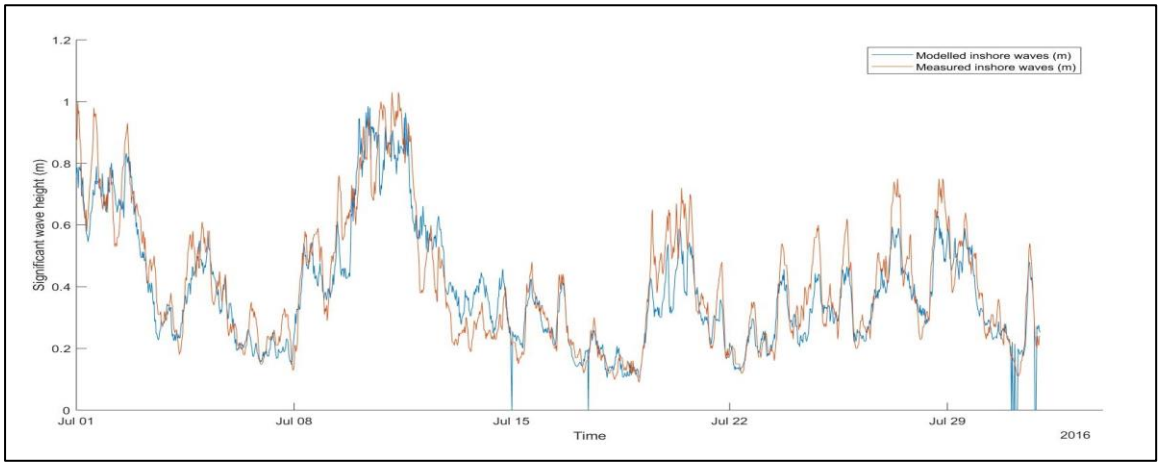
Modelled inshore waves (m)
Measured inshore waves (m)
Significant wave height (m)
Time
Jul 01
Jul 08
Jul 15
Jul 22
Jul 29
2016

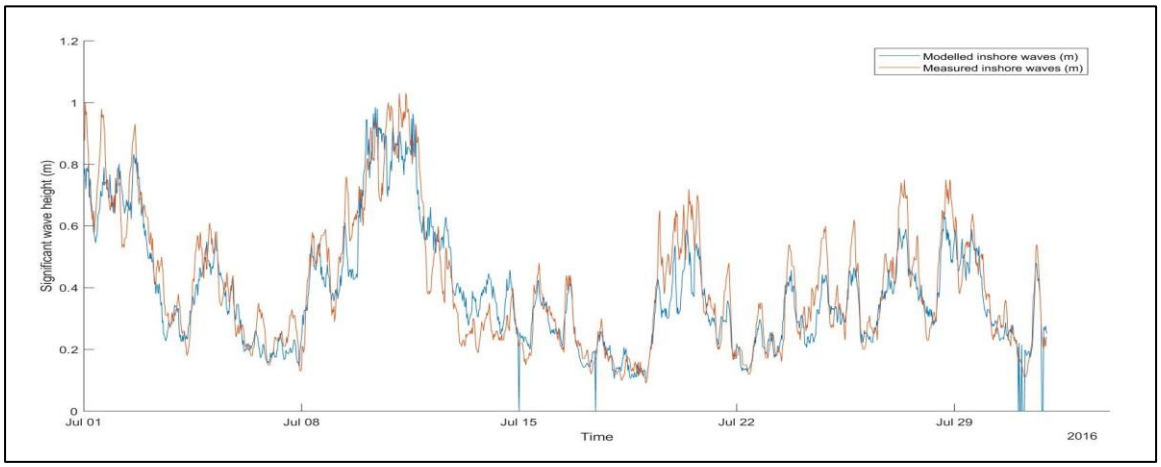
Modelled inshore waves (m)
Measured inshore waves (m)
Significant wave height (m)
Time
Jul 01
Jul 08
Jul 15
Jul 22
Jul 29
2016

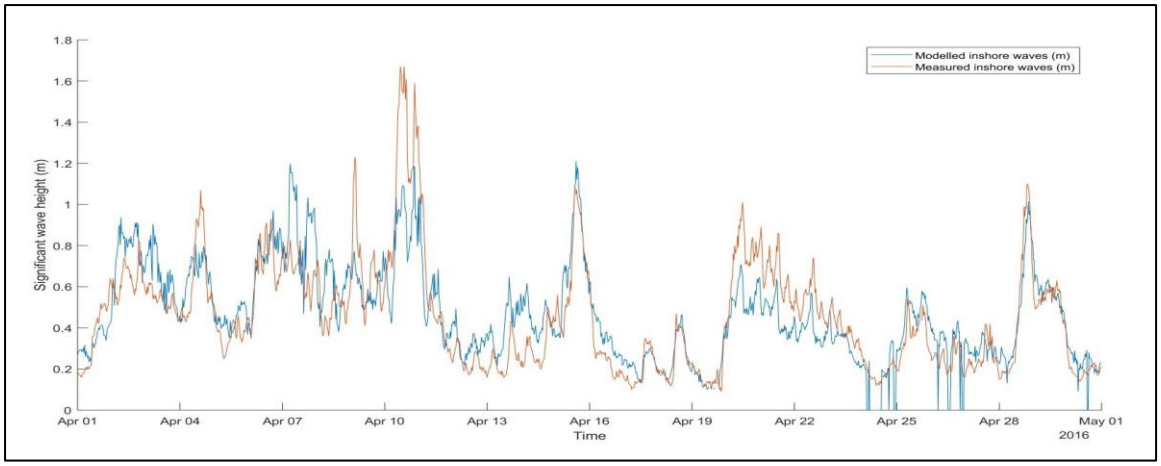
Modelled inshore waves (m)
Measured inshore waves (m)
Significant wave height (m)
0
0.2
0.4
0.6
0.8
1
1.2
1.4
1.6
1.8
Apr 01
Apr 04
Apr 07
Apr 10
Apr 13
Apr 16
Apr 19
Apr 22
Apr 25
Apr 28
May 01
Time
2016

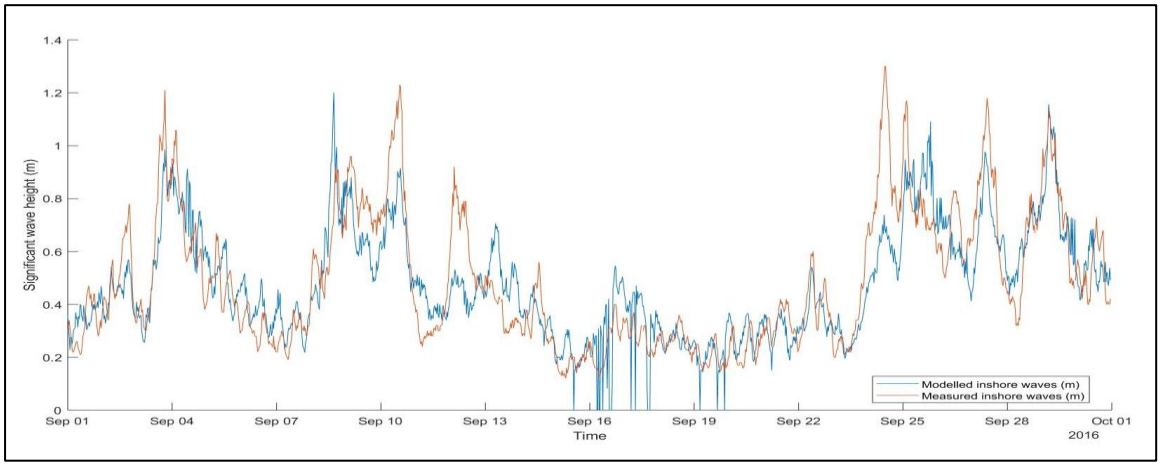
Modelled inshore waves (m)
Measured inshore waves (m)
Significant wave height (m)
0
0.2
0.4
0.6
0.8
1
1.2
1.4
Sep 01
Sep 04
Sep 07
Sep 10
Sep 13
Sep 16
Sep 19
Sep 22
Sep 25
Sep 28
Oct 01
Time
2016

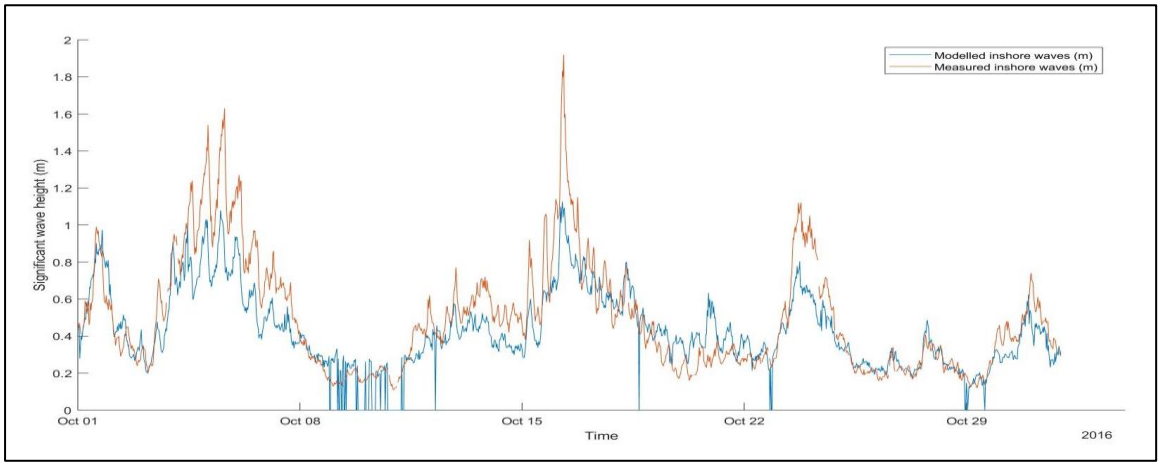
Modelled inshore waves (m)
Measured inshore waves (m)
Significant wave height (m)
0
0.2
0.4
0.6
0.8
1
1.2
1.4
1.6
1.8
2
Oct 01
Oct 08
Oct 15
Oct 22
Oct 29
Time
2016

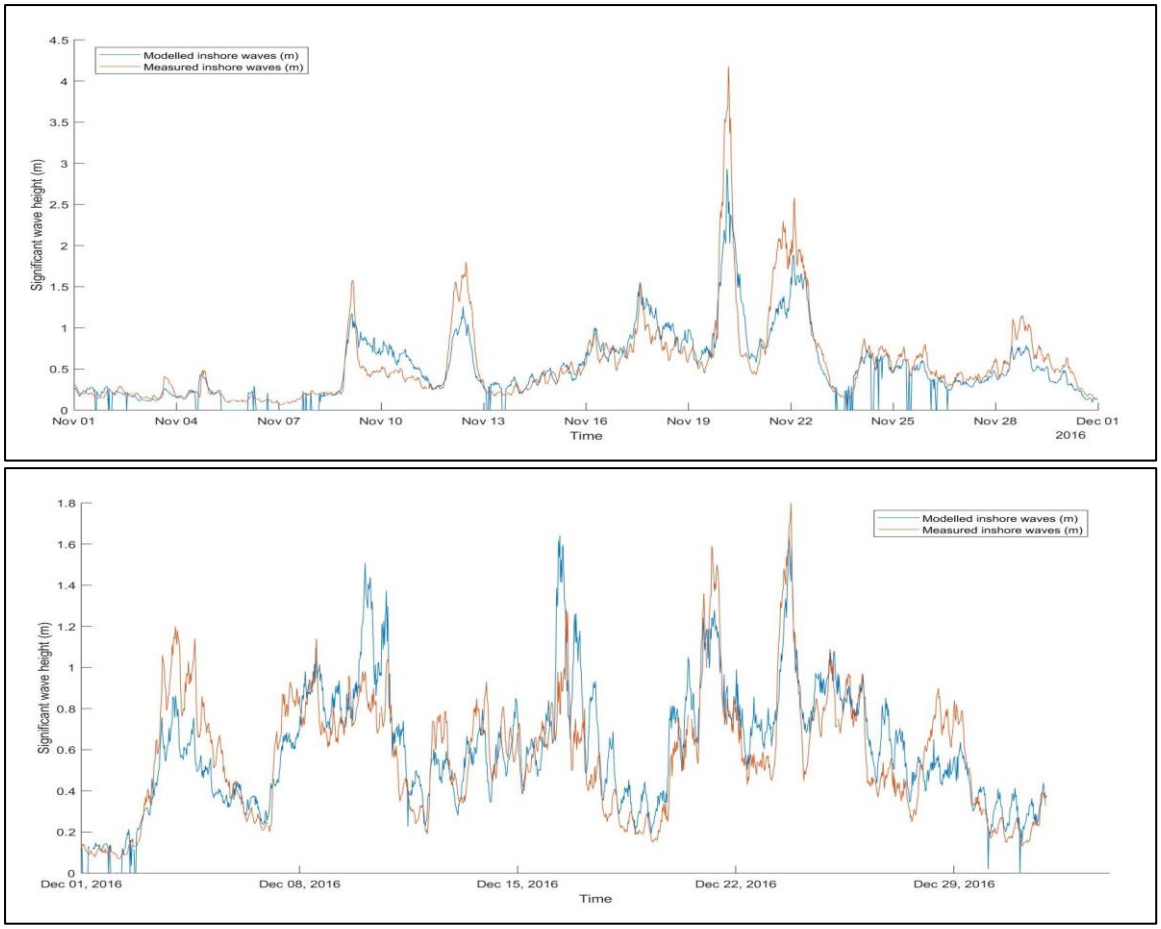

ii) Wave approach (deg)

The calibrated model produced inshore wave directions in the approximate same direction as the actual ones.

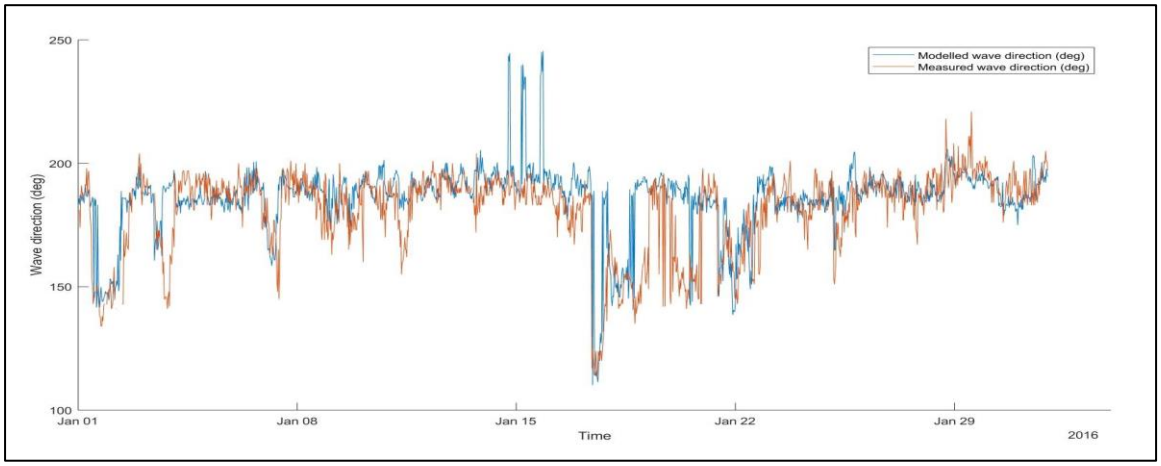

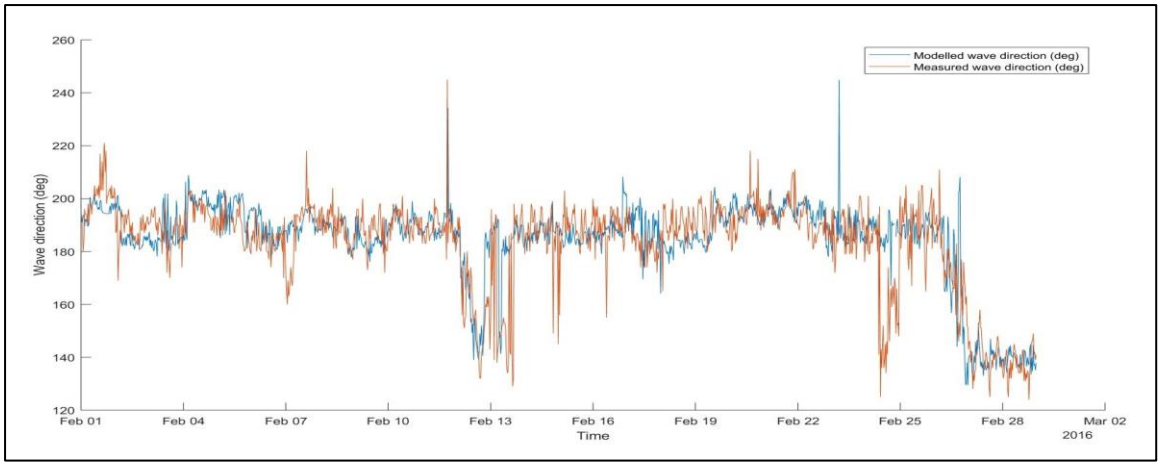
Modelled wave direction (deg)
Measured wave direction (deg)
Wave direction (deg)
260
240
220
200
180
160
140
120
Feb 01
Feb 04
Feb 07
Feb 10
Feb 13
Feb 16
Feb 19
Feb 22
Feb 25
Feb 28
Mar 02
Time
2016

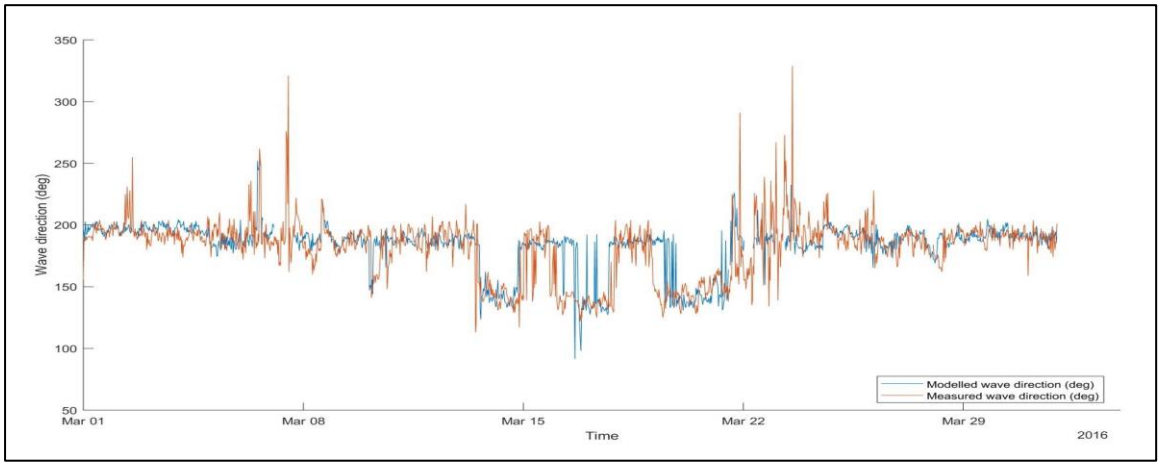
Wave direction (deg)
350
300
250
200
150
100
50
Modelled wave direction (deg)
Measured wave direction (deg)
Mar 01
Mar 08
Mar 15
Mar 22
Mar 29
Time
2016

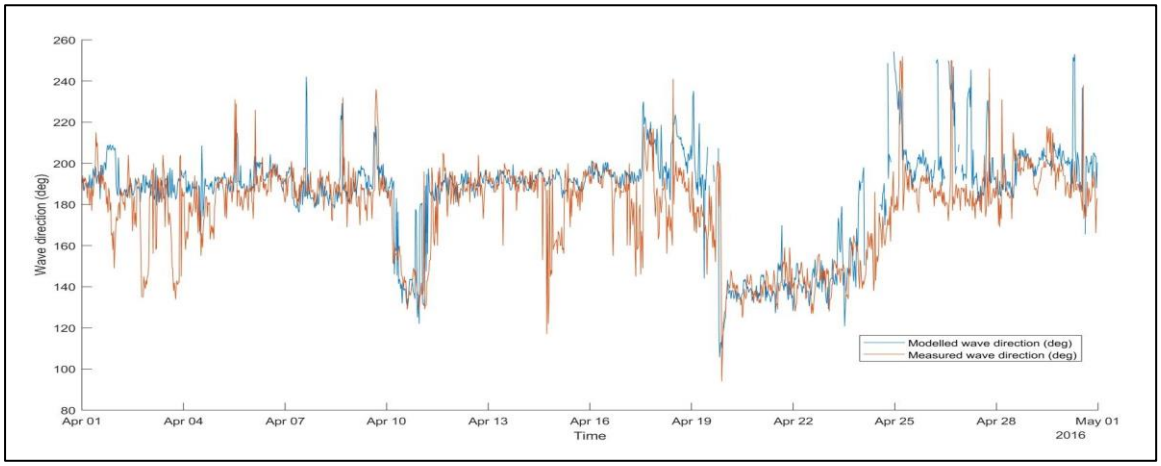
Wave direction (deg)
260
240
220
200
180
160
140
120
100
80
Modelled wave direction (deg)
Measured wave direction (deg)
Apr 01
Apr 04
Apr 07
Apr 10
Apr 13
Apr 16
Apr 19
Apr 22
Apr 25
Apr 28
May 01
Time
2016

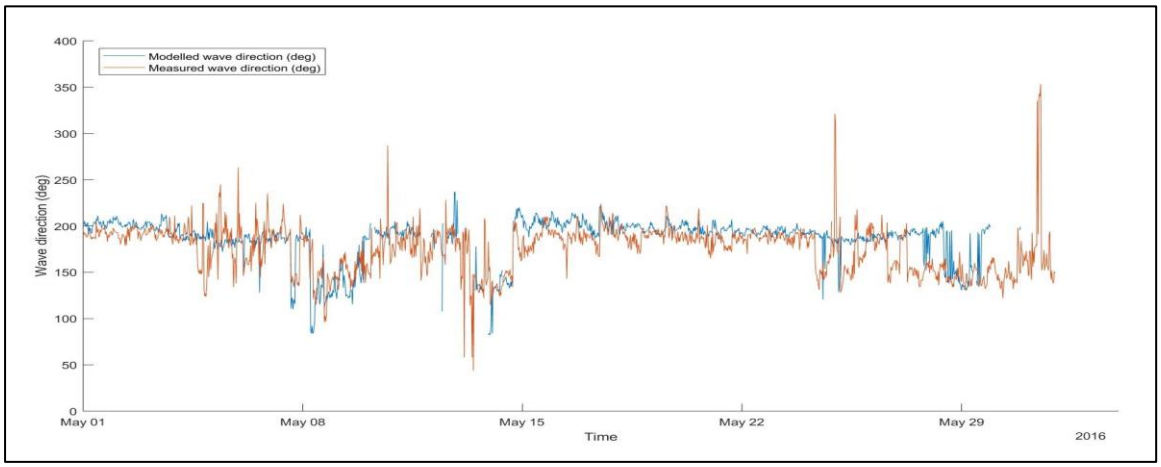
Modelled wave direction (deg)
Measured wave direction (deg)
Wave direction (deg)
400
350
300
250
200
150
100
50
0
May 01
May 08
May 15
May 22
May 29
Time
2016

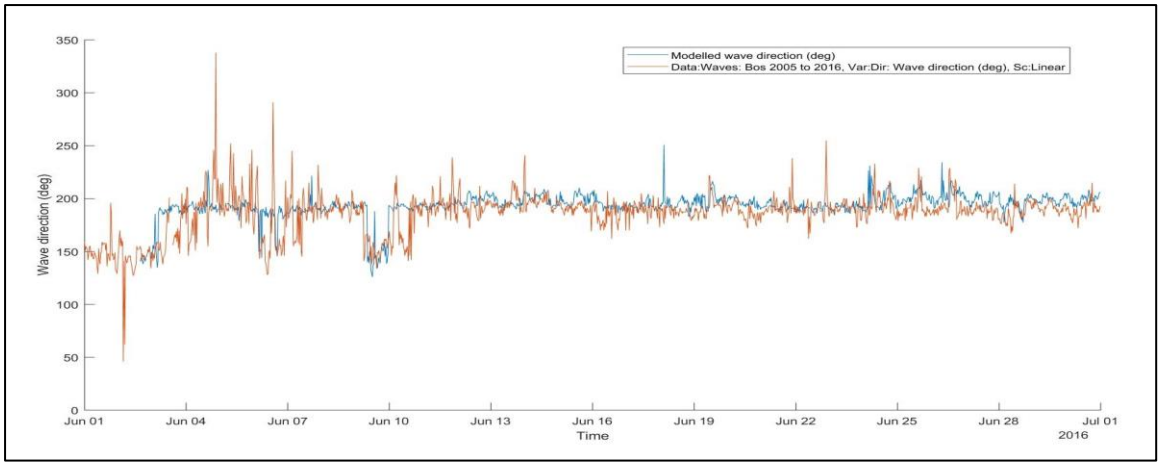
Modelled wave direction (deg)
Data:Waves: Bos 2005 to 2016, Var:Dir: Wave direction (deg), Sc:Linear
Wave direction (deg)
Time
2016

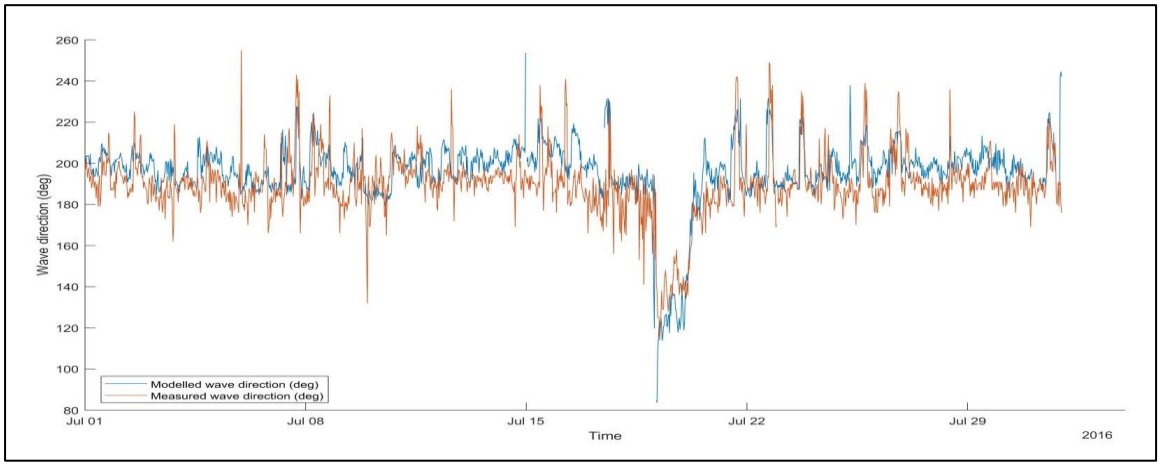
Modelled wave direction (deg)
Measured wave direction (deg)
Wave direction (deg)
Time
2016

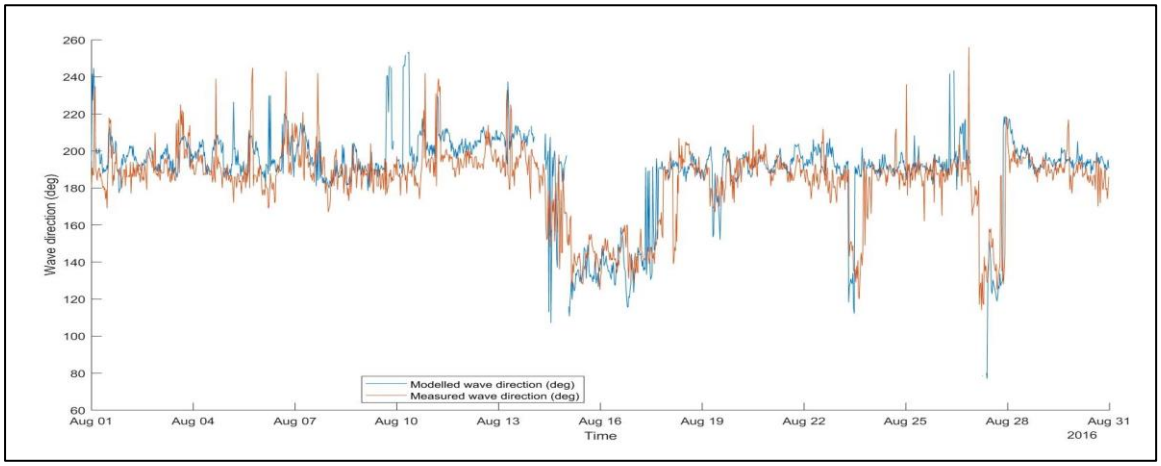
Modelled wave direction (deg)
Measured wave direction (deg)
Wave direction (deg)
Time
2016

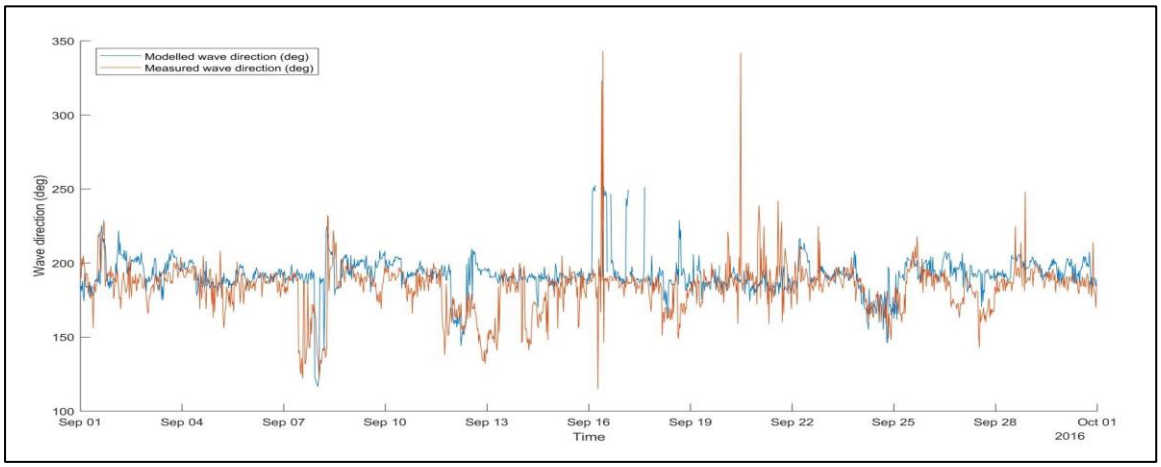
Modelled wave direction (deg)
Measured wave direction (deg)
Wave direction (deg)
Time
2016

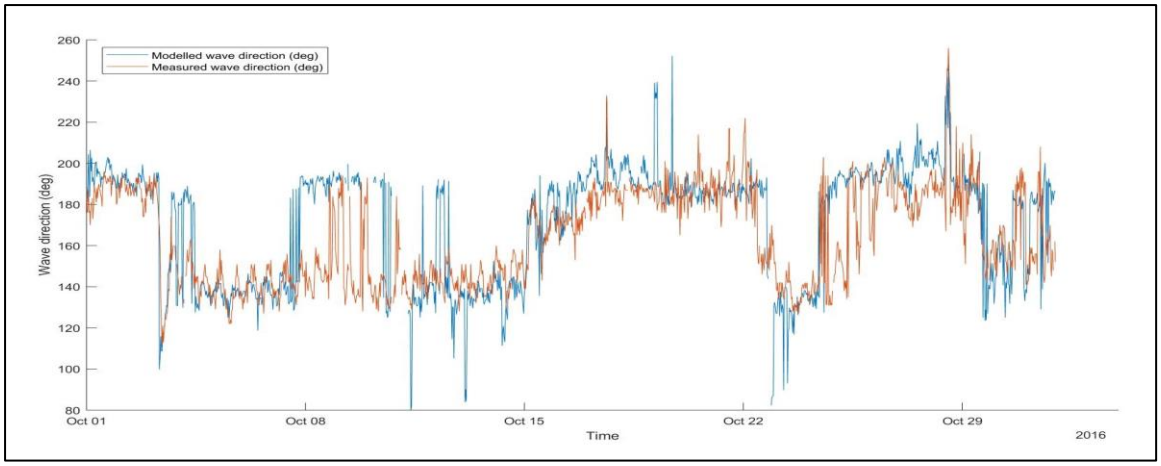
Modelled wave direction (deg)
Measured wave direction (deg)
Wave direction (deg)
260
240
220
200
180
160
140
120
100
80
Oct 01
Oct 08
Oct 15
Oct 22
Oct 29
Time
2016

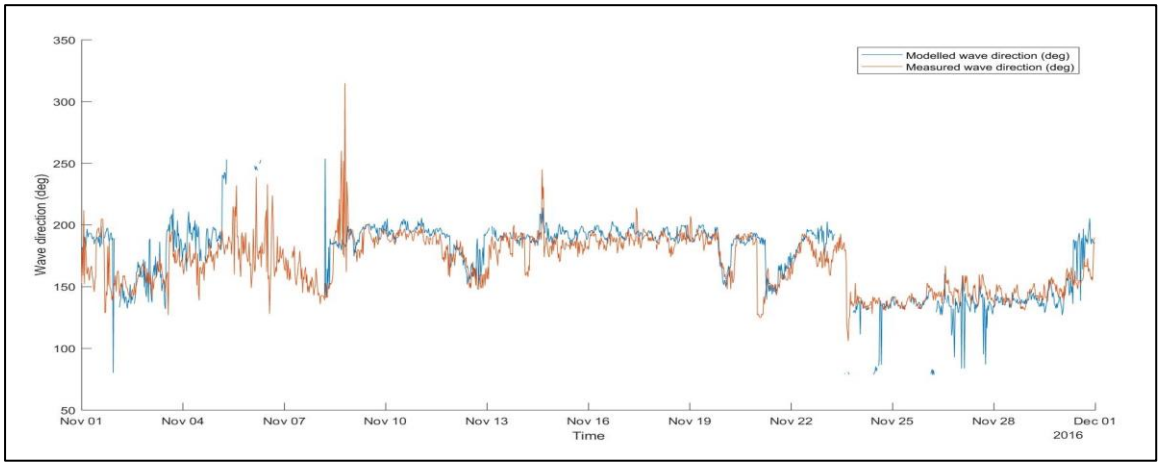
Modelled wave direction (deg)
Measured wave direction (deg)
Wave direction (deg)
350
300
250
200
150
100
50
Nov 01
Nov 04
Nov 07
Nov 10
Nov 13
Nov 16
Nov 19
Nov 22
Nov 25
Nov 28
Dec 01
Time
2016

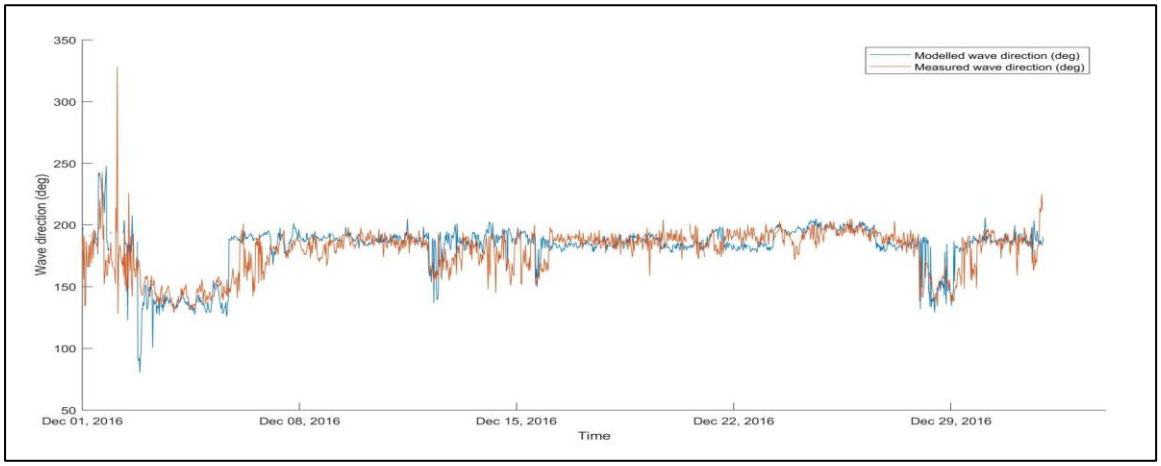
Modelled wave direction (deg)
Measured wave direction (deg)
Wave direction (deg)
350
300
250
200
150
100
50
Dec 01, 2016
Dec 08, 2016
Dec 15, 2016
Dec 22, 2016
Dec 29, 2016
Time

Appendix B

This section provides the PSD characteristics of the entire sampled population. This is used to supplement the discussion in Section 5 on the sediment characteristics in the longshore direction. The subsequent plots showed the Mean (Mn), Sorting (So), Skewness (Sk) and Kurtosis (Ku) plot at offshore (OS), Low Water (LW) and High Water (HW) across the Poole Bay coastline.

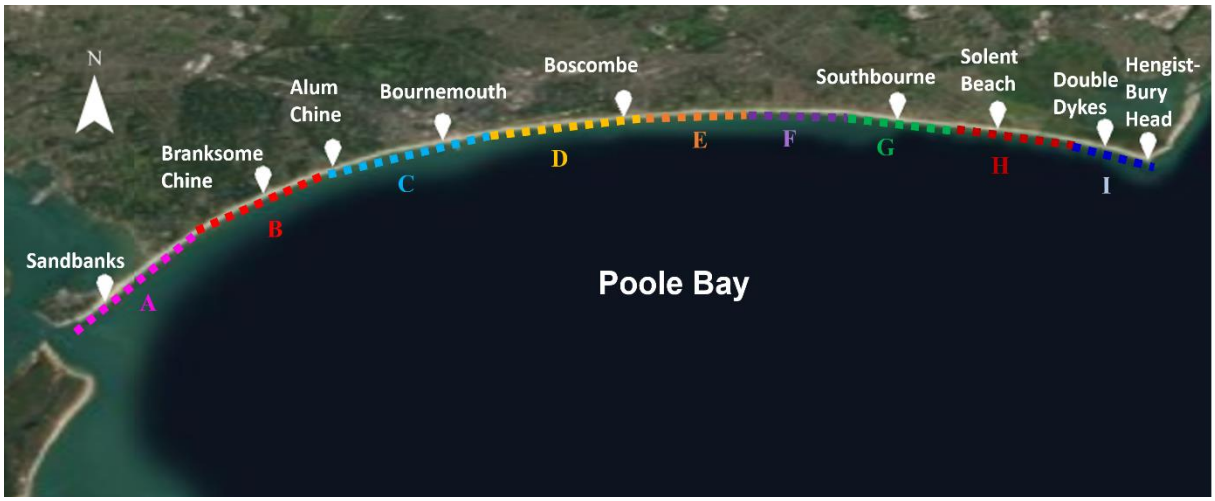

		A	B	C	D	E	F	G	H	I
OS	**Mn (φ)**	1.88	2.06	2.40	2.26	2.08	1.74	2.17	2.27	1.99
	So (φ)	0.76	0.87	0.62	0.55	0.57	1.08	0.51	0.55	0.72
	Sk (φ)	-0.29	-0.22	-0.25	-0.19	-0.01	-0.23	-0.01	-0.10	-0.17
	Ku (φ)	1.38	1.34	1.85	1.18	1.05	1.43	1.03	1.43	1.01
LW	**Mn (φ)**	1.98	1.64	1.62	0.71	0.61	0.09	0.38	-1.29	-0.74
	So (φ)	0.97	0.81	1.08	1.54	1.38	1.26	1.33	1.93	1.80
	Sk (φ)	-0.37	-0.18	-0.31	-0.31	-0.12	-0.09	-0.33	0.07	0.11
	Ku (φ)	1.18	1.20	1.53	1.96	1.29	1.45	1.08	0.81	0.93
HW	**Mn (φ)**	2.40	1.91	1.10	1.69	1.75	1.34	1.20	-0.04	0.14
	So (φ)	0.49	0.52	0.87	0.85	0.63	0.94	0.83	2.03	1.90
	Sk (φ)	-0.08	-0.08	-0.14	-0.29	-0.14	-0.21	-0.18	-0.34	-0.13
	Ku (φ)	1.10	1.00	1.40	1.96	1.58	1.23	1.56	1.34	1.48

Appendix C

This section tabled the overall sediment characteristics distribution in cross-shore direction. Mn and So of the offshore, low water and high water samples for Zone A to I are plotted in the cross shore direction.

	A	B	C	D	E	F	G	H	I
Distance from coast (m)	280	316	328	319	352	348	395	253	250
Mn (φ)	1.880	2.064	2.395	2.256	2.076	1.741	2.171	2.267	1.987
So (φ)	0.762	0.867	0.616	0.554	0.567	1.079	0.505	0.546	0.718
Sk (φ)	-0.291	-0.222	-0.247	-0.194	-0.006	-0.229	-0.012	-0.100	-0.167
Ku (φ)	1.380	1.335	1.850	1.178	1.054	1.425	1.027	1.434	1.012
Distance from coast (m)	55	42	34	37	32	47	28	35	47
Mn (φ)	1.982	1.635	1.616	0.705	0.610	0.090	0.381	-1.293	-0.740
So (φ)	0.966	0.810	1.075	1.538	1.378	1.263	1.331	1.928	1.798
Sk (φ)	-0.373	-0.175	-0.313	-0.311	-0.115	-0.093	-0.331	0.067	0.112
Ku (φ)	1.184	1.199	1.525	1.963	1.294	1.453	1.078	0.806	0.933
Distance from coast (m)	17	14	5	7	5	7	4	12	18
Mn (φ)	2.399	1.907	1.096	1.685	1.751	1.340	1.197	-0.038	0.137
So (φ)	0.487	0.516	0.867	0.854	0.631	0.939	0.830	2.029	1.903
Sk (φ)	-0.082	-0.083	-0.142	-0.286	-0.143	-0.210	-0.181	-0.340	-0.131
Ku (φ)	1.095	0.997	1.396	1.963	1.583	1.225	1.556	1.335	1.478

Mean grain size plots:

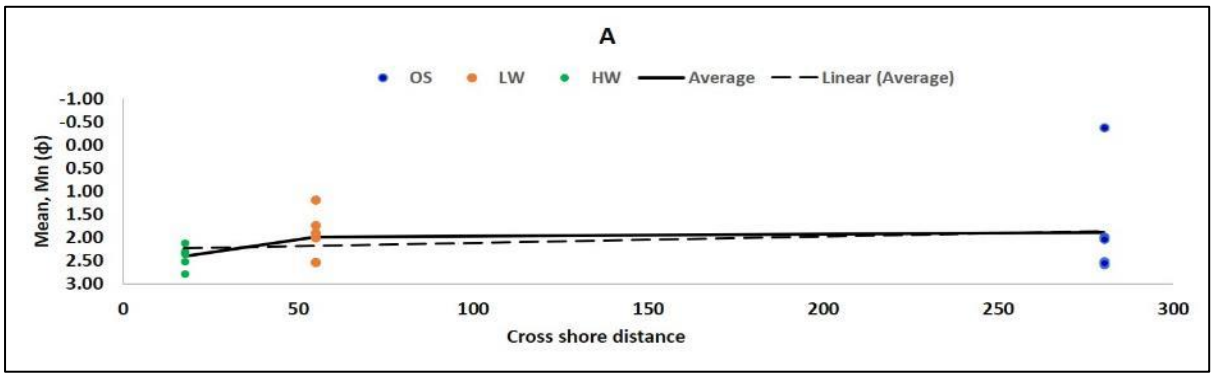

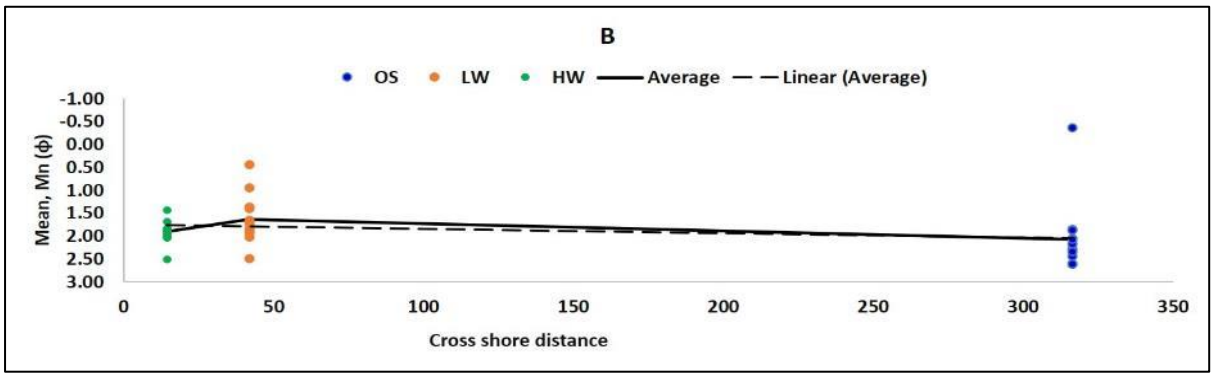

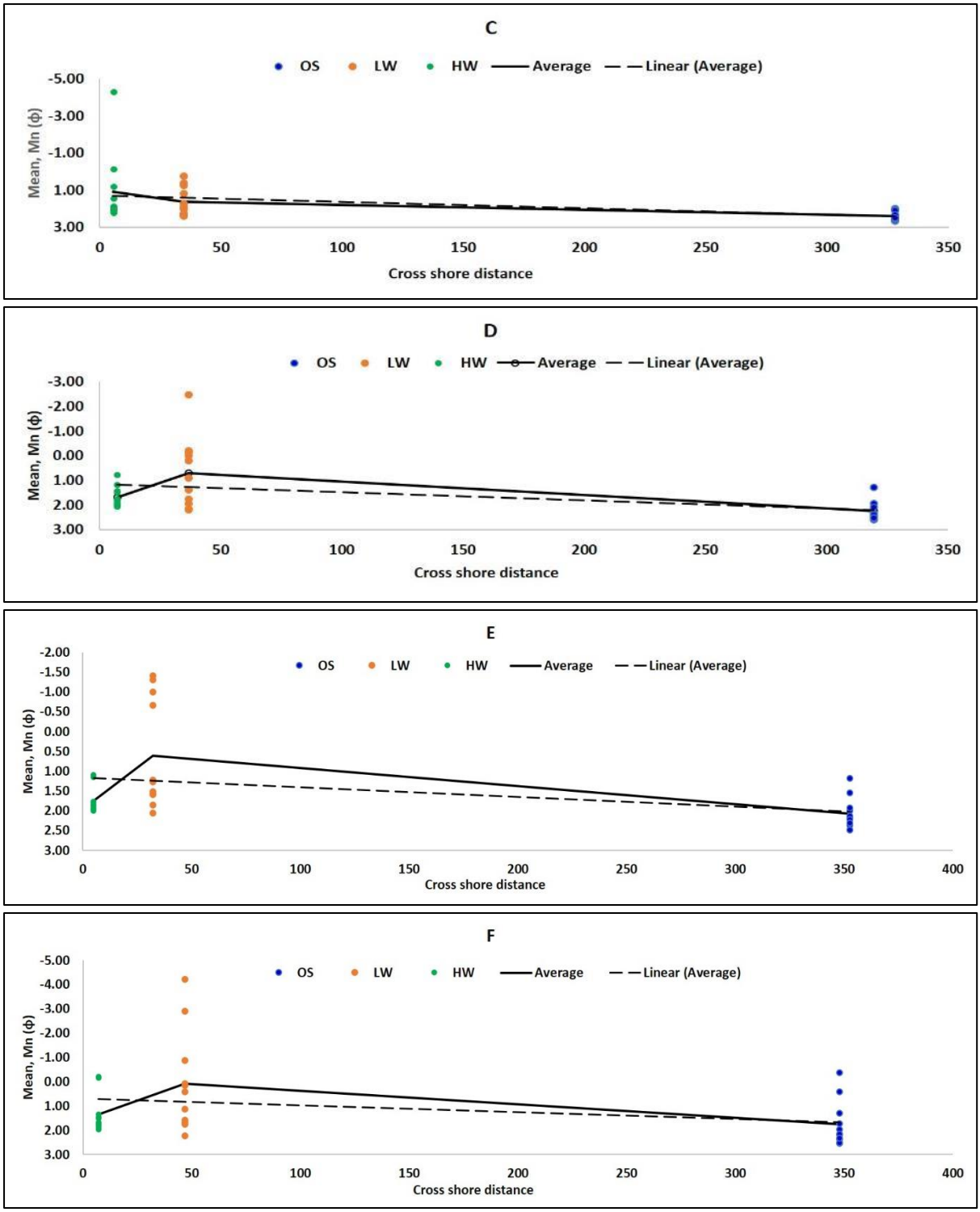
C
OS
LW
HW
Average
Linear (Average)
Mean, Mn (ϕ)
-5.00
-3.00
-1.00
1.00
3.00
0
50
100
150
200
250
300
350
Cross shore distance
D
OS
LW
HW
Average
Linear (Average)
Mean, Mn (ϕ)
-3.00
-2.00
-1.00
0.00
1.00
2.00
3.00
0
50
100
150
200
250
300
350
Cross shore distance
E
OS
LW
HW
Average
Linear (Average)
Mean, Mn (ϕ)
-2.00
-1.50
-1.00
-0.50
0.00
0.50
1.00
1.50
2.00
2.50
3.00
0
50
100
150
200
250
300
350
400
Cross shore distance
F
OS
LW
HW
Average
Linear (Average)
Mean, Mn (ϕ)
-5.00
-4.00
-3.00
-2.00
-1.00
0.00
1.00
2.00
3.00
0
50
100
150
200
250
300
350
400
Cross shore distance

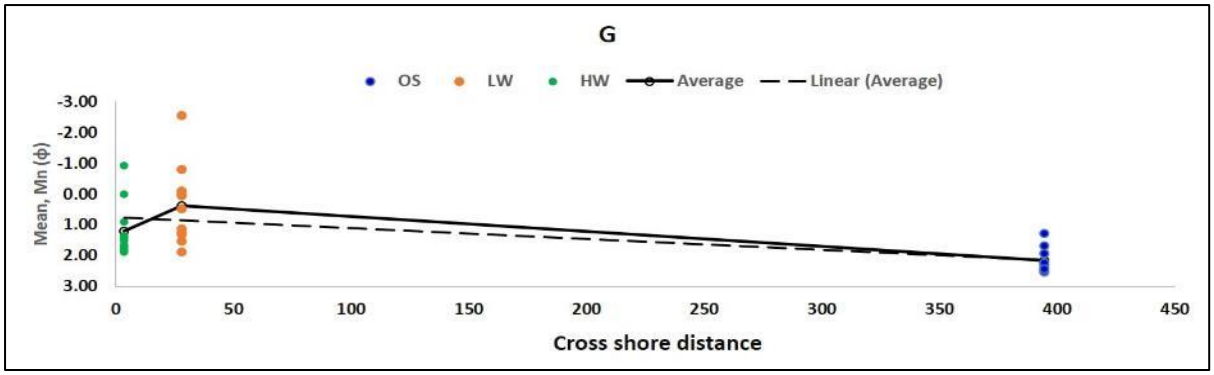

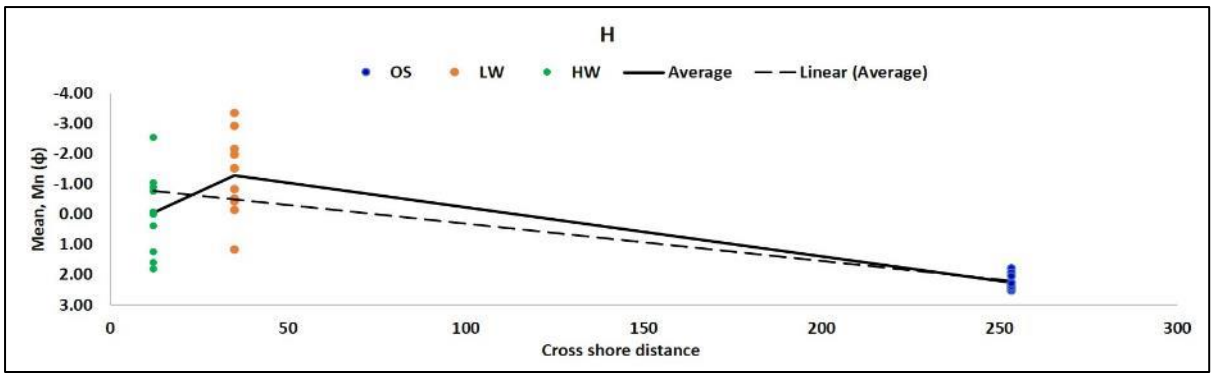

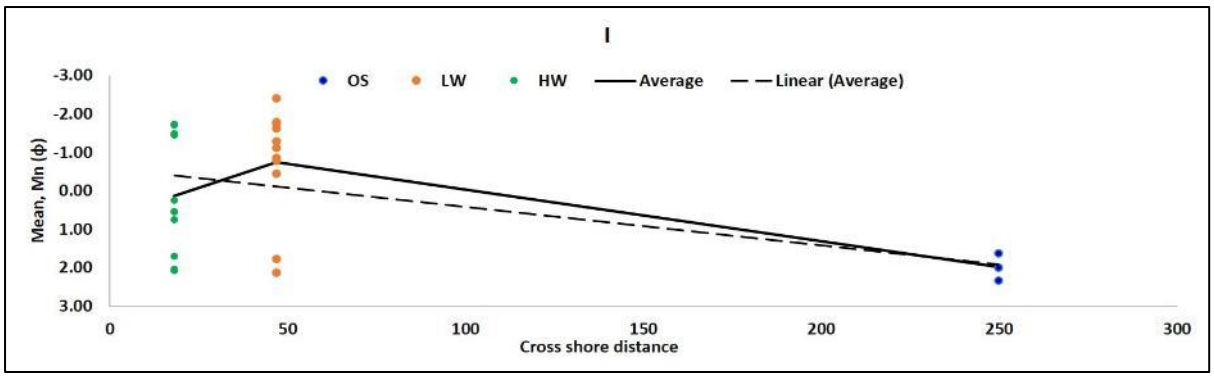

Sorting plots:

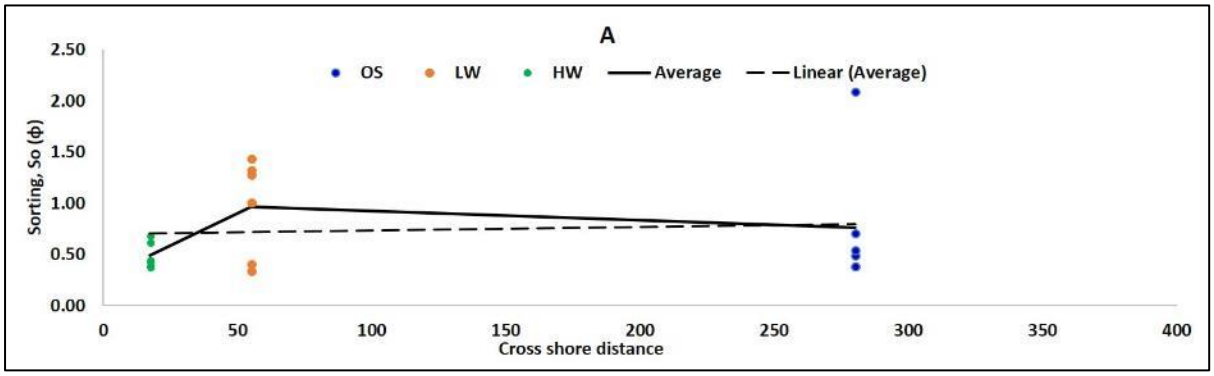

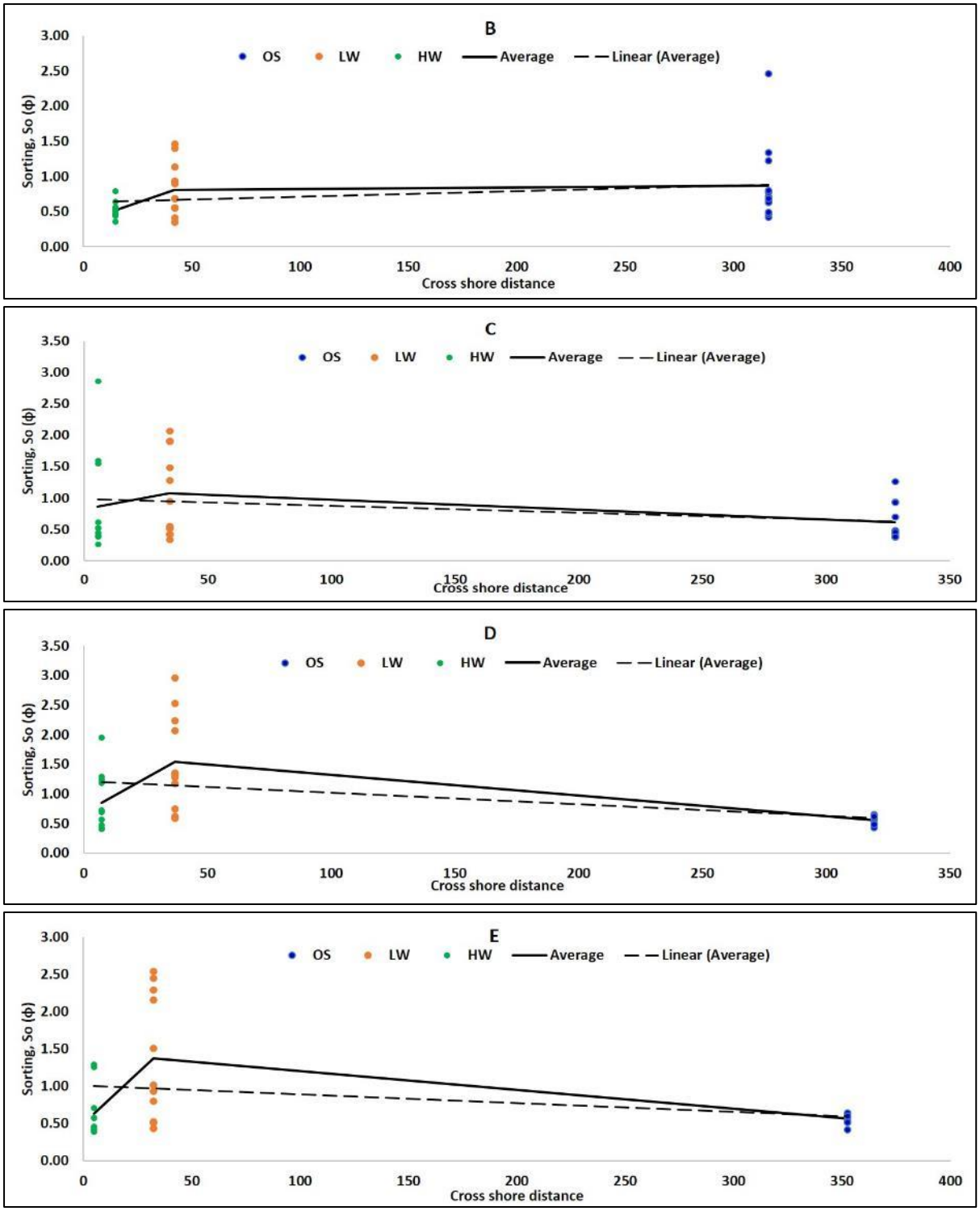
B
OS
LW
HW
Average
Linear (Average)
Sorting, So (ϕ)
Cross shore distance
C
OS
LW
HW
Average
Linear (Average)
Sorting, So (ϕ)
Cross shore distance
D
OS
LW
HW
Average
Linear (Average)
Sorting, So (ϕ)
Cross shore distance
E
OS
LW
HW
Average
Linear (Average)
Sorting, So (ϕ)
Cross shore distance

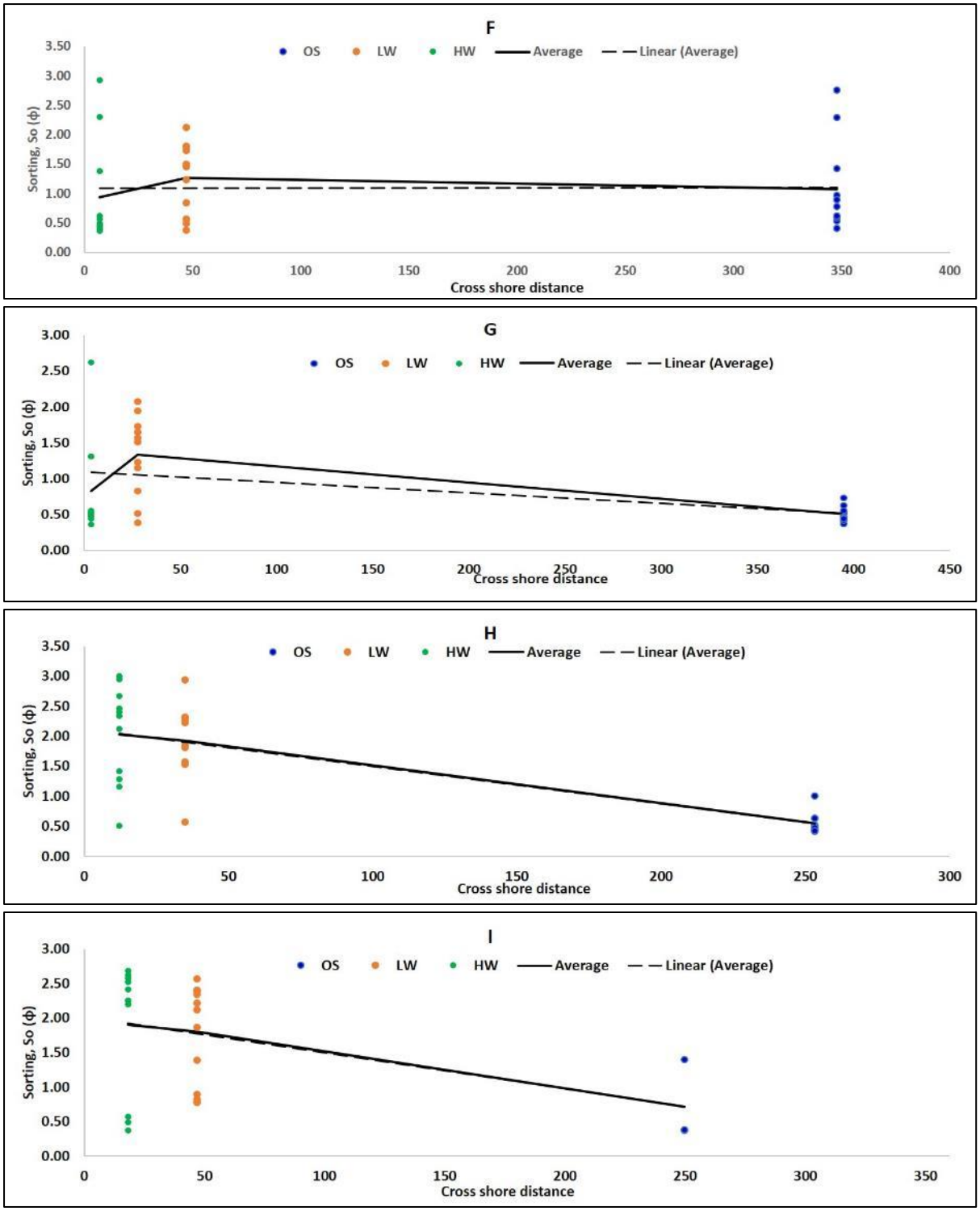
F
OS
LW
HW
Average
Linear (Average)
Sorting, So (ϕ)
Cross shore distance
G
OS
LW
HW
Average
Linear (Average)
Sorting, So (ϕ)
Cross shore distance
H
OS
LW
HW
Average
Linear (Average)
Sorting, So (ϕ)
Cross shore distance
I
OS
LW
HW
Average
Linear (Average)
Sorting, So (ϕ)
Cross shore distance

Appendix D

This section provides the annual dataset for wave properties from 2005 to 2016.

	2005								
	θ (deg)			Hs (m)			T (s)		
Zone	Mean	Min	Max	Mean	Min	Max	Mean	Min	Max
A	165	57	230	0.40	0.02	3.23			
B	177	67	244	0.43	0.01	3.47			
C	182	75	252	0.45	0.02	3.54			
D	185	82	258	0.46	0.04	3.57			
E	189	88	267	0.46	0.03	3.51			
F	192	94	272	0.51	0.03	3.80			
G	193	101	277	0.55	0.03	4.08			
H	196	110	284	0.58	0.01	4.48			
I	199	111	289	0.56	0.04	4.41	6.74	1.96	16.56

	2006								
	θ (deg)			Hs (m)			T (s)		
Zone	Mean	Min	Max	Mean	Min	Max	Mean	Min	Max
A	165	58	229	0.51	0.02	3.06			
B	177	67	244	0.54	0.03	3.21			
C	180	75	253	0.55	0.04	3.30			
D	183	83	258	0.56	0.06	3.34			
E	187	89	266	0.56	0.08	3.32			
F	189	96	272	0.62	0.09	3.62			
G	190	100	277	0.66	0.05	3.88			
H	193	108	283	0.70	0.04	4.32			
I	195	112	289	0.68	0.06	4.15	6.70	1.87	18.28

	2007								
	θ (deg)			Hs (m)			T (s)		
Zone	Mean	Min	Max	Mean	Min	Max	Mean	Min	Max
A	166	57	231	0.51	0.03	2.80			
B	177	68	245	0.55	0.02	2.93			
C	182	75	253	0.57	0.07	3.02			
D	186	82	258	0.58	0.03	3.08			
E	189	89	267	0.58	0.05	3.08			
F	192	95	272	0.64	0.09	3.37			
G	193	102	277	0.68	0.10	3.63			
H	195	111	283	0.73	0.05	4.03			
I	197	111	288	0.71	0.09	3.88	7.25	1.85	18.24

	2008								
	Wave Dir			Wave Height			(BOS) Wave Period		
Zone	Mean	Min	Max	Mean	Min	Max	Mean	Min	Max
A	166	59	227	0.50	0.03	3.24			
B	176	70	244	0.54	0.03	3.91			
C	182	76	252	0.55	0.06	3.97			
D	185	82	258	0.56	0.08	4.00			
E	188	90	267	0.56	0.06	3.93			
F	191	95	272	0.62	0.11	4.26			
G	192	103	277	0.66	0.03	4.56			
H	195	116	284	0.70	0.00	4.51			
I	195	116	284	0.68	0.09	4.93	7.06	1.78	21.06

	2009								
	θ (deg)			Hs (m)			T (s)		
Zone	Mean	Min	Max	Mean	Min	Max	Mean	Min	Max
A	166	57	225	0.53	0.03	3.23			
B	177	69	244	0.56	0.03	3.80			
C	182	78	253	0.58	0.07	3.90			
D	185	82	258	0.58	0.03	3.94			
E	189	89	267	0.58	0.07	3.91			
F	191	96	272	0.64	0.09	4.25			
G	193	100	277	0.68	0.03	4.56			
H	195	109	284	0.73	0.06	4.43			
I	197	112	289	0.71	0.09	4.92	7.34	1.88	18.57

	2010								
	θ (deg)			Hs (m)			T (s)		
Zone	Mean	Min	Max	Mean	Min	Max	Mean	Min	Max
A	164	58	226	0.43	0.03	2.59			
B	174	68	245	0.45	0.03	2.57			
C	180	76	253	0.46	0.05	2.57			
D	183	83	258	0.47	0.04	2.56			
E	187	88	267	0.47	0.06	2.52			
F	189	94	272	0.51	0.09	2.73			
G	191	102	277	0.55	0.07	2.94			
H	193	107	282	0.58	0.05	3.30			
I	195	113	289	0.56	0.06	3.17	7.11	1.85	18.43

	θ (deg)			Hs (m)			T (s)		
Zone	Mean	Min	Max	Mean	Min	Max	Mean	Min	Max
A	166	60	224	0.52	0.02	2.59			
B	177	67	244	0.55	0.01	2.68			
C	182	76	253	0.57	0.06	2.74			
D	185	82	258	0.58	0.06	2.77	7.59	1.98	19.68

E	188	89	266	0.58	0.01	2.75			
F	190	94	271	0.63	0.04	3.00			
G	192	101	273	0.68	0.04	3.23			
H	194	109	282	0.72	0.20	3.63			
I	196	112	286	0.70	0.06	3.50			

	2013								
	θ (deg)			Hs (m)			T (s)		
Zone	Mean	Min	Max	Mean	Min	Max	Mean	Min	Max
A	165	63	226	0.52	0.03	3.23			
B	175	72	245	0.55	0.03	3.71			
C	180	79	252	0.56	0.06	3.77			
D	183	82	258	0.57	0.09	3.79			
E	187	90	266	0.57	0.07	3.75			
F	189	94	272	0.62	0.04	4.07			
G	190	100	277	0.67	0.07	4.35			
H	193	108	284	0.71	0.03	4.43			
I	195	112	289	0.69	0.07	4.61	7.37	1.81	19.64

	2014								
	θ (deg)			Hs (m)			T (s)		
Zone	Mean	Min	Max	Mean	Min	Max	Mean	Min	Max
A	167	58	228	0.58	0.04	3.24			
B	177	67	244	0.61	0.03	4.61			
C	181	77	253	0.63	0.02	4.71			
D	184	82	258	0.64	0.06	4.74			
E	188	88	266	0.64	0.01	4.69			
F	190	94	272	0.70	0.07	5.08			
G	192	100	277	0.75	0.07	5.45			
H	194	106	284	0.80	0.03	4.52			
I	196	113	288	0.78	0.04	5.47	7.56	1.83	20.39

	2015								
	θ (deg)			Hs (m)			T (s)		
Zone	Mean	Min	Max	Mean	Min	Max	Mean	Min	Max
A	166	59	226	0.56	0.03	2.96			
B	176	67	245	0.60	0.02	3.05			
C	181	77	252	0.62	0.06	3.12			
D	184	82	258	0.63	0.05	3.15			
E	188	88	266	0.63	0.09	3.12			
F	190	94	272	0.69	0.08	3.39			
G	191	100	277	0.74	0.04	3.63			
H	194	115	283	0.79	0.04	4.08			
I	196	116	289	0.77	0.03	3.90	7.33	1.88	20.38

	2016								
	θ (deg)			Hs (m)			T (s)		
Zone	Mean	Min	Max	Mean	Min	Max	Mean	Min	Max
A	166	59	228	0.51	0.04	3.24			
B	176	67	241	0.54	0.02	3.49			
C	181	76	251	0.56	0.03	3.47			
D	184	83	258	0.56	0.06	3.45			
E	188	88	266	0.56	0.07	3.42			
F	190	97	272	0.62	0.03	3.73			
G	192	102	277	0.66	0.09	4.01			
H	194	109	282	0.70	0.03	4.37			
I	196	111	289	0.68	0.07	4.30	7.3	1.8	20.2

Appendix E

This section provides the details of the beach nourishment works in Poole Bay and the periodic change of mean grain size in the cross-shore direction.

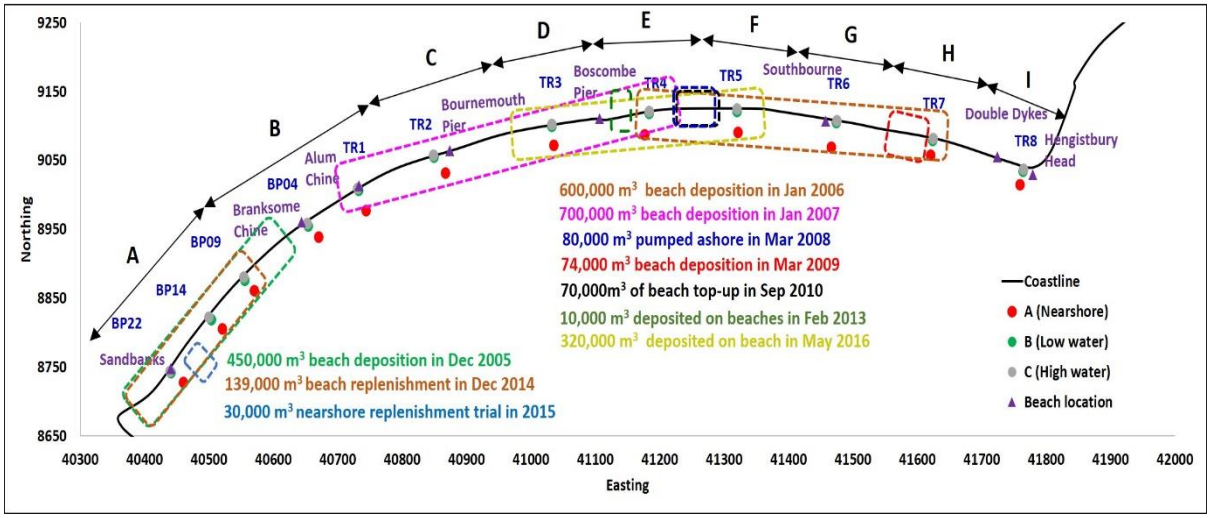

Year	Scheme	Quantity (m^3)	Notes
2006 to 2010	BIS 4	1,840,000	Poolebay.net: 1,840,000 m^3 • Swanage beach: 90,000 m^3 • Poole beaches between Shore Road and Branksome Dene Chine: 450,000 m^3 *[Work at Poole started in December 2005 and was completed on Monday, 16th January 2006]* • BIS 4.1 Bournemouth beaches between Boscombe Pier and Double Dykes: 600,000 m^3 *[winter of 2005/2006]* https://www.poolebay.net/PhaseI/ • BIS 4.2 Boscombe and Alum Chine: 700,000 m^3 *[winter of 2006/2007]* https://www.poolebay.net/PhaseII/ • BIS 4.3 A project to replenish a small section of beach between Boscombe & Southbourne. The dredger Oranje delivered sand to the coast between 8th -14th March 2008. Eight hopper loads dredged from Isle of Wight, pumped ashore from Groyne 32 (500 m), and west to Groyne 28 (300 m) *[Mar 2008]* https://poolebay.net/bournemouth-beach-2008-2010.html • BIS 4.4 A project to replenish a small section of beach at Southbourne. The dredger Crestway delivered sand to the coast between 4th -21st March 2009. 74,192 m^3 added to the beach between Groynes 50 & 53 at Southbourne beach *[March 2009]* • BIS 4.5 A project to replenish a section of beach at Southbourne between Portman Ravine and Fisherman's Walk. The third and final of the Bournemouth beach top-ups. 70,000m^3 of

			beach material top-up of a section of beach at Southbourne (Portman Ravine Groyne 28 to Fisherman's Walk Groyne 32) *[September 2010]*
2014		139,000	Replenished beach stretching from Sandbanks rock groyne to the end of the beach huts at Canford Cliffs by recycling sand from the Swash Channel, Poole Harbour *[Dec 2014]* (https://poolebay.net/shore-road.html)
2015		30,000	Nearshore replenishment trial: Recycled sand from Poole Harbour entrance, deposited on the seabed 300-400 m off Sandbanks beach (5f00506 to 5f00502) in water between 5-8 m deep *[Feb 2015]* (https://scopac.org.uk/wp-content/uploads/2018/04/EA-Report_Trialling_a_new_approach_to_beach_replenishment_in_Poole_Bay_-_report.pdf)
2015 to 2016		320,000	Recharge materials were dredged from west of Isle of Wight, deposit on beach between Bournemouth Pier and Southbourne.

Zone A

Year/ Sampling Site	2005	2006	2007	2008	2009	2010	2011	2013	2014	2015	2016
OS								0.58	0.19		
LW								0.24	0.29		
HW								0.21	0.17		

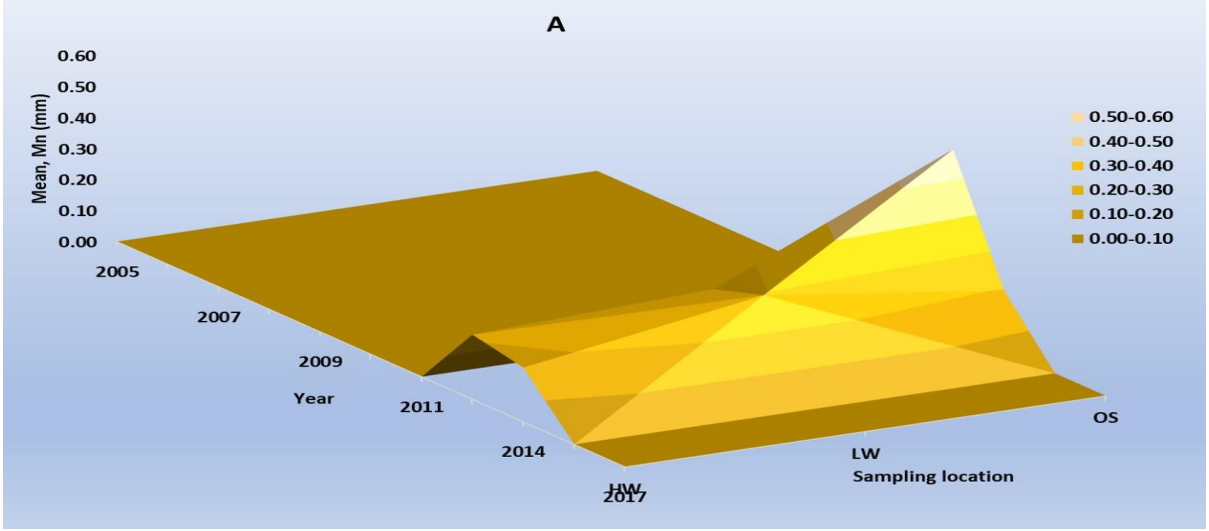

Zone B

Year/ Sampling Site	2005	2006	2007	2008	2009	2010	2011	2013	2014	2015	2016
OS	0.24	0.28	0.18	0.20	0.21	0.22	0.27	0.20	0.73	0.20	0.16
LW	0.32	0.39	0.30	0.28	0.31	0.27	0.18	0.26	0.63	0.26	0.38
HW	0.27	0.25	0.27	0.28	0.27	0.26	0.24	0.28	0.23	0.37	0.28

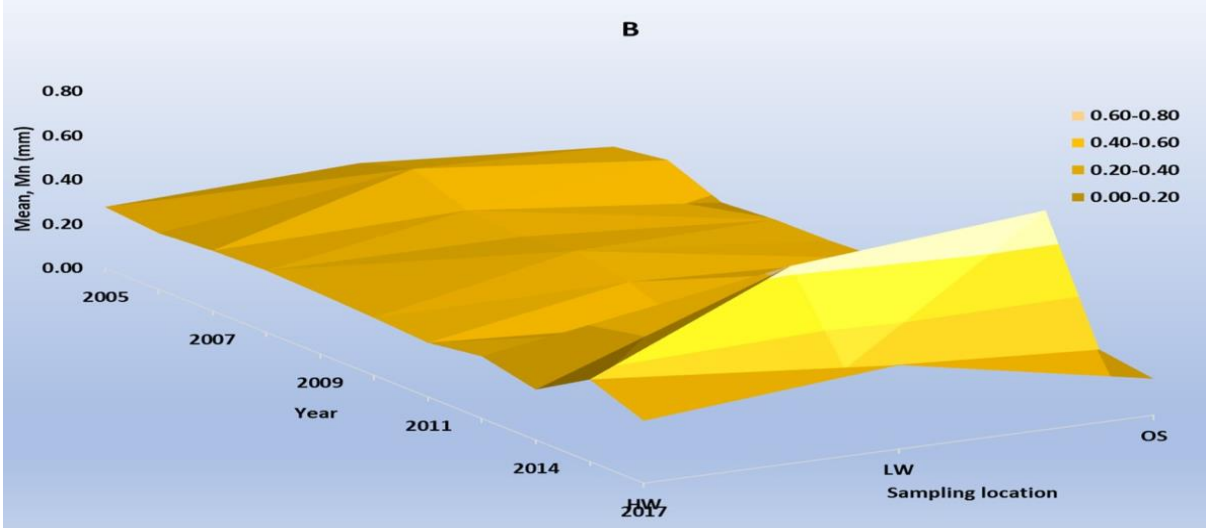

Zone C

Year/ Sampling Site	2005	2006	2007	2008	2009	2010	2011	2013	2014	2015	2016
OS	0.25	0.24	0.17	0.24	0.17	0.18	0.16	0.20	0.16	0.17	0.18
LW	0.65	0.84	0.27	0.21	0.24	0.59	0.19	0.21	0.44	0.19	0.30
HW	0.57	0.36	0.24	0.24	0.24	0.22	1.10	19.62	0.27	0.25	0.27

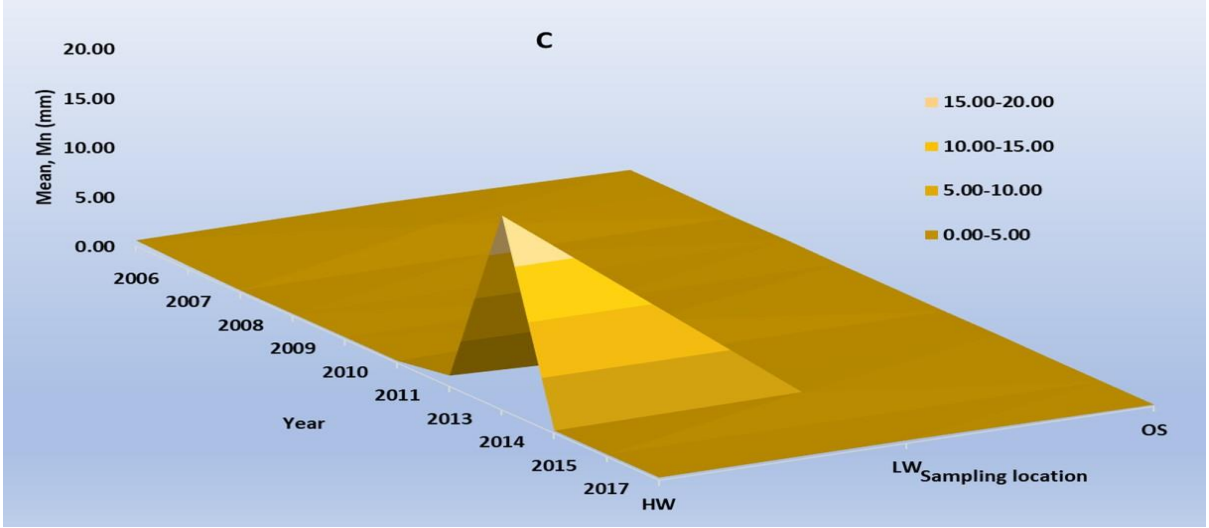

Zone D

Year/ Sampling Site	2005	2006	2007	2008	2009	2010	2011	2013	2014	2015	2016
OS	0.41	0.26	0.20		0.17	0.19	0.18	0.19	0.17	0.17	0.23
LW	0.53	0.38	0.29	1.15	1.00	5.62	0.22	0.22	1.10	0.26	0.86
HW	0.44	0.37	0.25	0.29	0.28	0.26	0.24	0.35	0.24	0.25	0.58

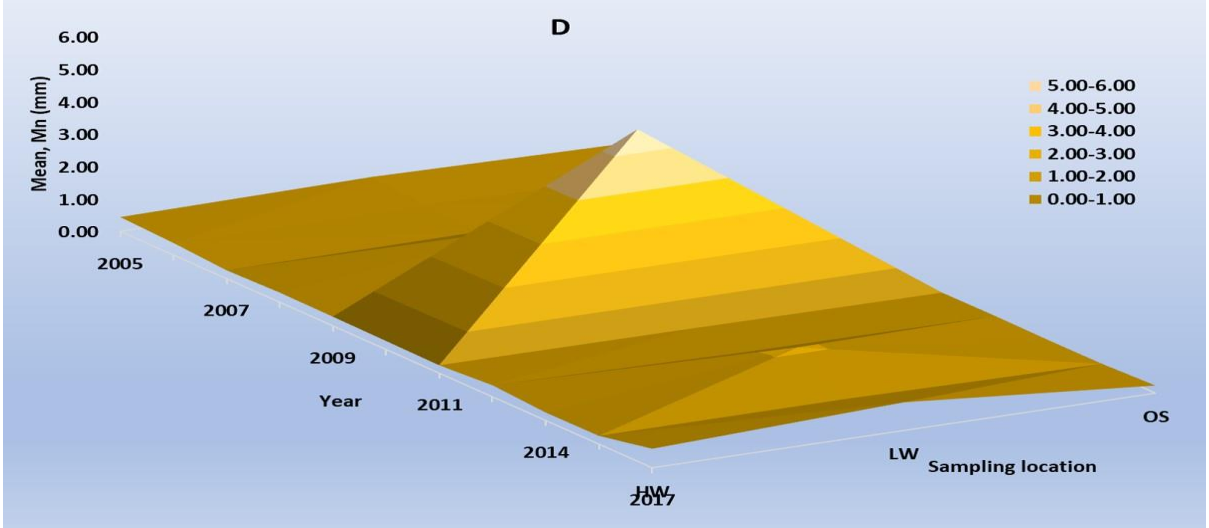

Zone E

Year/ Sampling Site	2005	2006	2007	2008	2009	2010	2011	2013	2014	2015	2016
OS	0.44	0.34	0.19	0.22	0.25	0.23	0.22	0.26	0.18	0.20	0.18
LW	0.43	0.41	0.33	1.58	2.48	0.34	2.01	0.24	0.35	0.28	2.66
HW	0.45	0.47	0.26	0.26	0.27	0.26	0.28	0.27	0.25	0.29	0.29

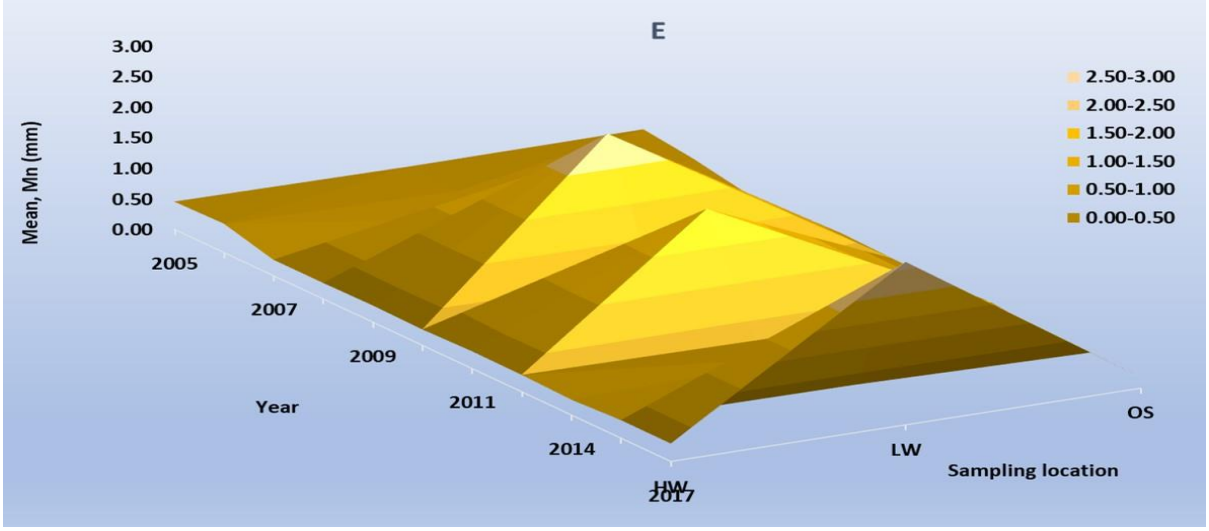

Zone F

Year/ Sampling Site	2005	2006	2007	2008	2009	2010	2011	2013	2014	2015	2016
OS	0.25	0.24	0.17	0.24	0.17	0.18	0.16	0.20	0.16	0.17	0.18
LW	0.91	0.30	1.82	0.33	7.47	18.70	0.21	0.46	0.75	0.31	0.95
HW	0.36	0.40	0.31	0.27	0.29	0.29	0.26	0.35	1.15	1.12	0.31

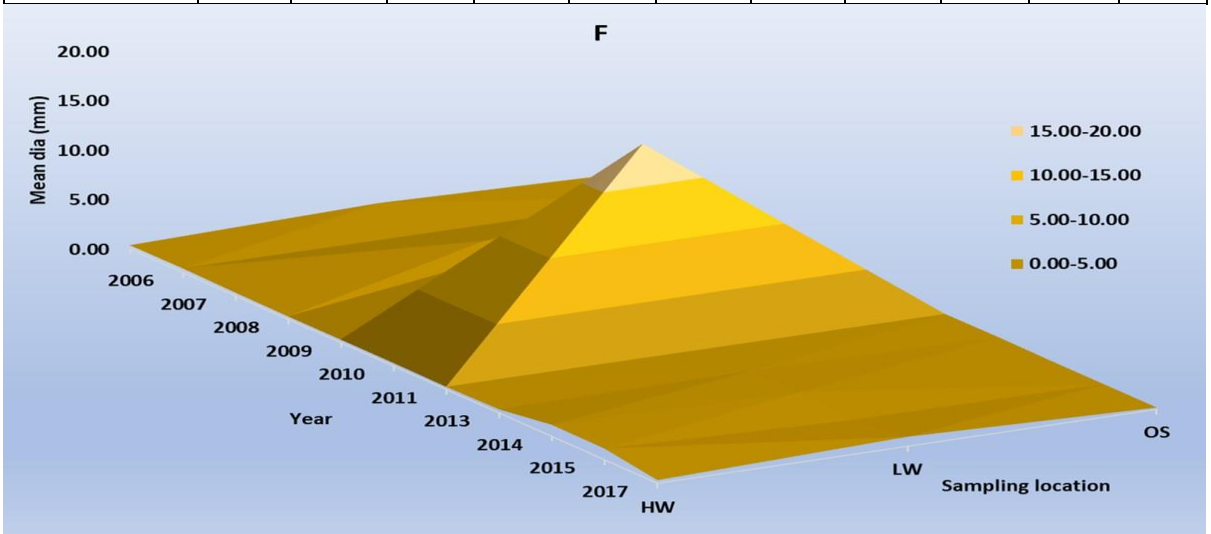

Zone G

Year/ Sampling Site	2005	2006	2007	2008	2009	2010	2011	2013	2014	2015	2016
OS	0.31	0.26	0.17	0.21	0.21	0.20	0.21	0.41	0.18	0.17	0.18
LW	1.08	0.99	0.41	0.35	0.27	5.95	0.46	0.40	1.75	0.96	0.72
HW	0.32	0.53	0.38	0.35	0.39	1.92	0.29	0.28	0.27	0.31	1.00

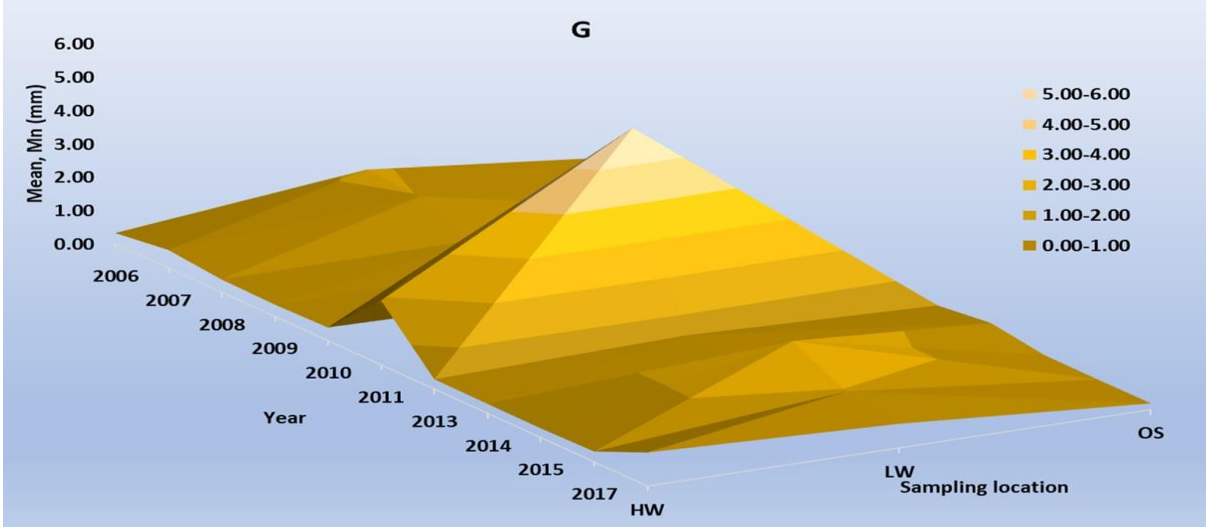

Zone H

Year/ Sampling Site	2005	2006	2007	2008	2009	2010	2011	2013	2014	2015	2016
OS	0.29	0.26	0.18	0.18	0.17	0.21	0.24	0.18	0.20	0.19	0.20
LW	1.34	2.87	1.78	3.90	7.63	0.45	1.10	1.43	10.28	4.49	2.89
HW	0.43	1.87	1.70	0.77	1.06	1.05	2.07	0.29	1.00	0.33	5.79

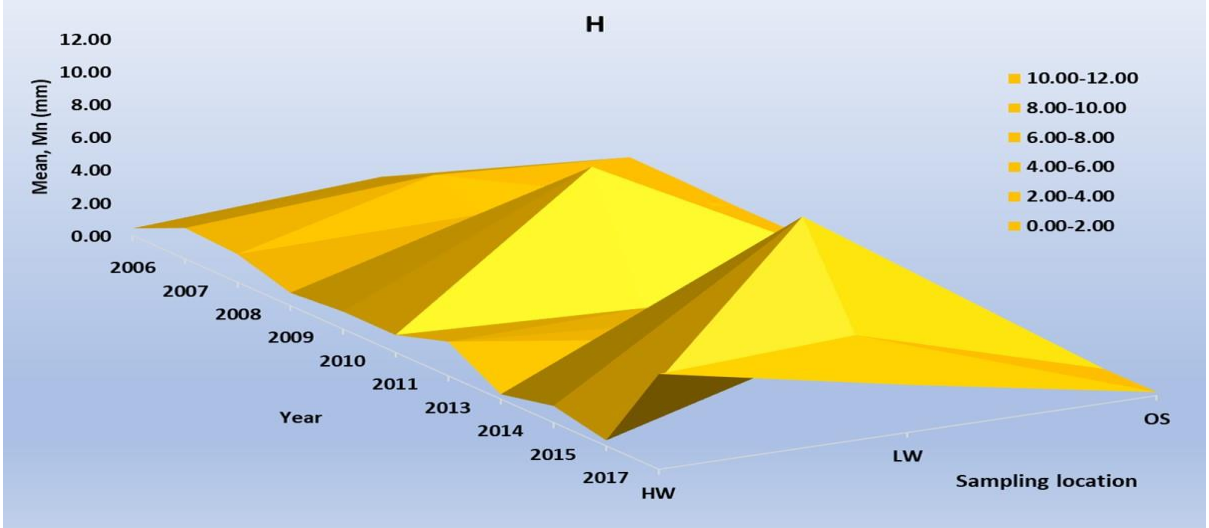

Zone I

Year/ Sampling Site	2005	2006	2007	2008	2009	2010	2011	2013	2014	2015	2016
OS		0.25	0.20			0.33					
LW	0.29	2.17	1.36	1.81	3.37	2.44	1.72	3.07	3.44	0.23	5.29
HW	3.32	2.81	0.84	0.31	0.24	0.24	0.68	2.74	0.59	0.68	3.28